University of Kentucky
UKnowledge

Theses and Dissertations--Physiology | Physiology

2019

TARGETING MALADAPTIVE PLASTICITY AFTER SPINAL CORD INJURY TO PREVENT THE DEVELOPMENT OF AUTONOMIC DYSREFLEXIA

Khalid C. Eldahan
University of Kentucky, khalid.eldahan@uky.edu
Author ORCID Identifier:
https://orcid.org/0000-0003-1674-2386
Digital Object Identifier: https://doi.org/10.13023/etd.2019.064

Right click to open a feedback form in a new tab to let us know how this document benefits you.

Recommended Citation

Eldahan, Khalid C., "TARGETING MALADAPTIVE PLASTICITY AFTER SPINAL CORD INJURY TO PREVENT THE DEVELOPMENT OF AUTONOMIC DYSREFLEXIA" (2019). *Theses and Dissertations--Physiology*. 41.
https://uknowledge.uky.edu/physiology_etds/41

This Doctoral Dissertation is brought to you for free and open access by the Physiology at UKnowledge. It has been accepted for inclusion in Theses and Dissertations--Physiology by an authorized administrator of UKnowledge. For more information, please contact UKnowledge@lsv.uky.edu.

STUDENT AGREEMENT:

I represent that my thesis or dissertation and abstract are my original work. Proper attribution has been given to all outside sources. I understand that I am solely responsible for obtaining any needed copyright permissions. I have obtained needed written permission statement(s) from the owner(s) of each third-party copyrighted matter to be included in my work, allowing electronic distribution (if such use is not permitted by the fair use doctrine) which will be submitted to UKnowledge as Additional File.

I hereby grant to The University of Kentucky and its agents the irrevocable, non-exclusive, and royalty-free license to archive and make accessible my work in whole or in part in all forms of media, now or hereafter known. I agree that the document mentioned above may be made available immediately for worldwide access unless an embargo applies.

I retain all other ownership rights to the copyright of my work. I also retain the right to use in future works (such as articles or books) all or part of my work. I understand that I am free to register the copyright to my work.

REVIEW, APPROVAL AND ACCEPTANCE

The document mentioned above has been reviewed and accepted by the student's advisor, on behalf of the advisory committee, and by the Director of Graduate Studies (DGS), on behalf of the program; we verify that this is the final, approved version of the student's thesis including all changes required by the advisory committee. The undersigned agree to abide by the statements above.

Khalid C. Eldahan, Student

Dr. Alexander G. Rabchevsky, Major Professor

Dr. Kenneth S. Campbell, Director of Graduate Studies

TARGETING MALADAPTIVE PLASTICITY AFTER SPINAL CORD INJURY TO PREVENT THE DEVELOPMENT OF AUTONOMIC DYSREFLEXIA

DISSERTATION

A dissertation submitted in partial fulfillment of the requirements for the degree of Doctor of Philosophy in the College of Medicine at the University of Kentucky

By
Khalid Charles Eldahan

Lexington, Kentucky, United States of America

Director: Dr. Alexander G. Rabchevsky, Professor of Physiology

Lexington, Kentucky

2019

Copyright © Khalid C. Eldahan 2019

ABSTRACT OF DISSERTATION

TARGETING MALADAPTIVE PLASTICITY AFTER SPINAL CORD INJURY TO PREVENT THE DEVELOPMENT OF AUTONOMIC DYSREFLEXIA

Vital autonomic and cardiovascular functions are susceptible to dysfunction after spinal cord injury (SCI), with cardiovascular dysregulation contributing to morbidity and mortality in the SCI population. Autonomic dysreflexia (AD) is a condition that develops after injury to the sixth thoracic spinal segment or higher and is characterized by potentially dangerous and volatile surges in arterial pressure often accompanied with irregular heart rate, headache, sweating, flushing of the skin, and nasal congestion. These symptoms occur in response to abnormal outflow of sympathetic activity from the decentralized spinal cord typically triggered by noxious, yet unperceived nociceptive stimulation beneath the level of lesion. Maladaptive plasticity of primary afferents and spinal interneurons influencing sympathetic preganglionic neurons is known to contribute to the development of AD. However, there are currently no treatments capable of targeting this underlying pathophysiology. The goal of this work was to test pharmacological agents for their potential to modify intraspinal plasticity associated with AD in order to prophylactically prevent the development of this condition altogether.

We first tested whether the drug rapamycin (RAP), a well-studied inhibitor of the growth promoting kinase “mammalian target of rapamycin” (mTOR), could prevent aberrant sprouting of primary c-fiber afferents in association with reduced indices of AD severity. Naïve and T4-transected rats undergoing 24/7 cardiovascular monitoring were treated with rapamycin (i.p.) for 4 weeks before tissue collection. RAP attenuated intraspinal mTOR activity after injury, however it also caused toxic weight loss. RAP treated SCI rats developed abnormally high blood pressure both at rest and during colorectal distension (CRD) induced AD, as well as more frequent bouts of spontaneous AD (sAD). These cardiovascular alterations occurred without altered intraspinal c-fiber sprouting. Our finding that rapamycin exacerbates cardiovascular dysfunction after SCI underscores the importance of screening potential pharmacological agents for cardiovascular side

effects and suggests that the mTOR pathway plays a limited or dispensable role in c-fiber sprouting after SCI.

We next examined the effects of the antinociceptive drug gabapentin (GBP) on AD development. Our previous work demonstrated that a single acute administration of GBP can reduce the severity of AD. The mechanism of action, however, remains unclear. Emerging evidence suggests that GBP may act by blocking *de novo* synaptogenesis. We investigated whether continuous GBP treatment could attenuate the development of AD by modifying synaptic connectivity between primary afferents and ascending propriospinal neurons. SCI rats were treated with GBP every six hours for four weeks. We found that GBP reduced blood pressure during CRD stimulation and prevented bradycardia typically observed during AD. However, GBP treated rats also had a higher sAD frequency and failed to return to pre-injury body weight. Moreover, SCI reduced the density of putative excitatory ($VGLUT2^+$) and inhibitory ($VGAT^+$) synaptic puncta in the lumbosacral cord, although GBP did not alter these parameters. Our results suggest that continuous GBP treatment alters hemodynamic control after SCI and that decreased synaptic connectivity may contribute to the development of AD.

These studies demonstrate the need for further research to better understand the cellular signaling driving maladaptive plasticity after SCI as well as the complex and dynamic changes in intraspinal synaptic connectivity contributing to the development of AD. Moreover, GBP treatment may offer clinical benefit by reducing blood pressure during AD, however the optimal dosage must be identified to avoid undesired side-effects.

KEYWORDS: Spinal cord injury, autonomic, rapamycin, gabapentin, synapse, plasticity

Khalid C. Eldahan

January 11, 2019

TARGETING MALADAPTIVE PLASTICITY AFTER SPINAL CORD INJURY TO PREVENT THE DEVELOPMENT OF AUTONOMIC DYSREFLEXIA

By

Khalid C. Eldahan

Dr. Alexander G. Rabchevsky
Director of Dissertation

Dr. Kenneth S. Campbell
Director of Graduate Studies

This dissertation is dedicated to my parents, Ismail and Cathy Eldahan.

ACKNOWLEDGEMENTS

First, I would like to extend gratitude to my advisor, Dr. Alexander Rabchevsky, for my experiences in his lab both as Technician/Lab Manager and later as a graduate student. I admire his unrelenting dedication to the scientific method and experimental rigor which are essential for the pursuit of new knowledge. I look forward to discovering how these experiences and lessons will continue to serve me and my career in the future.

To my committee members, Dr. Steve Estus, Dr. Bret Smith, Dr. Ai-Ling Lin and Dr. Jose Abisambra, as well as my Director of Graduate Studies, Dr. Kenneth Campbell: I am grateful for all of your advice, scientific discussion and encouragement over the years. You have each contributed positively to my scientific, professional and personal growth.

Next, thank you to all of the lab members that I have had the pleasure of working alongside over the years, especially Dr. Samir Patel, Dr. Jenna Gollihue, David Cox and Hannah Williams. I appreciate the comradery which made even the most grueling long experimental days fun and positive. Moreover, I most certainly appreciate all of your help with the early-morning and late-night animal care.

I would also like to thank all of the faculty and staff in the Department of Physiology and Spinal Cord and Brain Injury Research Center. I feel fortunate to have had such great educators and support staff that made this dissertation possible.

Last, but not least: thank you to all my family and friends who have been a constant source of support and advocacy. Your support has taken many forms over the years and kept me going when changing course would have been much easier.

TABLE OF CONTENTS

Acknowledgements iii
List of Figures vii

1 Chapter 1: Introduction
1.1 Introduction to the Autonomic Nervous System 1
1.1.1 Evolution and History of the Autonomic Nervous System 1
1.1.2 Anatomical Organization of the Autonomic Nervous System 3
1.1.3 Autonomic Control of the Heart 7
1.1.4 Autonomic Control of the Vascular System 11
1.2 Introduction and Overview of Spinal Cord Injury (SCI) 14
1.2.1 Etiology and Prevalence of SCI 14
1.2.2 Effects of SCI on the Autonomic Nervous System 15
1.3 Central Hypothesis of Dissertation 16

2 Chapter 2: Autonomic Dysreflexia After Spinal Cord Injury: Systemic Pathophysiology and Methods of Management
2.1 Introduction to Autonomic Dysreflexia 19
2.2 Clinical Description of Autonomic Dysreflexia (AD) 20
2.2.1 Who is at Risk of Developing AD? 20
2.2.2 Characteristic Features of AD 21
2.2.3 Temporal Development of AD after SCI 22
2.3 Mechanisms Contributing to AD 23
2.3.1 Loss of Supraspinal Control 23
2.3.2 Synaptic Reorganization of Sympathetic Preganglionic Neurons 24
2.3.3 Primary Afferent Sprouting 27
2.3.4 Propriospinal Plasticity 28
2.3.5 Peripheral Adrenergic Hypersensitivity 30
2.4 Clinical Management of AD 32
2.4.1 Nitrates 33
2.4.2 Nifedipine 33
2.4.3 Prazosin 34
2.4.4 Botulinum toxin 34
2.5 Systemic Effects of Recurrent AD 36
2.5.1 Cardiovascular Changes 36
2.5.2 Immunomodulatory Effects of AD 38
2.6 Emerging Research Strategies 41
2.7 Conclusions 43

3 Chapter 3: Rapamycin Exacerbates Cardiovascular Dysfunction After Complete High-Thoracic Spinal Cord Injury
3.1 Introduction 47
3.2 Methods and Materials 49
3.2.1 Cardiophysiological Monitoring 50
3.2.2 Spinal Cord Transections 51

3.2.3 Post-operative Care 51
3.2.4 Rapamycin Administration and Colorectal Distension 52
3.2.5 Western Blot Analysis 53
3.2.6 Tissue Fixation and Processing 54
3.2.7 Immunohistochemistry and Microscopy 55
3.2.8 Densitometric Analyses 56
3.2.9 Statistical Analyses 57
3.3 Results 57
3.3.1 Rapamycin Mitigates Elevated mTOR Activity in the Injured Spinal Cord 57
3.3.2 Rapamycin Treatment Impairs Normal Weight Gain and Exacerbates Weight Loss After SCI 59
3.3.3 Rapamycin Alters Daily Hemodynamic Measures Before and After SCI 61
3.3.4 Rapamycin Increases the Frequency of Spontaneous AD 62
3.3.5 Rapamycin Increases the Absolute Magnitude of Colorectal Distension Induced AD 63
3.3.6 Rapamycin Does Not Alter the Density of cFos or CGRP Immunolabeling 66
3.4 Discussion 71
3.5 Conclusion 76

4 Chapter 4: Assessing Continuous High Dose Gabapentin Delivery for the Treatment of Autonomic Dysreflexia
4.1 Introduction 78
4.2 Methods and Materials 80
4.2.1 Cardiophysiological Monitoring 80
4.2.2 Baroreflex Sensitivity 82
4.2.3 Spinal Cord Injury 83
4.2.4 Drug Administration and Noxious Colorectal Distension 83
4.2.5 Tissue Collection and Immunohistochemistry 84
4.2.6 Image Acquisition and Analysis 85
4.2.7 Statistical Analyses 88
4.3 Results 91
4.3.1 GBP Impairs Body Weight Recovery After SCI 91
4.3.2 Daily Mean Arterial Pressure and Heart Rate after SCI 92
4.3.3 Spontaneously Occurring Autonomic Dysreflexia 93
4.3.4 Colorectal Distension-Induced Autonomic Dysreflexia 96
4.3.5 Blood Pressure Recovery After Colorectal Distension 97
4.3.6 Effect of Experimental Handling and Restraint on Resting Blood Pressure 99
4.3.7 Sensitivity of the Spontaneous Baroreflex After SCI 99
4.3.8 Effects of SCI and GBP Treatment on Spleen Weight 101
4.3.9 Effects of SCI and GBP Treatment on Synaptic Density 102
4.3.10 Effects of SCI and GBP Treatment on Synaptic Colocalization 104
4.4 Discussion 106

4.4.1 Methodological Considerations 114
4.5 Conclusion 120

5 Chapter 5: Discussion, Future Research Directions and Conclusions
5.1 Conclusions 121
5.2 Discussion 122
5.3 Alternative Approaches and Future Directions 127
5.3.1 Determining the Mechanism by Which GBP Suppresses AD 127
5.3.2 Dissecting the Cellular Signaling Driving Maladaptive Plasticity 132
5.3.3 Homeostatic Plasticity: Does it Play a Role in the Pathogenesis of AD? 133
5.3.4 Further Elucidation of the Neuronal Circuitry Underlying AD 135
5.3.5 Interaction Between AD and the Immune System 138
5.4 Summary of Thesis 140

Appendices
Appendix 1. Abbreviations 142

References 144

Vita 176

LIST OF FIGURES

1.1 Anatomical organization of sympathetic and parasympathetic outflow ... 4
1.2 Autonomic Control of the Cardiovascular System ... 13
1.3 Maladaptive plasticity is associated with the development of AD weeks after spinal cord injury (SCI) ... 18
2.1 Diagrammatic representation of the neuroanatomical circuitry thought to be involved in autonomic dysreflexia triggered by pelvic visceral stimulation ... 45
3.1 Effects of rapamycin treatment on mTOR activity after spinal cord injury ... 58
3.2 Body weight dynamics following prolonged rapamycin treatment and spinal cord injury ... 60
Rapamycin effects on cardiophysiology of naïve and spinal cord injured rats ... 62
3.4 Rapamycin treatment effects on the daily frequency of spontaneously occurring AD events ... 63
3.5 Effects of prolonged rapamycin treatment on mean arterial pressure and heart rate during colorectal distension ... 65
3.6 c-Fos immunostaining in spinal cross sections ... 68
3.7 CGRP staining in spinal cross sections ... 70
4.1 Diagrammatic representation of synaptic quantification scheme ... 89
4.2 Representative thresholding and overlap identification ... 90
4.3 Daily change in body weight after complete spinal cord injury ... 91
4.4 Effects of spinal cord injury and gabapentin treatment on daily cardiophysiology ... 93
4.5 Effects of GBP treatment on the frequency of spontaneously occurring AD after injury ... 95
4.6 Gabapentin reduces blood pressure induced by noxious colorectal distension ... 97
4.7 Gabapentin reduces the time required for MAP to return to baseline after CRD ... 98
4.8 The effect of experimental handling and mild restraint stress on mean arterial pressure prior to weekly colorectal distension ... 99
4.9 Effects of SCI and gabapentin on the gain of the spontaneous baroreflex ... 100
4.10 Effect of injury and GBP treatment on terminal spleen wet weights ... 101
4.11 Density of synaptic puncta following complete spinal cord injury ... 103
4.12 Quantitative colocalization analysis of synaptic immunostaining ... 105
5.1 Proposed ascending pathways relaying visceral stimulation to sympathetic preganglionic neurons ... 136

CHAPTER 1

INTRODUCTION

1.1 Introduction to the Autonomic Nervous System

1.1.1 Evolution and History of the Autonomic Nervous System

The mammalian nervous system is a highly interconnected network of central and peripheral neurons with a multitude of functions that ultimately promote the survival and reproduction of the organism. This system of neurons, local and long-distance projections, and supporting cells enables the animal to respond behaviorally and physiologically to environmental challenges. These responses can be classified as voluntary or involuntary such as voluntary locomotion by an animal escaping a predator by its own volition, or involuntary responses such as an automatic increase in heart rate and blood pressure priming the animal's body for intense physical activity while escaping or fighting the predator. Such involuntary actions are a product of the autonomic nervous system (ANS).

The ANS is a multifaceted regulatory system found in all vertebrates (Nilsson, 1983; Nilsson, 2011) that serves essential bodily functions and maintains physiological homeostasis. As reviewed by Ackerknecht (1974), a vague conceptual understanding of the ANS has been traced as far back as ancient Greece. Galen (A.D. 130-200) described the theory of "sympathy" in reference to the coordinated functions he observed amongst the organs of the viscera (Debru, 1997). This concept, along with our understanding of physiology and neuroanatomy, has been developed and refined throughout the past millennium. The modern descriptions of the ANS started with physiologists Walter Gaskell and John Langley (Ackerknecht, 1974). The term "autonomic nervous system" was first applied over a century ago by Dr. Langley as a means of describing a system that is largely reflexive and self-governed. Prior to Langley (1898), the term "visceral nervous system" was widely used after being introduced by Dr. Gaskell (Gaskell, 1886) to describe the system of fibers

dispersed throughout the visceral organs. However, Langley contended that the term 'visceral nervous system' failed to depict the autonomous functioning and widespread innervation of both visceral and non-visceral tissues (Langley, 1898).

Gaskell and Langley also defined the three divisions of the ANS as still in use today. These are the sympathetic, parasympathetic and enteric nervous systems, the distinction of which was made on the basis of anatomical patterns and differential pharmacological responses in the peripheral ANS. Sympathetic and parasympathetic activity produces antagonistic effects on target tissues, with the actions of one system counterbalancing the other. Activity of the sympathetic nervous system promotes a physiological state of "fight or flight", with increased firing of sympathetic nerves producing increases in heart rate, myocardial contractility, shifting of blood from the viscera towards major skeletal muscles, dilation of the pupils, bronchodilation, sweating of the skin, increased fat and glycogen mobilization, and decreased digestive activity. These actions prepare the organism for high-intensity exercise needed to escape a potential threat.

On the other hand, a shift towards predominantly parasympathetic activity reduces heart rate, facilitates sexual arousal, stimulates digestive activity, and regulates defecation and urination. These functions promote a state of "rest and digest" or "feed and breed" when the animal is in an environment lacking threats or stressful stimuli. The third and last branch of the ANS is the enteric nervous system which is a vast network of neurons dispersed throughout the gastrointestinal system. This system has hundreds of millions of neurons and is sometimes referred to as the body's "second brain" due to its size and complexity. Rather than being intimately integrated with the CNS as the sympathetic and parasympathetic systems, the enteric nervous system functions largely independently and contains its own sensory neurons, local interneurons and efferent neurons controlling smooth muscle and secretory functions (Costa et al., 2000; Furness, 2012; Furness et al., 2014; Rao and Gershon, 2016). While this is a vast and fascinating system with many essential roles, this chapter will

focus on the sympathetic and parasympathetic divisions of the ANS which are critical for understanding cardiovascular control.

1.1.2 Anatomical Organization of the Autonomic Nervous System

The rodent and human ANS is comprised of peripheral effector cells whose activity is modulated by a network of central neurons which integrate and process a variety of inputs. During development, cells and neurons of the peripheral ANS arise from the neural crest and migrate to their final position as their axons grow towards target tissues under the guidance of chemoattractants and growth factors. Meanwhile, precursors of the central autonomic neurons of the brain and spinal cord grow into the neural tube formation along with the rest of the nascent central nervous system (Le Douarin and Smith, 1988; Sieber-Blum, 2000). Collectively, the central nuclei comprising the ANS are known as the central autonomic network (CAN) (Benarroch, 1993; Cersosimo and Benarroch, 2013). As reviewed by Cersosimo and Benarroch (2013), this network includes numerous structures in the forebrain, brainstem and spinal cord, including the insular cortex, anterior cingulate cortex, amygdala, hypothalamus, periaqueductal gray, parabrachial nucleus, nucleus tractus solitarius, rostral and caudal ventrolateral medulla, ventromedial medulla, caudal raphe, medullary reticular formation, intermediolateral cell column and sacral parasympathetic nucleus (Cersosimo and Benarroch, 2013). Primary regions comprising the sympathetic branch include the locus ceruleus, rostral and caudal ventrolateral medulla, serotonergic raphe nuclei of the brainstem and the intermediolateral cell column of the thoracolumbar spinal cord. Major regions involved in the parasympathetic branch include the central nucleus of the amygdala, dorsal motor nucleus of the vagus, nucleus ambiguus, raphe nuclei, periaqueductal gray, the parabrachial nucleus and nuclei within sacral spinal cord segments. In addition, the CAN receives input from regions involved in cognition and emotion, such as projections from the amygdala to the lateral hypothalamus (Lane et al., 2009; LeDoux et al., 1988). Such connections between the limbic

system and regions involved in cognition provide the physical basis for autonomic responses to fearful or stressful situations.

Peripheral outflow of the ANS follows a distinct anatomical organization. The parasympathetic system has a “craniosacral” arrangement, whereby parasympathetic signals flow out of the CNS through cranial nerves and sacral spinal cord segments. In contrast, the sympathetic system has a strict “thoracolumbar” outflow from the thoracic and upper lumbar spinal segments (**Figure 1.1**). Notably, although the craniosacral and thoracolumbar classification of the sympathetic and parasympathetic systems has been used for many decades after being introduced by Langley, some researchers have recently argued based on the similarities in developmental marker expression profiles, that the sacral outflow is sympathetic leaving the cranial nerves as the only conduit for parasympathetic outflow (Espinosa-Medina et al., 2016). This assertion led to a heated debate, with a series of rebuttals supporting the original description of sacral parasympathetic outflow by Langley (Horn, 2018; Janig and Neuhuber, 2017; Neuhuber et al., 2017). Notably, similar efforts to rename the anatomical organization of the ANS have been made previously, with Nilsson suggesting the use of “cranial autonomic” and “spinal autonomic” outflow as a more practical convention that disregards the distinction between sympathetic and parasympathetic outflow (Nilsson, 1983). The persistent discontent with the classification of peripheral ANS outflow exemplifies the challenges of accurately classifying this complex and multifaceted system.

In comparison to the somatic motor system outflow, which generally goes directly from spinal motoneurons to the peripheral target muscles, sympathetic and parasympathetic outflow is comprised of two neurons: a preganglionic neuron in the brain or spinal cord that projects to a peripheral ganglionic neuron, which in turn projects its postganglionic fiber to the final target tissue (**Figure 1.1**). One exception to this pattern is seen in the sympathetic innervation of the adrenal medulla. In this case, the central sympathetic preganglionic neuron sends its axon through the sympathetic ganglia without synapsing until it reaches

the adrenal medulla. For this reason, the secretory adrenal gland is sometimes described as a modified sympathetic ganglia (Ehrlich et al., 1994).

Virtually every peripheral tissue in the body is innervated by the ANS, with a number of organs receiving dual innervation from both sympathetic and parasympathetic nerves. From an evolutionary perspective, the dual-innervation of critical organs such as the heart occurred early in vertebrate evolution and has been retained, perhaps because it gives the organism the advantage of being able to reciprocally regulate sympathetic and parasympathetic activity, providing rapid and finely-tuned responses and adaptations (Burnstock, 1969). A characteristic feature common to the sympathetic and parasympathetic branches is a basal level of ongoing neural activity such that both systems maintain some level of “tone” (Laskey and Polosa, 1988). This arrangement adds an additional level of control; rather than having a unidirectional control ability, the sympathetic and parasympathetic systems can each increase or decrease their firing rate to produce a wider range of activity. The overall balance of sympathetic and parasympathetic tone on a target organ determines its functional state and can shift dramatically in response to physiological disturbances.

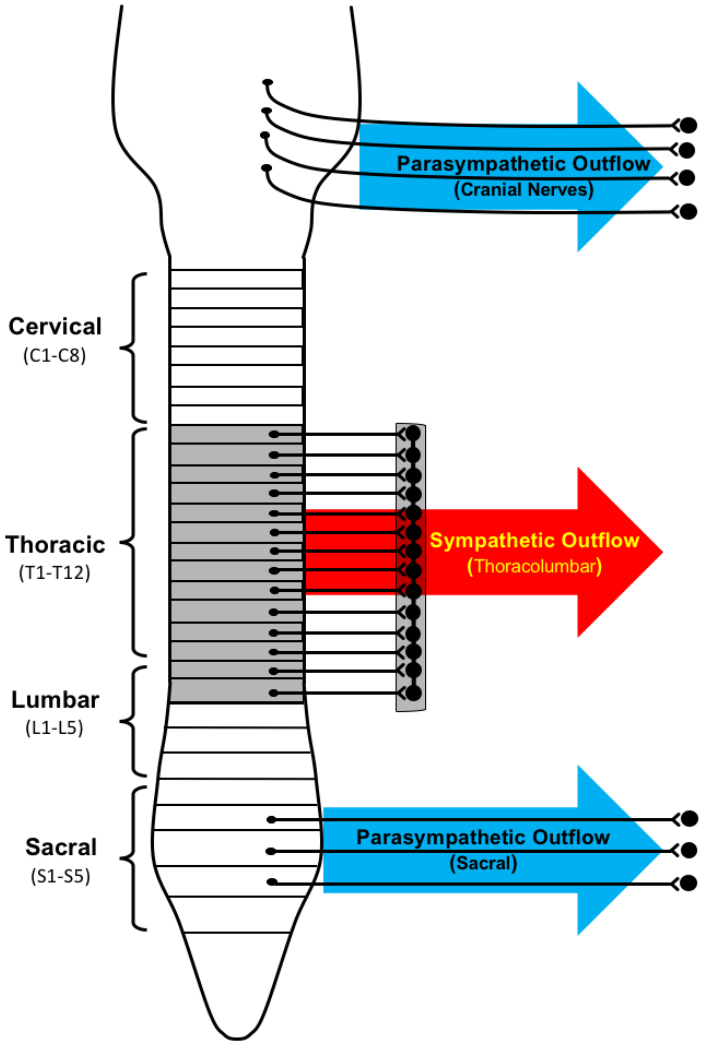

Figure 1.1. Anatomical organization of sympathetic and parasympathetic outflow. Diagrammatic representation of the anatomical organization of the peripheral autonomic nervous system. Sympathetic innervation of peripheral tissues follows a “thoracolumbar” pattern of outflow from central sympathetic preganglionic neurons distributed throughout the T1-L2 spinal segments (shaded grey). In contrast, the parasympathetic nervous system follows a “craniosacral” pattern of outflow from cranial nerves III, VII, IX, and X, as well as sacral spinal segments. Notably, both systems have a similar sequence of neural connections from the final central sympathetic or parasympathetic neurons in the brain or spinal cord, to a peripheral ganglionic neuron which then innervates the target

organs. However, peripheral sympathetic neurons coalesce to form paravertebral and prevertebral ganglia located proximal to the vertebral column whereas peripheral parasympathetic ganglia form more distally and have longer preganglionic projections.

1.1.3 Autonomic Control of the Heart

The mammalian cardiovascular system (CVS) is comprised of the heart and vasculature. This closed-loop system functions to deliver oxygen, nutrients and hormones to all organs while simultaneously removing metabolic wastes. Furthermore, the CVS has auxiliary roles in thermoregulation, fluid balance and immune function (Secomb, 2016). Cardiac muscles contract rhythmically to produce pressure pulses that generate the flow of oxygenated blood throughout an extensive arterial supply. Large elastic arteries, such as the aorta, expand with blood during the systolic phase and subsequently relax to produce a steady flow of blood through smaller downstream blood vessels during diastole, a phenomenon known as the Windkessel effect. After infiltrating and passing through the tissues, the low-pressure venous system collects deoxygenated blood to return to the lungs and heart for re-oxygenation and re-circulation.

Because the level of activity in a muscle or organ can change dramatically during normal behavior, the CVS must be able to rapidly alter the rate, volume and distribution of blood flow to match the metabolic needs of specific regions of the body. To accomplish this, the CVS is modulated through a combination of neural, humoral and local autoregulatory mechanisms which allow for both rapid and long-term adaptations. At the local level of the heart, a set of intrinsic cardiac nerves surrounds the myocardium and comprises an electrical conduction system referred to by some researchers as the heart's "little brain" (Brack, 2015; Wake and Brack, 2016). Notably, this intrinsic network contains a cluster of pacemaking cells in the sinoatrial node which can produce rhythmic contractions even in the absence of extrinsic autonomic control (Sebastian et al., 2013). Experimental autonomic blockade in humans using pharmacological adrenergic and cholinergic blockers results in an intrinsic basal heart rate averaging 100

bpm, indicating that the human heart is primarily under parasympathetic control at rest when the heart rate is typically 70 bpm (Jose and Collison, 1970; Jose and Taylor, 1969; Marcus et al., 1990).

Although the heart's intrinsic electrical system can produce a stable cardiac rhythm, it does not have the ability to independently adjust output to match the highly dynamic metabolic needs of the body. Instead, the heart is under constant autonomic influence via dual innervation by sympathetic and parasympathetic nerves. Parasympathetic and sympathetic modulation of the heart must be appropriately balanced to match the cardiac output with the metabolic demands of the entire body. Cardiac output is a function of heart rate (HR) and stroke volume:

$$Cardic\ Output = Heart\ Rate\ x\ Sroke\ Volume$$

This formula demonstrates that cardiac output can be increased by elevating the heart rate or the volume of blood ejected per beat. As described below, both of these parameters can be reciprocally altered by sympathetic and parasympathetic stimulation.

Parasympathetic supply to the heart courses through efferent fibers of the vagus nerve (cranial nerve X; **Figure 1.2**), with origins in the nucleus ambiguus and dorsal motor nucleus of the vagus located in the medulla oblongata (Ciriello and Calaresu, 1982; Jamali et al., 2017). A relatively minor proportion of cardiac parasympathetic innervation also runs through the laryngeal nerve, which itself is a bifurcation of the vagus nerve complex (Armour et al., 1997). Dense parasympathetic innervation from the vagus nerve is observed in the cardiac atria and, although there is a common misconception that the ventricles lack parasympathetic innervation (Coote, 2013), a sparse amount of vagal fibers have indeed been observed in the ventricles (Higgins et al., 1973; Loffelholz and Pappano, 1985).

Increased activity of vagal parasympathetic fibers produces negative chronotropic effects (decreased heart rate) and, to a lesser degree, negative inotropic (decreased contractility) effects (Machhada et al., 2016). Upon firing, parasympathetic nerve terminals release acetylcholine (ACh) which binds to

muscarinic acetylcholine receptors expressed on cardiomyocytes and cardiac pacemaker cells in the sinoatrial (SA) and atrioventricular (AV) nodes (Dhein et al., 2001). Muscarinic ACh receptors are members of the g-protein coupled receptor (GPCR) family, which is a large family of metabotropic receptors featuring a characteristic seven-pass transmembrane domain. There are 5 subtypes of muscarinic ACh receptors(M_1-M_5), of which the M_2 is most important for cardiac functioning. Upon binding of ACh released from parasympathetic fibers, M_2 receptors on the heart signal through the G_i second messenger cascade to open g protein-coupled inwardly rectifying potassium channels (GIRKs). The subsequent increase in inward potassium current through GIRKs results in hyperpolarization that promotes an increased inter-beat interval (decreased heart rate) and decreased force of contraction (Hartzell, 1988; Harvey and Belevych, 2003; Harvey and Hume, 1989; Lanzafame et al., 2003; Nishimaru et al., 2000).

In contrast to the vagal parasympathetic supply of the heart, which projects directly from the brainstem to the heart, cardiac sympathetic innervation first runs through the spinal cord. All sympathetic outflow originates from sympathetic preganglionic neurons (SPN) dispersed throughout the thoracic and upper lumbar spinal cord. As discussed by Deuchars and Lall (2015), a number of tracing and labeling methods have been employed to visual the SPN including visualization of sympathectomy-induced chromatolysis, retrograde tracing, and immunolabeling with choline acetyltransferase (ChAT). The SPN are distributed into four spinal nuclei: the intermediolateral cell column (IML), intercalated nucleus, central autonomic region and thoracolumbalis pars funicularis (Deuchars and Lall, 2015). Most attention is typically given to the IML, given that approximately 75% of all SPN are concentrated in this nucleus. The IML is located in the lateral horns of the thoracolumbar cord, forming bilateral clusters with a “ladder-like” architecture among segments (Deuchars and Lall, 2015; Markham and Vaughn, 1990; Rando et al., 1981). Cardiac SPN that control the heart are distributed throughout the T1-T6 spinal segments (Coote, 1988; Coote and Chauhan, 2016). As with all SPN, the cardiac SPN exit the cord through the

ventral root system to synapse with sympathetic ganglia in the periphery. These ganglia contain the final effector neurons that send postganglionic axons to innervate the target tissues. Greater than 90% of the post-ganglionic fibers innervating the heart arise from the middle and inferior/stellate cervical ganglia, with the remaining postganglionic fibers originating from the superior cervical ganglia and the 4th through 6th thoracic sympathetic ganglia (Pardini et al., 1989, 1990). In addition to direct sympathetic innervation of the heart, the sympathetic system also alters cardiovascular function through circulating catecholamines released from the adrenal medulla (Adameova et al., 2009). This is another notable distinction between sympathetic and parasympathetic control of the heart, as parasympathetic modulation is restricted to direct innervation.

The terminals of cardiac sympathetic fibers primarily release norepinephrine, which is a catecholamine that binds to and activates adrenergic receptors (AR) throughout the heart. The ARs are divided into α-AR and β-AR subtypes and, similar to the muscarinic ACh receptors, are members of the GPCR family. While the heart expresses both α-ARs and β-ARs, approximately 90% are β-ARs (O'Connell et al., 2014). The β-ARs include β_1, β_2 and the β_3-ARs, of which the β_1-ARs are the most widely expressed accounting for roughly 80% of β-ARs (O'Connell et al., 2014; Post et al., 1999). When activated by norepinephrine released from sympathetic terminals, or circulating epinephrine released from chromaffin cells of the adrenal medulla, the ARs have positive chronotropic, inotropic and lusitropic (rate of cardiac relaxation) actions. These effects are mediated by an array of intracellular changes resulting from g-protein signaling initiated by ligand binding. For example, AR activation increases intracellular cAMP and PKA activity leading to enhanced phosphorylation/activation of calcium channels, and contractile proteins. Notably, phospholamban is an inhibitor of the cardiac sarcoplasmic reticulum Ca^{++} ATPase (SERCA) pump in its non-phosphorylated state. Upon phosphorylation, the SERCA becomes disinhibited which allows for more rapid calcium sequestration that is responsible for the positive lusitropic effect of increased sympathetic tone (Hagemann and Xiao, 2002).

1.1.4 Autonomic Control of the Vascular System

The vascular system is a large and dynamic collection of blood vessels which bifurcates in an iterative fashion, with each subsequent iteration decreasing in diameter to form the microcirculation serving every organ. Far from a passive set of tubes, this system is highly dynamic and responsive to the needs of a given tissue. Blood vessels are critical for the delivery of oxygen, nutrients and hormones as well as the removal of metabolic wastes such as carbon dioxide. Moreover, the vascular system plays a major role in determining blood pressure and cardiac preload/afterload. The total peripheral resistance (TPR) to blood flow is a major factor in determining arterial pressure, with increases in TPR resulting in higher blood pressure. TPR is highly responsive to changes in the diameter of blood vessels. In fact, as described by Poiseuille's law, the relationship between TPR and vessel diameter is linked to the fourth power, demonstrating the powerful relationship between vessel diameter and blood pressure (Thomas, 2011).

Two systems contribute to the regulation of blood vessel diameter: 1) local autoregulation of regional blood flow and 2) autonomic-mediated control through direct neural innervation and indirect circulatory factors released from the adrenal medulla. Autoregulation occurs most notably in the critical renal, cardiac and cerebral vascular beds, and occurs through local monitoring of the levels of oxygen and metabolic wastes which indicate whether an increase or decrease of blood flow/vessel diameter is necessary. In addition to localized autoregulation, vascular smooth muscles of critical blood vessels throughout the body also receives autonomic. This allows for the rapid neural control of peripheral resistance and blood pressure, as well as the ability to allocate cardiac output to match the metabolic demands of specific tissues. Postganglionic sympathetic fibers arising from cardiovascular SPN innervate the smooth muscle of arteries, veins and large-diameter arterioles. Upon firing, norepinephrine released from these fibers activates α-ARs in the smooth muscle resulting in increased calcium release and contraction of the smooth muscle. In this fashion, increased sympathetic tone decreases vessel diameter to increase total peripheral

resistance and blood pressure. Catecholamines released from the adrenal gland produce similar vasoconstriction, however, because these effects are more widespread due to their release into the circulation (Guyton and Hall, 2006).

While much attention is paid to the sympathetic innervation of the vasculature, less is generally given to parasympathetic innervation. Indeed, sympathetic and parasympathetic systems are both involved in vascular regulation (Kaji et al., 1991; Ruocco et al., 2002; Sheng and Zhu, 2018). Notably, however, the parasympathetic vascular supply is limited to a few particular vascular beds in the cutaneous circulation, salivary glands and genitalia (Amiya et al., 2014; Emmelin, 1987; Ruocco et al., 2002; Sheng and Zhu, 2018). In comparison, the sympathetic innervation of arterial and venous circulation is extensive and plays a more critical role in regulating blood pressure and blood flow (Ruffolo et al., 1991; Sheng and Zhu, 2018).

Examination of adrenoceptor expression profiles reveal tissue-specific distribution patterns, allowing for the selective control of regional blood vessels in response to globally circulating catecholamines. Large coronary arteries, for example, express both α-AR and β-AR, whereas small coronary vessels only express β-AR (Bohr, 1967). Splanchnic and skeletal muscle vascular beds in humans express predominantly β-ARs, dilating in response to epinephrine. In contrast, the vessels of the renal and skin circulatory beds express predominantly α-ARs and constrict in response to epinephrine. With this pattern, epinephrine released into the circulation from adrenal chromaffin cells would tend to shunt blood away from the skin and kidneys towards skeletal muscle to increase muscle blood flow during the fight-or-flight response (Guimaraes and Moura, 2001). Sympathetic innervation is also observed in the cerebral vasculature, although the degree of innervation varies considerably across species. Whereas some species have a dense sympathetic cerebrovascular innervation, humans have a relatively low density of sympathetic nerve bundles surrounding cerebral arteries which is correlated with weak changes in cerebrovascular diameter upon sympathetic nerve stimulation (Bevan et al., 1998).

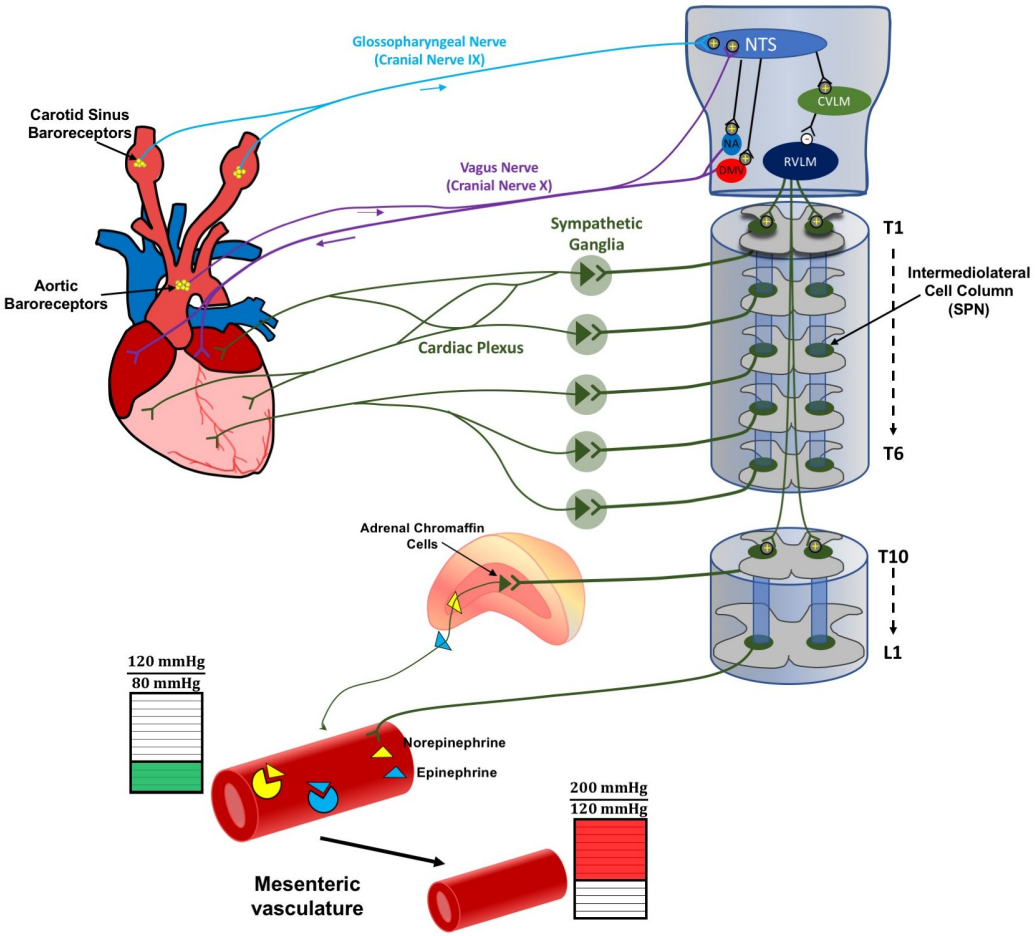

Figure 1.2. Autonomic Control of the Cardiovascular System. Dual sympathetic and parasympathetic innervation of the heart provides rapid neuronal control of cardiac function. While sympathetic cardiac innervation is mediated through sympathetic post-ganglionic fibers, parasympathetic supply comes directly from the vagus nerve (cranial nerve X). Cardiac sympathetic preganglionic neurons (SPN) are located primarily in the intermediolateral cell column of the first through sixth thoracic (T1-T6) spinal segments and project to sympathetic ganglia to form the cardiac plexus. These SPNs are stimulated by supraspinal regions including the rostral ventrolateral medulla (RVLM), which in turn receives inhibitory inputs from the caudal ventrolateral medulla (CVLM). The CVLM receives excitatory drive from neurons within the nucleus tractus solitarius (NTS) which are, in turn, stimulated by pressure sensitive baro-afferents located in the carotid sinus and aortic arch. With this arrangement, increased blood pressure results in inhibition of the RVLM and reduced vasomotor tone as part of

the baroreflex. SPN of the thoracolumbar cord innervate the adrenal medulla, stimulating the release of catecholamines into the circulation, as well as the extensive mesenteric vasculature to modify vascular diameter and total peripheral resistance.

1.2 Introduction and Overview of Spinal Cord Injury

1.2.1 Etiology and Prevalence of Spinal Cord Injury

Traumatic spinal cord injury (SCI) can wreak havoc on multiple body systems and functions, often resulting in the loss of motor and sensory functions as well as the development of neuropathic pain, irregular cardiovascular control, and disrupted autonomic function. The primary causes of traumatic SCI are automobile accidents, sports injuries, accidental falls, acts of violence and work-related accidents (Lee et al., 2014a). The worldwide incidence of traumatic injury to the spinal vertebral column is estimated at 10.5 patients per 100,000 individuals, with over 750,000 new cases each year. 30- 40% of these cases also involve SCI, defined by damage to the cord tissue itself (Kumar et al., 2018). Males are disproportionately affected with the male:female ratio ranging between approximately 3:1 globally (Kumar et al., 2018) to as high as 7:1 regionally in Brazil (Santos et al., 2009). There is indication that there is an increase in SCI among older individuals and an increase in the relative number of new injuries resulting in high-level tetraplegia (McCaughey et al., 2016). These trends are speculated to further increase an already significant financial burden of the lifetime costs of medical care for an individual with SCI, which can accumulate into several millions of dollars over a lifetime (McCaughey et al., 2016).

Based on current (2018) data from the National Spinal Cord Injury Statistical Center, the largest portion (47%) of new SCI cases since 2015 involves damage to the cervical spinal segment resulting in incomplete tetraplegia. The mechanisms of the primary injury are variable, ranging from complete cord transection to contusion or compression injury caused by fractured or dislocated vertebrae. The majority of cases involve contusion or compression

injury, resulting in a large degree of heterogeneity in functional deficits among the SCI population (Iencean, 2003).

While the primary mechanical insult is virtually unavoidable due to the inadvertent nature of SCI, secondary damage processes occurring over the hours and weeks after injury are potentially targetable processes that are the focus of much SCI research (Orr and Gensel, 2017). In the immediate aftermath of injury, a number of toxic interactions occur related to the release of free radicals, excitotoxic damage, and calcium overload. The respiratory capacity of mitochondria is greatly diminished, leading to inadequate energy production and additional apoptotic cell death (Sullivan et al., 2007). In the days and weeks after injury, neuroinflammatory processes occur, some of which are beneficial for functional recovery but some of which contribute to irreversible tissue loss (reviewed in Gensel and Zhang, 2015). At the level of neuronal networks, the loss of descending innervation promotes undirected compensatory fiber sprouting and synaptic remodeling in an uncoordinated and abnormal fashion, resulting in aberrant connectivity contributing to neuropathic pain, spasticity and cardiovascular dysfunction (Beauparlant et al., 2013; Brown and Weaver, 2012).

1.2.2 Effects of Spinal Cord Injury on the Autonomic Nervous System

The spinal cord functions both as a highway connecting the brain with the periphery as well as an independent control center capable of integrating numerous inputs and mediating reflex-level autonomic responses. While sensorimotor detriments are the most outwardly apparent effect of SCI, there can also be a plethora of cardiovascular and autonomic disruptions. Notably, the efferent sympathetic supply and sacral portion of the parasympathetic innervation flows out through the spinal cord (**Figure1.1**). Accordingly, damage to the cord often results in disrupted communication between supraspinal control centers and preganglionic neurons of the cord, which contributes to irregular autonomic and cardiovascular control in SCI (Weaver et al., 2012). Importantly, cardiovascular and autonomic dysfuntions are a major impact of SCI that present considerable hindrances to quality of life for those living with SCI (Anderson,

2004), demonstrating the clinical significance of developing therapeutic strategies to treat such dysfunction.

Arguably the most insidious manifestation of disrupted cardiovascular control is autonomic dysreflexia (AD), defined as abnormal and potentially harmful surges in blood pressure typically in response to noxious afferent stimuli below the lesion triggering unrestrained sympathetic reflexes. The earliest descriptions of AD were by two wartime doctors, Henry Head and George Riddoch, who observed “mass reflex” activity of sympathetic outflow in a subset of patients with SCI (Feustel, 1976; Guttmann and Whitteridge, 1947). Decades later, this phenomena came to be understood as autonomic hyperreflexia (Feustel, 1976) and today is referred to as AD (Karlsson, 1999). As discussed in depth in **Chapter 2**, AD develops in many patients with injury to the sixth thoracic segment or higher and presents a considerable health concern and detriment to a patient’s quality of life, making this an important topic of SCI research.

1.3 Central Hypothesis of Dissertation

A number of mechanisms are thought to contribute to the development of AD, including maladaptive sprouting of primary afferent fibers and propriospinal relay neurons (**Figure 1.3**). Previous experiments from our lab have demonstrated that the degree of sprouting correlates with the severity of AD, indicating maladaptive sprouting as a targetable process to modulate the development of AD (Cameron et al., 2006; Hou et al., 2009). Therefore, the overall hypothesis tested in this dissertation is that pharmacological targeting of cellular processes thought to underlie maladaptive plasticity can prophylactically block the development of AD.

First, the drug rapamycin (RAP) was administered in rats using a well-established T4-transection SCI model widely used for experimental investigation of AD. RAP is an FDA-approved immunosuppressant drug that inhibits the mammalian target of rapamycin (mTOR) pathway. Recently, the mTOR signaling complex has gained much interest in the field of neuroscience for its purported role in functional and structural plasticity. As presented in **Chapter 3**, we first

tested the hypothesis that chronic RAP treatment after SCI can suppress maladaptive plasticity of primary afferents activating propriospinal neurons, and the development of AD. Next, the drug gabapentin (GBP) was investigated for its potential to prevent aberrant synaptogenesis believed to coincide with maladaptive sprouting. GBP is a well-established drug developed decades ago as an analogue of γ-aminobutyric acid (GABA) and initially intended to treat epilepsy and neuropathic pain. Previous studies from our lab (Rabchevsky et al., 2011; Rabchevsky et al., 2012) showed that acute treatment with GBP attenuates the severity of AD and spasticity in SCI rats. In lieu of reports suggesting that prolonged GBP treatment can suppress excitatory synaptogenesis in the brain and spinal cord (Crosby et al., 2015; Yu et al., 2018), we administered GBP continuously (every 6 hours) after SCI to determine if prolonged GBP treatment can mitigate the development of AD by suppressing aberrant synaptogenesis believed to contribute to AD pathophysiology (**Chapter 4**). Cardiophysiological and histological analyses were conducted in both studies to determine if these drugs present clinically viable approaches in the prophylactic prevention of AD development.

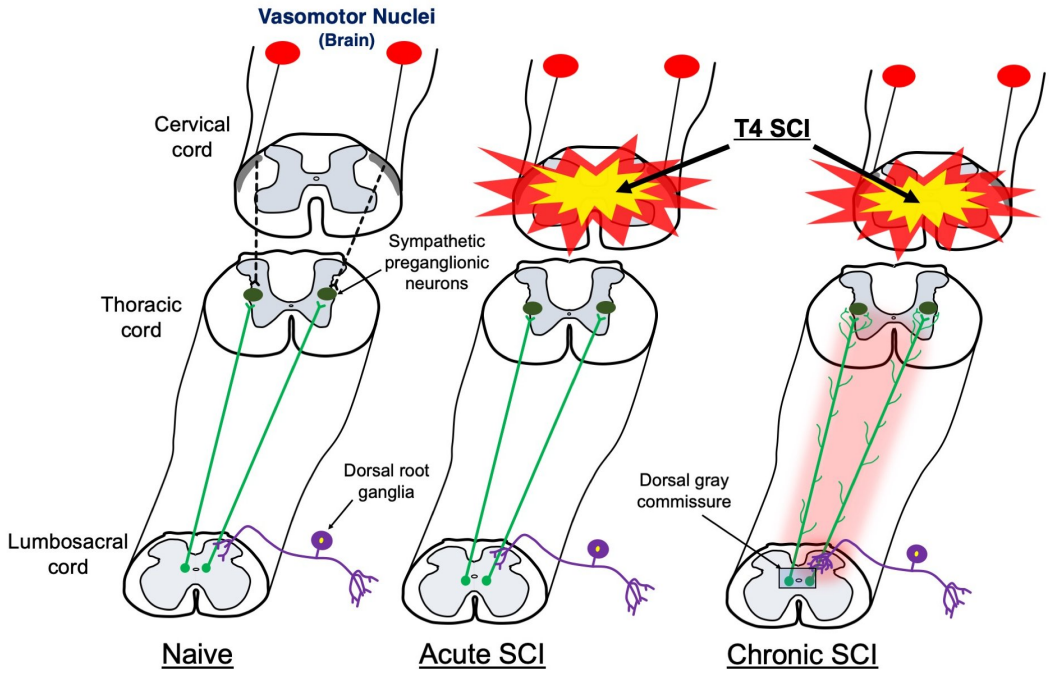

Figure 1.3. Maladaptive plasticity is associated with the development of AD weeks after spinal cord injury (SCI). In the uninjured Naïve rat spinal cord (left), sympathetic preganglionic neurons (SPN; dark green) distributed throughout the intermediolateral cell column of the thoracic cord receive inputs from descending vasomotor control centers in the brain, as well as from ascending propriospinal neurons (light green) which may be activated by primary afferents (purple). In the acute phase following high-thoracic SCI (middle), descending fibers are severed leaving the caudal SPN partially denervated. The resultant segregation of SPN from supraspinal control allows sympathetic reflexes to occur unopposed. In the chronic stage of SCI (right), sprouting is observed in the central projections of c-fiber afferents and ascending propriospinal neurons projecting rostrally towards the SPN. This maladaptive plasticity is associated with the development of AD and may present a clinically viable target for the treatment or prophylactic prevention of this syndrome.

Copyright © Khalid C. Eldahan 2019

CHAPTER 2

Autonomic Dysreflexia After Spinal Cord Injury: Systemic Pathophysiology and Methods of Management

2.1 Introduction to autonomic dysreflexia (AD)

In addition to motor and sensory deficits, traumatic spinal cord injury (SCI) causes a constellation of interrelated autonomic and cardiovascular abnormalities. Cardiovascular complications secondary to SCI are among the leading causes of mortality and morbidity in this population, underscoring the necessity to understand and properly manage resultant comorbidities (Cragg et al., 2013; Garshick et al., 2005; Myers et al., 2007; Sabre et al., 2013). In humans, SCI at or above the sixth thoracic (T6) spinal cord segment often results in the development of a potentially life-threatening syndrome called autonomic dysreflexia (AD). AD is clinically defined as acute hypertension generated by unmodulated sympathetic reflexes below the injury level that is often accompanied by baroreceptor-mediated bradycardia, which provides short-term control of blood pressure (Karlsson, 1999). In response to hypertension, the baroreflex system normally lowers blood pressure by reducing heart rate and decreasing activity of vasoconstrictor sympathetic preganglionic neurons (SPN) located throughout the thoracolumbar spinal cord that regulate peripheral vascular resistance. However, while vagal parasympathetic innervation of the heart remains intact after SCI, the disruption of descending vasomotor pathways to SPN produces an incomplete compensatory decrease in peripheral vascular resistance so that hypertension persists until the triggering stimulus is removed.

Typically, AD is precipitated by noxious visceral or somatic stimulation below the level of injury that activates a massive sympathetic reflex causing widespread vasoconstriction. While the most common triggers are over-distension of the bowel or bladder (Canon et al., 2015; Lindan et al., 1980; Snow et al., 1978), other noxious stimuli including skin lacerations, ingrown toenails, pressure sores, tight clothing and certain medical procedures such as bladder catheterization and cystometry are also reported to cause AD (reviewed in

Karlsson, 1999). During an episode of AD, arterial blood pressure can reach devastating levels, with systolic values as high as 325 mmHg (McBride et al., 2003), exemplifying that AD is a hypertensive crisis that requires immediate medical attention (Muzumdar, 1982; Showkathali and Antionios, 2007; Verghese, 1989). Severe cases that do not receive rapid and appropriate treatment can have serious consequences such as hypertensive encephalopathy, stroke, cardiac arrest, seizure and even death (Bjelakovic et al., 2014; Colachis and Clinchot, 1997; Eltorai et al., 1992; Fausel and Paski, 2014; Jain et al., 2013; Valles et al., 2005). Bouts of AD can arise multiple times daily due to the noxious yet unperceived afferent stimulation produced by normal, intermittent filling of the bladder and bowels (Fougere et al., 2016a; Hubli et al., 2015; Popok et al., 2016). In light of this, it is perhaps not surprising that eliminating AD is one of the highest priorities of the SCI population, based on a large national survey (Anderson, 2004) which reported that both quadriplegics and paraplegics prioritize the recovery of bowel/bladder function and elimination of AD over regaining walking movements, highlighting the need for research strategies to mitigate the development of AD altogether.

This chapter provides a clinical description of AD along with its pharmacological management, and discuss the underlying pathophysiological changes that contribute to such dangerous, episodic hypertension after high-level SCI. We further describe recent studies revealing body-wide disturbances that result from chronic recurring episodes of AD, including vascular, cardiac and immunological dysfunctions. Contemporary research strategies will be considered to understand more comprehensively the underlying mechanisms, the full physiological impact of this syndrome that typically occurs multiple times daily, and potential therapeutic approaches to abrogate its development.

2.2 Clinical description of autonomic dysreflexia

2.2.1 Who is at risk of developing AD?

The T6 spinal segment is critical to the development of AD (Lindan et al., 1980; Mathias and Frankel, 1988; Snow et al., 1978), as damage at or above this

level interrupts descending modulation of the thoracolumbar SPN that regulate vasomotor tone, notably in the extensive splanchnic vascular bed (Blackmer, 2003; Gao et al., 2002). These vessels are innervated by the splanchnic nerves arising from the T5-T12 levels (see (Loukas et al., 2010) and receive approximately 25% of the cardiac output (Greenway and Lister, 1974; Rowell, 1990), which can have a large influence on total peripheral resistance and blood pressure. There are, however, uncommon reports of AD occurring after lesions below T6 but the magnitude of hypertension and changes in heart rate tend to be relatively mild since some degree of control over splanchnic sympathetic outflow remains intact (Moeller and Scheinberg, 1973).

Not all individuals with SCI at or above the T6 level develop AD, with the prevalence reported between 48% and 91% (Curt et al., 1997; Lindan et al., 1980; Snow et al., 1978). This discrepancy is likely attributed to differences in the completeness of SCI, time elapsed since injury, and differences in the criteria used to confirm the presence of AD used among studies (Furusawa et al., 2011). Indeed, the clinical definition of AD is somewhat inconsistent (see section 2.2). Interestingly, AD has been documented in cases of non-traumatic abnormalities of the spinal cord such as intramedullary astrocytoma (Furlan et al., 2003) and multiple sclerosis (Kulcu et al., 2009), indicating that disruption of descending vasomotor pathways in any manner may contribute to the development of this syndrome.

2.2.2 Characteristic features of AD

The magnitude of hypertension required to be considered AD varies across studies. Snow et al. (1978) classified AD in adults as an increase of 40 mmHg systolic blood pressure whereas Popok et al. (2016) defined AD as an increase of 20 mmHg systolic blood pressure. Others (Lindan et al., 1980) diagnosed AD as a sudden rise in both systolic and diastolic blood pressure of any magnitude. Veteran's Affairs guidelines recommend that AD in adults is considered following abrupt elevation in systolic blood pressure of 20-40 mmHg above baseline, whereas in pediatric SCI an increase of 15-20 mmHg systolic

pressure warrants consideration (Canon et al., 2015; Consortium for Spinal Cord, 2002).

In addition to elevated blood pressure, individuals with an acute episode of AD can experience a diverse set of symptoms including debilitating headache, sweating, flushing of the skin above the injury level, piloerection, stuffy nose, blurred vision and anxiety (Karlsson, 1999). While these symptoms are not simultaneously present in all cases, headache and sweating above the lesion occurs 88% of the time (Lindan et al., 1980). Although the classical definition of AD is acute hypertension coincident with bradycardia (Erickson, 1980; Guttmann and Whitteridge, 1947; Trop and Bennett, 1991), the importance of heart rate in the diagnosis of AD is a matter of controversy. Lindan et al. (1980) reported an equal incidence of bradycardia and tachycardia (increase in heart rate) in documented cases of AD, whereas others report that tachycardia is more common (Hickey et al., 2004; Kewalramani, 1980; Scott and Morrow, 1978). Whether an episode of AD is concomitant with an increase or decrease in heart rate may depend on the injury level (Collins et al., 2006; Karlsson, 1999; Krassioukov et al., 2003). As suggested by Karlsson (1999), activation of sympathetic circuits in the spinal cord below a cervical injury may propagate rostrally towards cardiac-innervating SPN (i.e., T1-T4), explaining why tachycardia is frequently observed during AD. However, the correlation between injury level and the direction of heart rate change during episodes of AD has not been formally investigated.

2.2.3 Temporal development of AD after SCI

AD most often presents in the chronic phase of SCI, with a majority of cases first occurring 3-6 months after injury in humans (Lindan et al., 1980). While it may also occur in earlier stages of injury, the incidence of early AD is relatively low, with only 5.7% of individuals with SCI above T6 having clinically documented AD within the first month post-injury (Krassioukov et al., 2003). Though uncommon, the manifestation of AD in the early stage of injury is significant considering that treatment of acute, high-level SCI often includes

pressor agents to help combat the profound hypotension associated with such injuries (reviewed in Ploumis et al., 2010). In cases of acute AD occurring within days of injury, systolic blood pressure as high as 210 mmHg has been reported (Silver, 2000), suggesting that concurrent vasopressor support may compound damage during episodic hypertension.

In experimental SCI, the development of telemetric monitoring techniques, along with the advent of computer algorithms capable of processing large amounts of hemodynamic data, have allowed for detailed analysis of the temporal development of AD in conscious animals (Laird et al., 2006; Mayorov et al., 2001; Rabchevsky et al., 2012; West et al., 2015). In both rats and mice with high-thoracic SCI, spontaneous AD triggered by naturally occurring stimuli emerges in a biphasic pattern with a transient surge of events occurring within the first week, followed by a gradual rise in frequency beginning around 2-weeks post-injury (Rabchevsky et al., 2012; West et al., 2015; Zhang et al., 2013). Moreover, the magnitude of change in systolic pressure during these events increases over time (West et al., 2015). These observations generally correspond to the development of AD in humans, where the initial disruption to descending vasomotor pathways allows for early AD (Krassioukov et al., 2003) before maladaptive changes in viscerosympathetic circuitry associated with more frequent and severe cases occur during the more chronic stages (West et al., 2015). Recent capabilities of screening ambulatory blood pressure recordings for daily AD events in humans (Hubli and Krassioukov, 2014; Popok et al., 2016) will enable detailed analyses of temporal progression of this syndrome in humans, as well as the efficacy of drugs to reduce the frequency or magnitude of recurrent AD.

2.3 Mechanisms contributing to AD

2.3.1 Loss of supraspinal control

Within the intact nervous system, supraspinal vasomotor neurons residing in the paraventricular nucleus, rostral ventrolateral medulla, rostral ventromedial medulla, caudal raphe nuclei and A5 cell group (Calaresu and Yardley, 1988;

Chalmers et al., 1994; Hosoya et al., 1991; Jansen et al., 1995; Llewellyn-Smith, 2009; Strack et al., 1989; Sved et al., 2001) send projections to the intermediolateral cell column (IML), which is comprised of spinal nuclei containing sympathetic preganglionic neurons (SPN) that extends throughout the T1-L2 segments (Pyner and Coote, 1994; Tang et al., 1995; Zagon and Smith, 1993). These supraspinal neurons modulate the tonic firing of SPN which, in turn, send projections to the peripheral sympathetic chain ganglia or directly to the adrenal medulla (**Figure 2.1**). The sympathetic ganglia act as the final sympathetic effector cells and innervate blood vessels throughout the body, whereas stimulation of the adrenal medulla secretes epinephrine and norepinephrine (NE) into the circulation. Together, this provides both direct and indirect control of blood vessel diameter and peripheral resistance to facilitate hemodynamic homeostasis (reviewed in Thomas, 2011).

After high-level SCI, the descending autonomic pathways responsible for supraspinal modulation of SPN become interrupted, reducing sympathetic tone below the injury (Stjernberg et al., 1986) and leaving SPN under the control of spinal influences alone. In the initial “spinal shock” phase of injury, which can last for weeks in humans (Ditunno et al., 2004), this loss of descending control manifests as significantly reduced blood pressure and depression of sympathetic reflexes (Frankel et al., 1972). Over time, however, plasticity of SPN and reorganization of spinal circuitry create a hyper-excitable state that contributes to the aberrant reflex activation of SPN in response to afferent stimulation (**Figure 2.1**) (Krassioukov et al., 2002; Llewellyn-Smith and Weaver, 2001; Rabchevsky, 2006). Because of the interruption to descending modulatory pathways, which would normally inhibit the SPN during hypertension via the baroreflex (Guyenet and Cabot, 1981), AD persists until the stimulus is withdrawn.

2.3.2 Synaptic reorganization of sympathetic preganglionic neurons (SPN)

The damage to descending vasomotor pathways caused by SCI leaves many SPN partially denervated, causing a number of histological and functional changes in these neurons in both the human and rat (Krassioukov et al., 1999;

Krassioukov and Weaver, 1995, 1996). Whereas SPN activity is normally regulated by a confluence of supraspinal and intraspinal inputs, their ongoing activity after complete SCI depends solely on the influence of spinal sympathetic interneurons (Schramm, 2006). Spinally derived sources of input to SPN include interneurons residing in laminae V, VII and X (Cabot et al., 1994; Cano et al., 2001; Clarke et al., 1998; Deuchars et al., 2001; Deuchars and Lall, 2015; Joshi et al., 1995; Tang et al., 2004a). While there are no direct synaptic inputs to SPN from primary afferents, it is thought that sensory neurons can influence the SPN via such spinal interneurons (Laskey and Polosa, 1988; Schramm, 2006). The integration of supraspinal and intraspinal inputs on SPN is complex and involves both monosynaptic and polysynaptic pathways (reviewed in Deuchars and Lall (2015).

After experimental T4 spinal cord transection in adult rats, profound morphological changes occur to SPN within the IML below the lesion. Within 3 days of injury, the dendritic length and diameter of SPN soma decrease dramatically in response to the degeneration of terminals with supraspinal origins (Llewellyn-Smith and Weaver, 2001). By two-weeks, however, the somatic size and dendritic arbor of SPN appears normal again (Krassioukov and Weaver, 1996; Krenz and Weaver, 1998a). These dynamic changes in gross SPN morphology correspond temporally with the evolution of cardiovascular dysfunction in rats with high-level SCI, where pronounced resting hypotension occurs in the first days, followed by a gradual increase in basal blood pressure and the appearance of recurrent AD by two weeks post-injury (Laird et al., 2006; Mayorov et al., 2001; Rabchevsky et al., 2012; West et al., 2015).

While atrophied SPN regain a normal morphology in the weeks after injury, experimental evidence suggests that a radical reorganization of synaptic inputs controlling their activity occurs. Weaver et al. (1997) demonstrated altered expression patterns of GAP-43 (growth associated protein-43), a marker of reactive sprouting, in both mature axons and growth cones in close apposition to SPN caudal to a complete mid-thoracic transection weeks after injury. Because of the complete transection model used and absence of degenerating

supraspinal axons in the IML after 7 days, the source of these GAP-43 immunoreactive axons was limited to spinal neurons below the injury, suggesting reorganization of intraspinal sympathetic circuits that may contribute to the exaggerated sympathetic reflex during an AD event. Llewellyn-Smith and Weaver (2001) also observed a switch in the ratio of synapses on SPN containing glutamate or γ-aminobutyric acid (GABA), indicating a shift in the balance of excitatory and inhibitory influences, respectively. Specifically, T4-transection caused a decrease in the percentage of glutamatergic inputs versus an increase in the percentage of GABAergic inputs on SPN in the IML at the T8 spinal level after two-weeks, implying a predominantly inhibitory synaptic integration. While this observation is consistent with the resting hypotension and reduced sympathetic outflow seen after SCI, how this relates to the intense sympathetic outbursts that occur in response to noxious visceral stimulation is uncertain. Recent work by Huang et al. (2016) indicates that complete high-thoracic (T2) spinal cord transection in rats causes GABA neurotransmission to convert from an inhibitory to excitatory role in nociceptive circuits. While the influence of SCI on GABAergic regulation of SPNs was beyond the scope of this work, it provides evidence that GABAergic inputs onto SPN may provide excitatory drive after SCI (Rabchevsky, 2006).

An alternative explanation may be that glutamatergic synapses on SPN are the predominate input recruited by noxious visceral stimulation. It has been documented that glutamatergic signaling through both NMDA and AMPA receptors is important for the initiation of AD in response to noxious colorectal distension (CRD) (Maiorov et al., 1997). Ueno et al. (2016) recently demonstrated that chemogenetic silencing of Vglut2^{+} (vesicular glutamate transporter 2) interneurons after T3 SCI suppressed anti-inflammatory sympathetic reflexes related to AD (see section 5.2). This is further supported by studies testing the anti-epileptic and neuropathic pain medication gabapentin (GBP) as an experimental treatment for AD (Rabchevsky et al., 2011). GBP is known to inhibit pre-synaptic glutamate release by binding to the $\alpha_2\delta_1$ subunit of voltage-gated calcium channels (Coderre et al., 2005, 2007; Gee et al., 1996;

Shimoyama et al., 2000) and has been shown to reduce both the magnitude and frequency of AD in rats with complete T4-transection, specifically after acute but not chronic administration (Rabchevsky et al., 2011; Rabchevsky et al., 2012). Notably, however, the site(s) of action and mechanism(s) through which GBP mitigates AD remains uncertain. It is feasible that GBP acts by reducing glutamatergic transmission at the level of both primary afferents entering the spinal cord as well as glutamatergic spinal interneurons synapsing with SPN. GBP has also been reported to inhibit excitatory synaptogenesis both in-vitro and in-vivo by blocking the binding of synaptogenic thrombospondin proteins to the $\alpha 2\delta 1$ subunit (Eroglu et al., 2009). This suggests that GBP may work to reduce aberrant excitatory synapse formation in viscerosympathetic circuits after SCI. However, the short 2-3 hour half-life of GBP in rats (Radulovic et al., 1995; Vollmer et al., 1986) likely explains why once daily GBP treatment is insufficient to significantly reduce the frequency of spontaneous AD in the hours following administration; and likely insufficient to alter putative synaptic formation (Rabchevsky et al., 2012). Further studies into the synaptic mechanisms controlling SPN during noxious stimulation, as well as the precise means through which GBP mitigates AD may help identify novel therapeutic targets for prophylactically preventing the development of this syndrome.

2.3.3 Primary afferent sprouting

Intraspinal sprouting of primary afferent nociceptive fibers is also thought to contribute to the development of AD. After experimental SCI, the central arbors of unmyelinated c-fiber afferents expressing calcitonin gene-related peptide (CGRP), a marker of nociceptive fibers, sprout into the dorsal horn caudal to the injury (Hou et al., 2009; Krenz and Weaver, 1998b). The extent of $CGRP^+$ fiber sprouting into the lumbosacral spinal cord correlates with the magnitude of AD elicited by noxious CRD (Cameron et al., 2006; Krenz et al., 1999), suggesting that enhanced sprouting of nociceptive fibers increases reflex activation of SPN through propriospinal “relay” neurons (**Figure**1, see section 4.4). Increased $CGRP^+$ fiber density becomes apparent two weeks after

experimental injury (Hou et al., 2009; Krenz and Weaver, 1998b), a time at which AD develops reliably in spinal rats (Krassioukov and Weaver, 1995; Laird et al., 2006). Importantly, increased CGRP$^+$ fiber sprouting in the dorsal horn is also seen in the chronic stages of human SCI, and in one case has been associated with a well-documented history of AD (Ackery et al., 2007).

The sprouting of c-fibers appears to be primarily dependent on nerve growth factor (NGF) signaling. After transection or contusion SCI, resident neurons and glia upregulate the expression of intraspinal NGF rostral and caudal to the lesion (Bakhit et al., 1991; Brown et al., 2004). Blockade of NGF signaling through intrathecal delivery of anti-NGF antibodies for two-weeks after T4-transection SCI effectively mitigates injury-induced sprouting of CGRP$^+$ fibers throughout the spinal cord. Furthermore, animals receiving anti-NGF therapy had less severe AD in response to noxious CRD (Krenz et al., 1999), although this treatment did not abolish it completely. Cameron et al. (2006) used a proof-of-principle approach to overexpress NGF in the cord after T4-transection using adenovirus injections into either the T13/L1 or L6/S1 spinal levels innervating the distal colon and found that the pressor and bradycardic responses to CRD were significantly exacerbated. Conversely, injured cords injected with adenovirus encoding semaphorin 3a, a specific chemorepellant for both c-fibers and sympathetic fibers (Tang et al., 2004b), had significantly diminished pressor and bradycardic responses during CRD. Such exacerbations or ameliorations were significantly correlated with increased or decreased CGRP$^+$ fiber sprouting, respectively.

2.3.4 Propriospinal plasticity

Plasticity of ascending lumbosacral propriospinal fibers that relay pelvic sensory information rostrally towards SPN in the thoracic cord is also thought to contribute to the development of AD. There is compelling evidence for functional plasticity of propriospinal interneurons which comprise spinal sympathetic circuits after transection SCI in the rat. Krassioukov et al. (2002) investigated the response of sympathetically-correlated interneurons to both noxious and

innocuous stimuli hours following T3 transection (acute) as well as after one month (chronic). In the chronic but not acute stage of injury, interneurons whose electrical activity was cross-correlated with that of simultaneously recorded renal sympathetic nerve activity were excited by noxious CRD and cutaneous pinching, as well as non-noxious brushing of the skin caudal to the injury. This seminal study showed that in the weeks after injury, plasticity occurs within somatosensory relay neurons that influence the activity of SPN.

This electrophysiological evidence was supported histologically following anterograde tracer injections into the lumbosacral cord after complete T4-transection which significantly increased labeling of ascending propriospinal fibers originating in the dorsal gray commissure (DGC), notably found in juxtaposition to thoracic SPN labeled with Fluorogold (Hou et al., 2008). The DGC is a region in which pelvic visceral afferents terminate and send relay projections rostrally toward supraspinal targets (Al-Chaer et al., 1996; Hosoya et al., 1994; Matsushita, 1998; Pascual et al., 1993; Vizzard, 2000). Hou et al. (2008) found that a single session of prolonged, intermittent CRD performed two weeks after injury caused enhanced neuronal activation throughout the lumbosacral DGC, as indicated by increased expression of the immediate early gene *c-fos* in comparison to sham animals in which intact descending modulation prevents such expression. It remains unclear, however, whether the DGC neurons project directly to SPN or whether they project to excitatory interneurons to indirectly modulate the excitability of SPN (Rabchevsky, 2006).

Collectively, these findings support a model of AD in which plasticity of ascending propriospinal fibers, in conjunction with sprouting of primary afferents, creates an amplification of afferent stimuli below the injury such that noxious inputs are more likely to activate SPN to initiate unmodulated sympathetic reflexes leading to AD episode (**Figure 2.1**). Previous technical limitations made it difficult to directly test the neuroanatomical basis of the AD reflex in live animals. However, with the recent development of elegant genetic and chemogenetic silencing techniques (Kinoshita et al., 2012; Stachniak et al., 2014; Zhu and Roth, 2014), it may now be feasible to directly assess the role of specific

populations of ascending propriospinal neurons in conveying lumbosacral afferent input to rostral segments containing cardiovascular SPN (**Figure 2.1;** see section 2.5).

2.3.5 Peripheral adrenergic hypersensitivity

In addition to maladaptive plasticity of viscerosympathetic circuitry, there is also evidence of peripheral changes responsible for the exaggerated pressor response to afferent stimulation. In quadriplegics, resting blood pressure and plasma catecholamine levels are both significantly lower than in intact subjects (Mathias et al., 1976). This is consistent with the observation that sympathetic outflow below the lesion is lower both acutely and chronically after SCI (Mathias et al., 1979; Wallin and Stjernberg, 1984), which would be expected to produce lower concentrations of circulating catecholamines (Goldstein et al., 1983). However, it has been demonstrated that the vasomotor response to intravenously infused NE is enhanced in quadriplegics with a documented history of AD. Specifically, by measuring the diameter of the dorsal foot vein before and after local intravenous administration of NE, Arnold et al. (1995) found that the concentration of NE required to induce a 50% reduction in resting vessel diameter was significantly lower in tetraplegics compared to normal controls (1.6 mg/min vs. 10.9 ng/min). Similarly, Krum et al. (1992b) found that the dose of intravenously infused phenylephrine (a peripheral α-adrenergic receptor agonist) required to produce a pressor response of 20 mmHg is significantly lower in functionally complete quadriplegics compared to normal individuals. Furthermore, Krum et al. (1992a) reported that even modest increases in plasma NE during bladder cystometry after high-level SCI were sufficient to produce a significant pressor response greater than 20 mmHg systolic. Taken together, these studies indicate that SCI promotes hypersensitivity of the vasculature to catecholamines released through aberrant, unmodulated sympathetic reflexes, and that this hypersensitization may contribute to the severity of episodic hypertension after SCI.

There is indication that peripheral sensitization following SCI is limited to the vasculature caudal to the lesion and not within rostral vascular beds in which central sympathetic control remains intact. Following T4 transection in rats, Rummery et al. (2010) found evidence of enhanced neurovascular transmission in the saphenous artery which receives sympathetic outflow from the lower thoracolumbar cord. However, SCI-related neurovascular potentiation was not seen in the median artery which receives sympathetic outflow from the cord rostral to the lesion. Brock et al. (2006) similarly found that T4 transection in rats leads to increased neurovascular transmission within the mesenteric vasculature, with perivascular nerve stimulation producing a five-fold increase in contraction of mesenteric arteries seven weeks after SCI. This increased reactivity of mesenteric arteries was blunted by the adrenergic antagonist prazosin, further implicating that peripheral hypersensitization is secondary to changes in adrenergic transmission after injury. While the mechanism of this phenomena is not fully known, Brock et al. (2006) suggest that decreased norepinephrine reuptake is a contributing factor. Alternatively, Al Dera et al. (2012) report that complete SCI in rats also alters the role of L-type calcium channels in vasoconstriction, with their activation playing a larger role in smooth muscle contraction of tail arteries isolated after injury. Whether or not these two mechanisms are unique to specific vascular beds caudal to the lesion remains unclear.

Consistent with the hypothesis that SCI causes enhanced adrenergic sensitivity in peripheral vasculature, Lee et al. (2016) demonstrated increased protein expression of the α-adrenergic receptor in the femoral artery of rats after T10 spinal contusion. Furthermore, this increased receptor expression corresponded to an enhanced pressor response and vasoconstriction of isolated femoral arteries in response to phenylephrine stimulation. Whether or not the time-course of these changes corresponds to the timeline over which AD develops in rodents or humans remains unknown. Moreover, it is unclear whether these findings are applicable to AD since it does not develop after T10 contusion SCI. Although there is compelling evidence that peripheral

sensitization contributes to this syndrome, many questions remain regarding the underlying cellular processes and time-course over which adrenergic hyper-responsiveness develops, as well as the relative contribution compared to central maladaptive plasticity discussed.

2.4 Clinical management of AD

A variety of non-pharmacological and pharmacological strategies can be used to treat AD. Since AD often resolves once the inciting stimulus is removed, the current standard of care recommends identifying and eliminating the inciting factors, when possible, before pharmacological approaches are considered (Consortium for Spinal Cord, 2002). Immediate measures involve assessment of resting arterial pressure and monitoring for other symptoms associated with AD (see section 2.2). If hypertension is observed, it is advised to move patients into an upright position to facilitate the lowering of arterial pressure through hydrostatic redistribution of blood to the lower extremities. This postural maneuver causes a reduction of blood pressure in high-level SCI patients (Krassioukov and Harkema, 2006), although the efficacy to alleviate hypertension specifically during AD has not yet been formally investigated (Krassioukov et al., 2009). Since filling of the bladder and impaction of the bowel are the most common triggers of AD (Lindan et al., 1980), bladder voiding or bowel care routines should next be considered along with a general inspection for other possible sources of noxious stimulation such as pressure sores, tight clothing and skin laceration. Given that blood pressure can fluctuate rapidly in patients with AD, it is important to monitor blood pressure every 2-5 minutes for resolution or exacerbation of hypertension during physical examination (Consortium for Spinal Cord, 2002).

While some cases of AD are mild and resolve relatively easily, more severe cases can produce profound levels of hypertension and have no readily identifiable cause. Furthermore, it may be difficult to identify and remove the triggering stimuli, particularly for individuals with high thoracic and cervical injuries who have limited dexterity and mobility. Therefore, a variety of drugs and

medical procedures have been employed for the control of AD, primarily through managing hypertension. Some of the most common remedies are briefly discussed below.

2.4.1 Nitrates

Organic nitrates, such as nitroglycerine paste, are currently the most commonly prescribed medications for mitigating acute episodes of AD (Braddom and Rocco, 1991; Caruso et al., 2015). Nitrates are a class of drugs that are converted to or release nitric oxide (NO), an endogenous molecule that induces smooth muscle relaxation in the vasculature (Moncada and Higgs, 1993). For acute episodes of AD, it is recommended to apply 2% nitroglycerin paste onto the skin above the level of SCI (Braddom and Rocco, 1991). Vasodilation and subsequent reduction of blood pressure occurs rapidly after transdermal application and the paste can be wiped off once the therapeutic effect has been achieved (Grobecker, 1990). Moreover, a variety of oral and transdermal patch preparations are available and easy for patients and caregivers to administer. In severe cases of AD that are difficult to control, notably in a clinical setting, intravenous sodium nitroprusside may also be used to rapidly resolve hypertension (Valles et al., 2005).

2.4.2 Nifedipine

Nifedipine is an L-type calcium (Ca^{2+}) channel blocker that reduces the influx of Ca^{2+} into vascular smooth muscle cells, leading to a reduction in peripheral resistance and consequently blood pressure. Despite few controlled clinical trials, nifedipine has been widely used to treat AD in SCI patients (Braddom and Rocco, 1991; Caruso et al., 2015; Dykstra et al., 1987; Esmail et al., 2002; Krassioukov et al., 2009; Thyberg et al., 1994). In a survey of clinicians with extensive experience treating AD, Braddom and Rocco (1991) found that nifedipine was the most commonly prescribed agent to manage minor or severe symptoms of AD. More recently, nitrates have become slightly more prominent than nifedipine in treating minor or severe episodes of AD (Caruso et al., 2015),

likely stemming from safety concerns regarding the use of nifedipine during hypertensive crises because it may overshoot the therapeutic drop in blood pressure and cause severe hypotension and ischemia (Chobanian et al., 2003). Although there are no formal descriptions in the literature of adverse effects related to the use of nifedipine specifically for AD, it is possible that it may reduce arterial pressure below the range for critical renal, cerebral and cardiac vascular beds to autoregulate their perfusion, particularly since many with AD are predisposed to resting and orthostatic hypotension (Furlan and Fehlings, 2008).

2.4.3 Prazosin

The adrenergic receptor antagonist, prazosin, is another drug used to treat AD (Krum et al., 1992c; Phillips et al., 2015). Prazosin is an antihypertensive agent that works by specifically blocking □1-adrenergic receptors located on peripheral vasculature (Cavero and Roach, 1980). Unlike other hypertension medications, prazosin has little effect on cardiac function or resting blood pressure (Jaillon, 1980), making it safer to use in patients with chronic hypotension. Krum et al. (1992c) reported that, compared to placebo treatment, twice daily prazosin significantly decreased the magnitude of hypertension and severity of secondary symptoms during AD caused by a variety of genitourinary and colorectal stimuli. More recently, Phillips et al. (2015) reported that prazosin reduced the magnitude of hypertension during AD during sperm retrieval procedures involving penile vibrostimulation, which is a well-documented cause of AD. Collectively, research on the use of prazosin indicates that it may be useful as a prophylactic treatment for AD triggered by a variety of iatrogenic stimuli (Krum et al., 1992c; Phillips et al., 2015) .

2.4.4 Botulinum toxin

Conservative pharmacological approaches are not always effective, and some individuals require more aggressive treatments (Krassioukov et al., 2009). One such treatment is botulinum toxin (BTX), a neurotoxin derived from *Clostridium botulinum* that suppresses neuromuscular transmission by cleaving

synaptic proteins required for neurotransmitter exocytosis (reviewed in (Dolly, 2003). Due to its ability to temporarily cause detrusor muscle paralysis by preventing parasympathetic post-ganglionic acetylcholine release, delivery of BTX into the detrusor muscle has been used to treat bladder dysfunction secondary to SCI, such as neurogenic detrusor overactivity (NDO) (Dykstra, 2003; Dykstra et al., 1988; Orasanu and Mahajan, 2013; Schurch et al., 2005). As these conditions disrupt normal micturition and can lead to noxious distension of the bladder, they are associated with the occurrence of AD. While there have been no large-scale clinical trials for BTX as a prophylactic treatment of AD, there is indication that this could be a safe and tenable approach to minimize AD associated with bladder dysfunction and certain medical procedures such as cystoscopy. Schurch et al. (2000) reported a disappearance of AD caused by bladder voiding in a small subset of patients receiving BTX injections into the detrusor muscle to treat neurogenic bladder, though the duration of this improvement was not specified. Recently, Fougere et al. (2016a) conducted a small clinical trial specifically to assess the efficacy of intradetrusor injections of BTX to reduce bladder-related AD and observed a decrease in the severity of AD during cystometric filling of the bladder. Moreover, ambulatory blood pressure recordings revealed a decrease in the frequency of daily bladder-related AD for at least one month, accompanied by an increase in quality of life measures. Such reports indicate that BTX treatment may be a safe and potentially long-lasting means of prophylactically treating bladder-related AD. Notably, the duration of effect after BTX treatment is limited due to a combination of compensatory sprouting of peripheral nerve terminals and the gradual recovery of synaptic proteins necessary for neurotransmitter release (Dolly, 2003). While the duration of detrusor paresis is approximately 9 months (Schurch et al., 1996), it remains unknown how long intradetrusor BTX treatment can provide relief of AD.

In addition to temporary paralysis of bladder smooth muscle, there is also evidence that BTX treatment reduces AD by modulating sensory transmission into the spinal cord. Apostolidis et al. (2005) reported that intradetrusor injections of BTX in patients with NDO caused a decrease in the expression of both

purinoceptors ($P2X_3$) and capsaicin receptors (TRPV1) in sensory fibers innervating the bladder, and that this decrease was correlated temporally with a significant improvement in bladder function. These receptors are involved in bladder nociception (Birder et al., 2002; Cockayne et al., 2000), suggesting that decreased afferent signaling contributes to the improvement in urodynamic function after BTX treatment. In an experimental model, Elkelini et al. (2012) instilled BTX into the bladder of rats after T4-transection and observed a significant reduction in the magnitude of AD induced by bladder distension during cystometry, which was associated with reduced NGF expression in the bladder and sensory neurons in the dorsal root ganglia. As NGF regulates c-fiber density in the bladder (Schnegelsberg et al., 2010), it is also possible that BTX reduces bladder-related AD by decreasing the innervation or distribution of nociceptive fibers. Notably, intradetrusor BTX treatment has also been used to alleviate refractory AD in a pediatric SCI patient (Lockwood et al., 2016).

2.5 Systemic effects of recurrent AD

2.5.1 Cardiovascular Changes

Emerging evidence suggests that the recurrence of AD, which can occur more than 40 times a day for some individuals (Hubli et al., 2015), adversely affects multiple physiological systems over time. Alan et al. (2010) demonstrated that repeated instances of AD after experimental SCI exacerbate injury-induced peripheral vascular dysfunction. Isolated mesenteric arteries from rats which underwent 30-minutes of continuous CRD daily for two-weeks after T3 transection SCI had a more pronounced vasoconstrictor response to phenylephrine (an α_1-adrenergic agonist) compared to arteries from animals with SCI only. This suggests that injury-induced adrenergic hypersensitization, which itself is a mechanism involved in the etiology of AD (see section 3.2), is exacerbated by repeated instances of AD and may help explain why the severity of AD increases over time (West et al., 2015). If this is the case, it should be possible to dampen the temporal increase in AD severity by pharmacologically controlling adrenergic hypersensitization. However, as discussed in section 4.5,

the cellular processes leading to adrenergic hyper-responsiveness have yet to be elucidated.

Repetitive surges in blood pressure from recurrent AD may also induce maladaptive structural changes in peripheral vasculature (West et al. (2013). Vascular remodeling is a dynamic process that responds to changes in shear stress from normal hemodynamic fluctuations as well as hypertensive disease (Baeyens et al., 2015; Schiffrin, 2004; Silver and Vita, 2006). While SCI alone is associated with changes in vascular structure, this is believed to be an adaptation to the decreased metabolic demands of atrophied tissue below the injury (Olive et al., 2003). The hypothesis that blood pressure fluctuations from recurrent AD cause further remodeling of peripheral vasculature requires additional study, particularly since structural changes to resistance vessels, such as alterations in the ratio of wall thickness/lumen diameter, are strongly associated with cardiovascular disease (Rizzoni et al., 2003).

Deleterious changes in cardiac function are also associated with daily repeated bouts of experimental AD. West et al. (2016) investigated the effects of recurrent AD on cardiac structure and function in rats following T3 transection. Beginning 2-weeks after injury, rats received 60-minutes of repetitive CRD daily for 4 weeks. In-vivo echocardiography revealed that animals with daily induced AD (SCI-AD) had diminished basal contractility and their hearts developed significantly lower left ventricular pressure with a slower rate of ventricular contraction. These alterations in cardiac mechanics were accompanied by a dampened inotropic response to β-adrenergic stimulation during isoproterenol challenge in the SCI-AD group compared to SCI alone, despite no differences in β-adrenergic receptor expression. Taken together, this data suggests that recurrent AD leads to aberrant cardiac mechanics, which may be due to desensitization of adrenergic receptors in the heart. Notably, these experimental findings were corroborated with clinical data which indicated a relationship between the number of daily AD events and impaired cardiac mechanics in a small sample of humans with mid-cervical SCI (C4-C8). As suggested by the authors (West et al., 2016), this consequence of recurrent AD may also

contribute to the increased risk of cardiovascular disease in people with SCI (Cragg et al., 2013; Garshick et al., 2005).

In addition to peripheral vasculature, there are emerging reports of associations between AD and cerebrovascular function. Phillips et al. (2016) found that high-thoracic SCI in rats causes maladaptive changes in middle cerebral artery (MCA) structure and function. Seven weeks after T3 transection, ex-vivo analysis of MCA revealed decreased vessel compliance and diminished vascular reactivity to vasoconstrictive 5-hydroxytryptamine. The functional changes in MCA preparations were seen in conjunction with increased collagen deposition and wall thickness, suggesting that arterial stiffening and structural remodeling after SCI may impair cerebral autoregulation. Considering that T3 transection in rats reliably causes AD to develop within two weeks, and given the seven-week duration of this study, it is likely that recurrent AD contributed to these findings. Potential changes in cerebrovascular function may help explain cognitive dysfunction which has been documented after high-level SCI (Davidoff et al., 1990; Phillips et al., 2014; Wecht and Bauman, 2013). Phillips et al. (2016) provided preliminary data suggesting that cerebral autoregulation is capable of maintaining sufficient blood flow to the brain during mild and slowly evolving episodes of AD, though it remains unknown if the cerebral vasculature can respond appropriately during more severe and rapidly occurring episodes. Ultimately, it will be important for future studies to determine whether recurrent AD causes structural and functional modifications to peripheral and cerebral vasculature since these maladaptations have been proposed to contribute to cardiovascular and cognitive dysfunction after SCI (Phillips et al., 2016; Wecht and Bauman, 2013).

2.5.2 Immunomodulatory effects of AD

In addition to cardiovascular anomalies, AD is linked to aberrant functioning of the immune system (Ueno et al., 2016; Zhang et al., 2013). Compared to the general population, people with chronic SCI have a weakened immune system capacity (Campagnolo et al., 1994; Iversen et al., 2000) and are

more susceptible to lethal infections such as pneumonia (Brommer et al., 2016). This phenomenon, known as spinal cord injury-induced immune depression syndrome (SCI-IDS) (Riegger et al., 2007), is dependent on the level of SCI, with injuries above the level of the major sympathetic outflow being associated with more severe immunosuppression (Brommer et al., 2016; Campagnolo et al., 1997; Iversen et al., 2000; Lucin et al., 2007; Zhang et al., 2013). Iversen et al. (2000) collected blood and bone marrow samples from individuals with SCI and observed diminished lymphocyte activity and impaired proliferation of hematopoietic progenitor cells, particularly in tetraplegics with mid-cervical injuries. Similarly, Lucin et al. (2007) found that T3 but not T9 transection in mice causes a loss of splenocytes and B cells in association with enhanced levels of splenic NE and blood cortisol levels.

In intact subjects, the immune system is modulated by the hypothalamic-pituitary-adrenal axis (HPA) and sympathetic nervous system (SNS) (reviewed in (Irwin and Cole, 2011). In response to physical or psychological stress, the anterior pituitary gland releases adrenocorticotropic hormone to stimulate the release of glucocorticoids (GCs) from the adrenal cortex into the blood. There is also evidence for direct neural innervation of the adrenal cortex by SPN (Engeland and Arnhold, 2005), suggesting that sympathetic activity during AD may also promote GC release. GCs subsequently bind to the intracellular glucocorticoid receptor in leukocytes to alter the transcriptional programming and limit inflammatory responses (reviewed in (Rhen and Cidlowski, 2005). Additionally, activation of the SNS modulates the immune system through the release of NE directly into lymphoid tissues, where it binds to β_2-adrenergic receptors on a variety of immune cells, including lymphocytes and macrophages. Like GCs, NE can have immunosuppressive effects on a variety of immune cells, including B and T lymphocytes, by activating intracellular signaling cascades such as the cyclic adenosine monophosphate (cAMP) pathway. Ultimately, the result of such stimulation is to shunt cellular activity away from a pro-inflammatory state (reviewed in (Lorton and Bellinger, 2015).

Because of the immunosuppressive role of SNS stimulation, it is thought that SCI-IDS is caused by heightened sympathetic activity and catecholamine release during recurrent bouts of AD. Zhang et al. (2013) reported a causal link between AD and chronic immunosuppression. The temporal development of AD in mice with T3 transection SCI corresponded to an elevated level of circulating GCs and accumulation of NE within the spleen, along with a profound loss of greater than 50% of splenic leukocytes by 5-weeks post-injury. Compared to sham operated or low thoracic (T9) SCI mice which do not develop AD, those with spontaneously occurring AD measured telemetrically and quantified with a computer detection algorithm had a limited capacity to produce antibodies after injection of immunogenic ovalbumin. Additionally, this immunodeficiency was exacerbated by experimentally inducing AD with repeated bouts of noxious CRD. The immunosuppressive effects associated with established AD were reversed after treating injured mice with a cocktail of a selective β_2-adrenergic receptor antagonist and a GC receptor antagonist, concluding that immunosuppression after T3 SCI in mice is caused by AD-related elevations in NE and GC. Notably, however, this treatment cocktail was not reported to alter the occurrence of AD. These experimental findings in mice were corroborated with data from a mid-cervical SCI patient showing that tapping of the abdomen overlying the urinary bladder, which stimulated an episode of AD, caused an increase in catecholamine release with a concomitant reduction in lymphocyte proliferation. More recently, Ueno et al. (2016) used an inducible chemogenetic silencing approach in mice with T3 SCI to inhibit glutamatergic interneurons thought to facilitate reflex activation of SPN innervating the spleen. After silencing these neurons daily for 2-weeks, the quantity of splenic B and T cells was restored to pre-injury levels. Together, these studies may explain why individuals with high-level SCI, many of whom experience AD, have increased susceptibility to a variety of infectious diseases, and further implies that controlling or preventing AD is essential for overall well-being.

Importantly, the immunomodulatory effects of recurrent AD may only be a contributing factor to SCI-IDS rather than the primary driver. For example, direct sympathetic innervation of the bone marrow (Bjurholm et al., 1988; Denes et al., 2005) is thought to help regulate hematopoiesis and immune function in the normal, uninjured state (reviewed in Jung et al., 2017). Therefore, dysregulated activity of decentralized sympathetic fibers innervating bone marrow following SCI may also contribute to SCI-IDS. Moreover, it is well documented that SCI leads to decreased bone density as a result of diminished gravitational load (Biering-Sorensen et al., 1990; Zehnder et al., 2004). As the bone marrow is a major site of hematopoiesis, it is possible that bone atrophy after SCI compromises the hematopoietic niche, which may help to explain the reduced immune cell production seen after injury (Iversen et al., 2000). The relative contribution of these potential mechanisms warrants future investigation.

2.6 Emerging research strategies

Important questions remain regarding the underlying mechanisms responsible for episodic AD that develops after SCI. While strong correlative evidence supports a role in maladaptive plasticity of lumbosacral primary afferents and ascending propriospinal neurons, the relative contribution of these modified pathways to the AD syndrome is unclear. Recently developed genetic and chemogenetic neuronal silencing techniques should allow future investigations aimed at dissecting the precise role of these distinct neuroanatomical pathways. For example, Kinoshita et al. (2012) injected a complimentary set of viral vectors into regions of the spinal cord containing the terminals and soma of propriospinal neurons thought to be critical for the execution of dexterous hand movements. In their model, a highly efficient retrogradely transported lentiviral vector carrying enhanced tetanus toxin (HiRET-eTeNT) under the control of the tetracycline-responsive element was injected into the spinal segments containing the terminals of their target neurons. In addition, a second adeno-associated viral (AAV) vector carrying a reverse tetracycline transactivation sequence (AAV-rtTAV) was injected into the spinal cord segment

containing the cell bodies of those same neurons. With this approach, it was possible to silence neurons by inducing the expression of tetanus toxin through systemic delivery of doxycycline. Notably, only the neurons which were doubly infected with both HiRET-eTeNT and AAV-rtTAV were silenced, providing a reversible and spatially targeted method for investigating the role of specific neural pathways. Based on such an approach, it is feasible to doubly infect and silence ascending propriospinal relay neurons which originate in the lumbosacral cord that project rostrally towards thoracic SPN to directly test their contribution to AD induced through stimulation of lumbosacral afferents (**Figure 2.1**). As discussed in section 2.5.2, Ueno et al. (2016) employed a novel chemogenetic silencing approach to prevent the development of SCI-IDS associated with AD by blocking neurotransmission of glutamatergic spinal interneurons, though it is unknown whether this approach would also ameliorate hemodynamic changes during AD. Moreover, this method silenced all glutamatergic interneurons in the injected regions (T5-T7) and, therefore, does not allow for the precise dissection of specific neuroanatomical pathways.

Alternatively, a recent report by Iyer et al. (2016) demonstrated the ability to silence specific nociceptive primary afferents using a chemogenetic method in which AAV carrying the engineered inhibitory hMD4(Gi) DREADD receptor (designer receptor exclusively activated by a designer drug) was injected directly into the sciatic nerve. Upon activation with the highly specific ligand clozapine-n-oxide (CNO), the hMD4(Gi) receptor hyperpolarizes neurons through induction of the G-protein inward-rectifying potassium channel (Armbruster et al., 2007). They demonstrated that intraperitoneal injection of clozapine-n-oxide (CNO) significantly increased mechanical and thermal nociceptive thresholds in the foot pads of animals with DREADD infected afferents. Because the genetic and chemogenetic silencing methods discussed here have distinct ligand-receptor interactions, it may be possible within a single animal to serially silence propriospinal relay neurons and primary afferents to directly investigate their contributions to both spontaneous and CRD-induced AD.

In addition to further mechanistic studies, it will also be important to fully elucidate the systemic effects of recurrent AD. The metabolic consequences of sporadic, uncontrolled fluctuations in catecholamines and GCs released during AD are not well known. As suggested by Karlsson (1999), frequent daily bouts of AD accompanied with such abnormal surges in GCs and catecholamines may contribute to the high reported incidence of metabolic abnormalities in persons with SCI (Duckworth et al., 1980; Gorgey et al., 2014; Maruyama et al., 2008; Yekutiel et al., 1989). Considering that GC and catecholamines have a number of effects on energy metabolism in various tissues throughout the body, including the liver, spleen, pancreas, adipose tissue and skeletal muscle (reviewed in (Barth et al., 2007; Vegiopoulos and Herzig, 2007), it is possible that recurring AD predisposes or exacerbates the development of metabolic disease, such as insulin resistance and dyslipidemia. In support of this, Bluvshtein et al. (2011) reported that post-prandial insulin resistance is present in tetraplegics with cervical SCI, but not in paraplegics with thoracic SCI that preserves some level of supraspinal control over sympathetic outflow. Moreover, manual percussion of the abdomen overlying the bladder in people with high-thoracic or cervical SCI was found to activate lipolysis in tissues below the injury level in association with increased blood pressure and catecholamine release (Karlsson et al., 1997). Whether a relationship exists between the magnitude and frequency of AD and the incidence of insulin resistance or abnormal lipid metabolism has not yet been formally investigated.

2.7 Conclusions

AD can have a significant impact on the quality of daily living and, if not treated properly and timely, this hypertensive syndrome can have deleterious cardiophysiological and systemic consequences. The most common treatment paradigms involve vasoactive drugs intended to resolve the acute hypertensive crises rather than preventing them from occurring, though some evidence suggests that prazosin and botulinum toxin may provide prophylactic management of AD associated with normal and iatrogenic urogenital stimulation.

While well documented, the intracellular signaling processes underlying adrenergic hypersensitization in the context of AD are unknown. Recent methodological advances should allow for more detailed investigation into the relative contribution of specific propriospinal neurons and primary afferent fibers to this aberrant viscerosympathetic reflex after SCI. The widespread physiological consequences of recurrent AD, which can happen dozens of times daily, have only recently been investigated. Animal models and clinical data indicate that repeated episodes of AD exacerbate peripheral adrenergic hypersensitization, suppress immune function, compromise cardiac mechanics, and potentially alter cerebrovascular and cognitive function. However, the potential effects of recurrent AD on peripheral and central vasculature structure, as well as widespread metabolism have only begun to be investigated. In light of recent data describing profound systemic effects of chronic AD, it is increasingly important to develop more targeted therapies capable of preventing the development of this syndrome and its associated maladies altogether in order to improve quality of lives for individuals with SCI who are predisposed to this syndrome.

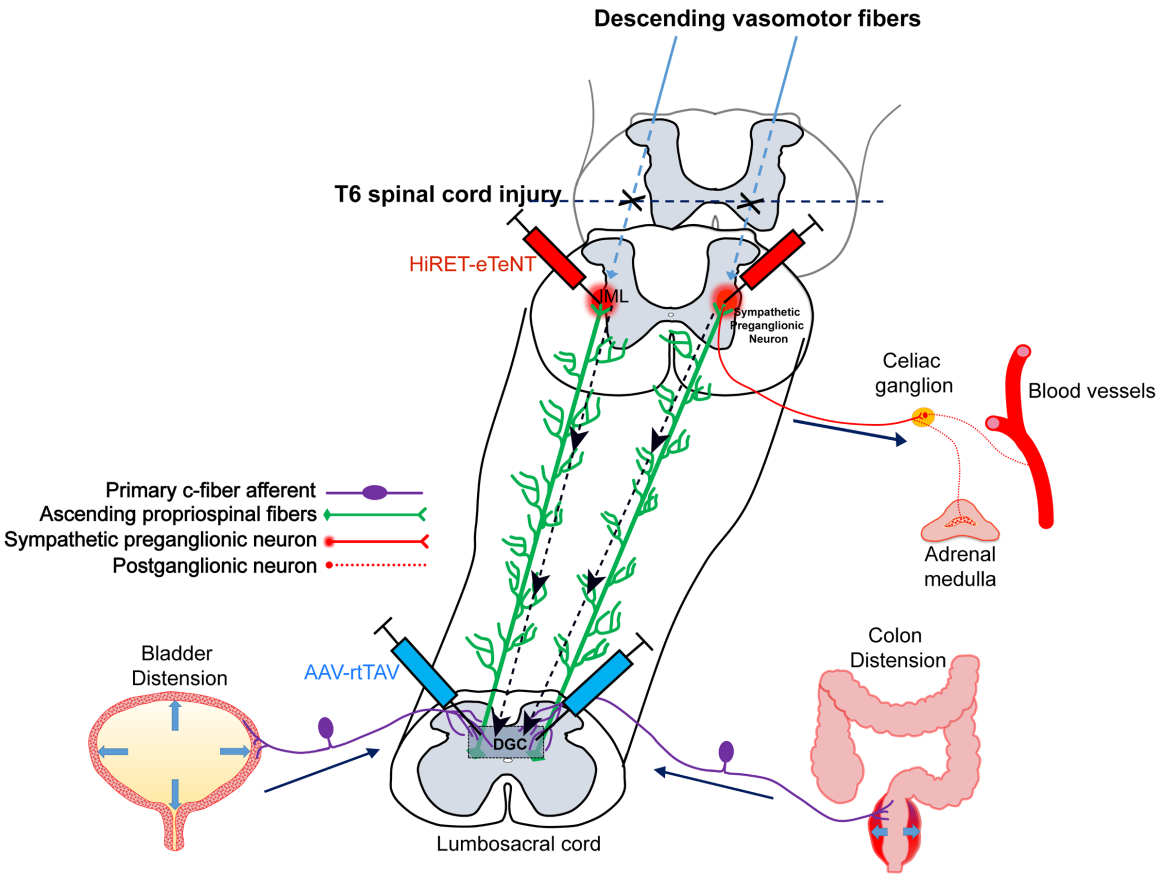

Figure 2.1. Diagrammatic representation of the neuroanatomical circuitry thought to be involved in autonomic dysreflexia triggered by pelvic visceral stimulation. Descending vasomotor fibers (blue) originating in the brainstem and hypothalamus modulate the tonic activity of sympathetic preganglionic neurons (SPN; red) throughout the intermediolateral cell column (IML) in the thoracolumbar spinal cord. After complete spinal cord injury at or above the T6 segment, SPN which innervate the adrenal medulla and blood vessels below the injury are segregated from descending control pathways, allowing for unrestrained sympathetic reflex activity that leads to hypertension. Injury further leads to maladaptive sprouting of both primary afferent c-fibers (purple) and ascending propriospinal tracts (green) originating in the lumbosacral dorsal gray commissure (DGC). These ascending "relay" neurons are thought to convey sensory information from the bladder and colon (i.e., distension) rostrally towards SPN. Emerging neuronal silencing techniques may allow for investigations into

the role of specific neuroanatomical pathways involved in AD. One example might be to employ double infection of ascending lumbosacral propriospinal neurons with the HiRET-eTeNT vector (red syringe), which is retrogradely transported (dotted black lines) from nerve terminals in the IML to lumbosacral DGC also infected with AAV-rtTAV vector (blue syringe). Doxycycline-induced silencing of these neurons could then allow for direct investigation into their roles in facilitating AD during pelvic visceral stimulation.

Note:

This chapter has been reprinted with permission from Elsevier: Eldahan, K.C., Rabchevsky, A.G., 2018. Autonomic dysreflexia after spinal cord injury: Systemic pathophysiology and methods of management. Auton Neurosci 209, 59-70.

Copyright © Khalid C. Eldahan 2019

CHAPTER 3

Rapamycin Exacerbates Cardiovascular Dysfunction After Complete High-Thoracic Spinal Cord Injury

3.1 Introduction

In addition to loss of sensory and motor function, traumatic spinal cord injury (SCI) can also disrupt central autonomic pathways that are important for maintaining cardiovascular homeostasis. Autonomic dysreflexia (AD) is an abnormal hypertensive syndrome that presents in many individuals with a spinal cord injury (SCI) above the sixth thoracic (T6) spinal level; the majority of cases (Devivo, 2012). Injuries above this level segregate critical spinal sympathetic preganglionic neurons (SPN) involved in blood pressure regulation from important vasomotor nuclei in the brainstem and hypothalamus, leaving them susceptible to unrestrained reflex activation by stimuli below the lesion level. Notably, SPNs below T6 control vasomotor tone of the extensive mesenteric vasculature, which accounts for approximately 30% of the total blood volume (Greenway and Lister, 1974; Rowell, 1990). Noxious distension of the bladder or bowel are among the most common triggers of AD (Lindan et al., 1980; Snow et al., 1978), though a variety of other noxious and non-noxious stimuli are also known to precipitate an event (Karlsson, 1999; Marsh and Weaver, 2004). AD presents as episodic hypertension accompanied with baroreflex-mediated bradycardia, although tachycardia may alternatively be present (Lindan et al., 1980). While the severity of hypertension during an AD episode can vary widely, if not treated promptly and properly then severe episodes can lead to stroke, hypertensive encephalopathy, seizures, cardiac arrest, and even death(Bjelakovic et al., 2014; Colachis and Clinchot, 1997; Eltorai et al., 1992; Fausel and Paski, 2014; Jain et al., 2013; Valles et al., 2005).

A contributing factor to the development of AD is maladaptive plasticity of sympathetic reflex circuitry (Krassioukov et al., 2002). After transection SCI, the sprouting of unmyelinated afferent c-fibers carrying nociceptive signals from the pelvic viscera into the lumbosacral cord, as well as ascending propriospinal fibers

which project rostrally and relay these signals towards SPNs in the thoracic cord, are associated temporally with the development of AD (Cameron et al., 2006; Hou et al., 2008; Krenz et al., 1999). Moreover, the extent of nociceptive afferent fiber sprouting, which is dependent upon injury-induced elevations in nerve growth factor (Brown et al., 2004; Krenz et al., 1999), positively correlates with the extent of mean arterial pressure (MAP) increases during AD induced experimentally through noxious colorectal distension (CRD) (Cameron et al., 2006; Krenz et al., 1999). While therapeutic strategies aimed at mitigating such maladaptive plasticity are attractive for their potential to prevent or reduce the development of AD, no such treatments exist in the clinical setting.

Recently, the mammalian target of rapamycin (mTOR) has gained considerable interest as a target to modulate post-traumatic plasticity within the central nervous system. Considered a “master regulator” of protein synthesis, mTOR is expressed ubiquitously in eukaryotic cells and integrates a variety of environmental cues such as nutrient availability and growth factors to coordinate important cellular processes such as cell growth, proliferation and autophagy (Dibble and Manning, 2013; Laplante and Sabatini, 2012; Sandsmark et al., 2007). Several lines of evidence indicate that mTOR is also a critical mediator of neuronal sprouting and regeneration after neurotrauma. Following crush injury of the optic nerve in mice, deletion of phosphatase and tensin homologue (PTEN), a negative regulator of mTOR, promotes robust regeneration in an mTOR-dependent manner (Sun et al., 2011). Genetic mouse models of enhanced mTOR activity after SCI via PTEN deletion in the motor cortex demonstrate increased regeneration and compensatory sprouting of injured descending corticospinal tract axons (Jin et al., 2015; Liu et al., 2010). Moreover, pharmacological inhibition of mTOR signaling with rapamycin after traumatic brain injury has been shown to decrease seizure frequency and associated maladaptive sprouting of hippocampal mossy fibers (Guo et al., 2013). Together, these studies suggest that this highly conserved signaling pathway which is present in all mammalian cells (Schmelzle and Hall, 2000) may also be involved

in the sprouting of ascending afferent pathways underlying the development of AD.

In addition to its involvement in CNS structural plasticity, mTOR regulates nociceptive sensitivity in both the normal and injured states. In naïve rats, pharmacological blockade of spinal mTOR with rapamycin prevents the development of neuronal hyperexcitability and behavioral hypersensitization associated with pain induced by injection of formalin into the hindpaw (Asante et al., 2009). In rats with cyclophosphamide-induced cystitis, a condition characterized by bladder hyperactivity and pelvic pain, rapamycin significantly reduces the expression of CGRP and substance P in the spinal cord dorsal horn (Liang et al., 2016). Furthermore, inhibition of mTOR following SCI in rats treated with rapamycin attenuates the development of neuropathic pain in correlation with reduced expression of both calcitonin gene related peptide (CGRP) and substance P, two neuropeptides involved in the regulation of nociceptive sensitivity (Wang et al., 2016). Collectively, these studies suggest that mTOR is involved in the regulation of both intraspinal plasticity and nociceptor sensitivity, but it is not yet known whether mTOR modulates the sprouting of sensory and/or propriospinal pathways after SCI in relation to the development of AD. Therefore, in contrast to SCI studies attempting to promote sprouting and regeneration of descending corticospinal tracts by enhancing mTOR activity, we carried out experiments to test how the inhibition of mTOR after complete high-thoracic SCI with the drug rapamycin alters the temporal development of AD, and whether it modulates injury-induced maladaptive plasticity of primary afferent fibers and/or propriospinal neurons.

3.2 Methods and Materials

Collectively, a total of 33 age and sex-matched rats were used for all experiments, which includes n=23 for telemetric monitoring (n=3 naïve + vehicle, n=3 naïve + rapamycin, n=7 SCI + vehicle, n=10 SCI + rapamycin) and n=10 for western blot analysis (n=2 naïve, n=2 10 days post-injury [DPI], n=2 21 DPI, n=2 21 DPI + CRD, n=2 21 DPI + CRD + RAP).

3.2.1 Cardiophysiological Monitoring

All animal housing conditions, surgical procedures, and postoperative care were conducted according to the University of Kentucky Institutional Animal Care and Use Committee and the National Institutes of Health animal care guidelines. As described in detail (Rabchevsky et al., 2011; Rabchevsky et al., 2012), seven days prior to SCI, naïve anesthetized (2% isoflurane) 3 to 3.5 month old female Wistar rats (~275 grams, n=23) were implanted with telemetric blood pressure transmitters (model HD-S10, Data Sciences International, Inc., St. Paul, MN) into the descending aorta. The probes were secured to the abdominal wall with silk sutures before closing the skin with 3-0 vicryl sutures and surgical staples. Animals were then treated post-operatively, as described below. Blood pressure was monitored 24/7 (500 Hz sampling rate) using the Dataquest A.R.T. acquisition system (Data Sciences International, Inc., St. Paul, MN) beginning 2 days pre-injury through 4-weeks post-injury. Rats were single-housed, with each cage placed directly on top of its corresponding data receiver plate (model RPC-1, Data Sciences International, Inc., St. Paul, MN). Captured recordings were binned into 24-hour segments for analysis of daily blood pressure, heart rate, and spontaneous AD (sAD). As previously described in detail (Rabchevsky et al., 2012), sAD was analyzed using a custom algorithm written and implemented in Matlab software (The MathWorks, Inc., Natwick, MA). Briefly, this algorithm simultaneously processes 24-hour mean arterial pressure (MAP) and heart rate (HR) traces for instances where a rise in MAP of 10 mmHg or more above baseline is accompanied by a decrease in HR of at least 10 beats per minute. While this algorithm does not require such events to be sustained above baseline for a specific duration, it does require the rise in MAP over baseline to occur within a 35-second window. MAP rises that were accompanied by tachycardia (an increase in HR) were not included in these detections. From the computer automated AD event detections, a single human observer then manually eliminated false-positive results stemming from technical artifacts that can arise during normal rat movements and during planned CRD procedures.

3.2.2 Spinal Cord Transections

One week following telemetry probe implantation, 17 out of 23 rats undergoing cardiophysiological monitoring were were designated for the SCI groups. These randomly selected telemetry rats were anesthetized (ketamine, 80 mg/kg; xylazine 7 mg/kg i.p.) and underwent a T3 laminectomy prior to complete transection of the T4 spinal cord (T4Tx) using a scalpel blade, as previously described (Cameron et al., 2006; Rabchevsky et al., 2012). In addition, 8 out of 10 non-telemetered rats from the western blot cohort were designated for T4Tx in order to examine the effect of rapamycin treatment on mTOR activity after SCI. Altogether, a total of 25 rats underwent T4Tx, including n=17 for telemetry experiments and n=8 for western blot experiments. Two independent observers confirmed complete spinal cord transection of each rat based on full separation of the rostral and caudal stumps. Immediately afterwards, gelfoam was placed into the transection site to achieve hemostasis and the overlying muscles were sutured with 3-0 vicryl before stapling the skin with wound clips (Stoelting, Wood Dale, IL).

3.2.3 Post-operative Care

All rats which underwent ketamine/xylazine anesthesia received i.p. injections of yohimbine (3.2 mg/kg Lloyd Laboratories, Shenanhoah, IA) to reverse the effects of xylazine. Injured rats were then housed one per cage with food and water *ad libitum*. A heating pad was placed between each cage and its corresponding data receiver plate for the duration of the study period. Immediately post-op, rats were administered 10 mL of lactated Ringer's solution, s.c. Post-surgical pain management was achieved with twice daily buprenorphine-HCl injections (0.03mg/kg, s.c.; Reckitt-Benckiser Pharmaceuticals Inc., Richmond, VA) for three days. All rats received two daily injections of the antibiotic cefazolin (33.3 mg/kg, s.c.; WG Critical Care, LLC, Paramus, NJ) for 5-days post-surgery and injured rats received twice daily

manual bladder expression for 2-3 weeks or until they regained spontaneous bladder voiding reflexes without signs of urinary tract infection.

3.2.4 Rapamycin Administration and Colorectal Distension (CRD)

All rats were weighed prior to injections to ensure accurate drug dosage throughout the study period. Rapamycin (RAP; 3 mg/kg, LC Labs, Woburn, MA) or vehicle (4% ethanol, 5% polyethylene glycol-400, 5% polysorbate-80 in 0.1M PBS) was injected i.p. immediately after injury and then every other day until euthanasia at 10 and 21 days post-injury (DPI) for the western blot cohort, or 28 DPI for telemetered rats. In rodent SCI models, RAP has been administered at 6 mg/kg every other day(Liu et al., 2012), 3 mg/kg daily (Sun et al., 2013), or 1 mg/kg daily (Song et al., 2015). We chose a 3 mg/kg alternate day dosage based on optimal effectiveness in blocking mTOR signaling (Zeng et al., 2008). Moreover, we found that this dosage attenuates mTOR activity in the spinal cord after T4Tx, as assessed by phosphorylation of the downstream S6 ribosomal protein (see **Figure 3.1**).

On days 14, 21 and 28 post-SCI, naïve and injured rats undergoing telemetric monitoring underwent 2 consecutive trials of CRD using a balloon-tipped catheter (Swan-Ganz, model# 111F7, Edwards Lifesciences, Irvine, CA) inserted 2 cm into the rectum and secured to the tail with surgical tape, as described(Rabchevsky et al., 2012). Additionally, non-telemetered western blot rats designated for SCI + CRD similarly underwent two consecutive CRD trials at 21 DPI prior to euthanasia and tissue collection. Following catheterization, rats were placed into cylindrical plastic restrainers (Cat # 51335, Stoelting, Wood Dale, IL) to prevent them from tampering with the catheter. All rats were then left in a quiet and dark environment to acclimate to the catheter and restrainer for 30 minutes before balloon inflation and CRD measurements. During each CRD trial, the balloon was inflated with 2 mL of air for 60 seconds, followed by a 10-minute rest interval. Using the Dataquest A.R.T. Acquisition software (Data Sciences International, Inc., St. Paul, MN), “event markers” were placed at the beginning and end of each CRD trial trace to demarcate CRD-induced cardiovascular

changes. Immediately following the second CRD trial at 28 DPI, a final session of prolonged, intermittent CRD was initiated to induce c-Fos expression as described (Hou et al., 2008). Briefly, this procedure lasted 90 minutes with 30-second inflation periods separated by 60-second rest periods. With this paradigm, a total of 60 rounds of catheter inflation were performed. For all CRD trials, the balloon catheter was fully inflated with 2 mL of air within 5 seconds.

For measurements of CRD-induced changes in blood pressure and heart rate, the raw pulsatile arterial pressure data was averaged every 2 seconds and converted into mean arterial pressure (MAP) traces for analysis in the Dataquest A.R.T. Analysis software. The inter-beat interval was derived from the pulsatile arterial pressure waveform and converted to beats per minute (BPM) to generate a separate heart rate (HR) trace. For each trial, the absolute MAP and HR values achieved during CRD stimulation were measured by averaging all data points within the 60-second window of balloon inflation. Additionally, pre-CRD baseline MAP and HR values were generated by averaging all data points within the 30-second window immediately prior to the balloon inflation event marker, and CRD-induced changes in MAP and HR were then calculated as the difference between the respective 30-second baselines and the values achieved during CRD. At each time-point (14, 21, 28 DPI), the values of the two replicate CRD trials were averaged for each rat in the data analyses.

3.2.5 Western Blot Analysis

For the cohort of age and sex-matched Wistar rats (n=10) used for western blotting, the L6-S2 spinal cord segment was rapidly dissected and flash frozen in liquid nitrogen, following CO_2 euthanasia and decapitation. Samples were mechanically homogenized in ice-cold RIPA buffer with 5mm sodium fluoride and protease inhibitors (Cat# 11836153001, Sigma Aldrich, St. Louis, MO) added to preserve protein phosphorylation status and maintain total protein integrity. 1 mL of RIPA buffer was added per gram of tissue to manually grind samples in a dounce homogenizer before brief (3 x 10 seconds) ultrasonic homogenization. The Pierce BCA Protein Assay Kit (Cat# 23225, Thermo Fisher

Scientific, Waltham, MA) was used to estimate the total protein concentration of each sample, and 20 µg of total protein from each spinal cord sample were suspended in Laemmli buffer under reducing conditions (5% β-mercaptoethanol) and then separated by SDS–PAGE using Criterion 4-20% Criterion TGX precast gels (Cat# 5671094, Bio-Rad, Hercules, CA). Separated proteins were transferred onto nitrocellulose membranes using the Trans-Blot Turbo Transfer System (Cat# 1704150, Bio-Rad, Hercules, CA). Nitrocellulose membranes were blocked with non-fat dry milk (5% in TBST) for one hour at room temperature. Blocked membranes were then incubated at 4° C overnight in primary antibody diluted in blocking buffer. Following primary incubation, membranes were washed for 3 x 20 minutes in TBST before incubating for 1 hour at room temperature in secondary antibody diluted in blocking buffer. Excess secondary antibody was then removed by washing for 3 x 20 minutes in TBST. Immunolabeled membranes were developed using enhanced chemiluminescence (Amersham ECL Advance Western Blotting Detection Kit, GE Healthcare, UK) and imaged with the ChemiDoc MP system (Bio-Rad, Hercules, CA). Quantification was then performed with ImageJ software (National Institutes of Health, Washington, USA) by plotting individual lanes and quantifying the area under the curve (Gassmann et al., 2009; Guo et al., 2013). Antibodies were used according to manufacturer data sheets: pS6 (1:1,000; Cell Signaling Technology # 2215), S6 (1:1,000; Cell Signaling Technology # 5G10), α-Tubulin (mouse monoclonal 1:10,000; Abcam #ab7291), HRP conjugated goat-anti-rabbit (1:5000; Jackson Immunoresearch Cat# 111-035-144), HRP conjugated goat-anti-mouse (1:5000; Jackson Immunoresearch Cat#115035166). All lanes were normalized to their respective α-Tubulin loading control, and fold-changes were expressed relative to naïve values.

3.2.6 Tissue Fixation and Processing

At 28 DPI, all rats undergoing cardiophysiological monitoring were euthanatized within 10 minutes following the 90-minute CRD protocol with an overdose of sodium pentobarbital (Fatal Plus, Vortex Pharmaceuticals, Dearborn,

MI) before perfusion transcardially with 0.1 M phosphate-buffered saline (PBS), pH 7.4, followed by 4% paraformaldehyde in PBS (Cameron et al., 2006). A 3-cm segment of cord measured from the conus medullaris was dissected and the dura mater carefully removed before post-fixing in 4% PFA for 4 hours and storing overnight in 0.1M PB at 4°C. Tissue was then cryopreserved with 20% sucrose in 0.1M PBS solution with 0.002% sodium azide at 4°C until all cords had sunk to the bottom of their container. Spinal cords were embedded in a mixture of gum tragacanth (Sigma Aldrich, St. Louis, MO) and 20% sucrose in 0.1M PBS by evenly aligning 4-6 cords side by side within plastic cryomolds that were then snap frozen in –40°C acetone and stored at –80°C until sectioning on a cryostat (Microm Laborgerate, Walldorf, Germany). Frozen tissue blocks were sectioned in the transverse plane at a thickness of 20 µm, and every fifth section (100 µm spacing) was mounted onto one of three series of 10 slides (Superfrost, Fisher Scientific, Waltham, MA), consecutively (i.e., 1-10 thoracolumbar; 1a-10a lumbar; 1b-10b lumbosacral). Up to 15 consecutive rows of cryosections from each block were placed onto each of 10 slides in all three series. In this manner, 0.5 mm separation is represented by two slides separated by 5 within the series of 10 processed for histological analysis (i.e., slides 1 and 6, 1a and 6a, 1b and 6b). All slides were stored at -20°C until used for histological staining.

3.2.7 Immunohistochemistry and Microscopy

Mounted slides were removed from the freezer to thaw at room temperature for 30 minutes before a series of 3 x 10-minute washes in 0.1M PBS with gentle agitation to rehydrate tissue and remove excess embedding media. They were then pre-incubated in blocking buffer consisting of 0.1M PBS containing 0.3% Triton-X and 5% normal goat serum. Tissue was then incubated with primary antibody overnight at 4°C in blocking buffer containing rabbit-anti-calcitonin gene related peptide (CGRP; 35.3 ug/ml; Sigma #C8198) and mouse-anti-cFos (2 ug/ml; Encor Biotechnology #MCA-2H2). Following primary antibody incubation, slides were washed 3 x 10 minutes in 0.1M PBS. Next, slides were incubated overnight at 4°C in blocking buffer containing goat-anti-rabbit

conjugated to Alexa-488 (4 ug/ml; Life Technologies #A11008) or biotinylated goat-anti-mouse (7.5 ug/ml; Vector #BA9200). The following day, slides were washed 3 x 10 minutes in 0.1M PBS and cFos sections were shielded from light and incubated for another 4 hours at room temperature with Texas Red conjugated streptavidin (3.33 ug/ml, Vector #SA-5006) in 0.1M PBS. All slides were washed 3 x 10 minutes in 0.1M PBS before cover-slipping with Vectashield mounting media (Vector #H-1000) containing 5 uM Hoechts dye (#H3570, Thermo Fisher) to stain nuclear DNA. All images acquired for both CGRP and c-Fos quantification were captured using an Olympus BX51 microscope paired with an Olympus Magnafire digital camera (Melville, NY). Image exposure times were kept constant to help maintain a consistent level of background staining.

3.2.8 Densitometric Analyses

For both cFos and CGRP densitometry analyses in the thoracic and lumbosacral cord, five serial coronal sections (1mm spacing) centered on each of the 3 levels evaluated (T5/T6, T13/L1 and L6/S1 segments) were used for each rat. For cFos quantification, densitometry was performed using ImageJ software (National Institutes of Health, Bethesda, MD, USA). All 24-bit RGB photomicrographs were converted into 8-bit black and white images, and the regions of interest (ROI) included the entire right dorsal horn for the L6/S1 level (**Figure 3.6a**) or the dorsal gray commissure for T5/T6 and T13/L1 levels. Thresholds for each cFos ROI were manually identified by a single experimenter based on the lowest pixel value above which cFos+ nuclei were included, and final values were expressed in arbitrary units. For CGRP quantification, densitometry of digitized 24-bit RGB photographs from the thoracic and lumbosacral levels was performed using Bioquant image analysis software (Nova Prime; V6.70.10; Bioquant Image Analysis Corp., Nashville, TN) with the ROI demarcated by laminae III-V in the dorsal gray matter for the L6/S1 level (**Figure 3.7E**) or laminae IV for the T5/T6 and T13/L1 levels (**Figure 3.7A,C**) to account for differential cytoarchitecture. Thresholds for each CGRP ROI were chosen by a single experimenter based on the pixel values above which the faintest $CGRP^+$

fibers were included. CGRP measurements were calibrated inside of Bioquant software to express results in um^2.

3.2.9 Statistical Analyses

All statistical analyses were conducted using Prism 6.0 software (Graphpad Software, La Jolla, CA), with alpha set at 0.05. For measurements over time of body weight, daily mean arterial pressure and heart rate, CRD-induced changes, and daily spontaneous AD data sets, two-way repeated measures analysis of variance (ANOVA) were conducted followed by Sidak's post-hoc when appropriate. The Geisser-Greenhouse correction factor was used for all repeated measures ANOVAs to adjust for deviations from the compound symmetry assumption within our data. For analysis of c-Fos and CGRP histological data, ANOVA and Sidak's post-hoc were used, followed by unpaired t-tests on collapsed data when warranted.

3.3 Results

We recorded a 30% attrition rate in the SCI + RAP group undergoing telemetric monitoring, with 3/10 rats in this group dying of unknown causes within 3-weeks post-injury and the start of treatment. These animals were accordingly excluded from all analyses, resulting in a final group size of n=7. Notably, no unexpected attrition occurred in the naïve or SCI + vehicle groups, or in any of the groups used for western blotting.

3.3.1 Rapamycin Mitigates Elevated mTOR Activity in the Injured Spinal Cord

We examined mTOR activity in the lumbosacral segments following SCI and noxious CRD using Western blot assessments of phosphorylated S6 ribosomal protein (pS6), a widely used downstream marker of mTOR activity (Guo et al., 2013; Harlan et al., 2013; Obara et al., 2011). Relative to naïve spinal cords, those from 10 and 21 DPI showed heightened S6 phosphorylation in the lumbosacral spinal cord (**Figure 3.1**). CRD at 21 DPI further augmented mTOR

activity by approximately 2-fold, however prolonged RAP administration prevented such increases, notably reducing pS6 levels below even naïve values.

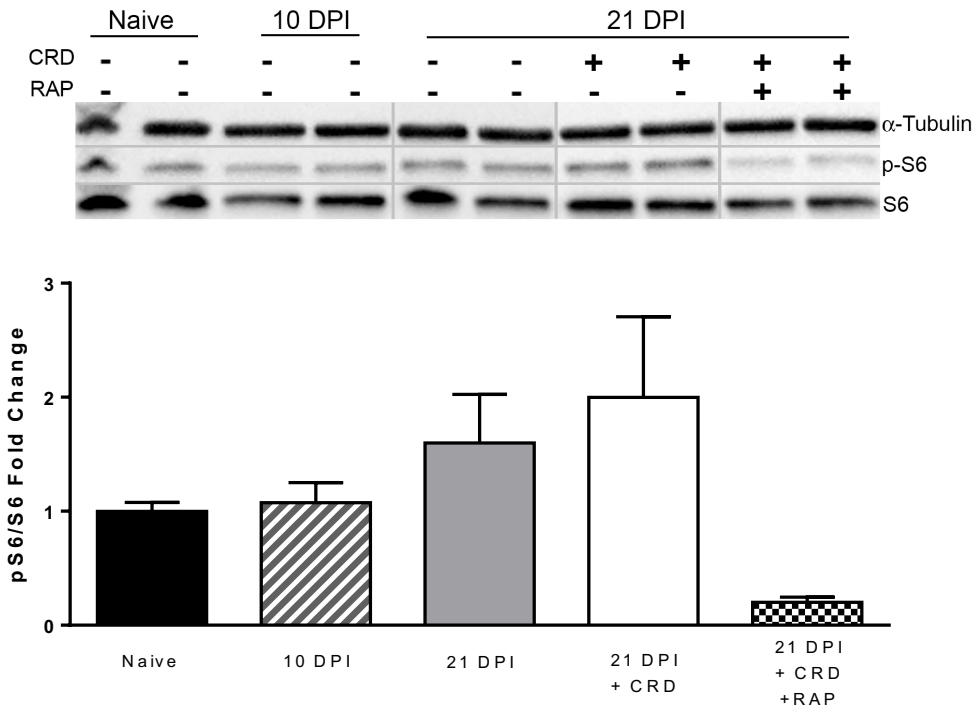

Figure 3.1. Effects of rapamycin treatment on mTOR activity after spinal cord injury (SCI). Western blot analysis showed that while mTOR activity was elevated by both SCI and CRD at 21 DPI, prolonged systemic treatment with rapamycin (RAP; 3 mg/kg i.p., every other day) suppressed mTOR activity in the lumbosacral spinal cord. The ratio of phosphorylated-S6 ribosomal protein to total S6 was used as a downstream surrogate of mTOR activity. α–tubulin was used as a loading control and values are expressed relative to naïve control values. Vertical grey lines indicate where lanes containing groups which were not included in this study were removed. Statistical analysis not performed due to the low sample size (n=2 per group). Symbols are means ± SD.

3.3.2 Rapamycin Treatment Impairs Normal Weight Gain and Exacerbates Weight Loss After SCI

Body weight data was compared between vehicle control and RAP-treated groups prior to and during prolonged RAP administration. In naïve rats, there were significant effects of time ($p<0.0001$), treatment ($p=0.0079$), and interaction ($p<0.0001$) on body weight (**Figure 3.2A**). Naïve + vehicle rats gained approximately 30g of body weight by 10 DPI, whereas naïve + RAP rats maintained stable body weights for the duration of the study and weighed significantly less than naïve + vehicle rats beginning at 10 DPI ($p<0.0001$). In injured rats, there were also significant effects of time ($p<0.0001$), treatment ($p=0.0002$), and interaction ($p<0.0001$) on body weight (**Figure 3.2B**). SCI + vehicle rats lost approximately 15g of body weight over the first 10 DPI, and subsequently returned to their pre-injury weight by 16 DPI. Conversely, SCI + RAP rats lost approximately 40g in the first 10 DPI and failed to return to pre-injury weights by the end of the study (**Figure 3.2B**). Similar to the naïve groups, a significant treatment effect to reduce weight was apparent by 10 DPI, which remained significantly lower for the remainder of the study ($p< 0.05$).

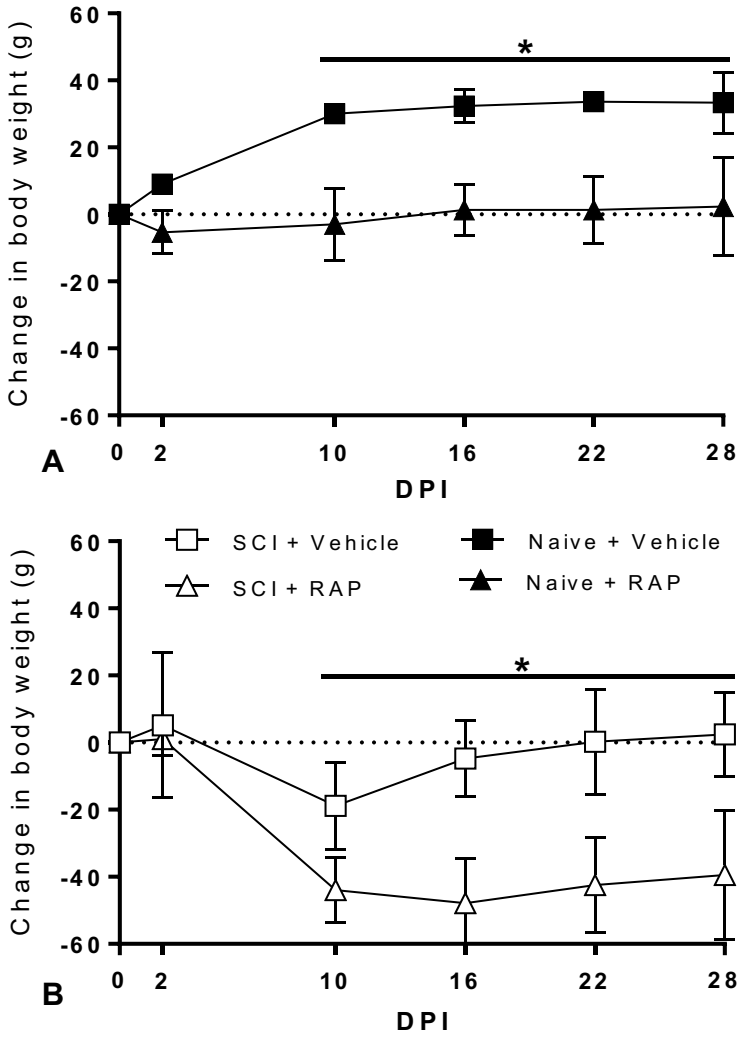

Figure 3.2. Body weight dynamics following prolonged rapamycin (RAP) treatment and spinal cord injury (SCI). RAP treatment prevents weight gain in both naïve and SCI rats. (**A**) RAP prevented the normal increase in body weight over time in naïve, vehicle-treated rats. (**B**) After SCI, vehicle-treated rats started to regain weight by 16 days post-injury (DPI), whereas RAP-treated rats lost significantly more weight loss by 10 DPI and failed to approach pre-injury body weights. n=3 naïve + vehicle; n=3 naïve + RAP (3 mg/kg); n=7 SCI + vehicle; n=7 SCI + RAP (3 mg/kg). Symbols are means ± SD, *$p \leq 0.05$, Vehicle vs. RAP treatment.

3.3.3 Rapamycin Alters Daily Hemodynamic Measures Before and After SCI

We investigated the effect of prolonged rapamycin treatment on the average daily mean arterial pressure (MAP) and heart rate (HR) in naïve and injured rats over 4 weeks. In naïve rats, there was a significant effect of time on daily MAP (**Figure 3.3A**; $p<0.0001$), but no differences in the average daily MAP between naïve groups across time ($p=0.4758$). In SCI rats, there were significant effects of time post-injury (**Figure 3.3B**; $p<0.0001$) and treatment ($p=0.0003$) on daily MAP, along with a significant interaction between time and treatment ($p<0.0001$). When compared to their respective pre-injury values, the average daily MAP in both vehicle- and RAP-treated SCI groups declined significantly ($p<0.001$) for two days post-injury before returning to pre-injury values (**Figure 3B**). RAP significantly elevated daily MAP above vehicle controls ($p<0.05$) beginning at 9 DPI and lasting through the remainder of the study period; notably being maintained well above pre-injury control values (**Figure 3.3B**).

In naïve rats, there were significant effects on daily HR based on time post-injury ($p<0.0001$) and treatment ($p=0.0133$), as well as a significant interaction ($p=0.0008$) (**Figure 3.3C**). Specifically, daily HR was significantly lower in naïve rats with RAP treatment versus naïve + vehicle controls between 5 and 21 DPI ($p<0.05$). However, despite a trend for increased daily HR in SCI + RAP rats during weeks 2 and 3 post-injury, there was no significant treatment effect on HR ($p=2.066$). In sum, and paradoxically, RAP treatment in naïve rats did not alter MAP but significantly lowered HR, whereas after SCI it significantly increased daily MAP accompanied by only moderate HR increases.

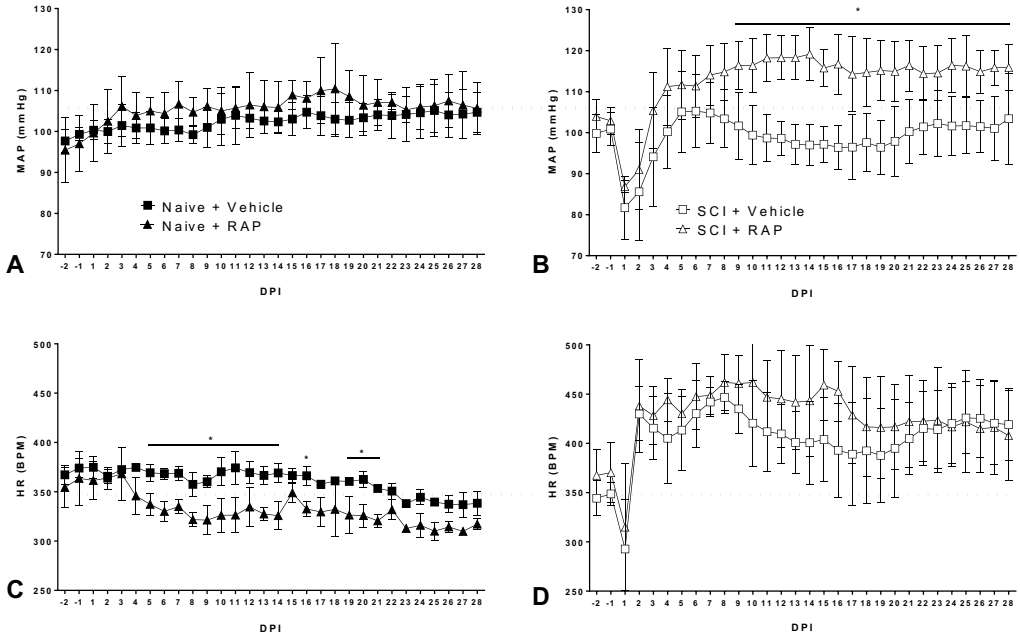

Figure 3.3. Rapamycin (RAP) effects on cardiophysiology of naïve and spinal cord injured (SCI) rats. (**A**) While chronic RAP treatment did not alter daily mean arterial pressure (MAP) in naïve rats across days post-injury (DPI), it caused significantly elevated MAP in SCI rats (**B**) beginning at 9 DPI to levels much higher than naïve controls (horizontal dotted lines). (**C**) In naïve rats, RAP significantly decreased heart rate (HR) across DPI, whereas highly elevated HR starting days after SCI was unaltered by RAP (**D**). n=3 naïve + vehicle; n=3 naïve + RAP (3 mg/kg); n=7 SCI + vehicle; n=7 SCI + RAP (3 mg/kg). Symbols are means ± SD, *$p \leq 0.05$ Vehicle vs. RAP treatment.

3.3.4 Rapamycin Increases the Frequency of Spontaneous AD

We assessed the effects of RAP treatment on the daily frequency of spontaneously occurring AD (sAD) in freely moving naive and SCI rats using our sAD event detection algorithm applied to MAP and HR data corresponding to each day pre- and post-injury (**Figure 3.4**). While there were negligible sAD events detected in the naïve groups across all time points, there were significant effects on the frequency of sAD events based on time post-injury ($p<0.0001$) and treatment ($p<0.0001$), along with a significant interaction ($p<0.0001$). Notably, the

RAP-treated SCI group showed significantly higher frequencies of daily sAD compared to the SCI + vehicle group, such that by 16 DPI, a time by which AD becomes fulminant in T4Tx rats, the SCI + RAP group had ~100 AD events/day compared to ~20 events/day in the SCI + vehicle group.

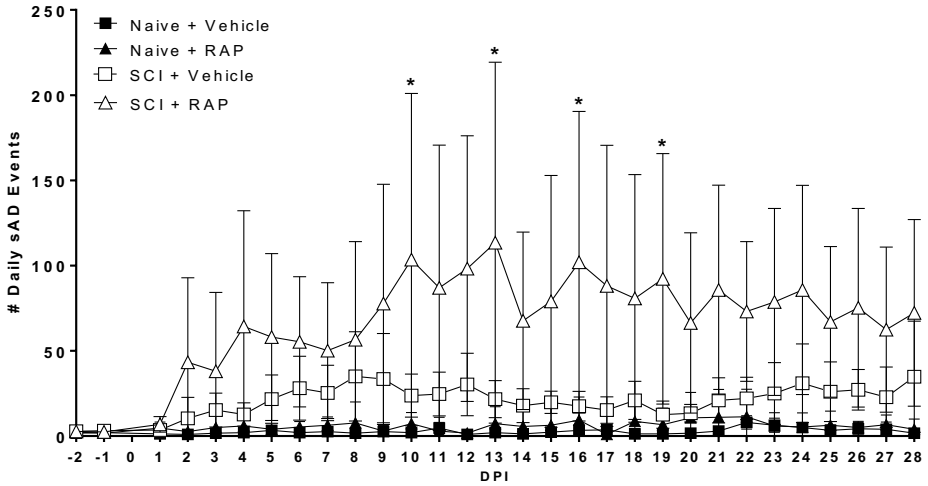

Figure 3.4. Rapamycin (RAP) treatment effects on the daily frequency of spontaneously occurring AD (sAD) events. Compared to vehicle-treated naive rats, the vehicle-treated SCI group had conspicuously more sAD events over all days post-injury (DPI). However, RAP significantly increased the frequency of sAD compared to vehicle-treated SCI rats. n=3 naïve + vehicle; n=3 naïve + RAP (3 mg/kg); n=7 SCI + vehicle; n=7 SCI + RAP (3 mg/kg). Symbols are means ± SD, *$p \leq 0.05$ vs SCI + Vehicle.

3.3.5 Rapamycin Increases the Absolute Magnitude of CRD-Induced AD

We first examined the extent of MAP increase during CRD in relation to 30-second baselines, as is typically reported (**Figure 3.5A**), and found significant effects of time ($p<0.0001$) and injury ($p=0.0037$), along with interaction of time and injury ($p=0.0292$). When compared to naïve + vehicle, SCI + vehicle rats had significantly reduced MAP increases during CRD at 14 and 21 DPI ($p<0.05$). However, in both naïve and injured groups, RAP did not alter the extent of such

MAP increases during CRD compared to respective 30-second baselines (**Figure 3.5A**).

In both naïve and injured groups, there was an overall effect of time post-injury on HR changes during CRD ($p=0.0052$), but no significant treatment effects ($p>0.05$; **Fig 3.5B**). Notably, irrespective of treatment, naïve rats responded to CRD with pronounced tachycardia whereas injured rats showed bradycardia that is characteristic of AD. Both SCI groups had significant drops in HR during CRD compared to the naïve groups at 14 and 21 DPI ($p < 0.005$), with only a trend for lower HR in the injured groups at 28 DPI ($p=0.056$).

While this would appear to indicate no effect of RAP on CRD-induced AD, we next compared baseline MAP values of naïve and injured rats at rest during the 30 seconds preceding CRD (**Figure 3.5C**). There was an overall significant treatment effect on the pre-CRD baseline MAP values ($p=0.0008$), but no effect of time post-injury ($p=0.1291$). The baseline MAP was significantly ($p < 0.05$) lower in the SCI + vehicle groups compared to the naïve + vehicle groups at 14, 21 and 28 DPI. Critically, however, the SCI + RAP group had significantly higher pre-CRD baseline MAP compared to the SCI + vehicle group at 14 and 21 DPI ($p<0.05$), effectively normalizing pre-CRD baselines to naïve control levels. Notably, the significant increase in pre-CRD MAP in SCI + RAP versus SCI + vehicle rats is consistent with the significantly increased daily 24-hour MAP in RAP- versus vehicle-treated SCI rats.

Accordingly, there were significant effects of RAP on the absolute magnitude of MAP reached during CRD based on time ($p<0.0001$) and treatment ($p<0.0001$), with no interaction ($p=0.2455$) (**Figure 3.5D**). SCI alone resulted in significantly lower absolute MAP induced by CRD compared to both naïve groups at 14, 21 and 28 DPI ($p < 0.05$). However, while RAP treatment did not alter the absolute MAP reached during CRD in naïve rats, the SCI + RAP group had a significantly higher MAP during CRD (125 mmHg) compared to SCI + vehicle rats (143 mmHg) at 21 DPI ($p < 0.05$). While the absolute MAP reached during CRD did not change over time in the naïve groups, there were significant increases over time in both SCI groups. In the SCI + vehicle group, the absolute

CRD-induced MAP increased significantly from 14 to 21 DPI ($p<0.005$), 14 to 28 DPI ($p<0.0001$), and 21 to 28 DPI ($p<0.005$). Similarly, the absolute CRD-induced MAP in the SCI + RAP group increased from both 14 to 21 DPI ($p < 0.0005$) and 14 to 28 DPI ($p < 0.0001$). While not statistically significant, there was a trend for the CRD-induced MAP to increase from 21 to 28 DPI in the SCI + RAP group ($p=0.055$).

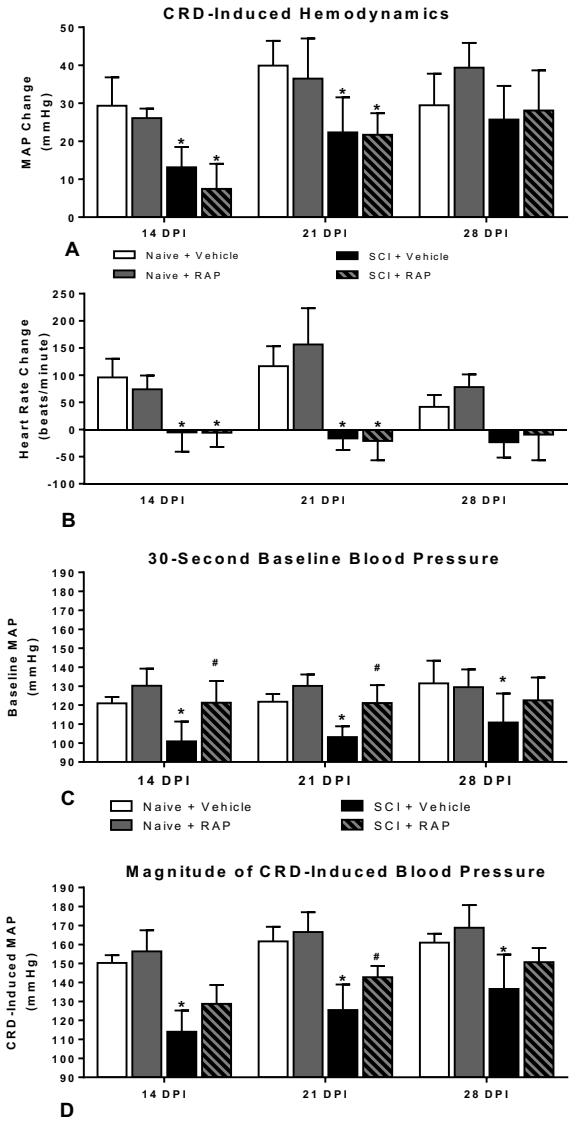

Figure 3.5. Effects of prolonged rapamycin (RAP) treatment on mean arterial pressure (MAP) and heart rate (HR) during colorectal distension (CRD). (**A**) In naïve rats, RAP treatment did not affect the extent of CRD-induced

MAP change relative to baseline at any time point. SCI alone significantly attenuated the extent of CRD-induced MAP changes at 14 and 21 days post-injury (DPI), but RAP treatment after SCI did not alter the extent of MAP response to CRD at any time-point. (**B**) Naïve rats responded to CRD with tachycardia, whereas injured rats displayed bradycardia that is characteristic of AD. While the HR responses to CRD were diametrically opposite in injured compared to naïve rats at all DPI, RAP treatment did not alter the extent of CRD-induced HR changes in either naïve or SCI groups. (**C**) RAP treatment did not alter the baseline MAP in naïve rats at any time point. However, spinal cord injury (SCI) significantly reduced the baseline MAP compared to the naïve + vehicle group at 14, 21 and 28 DPI. In SCI rats, RAP significantly increased the BL-MAP to naïve levels compared to the SCI + vehicle group at 14 and 21 DPI. (**D**) The absolute MAP achieved during CRD was lower in SCI rats at all time points. Whereas RAP treatment had no effect in naïve rats, it significantly increased the CRD-induced MAP in injured rats at 21 DPI. n=3 naïve + vehicle; n=3 naïve + RAP (3 mg/kg); n=7 SCI + vehicle; n=7 SCI + RAP (3 mg/kg). Symbols are means ± SD, *$p<0.05$ vs. naïve + vehicle; # $p<0.05$ vs. SCI + vehicle.

3.3.6 Rapamycin Does Not Alter the Density of cFos or CGRP Immunolabeling

Following prolonged, intermittent CRD, we measured the density of c-Fos immunolabeling in the dorsal gray commissure (DGC) at the T5/T6 and T13/L1 spinal cord levels (**Figure 3.6A-D**) which contain propriospinal interneurons that relay noxious pelvic sensory information towards thoracic SPNs (Hou et al., 2008; Lu et al., 2001; Matsushita, 1998), as well as the dorsal horn of the L6/S1 spinal cord (**Figure 3.6E,F)**, which receives colorectal afferents. c-Fos is an immediate early gene widely used as a marker of neuronal activation in response to electrical or sensory stimulation (Dragunow and Faull, 1989). In naïve rats with intact descending modulatory pathways, we observed sparsely distributed $cFos^+$ nuclei throughout the thoracic DGC (**Figure 3.6A,C**) and lumbosacral dorsal horn gray matter (**Figure 3.6E**) after prolonged CRD, which qualitatively increased in density after SCI (**Figure 3.6B,D,F**). An ANOVA revealed that the density of c-

Fos was unaltered by RAP treatment in the T5/T6, T13/L1 or L6/S1 spinal levels (**Figure 3.6G**). When data were collapsed into two groups based on injury status (naïve or injured), t-tests showed that SCI rats had significantly increased c-Fos density at all three spinal levels when compared to naïve rats ($p<0.05$).

We also evaluated the density of $CGRP^+$ fiber labeling in the thoracic and lumbosacral dorsal horn to determine whether RAP altered sprouting of unmyelinated primary afferents conveying noxious stimuli into the spinal cord. In naïve rats, thoracic CGRP immunolabeling was primarily restricted to the substantia gelatinosa and lamina IV (**Figure 3.7A-D**). In the lumbosacral cord, $CGRP^+$ labeling was typically located in the substantia gelatinosa, dorsal gray commissure, and around the sacral parasympathetic nucleus (**Figure 3.7E,F**). After injury, there were qualitative increases in fiber labeling throughout the L6/S1 segments (**Figure 3.7E**) that were not apparent in the thoracic segments (**Figure 3.7B,D**). An ANOVA across all groups at each level showed no significant treatment effects in naïve or injured rats. When data were collapsed into two groups based on injury status (naïve or injured), the lumbosacral segment had significantly more $CGRP^+$ fiber density after SCI compared to naïve groups ($p=0.0081$; **Figure 3.7G**), but no injury effects were observed at either thoracic level ($p>0.05$; **Figure 3.7B,D**).

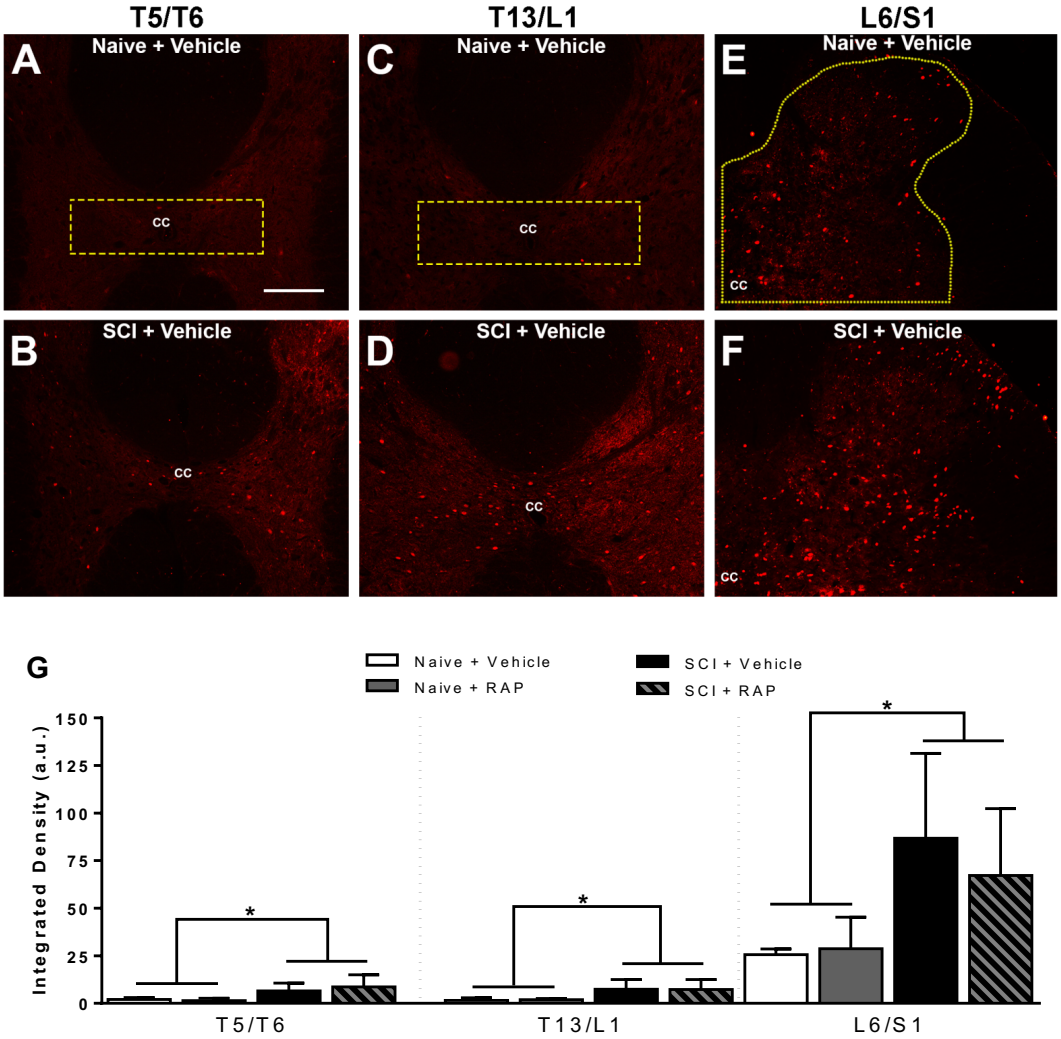

Figure 3.6. c-Fos immunostaining in spinal cross sections from the T5/T6, T13/L1 and L6/S1 spinal segments of vehicle-treated naïve (A,C,E) and SCI (B,D,F) rats following prolonged, intermittent colorectal distension (CRD). At all levels examined, the loss of descending inhibitory inputs lead to an increase in c-Fos expression throughout the dorsal gray commissure (DGC) of thoracic (**A-D**) segments and the dorsal horn in the lumbosacral cord (**E,F**) after SCI compared to naïve cords, but treatment with rapamycin (RAP) did not alter expression qualitatively (**G**). The region of interest (ROI) used for quantification of the T5/T6 and T13/L1 levels (yellow dotted lines in **A, C**) included the bilateral DGC. For the L6/S1 level. the ROI (yellow dotted line in **E**) began at the central canal (CC) and included the entire unilateral dorsal gray matter. Bar = 200 uM, applies to all. (**G**) Densitometric analysis showed that CRD led to increased c-

Fos immunoreactivity at all levels in the SCI groups compared to naïve, but there were no significant treatment effects within groups. When groups were collapsed according to injury status, there was a significant increase in c-Fos density in the thoracic DGC and lumbosacral dorsal horn after SCI. n=3 naïve + vehicle; n=3 naïve + RAP (3 mg/kg); n=7 SCI + vehicle; n=7 SCI + RAP (3 mg/kg). Symbols are means ± SD. * $p < 0.05$ naïve vs. SCI groups.

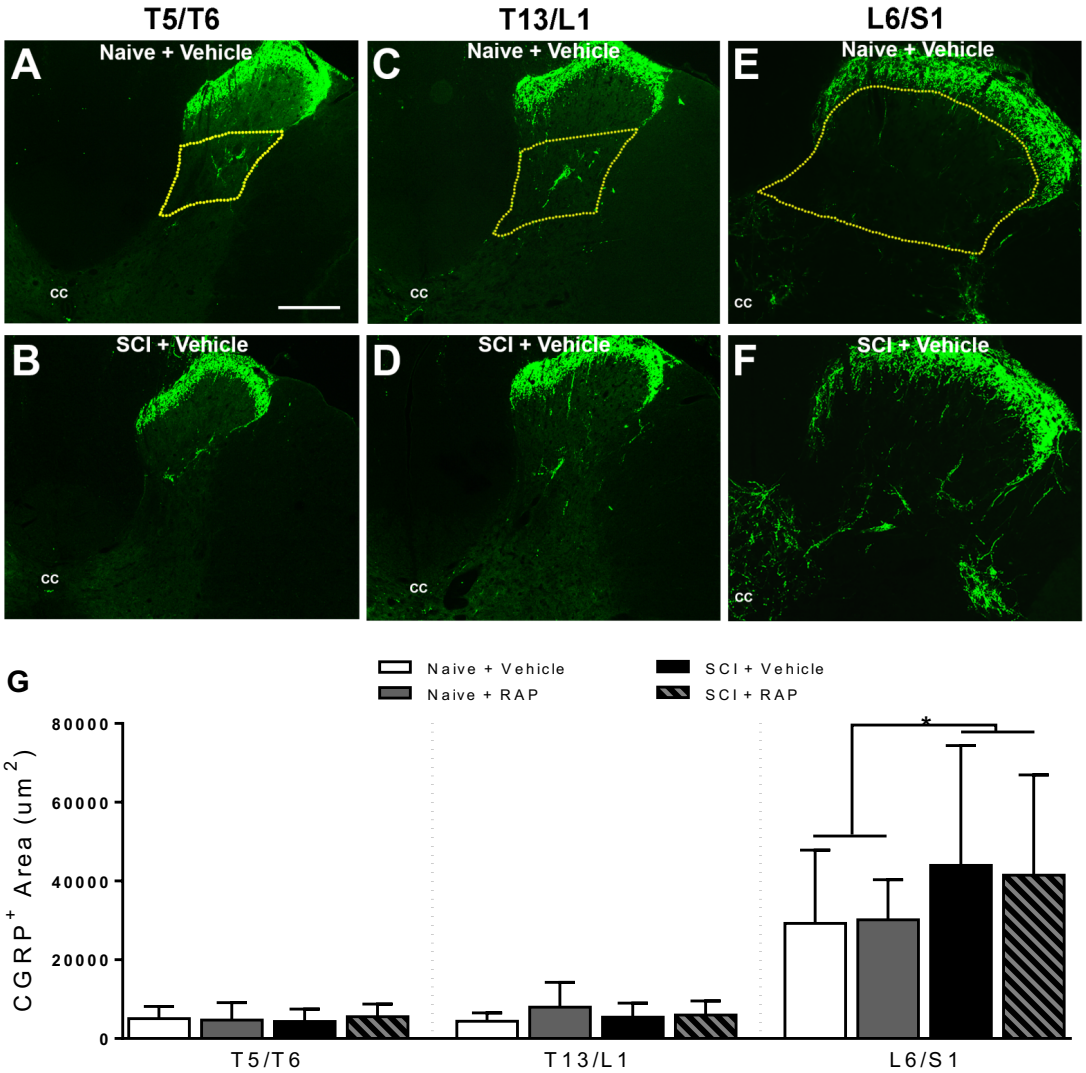

Figure 3.7. CGRP staining in spinal cross sections from the T5/T6, T13/L1 and L6/S1 segments of naïve (A,C,E) and injured (B,D,F) spinal cords four weeks after SCI. CGRP$^+$ fibers in thoracic segments (**A-D**) were located in the substantia gelatinosa (laminae I-II) and laminae IV, whereas CGRP staining in the lumbosacral cord (**E,F**) was primarily located in laminae I-II with fibers extending throughout deeper dorsal laminae. After SCI, there was a qualitative increase in the density of CGRP$^+$ fibers located in the deeper dorsal horn laminae of the L6/S1 spinal level (**F**), but not in the thoracic levels examined (**B,D**).The region of interest (ROI) used for quantification included laminae IV of the thoracic cord (yellow dotted lines in **A,C**) and laminae III-V of the lumbosacral

cord (yellow dotted line in **E**). Bar = 200 uM, applies to all. (**G**) Densitometric analysis showed that rapamycin (RAP) did not alter injury-induced sprouting of CGRP+ c-fibers in the lumbosacral dorsal horn. No significant treatment effects were observed in naïve or injured groups, however collapsed data sets revealed a significant injury effect for increased $CGRP^+$ fiber densities in the L6/S1 segment. CC=central canal. n=3 naïve + vehicle; n=3 naïve + RAP (3 mg/kg); n=7 SCI + vehicle; n=7 SCI + RAP (3 mg/kg). Symbols are means ± SD. * $p < 0.05$ naïve vs. SCI groups.

3.4 Discussion

While the mTOR pathway has been targeted as a modulator of post-traumatic plasticity as well as pain development, no studies have examined the effects of mTOR inhibition on cardiovascular and autonomic dysfunction after SCI. Herein we report that prolonged every-other-day rapamycin treatment leads to elevated resting blood pressure, increased blood pressure volatility, and exacerbated weight loss after experimental SCI. While the extent of MAP increases relative to 30-second baseline during noxious CRD was unaltered by treatment, the baseline MAP preceding CRD was significantly higher at 14 and 21 DPI, and the absolute magnitude of CRD-induced MAP was significantly higher three-weeks post injury in rapamycin treated rats.

It is unclear whether the higher resting blood pressure, in conjunction with the increased frequency of sAD and decrease in body weight, contributed to the higher attrition we recorded in rapamycin-treated rats after SCI. Since there were no treatment effects on the sprouting of c-fiber afferents or c-Fos expression in interneurons, these confounding cardiovascular effects of rapamycin after SCI appear to result from other unidentified central and/or peripheral mechanisms. Moreover, these results indicate that, unlike hippocampal pathways after traumatic brain injury (Guo et al., 2013), intraspinal plasticity of ascending nociceptive pathways contributing to AD after SCI is not dependent upon mTOR signaling. Although we did not investigate the effects of a single administration of rapamycin at a clinically relevant time-point, our data

show that the adverse cardiovascular effects started soon after the first drug administration. Notably, there were trends for increased daily MAP and sAD in the SCI + rapamycin group as early as 2-3 days post-injury, and given our every-other-day treatment paradigm, this suggests that a single dosage immediately after SCI can elicit adverse cardiovascular effects. This would again support a mechanism that is not dependent upon inhibiting intraspinal plasticity, but rather altering resistance of peripheral vasculature.

The marked increase in sAD events in SCI rats treated with rapamycin may stem from a lowering of the threshold needed for afferent stimulation to trigger an AD event. For instance, long-term treatment of cancer patients and organ transplant recipients with mTOR inhibitors, including rapamycin and closely associated derivatives such as everolimus, increases the incidence of pain development (Budde et al., 2011; Massard et al., 2010; McCormack et al., 2011; Molina et al., 2008). Moreover, rapamycin also induces significant tactile hypersensitivity in both naïve and spinal nerve ligated rodents(Melemedjian et al., 2013). Chronic mTOR inhibition can result in over-activation of the extracellular signal-regulated kinase (ERK) signaling pathway in sensory neurons, purportedly through disinhibition of the insulin receptor substrate (IRS) which functions upstream of ERK (Melemedjian et al., 2013). Notably, ERK activation is involved in the regulation of nociceptive neurons (Karim et al., 2001; Melemedjian et al., 2010), suggesting that prolonged rapamycin treatment may increase nociceptor sensitivity by inducing feedback stimulation of the ERK pathway. Such feedback stimulation may lower the threshold of afferent stimulation needed to trigger AD, thus increasing the frequency of sAD in rapamycin-treated SCI rats independent of structural plasticity associated with the development of AD (Cameron et al., 2006; Hou et al., 2008).

Conversely, a number of studies suggest that rapamycin treatment can prevent the development of pain after SCI. A single intraperitoneal injection of rapamycin given 4 hours after T10 contusion SCI in mice suppresses microglial activation and neuropathic pain weeks after injury (Tateda et al., 2017). Similarly, pharmacological inhibition of mTOR has been associated with reduced CGRP

protein expression in the spinal cord after traumatic SCI in rats (Wang et al., 2016). A single intrathecal infusion of rapamycin (10 μg) or LY294002 (10 μM), an inhibitor of the upstream PI3K, administered after SCI attenuates injury-induced increases in CGRP protein expression in the dorsal horn (Wang et al., 2016). This finding was in correlation with reduced indices of neuropathic pain after SCI, suggesting that acute and local rapamycin administration attenuates the development of neuropathic pain after injury by disrupting the production or release of CGRP in the spinal cord dorsal horn. Importantly, our findings instead show that prolonged i.p. rapamycin administration does not change $CGRP^+$ fiber density in the lumbosacral cord but suggests that it may possibly increase nociceptive neurotransmission as indicated by a significantly higher frequency of spontaneous AD events. These opposing effects of rapamycin on CGRP expression may be due to the difference in route and length of rapamycin administration, possibly reflecting an unintended feedback stimulation of ERK (Melemedjian et al., 2013) or other nociceptive signaling pathways in our chronic treatment paradigm. In support of this notion, in-vitro and in-vivo studies suggest that prolonged versus acute rapamycin administration has differential effects on metabolism and cellular signaling (Fang et al., 2013; Sarbassov et al., 2006).

Regarding the significantly increased basal MAP with rapamycin treatment, it is important to note that both resting and orthostatic hypotension are clinically vital issues, particularly for individuals with severe cervical or high-thoracic SCI (Frankel et al., 1972; Furlan and Fehlings, 2008). Therefore, treatments capable of increasing resting MAP may be therapeutically valuable for the SCI population. Similar to previous reports (Laird et al., 2006; Mayorov et al., 2001; Rabchevsky et al., 2012; West et al., 2015), we observed that SCI resulted in a decreased daily MAP lasting for several days that gradually returned to near-normal levels within three weeks post-injury in vehicle-treated rats. Conversely, the acute decrease in daily MAP after SCI was followed by significant elevations in daily MAP in rapamycin-treated rats within approximately one week after injury. In fact, the daily MAP levels reached were higher than pre-injury levels or even controls, indicating that prolonged rapamycin treatment may alleviate

symptoms associated with hypotension, such as weakness and dizziness. We did not, however, examine daily systolic blood pressure to assess whether prolonged rapamycin treatment after complete SCI significantly increases resting systolic blood pressure to potentially harmful levels.

We observed that rapamycin significantly exacerbated injury-induced weight loss and prevented rats from returning to their pre-injury weight. A significant decrease in body weight has been observed in naïve male Wistar rats treated daily for 3 weeks with Sirolimus (i.p. 2 mg/kg), which is a clinical formulation of injectable rapamycin (Deblon et al., 2012). This was associated with significantly decreased food intake, suggesting that the effects of rapamycin on body weight are mediated through changes in appetite and energy intake. Single i.p. injections of rapamycin are sufficient to reduce daily food intake and weight gain for several days in naïve rats (Hebert et al., 2014). Notably, the effects of such injections on body weight persisted for at least 10 weeks, indicating that a singly dosage of rapamycin can cause a permanent shift in body weight set point. Hypothalamic mTOR activity is thought to play a role in the control of feeding, as intracerebroventricular delivery of rapamycin decreases food intake in rats treated with the appetite-stimulating hormone, ghrelin (Martins et al., 2012). Although we did not monitor food intake in our study, it is possible that the effects of rapamycin we observed in both naïve and SCI rats are due, at least in part, to changes in feeding behavior since rapamycin can cross the blood-brain barrier (Cloughesy et al., 2008). Importantly, it is also possible that the significant reduction in body weight following rapamycin treatment in our study, in conjunction with the elevation in resting blood pressure, contributed additional stress to the cardiovascular system. There are documented associations between body size and arterial load (Chirinos et al., 2009), indicating that the relatively rapid loss in body that we observed, in conjunction with the elevated resting MAP, contributed to overall toxicity and the increased attrition rate observed in the SCI + RAP group.

While the change in MAP relative to the baseline calculated from the 30 seconds prior to CRD was not altered by rapamycin treatment, the absolute

magnitude of blood pressure reached during CRD was significantly higher in SCI + rapamycin rats 3 weeks after injury. This elevation in absolute CRD-induced MAP indicates that rapamycin treatment has cardiophysiological consequences which could potentially increase the secondary consequences of AD, including stroke or hypertensive encephalopathy (Bjelakovic et al., 2014; Valles et al., 2005). There are other reports of hypertension induced by rapamycin in otherwise healthy rats. Daily oral administration of 1 mg/kg rapamycin to male Wistar rats for 7 weeks significantly elevated systolic (115 mmHg to 148 mmHg) and diastolic (99 mmHg to 126 mmHg) blood pressure compared to vehicle-treated rats (Reis et al., 2009). This rapamycin-induced hypertension was associated with significantly elevated levels of plasma serotonin (5-hydroxytryptamine; 5-HT). Because vasoactive plasma 5-HT can cause vasoconstriction in multiple vascular beds (Watts et al., 2012), such rapamycin-induced increases in plasma 5-HT may manifest as increased peripheral vascular resistance and resting blood pressure. While we did not measure plasma 5-HT, it is feasible that the increased resting MAP observed in our study following prolonged rapamycin treatment was due to such alterations in plasma 5-HT. Given our peripheral (i.p.) route of drug administration, we are unable to delineate whether the rapamycin-induced hypertension seen in our SCI model was due to central or peripheral sites of action.

Although rapamycin treatment did not significantly increase daily HR after injury, it is feasible that the slightly higher HR in rapamycin animals contributed to the significant increase in daily MAP. One possible mechanism for such a tachycardia-mediated increase in MAP is through increasing cardiac output (CO), which can be described as the product of stroke volume (SV) and heart rate (CO=SV x HR). In relation to MAP, which is broadly determined as the function of cardiac output and peripheral resistance (MAP=CO x PR), the enhancement in CO could increase MAP in the absence of modified peripheral resistance (Mayet and Hughes, 2003). In our injury model, supraspinal sympathetic control of the heart remains intact as the heart is innervated by T1-T3 SPNs (Sundaram et al., 1989). Moreover, evidence suggests that mTOR activity in the hypothalamus is

involved in the regulation of blood pressure and sympathetic nerve activity (Harlan et al., 2013), and hypothalamic mTOR controls feeding behavior that could partially explain both the decreased body weight and increased daily MAP in SCI + rapamycin animals in our study.

Other studies have investigated rapamycin as a neuroprotective agent after contusion SCI. A single 1 mg/kg (i.p.) dosage of rapamycin administered 4 hours after SCI in mice increases tissue sparing and functional recovery correlated with augmented cell autophagy (Sekiguchi et al., 2012). Injections of 1 mg/kg (i.p.) of rapamycin daily for 3 days starting 4 hours after SCI in rats also promotes neuronal survival by attenuating inflammatory responses (Song et al., 2015). A dosage of 6 mg/kg rapamycin (i.p., every other day) administered for three weeks post-injury in rats normalizes increased mTOR activity after complete T10 transection in combination with passive exercise (Liu et al., 2012). Whether the adverse cardiovascular effects of rapamycin we noted occur in the more clinically relevant contusion SCI model remains uncertain, although rodent contusion models of AD exist to test this (Squair et al., 2017).

3.5 Conclusion

While we sought to determine whether inhibiting mTOR activity with rapamycin could mitigate the development of AD by preventing injury-induced intraspinal plasticity, we found instead that rapamycin evoked significant physiological alterations in rats with complete high-thoracic SCI, including exacerbated body weight loss, increased resting blood pressure, increased spontaneous AD events, and an increase in the absolute magnitude of CRD-induced AD. Since inhibition of mTOR activity with rapamycin did not correlate with altered injury-induced sprouting of nociceptive afferents or activation of propriospinal neurons after noxious CRD, this indicates that mTOR does not act as a critical mediator of maladaptive plasticity thought to underlie AD. More broadly, the adverse cardiovascular effects are due to other unidentified central and/or peripheral mechanisms that could arise from actions of rapamycin on dorsal root ganglia, peripheral sympathetic ganglia, or cardiovascular

mechanisms involved in the modulation of peripheral vascular resistance. Critically, since cardiovascular complications after SCI are among the top health concerns clinically, studies investigating rapamycin as a neuroprotective therapy for SCI must take precaution in interpreting any outcome measures without considering unmonitored risks to already compromised cardiovascular and autonomic functions.

Note:

This chapter has been reprinted with permission from Mary Ann Liebert, Inc.: Khalid C. Eldahan, David H. Cox, Jenna L. Gollihue, Samir P. Patel, and Alexander G. Rabchevsky. (2018) Rapamycin Exacerbates Cardiovascular Dysfunction after Complete High-Thoracic Spinal Cord Injury. Journal of Neurotrauma. March 15 2018 DOI: 10.1089/neu.2017.5184

Copyright © Khalid C. Eldahan 2019

CHAPTER 4

Assessing Continuous High Dose Gabapentin Delivery for the Treatment of Autonomic Dysreflexia

4.1 Introduction

The spinal cord is a critical component in the central control of the cardiovascular and autonomic nervous systems. Accordingly, traumatic spinal cord injury (SCI) can result in a constellation of related cardiovascular and autonomic dysfunctions (Hou and Rabchevsky, 2014; Weaver et al., 2012), notably with injuries above the sixth thoracic (T6) segment frequently resulting in the development of a condition called autonomic dysreflexia (AD). This syndrome is characterized by episodes of volatile and potentially lethal hypertension in response to exaggerated sympathetic reflexes triggered by unperceived afferent stimuli below the injury level. As described in **Chapter 2**, patients may experience cardiac arrhythmia, pounding headache, anxiety, flushing of the skin and profuse sweating above the lesion during an episode of AD. For many people with AD, this episodic syndrome can occur frequently throughout the day due to regular filling of the bowel and bladder creating noxious stimuli, or by irregular and less predictable triggers such as pressure sores and seemingly benign over-tightening of shoes or clothing (Fougere et al., 2016b; Hubli et al., 2015; Squair et al., 2017). Because of the unpleasant and potentially dangerous manifestation of this syndrome, prevention or effective treatment of AD is cited as a top priority in the SCI population for enhancing quality of life (Anderson, 2004).

Several injury related mechanisms are known to contribute to the development of AD. These include the loss of descending vasomotor modulatory pathways, hyperreactivity of peripheral vasculature to adrenergic stimulation, and a number of pathophysiological changes within spinal circuitry influencing sympathetic outflow below the lesion (Cameron et al., 2006; Eldahan and Rabchevsky, 2018; Rabchevsky, 2006; Schramm, 2006; Teasell et al., 2000). These intraspinal changes include sprouting of both unmyelinated afferent c-fibers and ascending propriospinal ‘relay’ projections towards sympathetically-

correlated neurons in the thoracic spinal cord (Rabchevsky, 2006). In addition to structural sprouting, dynamic alterations of synaptic inputs to sympathetic preganglionic neurons (SPN) in the thoracolumbar cord are also known to occur. For example, synapses derived from descending supraspinal projections onto SPN are eliminated within one week after complete spinal transection at the fourth thoracic (T4) segment (Llewellyn-Smith and Weaver, 2001; Weaver et al., 1997). However, by two weeks after transection there is a restoration of the number of synaptic terminals on SPN to normal levels indicating the formation of new synaptic inputs derived from spinal interneurons and/or primary afferents below the injury. Because the development of AD also becomes apparent two-weeks after SCI in rodents (Krassioukov and Weaver, 1995; Laird et al., 2006), it has been suggested that injury induced synaptogenesis onto SPN contributes to AD pathophysiology (Eldahan and Rabchevsky, 2018; Llewellyn-Smith and Weaver, 2001; Weaver et al., 1997). Taken together, a model of AD development has emerged in which the loss of supraspinal control, coupled with increased synaptic convergence from both primary afferents and interneurons onto sympathetically correlated interneurons, enhances the transmission of noxious stimuli to SPN, triggering unrestricted sympathetic reflexes during AD. As part of this model, synaptogenesis of newly sprouted c-fiber terminals onto lumbosacral propriospinal neurons is thought to be involved in the etiology of AD, however this has remained unexamined (Rabchevsky, 2006).

We previously reported that in rats with complete T4-transection SCI, acute administration of the epilepsy drug gabapentin (GBP; 50 mg/kg, i.p.) significantly reduces the magnitude of colorectal distension (CRD) induced AD and tail spasticity shortly after treatment (Rabchevsky et al., 2011; Rabchevsky et al., 2012). The mechanism of this clinically valuable effect, however, remains unknown. GBP was first developed for the treatment of epilepsy and gained subsequent traction as a treatment for neuropathic pain (Sirven, 2010). Despite being a structural analog of y-aminobutyric-acid (GABA) with enhanced blood-brain barrier penetration (Crawford et al., 1987), most studies suggest that it's actions are independent of GABAergic modulation. Purification and binding

studies revealed GBP's high-affinity binding site as the L-type calcium channel $\alpha_2\delta$ subunits (Gee et al., 1996). This discovery suggested that GBP may act by modulating calcium channel activity and, subsequently, reducing presynaptic neurotransmitter release. Others have demonstrated that large daily doses of GBP can block the formation of excitatory glutamatergic synapses in the CNS by interfering with the action of thrombospondin proteins (Baldwin and Eroglu, 2017; Eroglu et al., 2009). Thrombospondins are extracellular proteins secreted by astrocytes and are believed to play a role in astrocyte-induced synaptogenesis (reviewed in Baldwin and Eroglu, 2017). Upon binding to the $\alpha_2\delta_1$ subunit, thrombospondin-4 can activate synaptogenic signaling to drive the formation of new glutamatergic synapses. By competing with thrombospondin for the same $\alpha_2\delta_1$ binding site, GBP treatment has been shown to prevent aberrant excitatory synapse formation in models of facet joint injury (Crosby et al., 2015), cortical trauma (Lau et al., 2017; Li et al., 2012b; Takahashi et al., 2018), neuropathic pain (Li et al., 2014; Yu et al., 2018) as well as regular neonatal development (Eroglu et al., 2009). Based on these studies which together suggest this mechanism may underlie the clinical actions of GBP, we sought to determine whether continuous high dose GBP treatment after SCI can prevent aberrant synaptogenesis of intraspinal pathways and thereby mitigate the development of AD.

4.2 Methods and Materials

4.2.1 Cardiophysiological monitoring:

All animal housing conditions, surgical procedures, and postoperative care were conducted according to the University of Kentucky Institutional Animal Care and Use Committee and the National Institutes of Health animal care guidelines. Animals were housed in a temperature and humidity-controlled room with a 12/12-hour light/dark cycle. Efforts were made to minimize unnecessary foot traffic and other potential environmental disturbances in the room. One week prior to SCI, a total of 24 naïve 3 to 3.5 month old female Wistar rats (250-275 grams) were anesthetized (2% isoflurane) and implanted with telemetric blood

pressure transmitters (model HD-S10, Data Sciences International, Inc., St. Paul, MN) into the descending abdominal aorta according to the manufacturer's surgical guidelines as previously reported (Eldahan et al., 2018; Rabchevsky et al., 2012). Telemetry probes were secured intra-abdominally by tying to the ventral abdominal wall using non-absorbable silk sutures before closing the skin with 3-0 vicryl sutures. Animals were then treated post-operatively as described below. Blood pressure was recorded 24/7 (500 Hz sampling rate) using the Dataquest A.R.T. acquisition platform (Data Sciences International, Inc., St. Paul, MN) for the duration of the study. Recordings were briefly paused during daily animal care and re-started immediately. Rats were single-housed, with each cage placed directly on top of its corresponding data receiver plate (model RPC-1, Data Sciences International, Inc., St. Paul, MN). All recordings were binned in a single parent folder and later analyzed in 24-hour segments beginning at 6 a.m. each day which corresponds to the beginning of the light-cycle. "One day post-injury" is defined as the time immediately after SCI (approximately 9:30 a.m.) until 6 am the following day. All days thereafter were defined as 6 a.m. to 5:59 a.m. the following day.

Naturally occurring spontaneous AD (sAD) was analyzed using a modified version of our previously reported custom computer algorithm using Matlab software (The MathWorks, Inc., Natwick, MA) (Eldahan et al., 2018; Rabchevsky et al., 2012). Our modified algorithm screens for instances of multiple sAD detections occurring within a 120-second window, such that multiple events beginning within two minutes of each other are counted as a single unified event, similar to recent AD algorithms described by West et al. (2015) and Mironets et al. (2018). The algorithm simultaneously processes 24-hour mean arterial pressure (MAP) and heart rate (HR) traces for instances where a rise in MAP of either 10 or 20 mmHg or more above baseline is accompanied by a decrease in HR of at least 10 or 20 beats per minute. While this algorithm does not require such events to be sustained above baseline for a specific duration, it does require the rise in MAP over baseline to occur within a 35-second window. MAP rises that were accompanied by tachycardia (an increase in HR) were not

included in these sAD detections. Following automated computer detected sAD events, a single human observer manually screened all detections to remove false-positive events stemming from technical artifacts, such as non-physiological rises in MAP associated with movement of the pressure-sensing catheter tip against the lumen of the aorta. For each of the four daily injections (12:00 a.m., 6:00 a.m., 12:00 p.m. and 6:00 p.m.), recordings were stopped simultaneously for all animals and an "event marker" was placed for each animal immediately after injection to allow for accurate tracking of all injection timepoints. Routine animal care, including twice daily bladder expression for the duration of the study, was performed at 6 am and 6 pm along with corresponding treatment injections. Cardiophysiological recordings were paused any time a cage was moved or an animal was handled to ensure that such disruptions were not included in any analyses.

4.2.2 Baroreflex Sensitivity

To test the hypothesis that continuous high doses of GBP suppress the cardiac baroreflex after SCI, we quantified the sensitivity, or "gain", of the spontaneous baroreflex (sBR) in saline and GBP treated rats one day before injury and the start of treatment as well as 14, 21 and 28 DPI. Assessment of the sBR sensitivity was performed using the sequence technique developed by Bertinieri et al. (1985). This method identifies sequences of at least three consecutive pressure pulses in which there is a positive relationship between systolic blood pressure and inter-beat interval, (i.e. heart rate). Linear regression plots are then created from identified sequences and the average slope of the fitted lines was calculated to indicate the sensitivity, or "gain" of the sBR (**Figure 4.9**). HemoLab software written and freely distributed by Dr. Harold Stauss was used for this analysis. Two-hour segments of raw waveform blood pressure data were selected at the same time of day for all animals. Peak systolic pressure values were used to calculate the pulse intervals to compare the relationship between blood pressure and heart rate. All detected sBR sequences were

visually screened to remove abnormal detections caused by technical artifacts which would otherwise skew the average slope of the regression lines.

4.2.3 Spinal cord injury

All rats were allowed to recover from telemetry probe implantation for one week. We have observed that elevated daily blood pressure and heart rate occurring following the abdominal probe implantation return to a normal level by 5 days post-implantation. A total of n=24 rats were anesthetized (ketamine, 80 mg/kg; xylazine 7 mg/kg i.p.) and underwent a T3 laminectomy prior to complete transection of the T4 spinal cord (T4Tx) using a scalpel blade, as previously described (Cameron et al., 2006; Rabchevsky et al., 2012). Two independent observers confirmed complete spinal cord transection of each rat based on full separation of the rostral and caudal stumps. Immediately afterwards, a square gelfoam pledget was placed into the transection site to achieve hemostasis and the overlying muscles were sutured with 3-0 vicryl before stapling the skin with wound clips (Stoelting, Wood Dale, IL).

4.2.4 Drug Administration and Noxious Colorectal Distension (CRD):

Gabapentin (GBP; 100 mg/kg, i.p, 4x daily, Spectrum Chemicals, New Brunswick, NJ) was injected after injury and then every 6 hours for 4 weeks. On days 14, 21 and 28 post-injury, rats were subjected to 2 trials of colorectal distention one hour after treatment using silicone balloon catheters (Coloplast Cysto-Care Folysil 2-Way Pediatric Silicone Foley Catheter, Fr10 3 cc) inserted into the rectum. Bladder expression was performed immediately prior to catheter insertion. Rats were gently restrained using a surgical towel wrapped around each rat, leaving the lower body exposed to avoid over-heating and allow for observation of hindlimb spasticity during CRD. After removing fecal pellets in the distal rectum, catheters were inserted a distance of 2.5 cm from the center of the balloon and secured to the tail with two pieces of Transpore ™ tape. Following restraint and catheter insertion, rats were allowed to acclimate for 20-30 minutes. All efforts were made to minimize distractions and potentially stressful stimuli. A

hood fan was left running to provide white noise and buffer unpredictable, irregular sounds occurring outside of the experimental room. All CRD testing was performed in the same room that all animals were regularly housed in. For each distention cycle, the balloon was inflated with 2.2 mL of air over the course of 5 seconds. Each distention trial lasted 60 seconds, separated by 30 minutes of rest. At 28 DPI, following the second CRD trial, a 90-minute session of intermittent CRD (30-second inflation periods separated by 60 seconds of rest) was performed to induce c-Fos expression. To quantify the MAP recovery time after CRD, the length of time required for the MAP trace to revert back to the 30-second baseline value was measured for each CRD trial using a modification of the methods used by Mironets et al. (2018) and Cloutier et al. (2016). Notably, the MAP was required to remain at or below the 30-second baseline value for at least 6 seconds before being considered stably recovered.

4.2.5 Tissue Collection and Immunohistochemistry

Terminal body weights were recorded and rats received a fatal overdose of sodium pentobarbital within 15-minutes following the end of the 90-minute CRD. After the loss of pinch-reflex in the forelimbs, a lateral abdominal incision was made to access the spleen. Bulldog clamps were applied to the vascular bundle serving the spleen before rapid dissection. Rats were then transcardially perfused with 0.1M PBS followed by 4% PFA (in 0.1M PBS). Excess fat and connective tissue was removed from the spleens using and raw spleen weights were measured prior to soaking them in 4% PFA overnight. The spinal cord caudal to the T4-transection site was carefully dissected and post-fixed for 3-4 hours in 4% PFA before being placed in 0.2M PB solution overnight at 4° to remove excess PFA. Cords were then cryopreserved in 20% sucrose (in 0.1M PBS) with sodium azide until all cords sank, after which they were embedded in gum tragacanth mixed with 20% sucrose and stored at -80° until cryosectioning. Every fifth serial cryosection (uM) was collected and placed on a series of Superfrost Plus™ slides (Thermo Fisher Scientific, Waltham, MA). This cutting scheme results in 10 adjacent sets of slides with each slide containing 10

consecutive spinal sections separated by 1mm. Slides were stored at -20 degrees C until further use. For immunohistochemistry, slides were removed from the freezer and warmed on a 37 degree slide warmer for 10 minutes. A pap-pen (Ted Pella, Redding, CA) border was then applied to all tissue slides before washing 3 x 30 minutes in 0.1M PBS. Slides were then blocked for 1-hour at room temperature in 5% normal serum and 0.3% Triton X-100 in 0.1M PBS. To immunoreact tissue sections with primary antibodies, slides were incubated for either 24-hours (VGLUT2 and synaptophysin) or 72-hours (VGAT) in primary antibody buffer containing 2 ug/ml rabbit anti-VGLUT2 (Synaptic Systems Cat #135-403) and 1 ug/ml mouse anti-synaptophysin (Clone SY3; Synaptic Systems Cat #101-011), or rabbit anti-VGAT (Synaptic Systems Cat #131-002) and 1:1,000 mouse anti-synaptophysin (Synaptic Systems Cat #101-011). Excess primary antibodies were washed 3x10 minutes in 0.1 M PBS before incubation with secondary antibodies (Goat anti-Rabbit-Alexa488 @ 1:500 or biotinylated goat anti-mouse @ 1:200) for 24-hours at 4 degrees. Following removal of excess secondary antibody with 3x10 minute 0.1 M PBS washes, slides were incubated in tertiary solution containing 1:200 streptavidin conjugated Texas Red in 0.1 M PBS. Two batches of tissue staining were performed: one with VGLUT2 and synaptophysin, and the second set with VGAT and synaptophysin. Within each batch of staining, all treatment groups were stained simultaneously using the same buffers and lot of antibody. Due to availability, separate lots of synaptophysin antibody were used in each staining set.

4.2.6 Image Acquisition and Analysis

High-resolution (2048 x 2048 pixels) images were collected using a Nikon Ti Eclipse inverted confocal microscope paired with a C2+ controller system and Nikon NIS Elements Advanced Research software (Nikon Inc., Melville, NY, USA). Laser settings for each fluorescent marker were optimized on naïve spinal cord tissues and maintained constant for all sections assessed. The histogram was used to monitor pixel intensity and ensure that the total fraction of saturated pixels remained below 2% for all images. For each tissue section, confocal

stacks were collected with a 40x oil-immersion lens. Image stacks were acquired by setting the central plane of the tissue section as “home”, and acquiring two additional optical sections 2 μM above and below the central plane (4 μM total thickness). Each optical section represented a thickness of 0.86 μM, with an individual pixel size of 0.16 μM. The pinhole size was maintained at 40 μM, and pixel dwell time set to 4.4 seconds/pixel. After image acquisition, the optical plane with the most uniform staining was selected for analysis. This selection was performed objectively in an unbiased and blinded fashion by selecting the optical plane with the highest mean fluorescence intensity within the desired region of interest measured by the Nikon software. Similar selection of the optical plane with the brightest staining has been used previously to help correct for potential issues with antibody penetration (Ferguson et al., 2008).

Synaptic quantification was performed using densitometric analysis. For each subject, 3 spinal sections centered on the L6/S1 spinal segment and separated by 1 mm were analyzed (**Figure 4.1**). The right dorsal horn was used for all animals, with the rare exception of tissue sections where the right horn was unusable due to folding of the section on the slide during tissue processing, in which case the left dorsal horn was used. A local contrast was applied using a radius of 1.0 μM to more clearly delineate the border of individual synaptophysin^{+}, VGLUT2^{+} and VGAT^{+} puncta. Thereafter, each fluorescent channel was thresholded to exclude non-specific background signal. All contrast and threshold settings were optimized on naïve spinal cord tissues and remained constant for all subjects thereafter (see **Figure 4.2**). After applying a threshold for each fluorescent channel, a binary layer mask was created for each marker (VGLUT2 or VGAT and synaptophysin) indicating the location of pixels above threshold. These two layers (VGLUT2 and synaptophysin or VGAT and synaptophysin) were then overlaid to create a third layer representing the area of overlap between markers. Using these three binary layers, either the area occupied by VGLUT2, VGAT, synaptophysin or the area occupied by the overlap of VGLUT2/synaptophysin and VGAT/synaptophysin puncta was measured using a standardized region of interest box measuring 175 x 175 μM. One ROI,

designated “R1”, represented the upper dorsal horn (rexed laminae I-II). The top of the ROI box was aligned with the upper edge of lamina I, and the box was centered in the middle of the right dorsal horn. The bottom of the ROI box extended to the approximate lower edge of laminae II. The other ROI, designated “R2”, was similarly sized 175 x 175 μM and placed in the dorsal grey commissure (laminae X) just above the central canal. To control for potential variation in antibody labeling efficiency between sets of synaptic staining, data was normalized to naïve control values within a respective set of staining. These methods were adapted from McKillop et al. (2016), who used a threshold-based method to quantify the area occupied by VGLUT1, synaptophysin and VGAT in the mouse spinal ventral horn after SCI.

Quantitative colocalization analysis was also performed using the JACoP plugin (https://imagej.nih.gov/ij/plugins/track/jacop.html) implemented in the ImageJ/FIJI platform. This plugin, which has previously been described in depth (Bolte and Cordelieres, 2006), contains a collection of commonly used tools to measure intensity correlation and co-occurrence of dual-color molecular probes. The same ROIs used for density analysis were cropped for JACoP analysis. To reduce confounding influences of non-specific background pixels, a threshold was applied to restrict analysis to pixels containing positive staining. The Costes’ automated thresholding algorithm was determined to yield inappropriately low thresholds, likely due to the high density of labeling and variability of pixel intensity which others have reported to be problematic for appropriate automated thresholding and image segmentation (Comeau et al., 2006; Dunn et al., 2011; Verstraelen et al., 2018). Therefore, threshold values were determined based on the background pixel intensity in a set of negative primary antibody control slides processed and imaged using identical settings. These threshold values were visually validated on a set of naive group images and subsequently applied equally to all images/treatment groups. The Manders overlap coefficient (MOC) and fractional overlap coefficients (tM1 and tM2) were calculated using the equations below, notably only using supra-threshold pixels with positive staining to avoid inflated results due to low-level background signal. To determine the

likelihood that positive colocalization results could be due to chance, the Costes' randomization test was run on a subset of images. The resulting P values[1] were 100%, along with r-values of 0.0±0.001, indicate that virtually none of the colocalization measured in our original images could be attributed to random chance.

$$MOC = \frac{\sum_i (R_i \times G_i)}{\sqrt{\sum_i R_i^2 \times \sum_i G_i^2}}, \qquad tM1 = \frac{\sum_i R_{i,coloc}}{\sum_i R_i}, \qquad tM2 = \frac{\sum_i G_{i,coloc}}{\sum_i G_i}$$

Where:

R_i: $pixel\ intensity\ in\ red\ channel\ (synaptophysin)$

G_i: $pixel\ intensity\ in\ green\ channel\ (VGLUT2/VGAT)$

$R_{i,coloc}$: $pixel\ intensity\ in\ red\ channel\ (synaptophysin), where\ a\ given\ pixel\ value\ is > 0\ in\ both\ channels$

$G_{i,coloc}$: $pixel\ intensity\ in\ green\ channel\ (VGLUT2/VGAT), where\ a\ given\ pixel\ value\ is > 0\ in\ both\ channels$

4.2.7 Statistical Analyses

For daily body-weight, MAP, HR, spontaneous AD and spasticity measurements, a repeated measures two-way analysis of variance (2-way RM ANOVA) was performed with Sidak's multiple comparisons post-hoc test when appropriate. The Geisser-Greenhouse correction was used for repeated measures analyses to provide additional rigor and minimize type-I errors. Unpaired t-tests were performed on CRD and spleen weight data. One-way ANOVA tests were used for synaptic histology, with Sidak's post-hoc analysis when appropriate. All statistical analyses were conducted with GraphPad Prism 7 software using alpha = 0.05.

[1] The P value, not to be confused with a *p-value*, is a measure of how likely a set of randomized images are to contain an equal or higher amount of signal colocalization than the original images. A value of 100% indicates a virtually non-existent chance that colocalization in the original image is due to random chance.

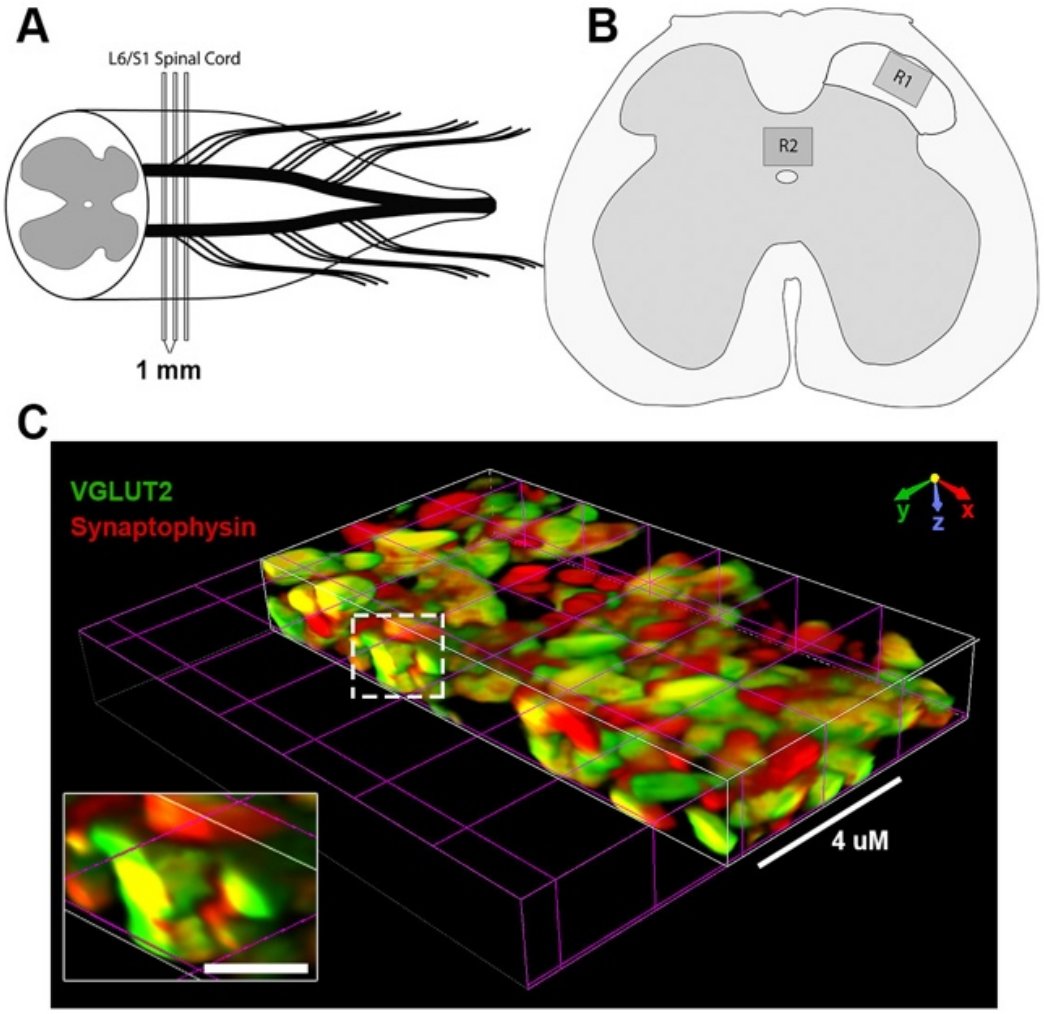

Figure 4.1. Diagrammatic representation of synaptic quantification scheme. Tissue from the L6/S1 spinal segment (**A,B**) was sampled for histological analysis of synaptic density. High-resolution confocal images were acquired from rexed laminae I-II of the upper dorsal horn (**B,** R1) and the laminae X region containing the dorsal gray commissure (**B,** R2). (**C**) Volumetric reconstruction shows colocalization of VGLUT2 and synaptophysin in 3D, indicating the co-occurrence of these presynaptic markers. Scale bar is 4 uM or 1 uM (inset, C).

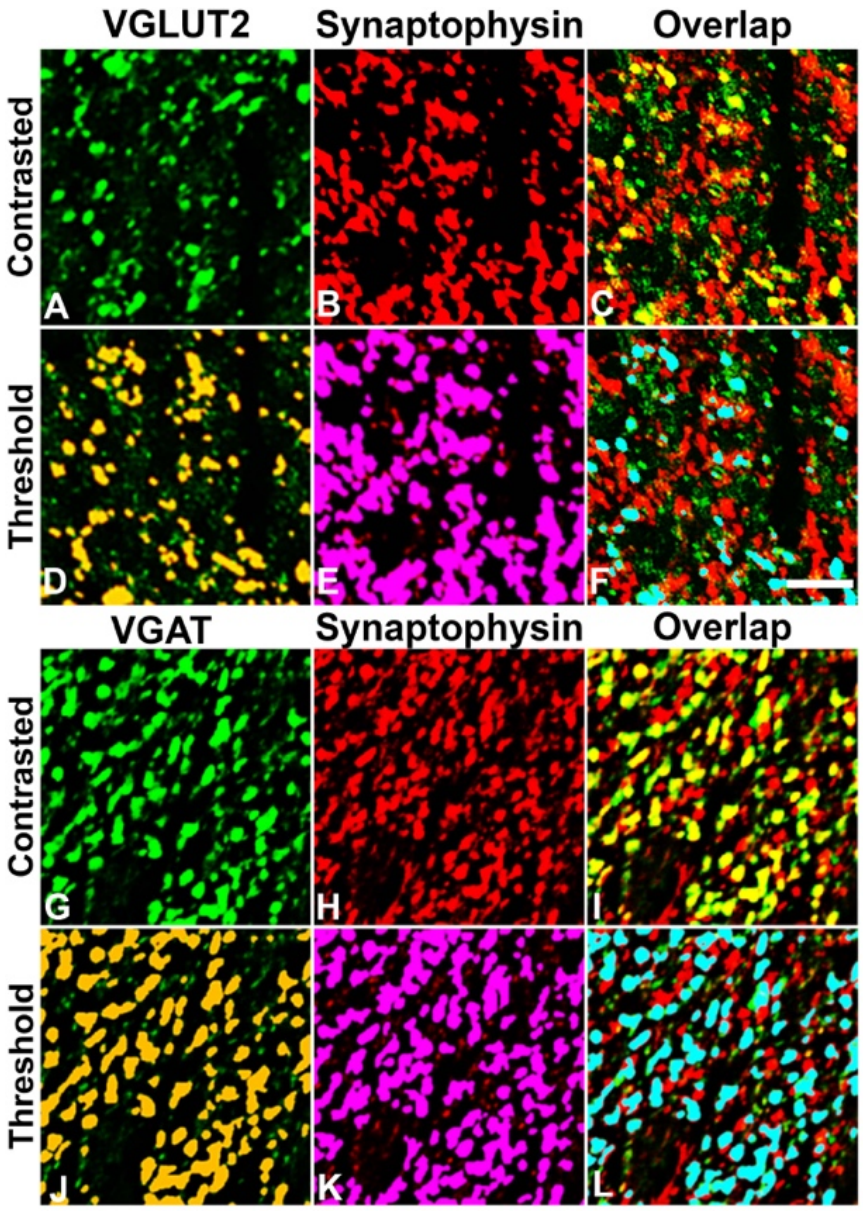

Figure 4.2. Representative thresholding and overlap identification. Adjacent tissue sections were double-labeled with VGLUT2+synaptophysin (**A-F**) or VGAT+synaptophysin (**G-L**). Contrasted images (top rows **A-C; G-I**) were thresholded (bottom rows **D-F; J-L**) to segregate positive staining from background, and a mask was applied representing supra-threshold pixels in VGLUT2 (**D**), VGAT (**J**) and synaptophysin (**E,K**) channels. Colocalization of VGLUT2+SYP or VGAT+SYP was determined based on overlapping of signal (**F,L**). Images represent a cropped and enlarged area taken from the full R1 field quantified as shown in **Figure 4.11**. Scale bar is 5 uM.

4.3 Results

We had a 13% attrition rate with early deaths occurring during recovery in the critical first week after injury and occured with similar frequency in the saline and GBP groups (n=1-2 per group).

4.3.1 GBP impairs body weight recovery after SCI

We compared the effects of time and chronic GBP treatment on the change in body weight after complete SCI and observed a significant effect of time ($p<0.0001$), but no significant treatment effect ($p=0.4197$) (**Figure 4.3**). There was, however, a significant interaction between time and treatment ($p<0.0001$). Within one-week after SCI, both groups lost a significant amount of body weight compared to their respective pre-injury values ($p<0.05$). Whereas vehicle-treated rats returned to pre-injury weight by 20 DPI, rats treated continuously with GBP did not return to their baseline body weight by the end of the study period.

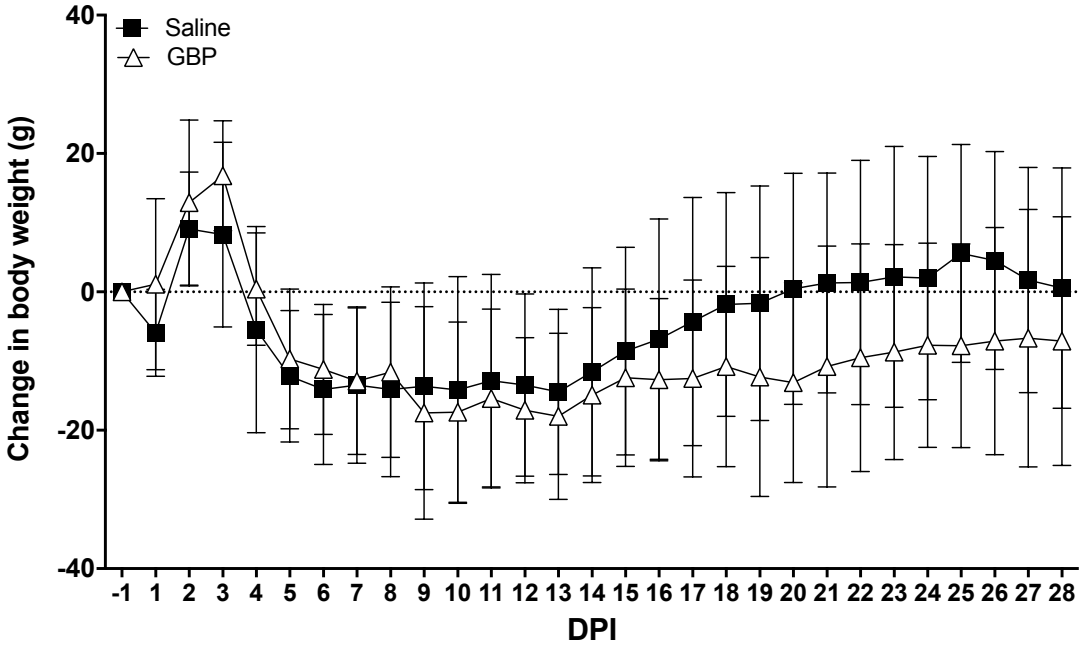

Figure 4.3. Daily change in body weight after complete spinal cord injury (SCI). All rats experienced an initial gain in weight in the first 2-3 days before

losing significant body weight for the first 2 weeks. Saline-treated control rats started to regain body weight by 14 days post injury (DPI) and returned to pre-injury weights (dotted line) by 20 DPI. In contrast, injured GBP treated rats maintained reduced body weight below pre-injury levels. N=11 Saline, N=10 GBP. Symbols are mean ± SD.

4.3.2 Daily Mean Arterial Pressure (MAP) and Heart Rate (HR) after SCI

We examined whether continuous high-dose GBP had temporal effects on daily hemodynamics post-injury. There was an overall significant effect of time post-injury ($p<0.0001$) on daily MAP (**Figure 4.4A**), with no treatment effect ($p=0.65$). Compared to pre-injury values, the daily MAP was significantly lower for the first three days post-injury (DPI) in both groups ($p<0.0.0001$) before stabilizing to slightly below naïve levels after the first two weeks post-injury. There was a significant effect of time post-injury on daily HR ($p<0.0001$), with no treatment effect ($p=0.65$). HR dropped significantly in both groups from approximately 350 beats per minute (bpm) at -1 DPI to approximately 260 bpm at 1 DPI (**Figure 4.4B**). Beginning at 2 DPI, however, daily HR was elevated in all rats to approximately 400 bpm and remained statistically higher than pre-injury values for the remainder of the study ($p<0.001$). While the mean daily HR of the GBP treated group was maintained approximately 20 bpm higher than the control group at all DPI, this observation was not statistically significant ($p=0.69$).

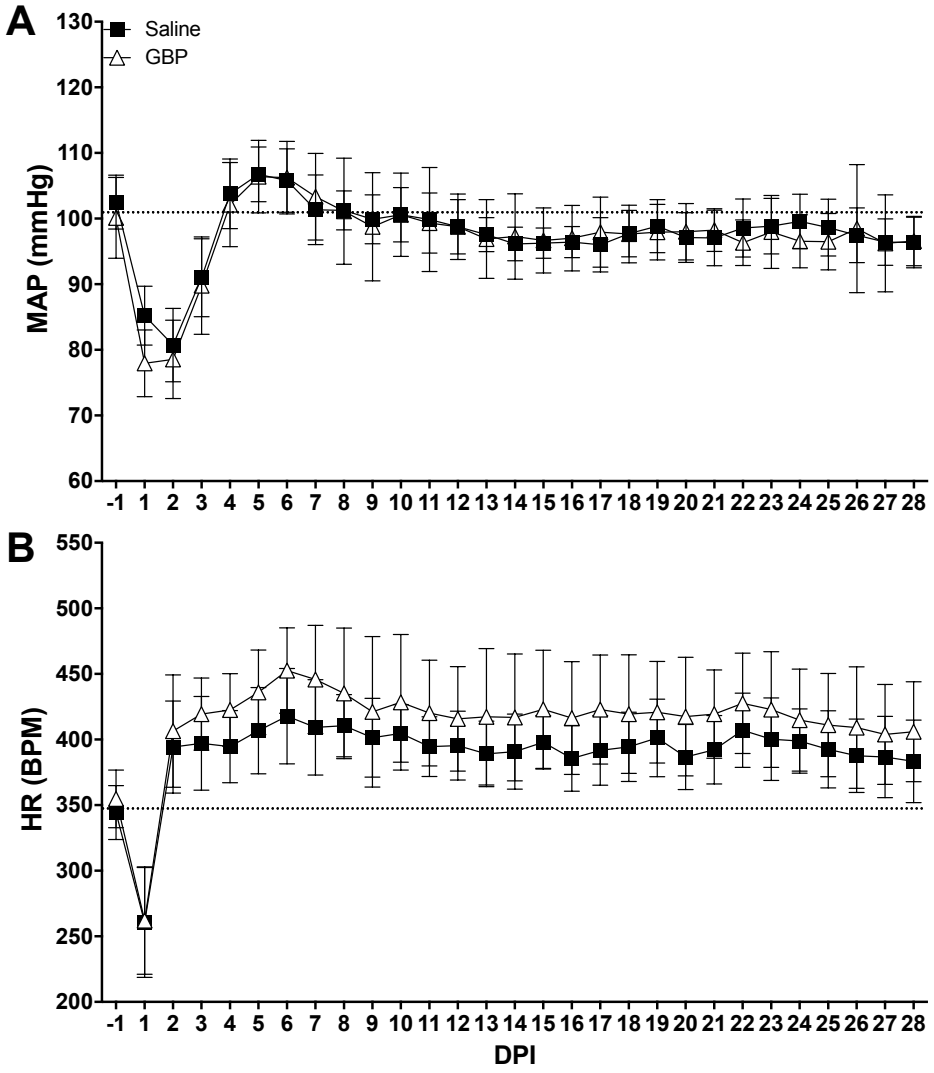

Figure 4.4. Effects of spinal cord injury and gabapentin (GBP) treatment on daily cardiophysiology. Daily (24-hour) mean arterial pressure (MAP, A) and heart rate (HR, B) measured across days post-injury (DPI). Daily MAP dropped markedly in the immediate days post-injury before returning to near-normal values after one week. The daily HR sharply decreased the first day after injury before rising above pre-injury levels beginning at 2 DPI. Dotted lines indicate pre-injury control values. N=11 Saline, N=10 GBP. Symbols are mean ± SD.

4.3.3 Spontaneously occurring autonomic dysreflexia (sAD)

Daily MAP and HR traces were analyzed with a computer algorithm to identify sAD events (**Figure 4.5A,B**). Two algorithm threshold settings were

employed to detect relatively small events (MAP increase ≥ 10 mmHg with HR drop ≥ 10 BPM; 10/10) as well as larger events (MAP increase ≥ 20 mmHg with HR drop ≥ 20 BPM; 20/20). With the 10/10 threshold settings, there was an overall effect of time post-injury ($p<0.0001$) on the frequency of sAD detections (**Figure 4.5C**). Moreover, there was an overall significant ($p=0.026$) treatment effect with GBP treated rats having a higher daily sAD frequency. The average number of daily sAD events was 16 between 14 and 28 days post-injury in the saline treated group, compared to 26 in the GBP treated group. Post-hoc multiple comparisons of individual time-points revealed a significant difference at 6 DPI ($p=0.0016$). When detection thresholds were set to 20/20, we similarly observed an overall significant effect of time ($p<0.0001$) and treatment ($p=0.0093$; **Figure 4.5D**). GBP-treated rats had significantly more events compared to the saline-treated control group. Between 14 and 28 days post-injury, GBP treated rats had an average of 4 events per day compared to 2 in the saline group. Post-hoc multiple comparisons of individual time-points revealed a significant difference at 6 DPI ($p=0.0049$). In the 10/10 data set, the pre-injury false detection rate was 0-3 events/day, which was negligible compared to post-injury detections typically between 20-40 events post-injury. Similarly, pre-injury detections rates were typically 0-1 when thresholds were set to 20/20, compared to a higher frequency of 2-7 events/day post-injury.

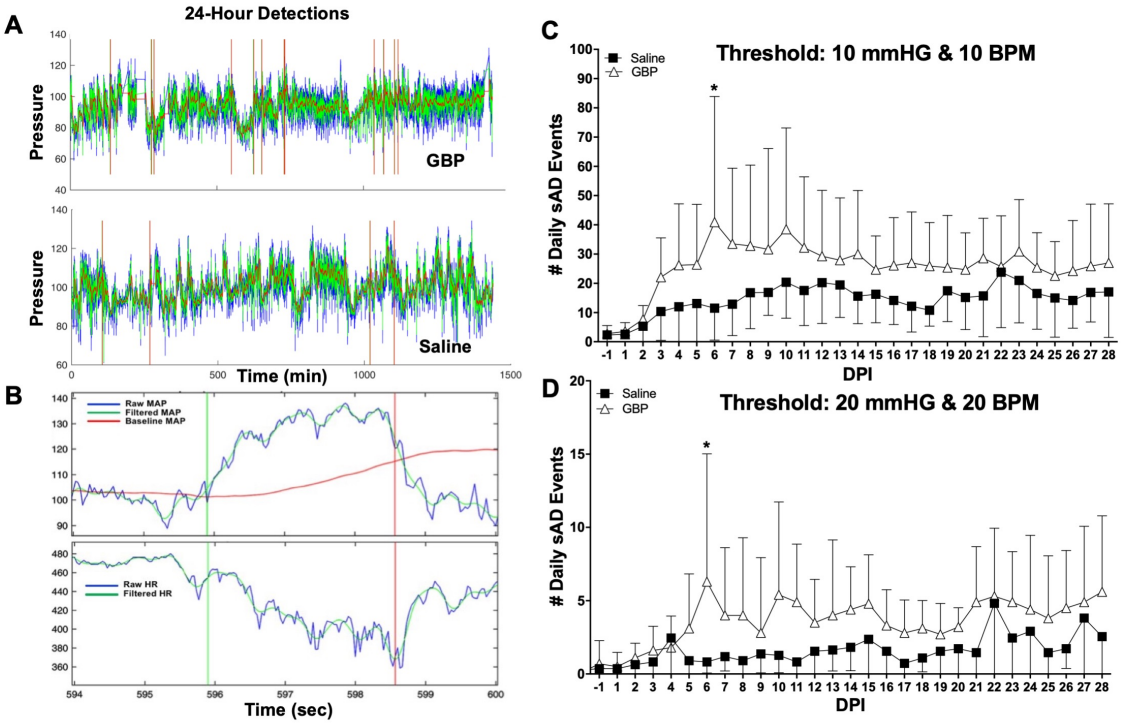

Figure 4.5. Effects of GBP treatment on the frequency of spontaneously occurring AD (sAD) after injury. Representative 24-hour traces show more overall sAD events with GBP treatment compared to saline controls (**A**; vertical bars indicate detected events). A typical event with a MAP rise >20 mmHg and HR drop >20 bpm is depicted in **B.** The frequency of small (MAP rise ≥ 10mmHg, HR drop ≥ 10 bpm; **C**) and larger (MAP rise ≥ 20mmHg, HR drop ≥ 20 bpm, **D**) sAD detections was monitored increased across days post-injury (DPI). Overall, GBP treated rats had a significantly higher frequency of both small sAD events (10/10; **C**) and larger detections (20/20; **D**) compared to saline-treated control rats. N=10 GBP, N=11 Saline. *$p<0.05$ vs saline control. Symbols represent mean ± SD.

4.3.4 Colorectal Distension-Induced Autonomic Dysreflexia

When we examined the severity of AD as assessed by the magnitude of hypertension during experimentally-induced AD, there was an overall significant treatment effect on the MAP reached during noxious colorectal distension (CRD) stimulation ($p<0.0001$; **Figure 4.6A**). GBP-treated rats had a lower MAP during CRD stimulation, with significant reductions at 21 and 28 DPI ($p<0.05$) that did not become more severe over time post-injury. In contrast, the magnitude of CRD-induced MAP became higher over time post-injury in the saline-treated group, with 28 DPI being significantly higher compared to 14 DPI ($p=0.001$).

In parallel, the baseline MAP measured immediately prior to CRD revealed an overall treatment effect ($p<0.0005$; **Figure 4.6B**), with GBP-treated rats having significantly lower baseline MAP at 21 ($p=0.0008$) and 28 DPI ($p=0.002$). The baseline MAP in saline rats did not change over time but was significantly lower at 28 DPI compared to 14 DPI in GBP-treated rats ($p=0.046$).

When the CRD-induced changes in MAP relative to baseline were measured, there was a significant effect of time ($p<0.0001$) but not treatment ($p=0.669$) on the MAP change during CRD (**Figure 4.6C**). The magnitude of change increased over time in both groups, with significant increases from 14 and 21 to 28 DPI ($p<0.05$). There was no effect of time on the change in HR during CRD ($p=0.16$), however there was an effect of treatment ($p=0.0047$). GBP significantly reduced changes in HR during CRD at 28 DPI ($p=0.012$; **Figure 4.6D**). Notably, saline-treated injured rats had typical bradycardic responses during CRD, but GBP-treated animals responded with little to no reduction in heart rate; in fact, tachycardic responses were noted in many instances.

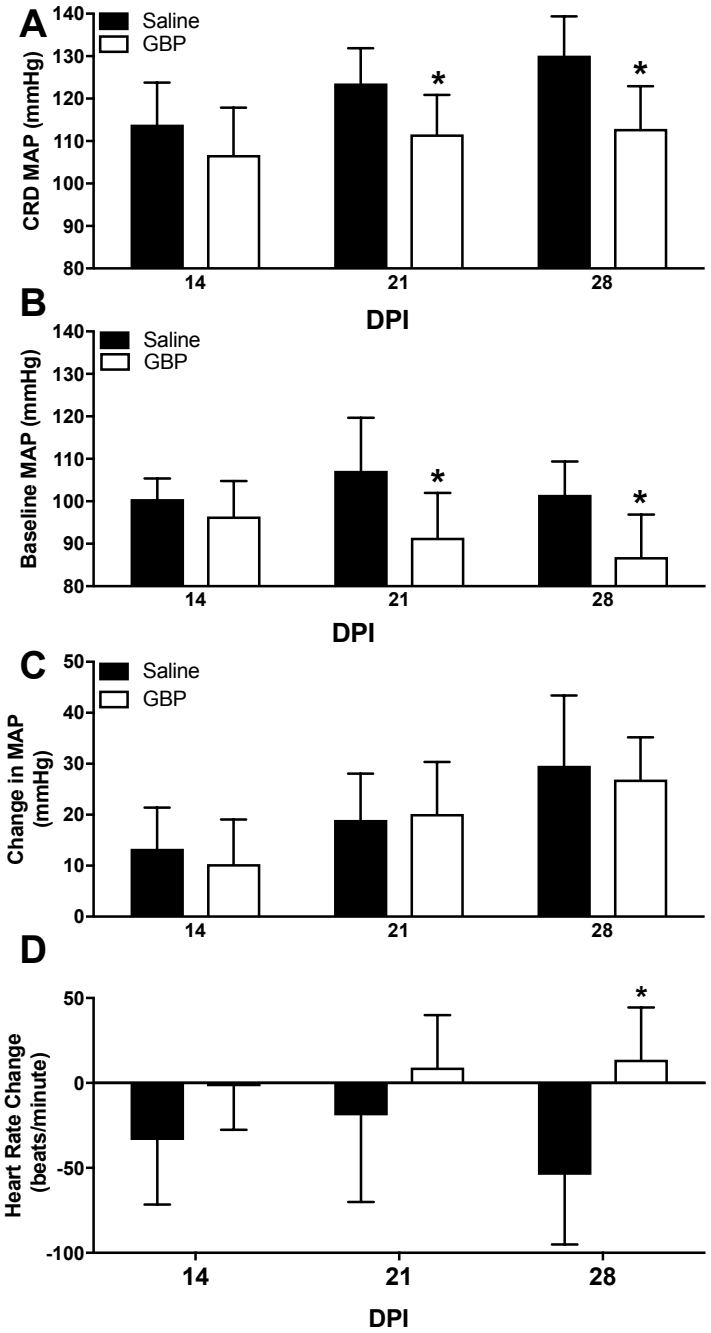

Figure 4.6. Gabapentin reduces blood pressure induced by noxious colorectal distension. AD was experimentally induced on 14, 21, and 28 days post-injury (DPI) through noxious colorectal distension (CRD). (A) GBP reduced the absolute mean arterial pressure (MAP) achieved during CRD at 21 and 28 DPI. (B) Similarly, the baseline MAP calculated from the 30 seconds immediately prior to each CRD trial was significantly lower in GBP treated rats. (C) The CRD-

induced change in MAP relative to baseline was not different between groups, however this parameter increased over time reflecting the gradual development of fulminant AD. (D) CRD-induced changes in heart rate were significantly altered by GBP, notably with treated rats having little change in heart rate, or occasionally displaying tachycardia. N=11 Saline, N=10 GBP. *p<0.05 vs saline control. Bars are mean ± SD.

4.3.5 Blood pressure recovery after induced AD

There was a significant effect of time (p=0.0057) and treatment (p=0.017) on the length of time for MAP to return to baseline values after CRD (**Figure 4.7**). The MAP recovery period to pre-CRD levels increased with time post-injury, paralleling the increased AD severity observed across weeks post-injury (**see Figure 4.6**). Post-hoc analyses did not indicate significant treatment differences at individual time points, but there was a significant increase between 14 and 28 DPI (p=0.0450) in the saline group, with the MAP recovery time increasing from 130 to 360 seconds.

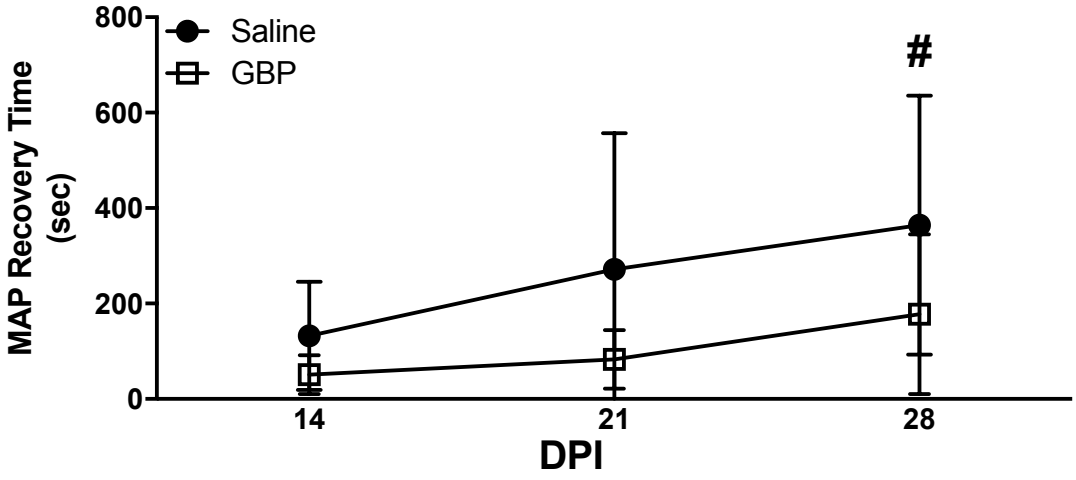

Figure 4.7. Gabapentin (GBP) reduces the time required for MAP to return to baseline after CRD. MAP recovery time following each CRD trial at 14, 21 and 28 DPI revealed a significant decrease with GBP treatment. N=11 Saline, N=10 GBP. #p<0.05 when comparing the 28 DPI saline vs 14 DPI saline group. Symbols are mean ± SD.

4.3.6 Effect of experimental handling and restraint on resting blood pressure

To evaluate the effect of potentially stressful handling on baseline blood pressure, we compared the resting MAP before the start of weekly CRD to the MAP after placing rats under gentle restraint for the CRD testing session. There was an overall effect of treatment ($p=0.004$), but not time ($p=0.50$) on the pressor response (**Figure 4.8**). Prior to CRD, saline-treated rats had resting MAP elevations of 15-20 mmHg during handling at 14, 21 and 28 DPI, whereas GBP-treated rats had significantly lower MAP at 21 and 28 DPI ($p<0.05$), with an average increase of 5 mmHg.

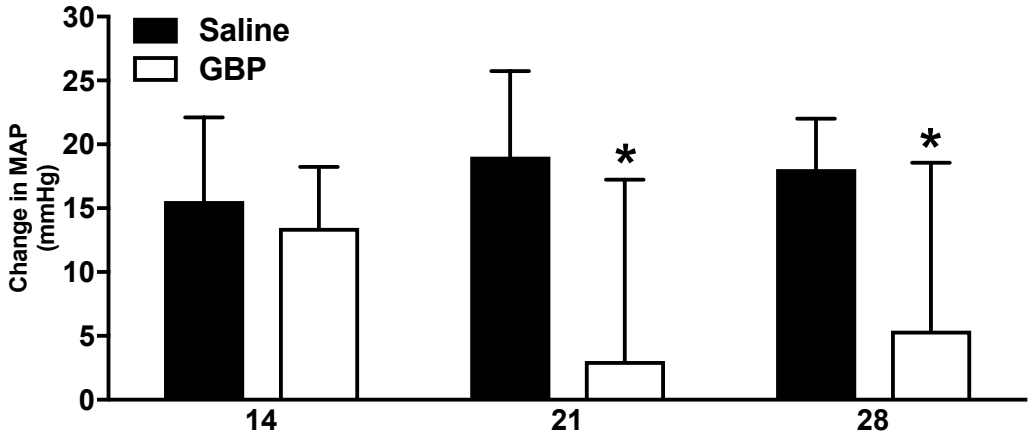

Figure 4.8. Effect of experimental handling and gentle restraint on MAP prior to CRD. The MAP measured in the mornings before the start of weekly CRD testing sessions was compared to the MAP measured during CRD test preparation. Pre-treatment with GBP minimized handling-induced pressor responses at 21 and 28 DPI. N=11 Saline, N=10 GBP. *$p<0.05$ vs saline control. Bars are mean ± SD.

4.3.7 Sensitivity of the spontaneous baroreflex after SCI

Based on the observation that GBP treated rats did not display reflex bradycardia normally observed during CRD in injured rats (**Figure 4.9**), we examined the spontaneous baroreflex (sBR) with the sequence method of Bertinieri et al. (1985) to test the hypothesis that GBP decreases baroreflex

sensitivity, or the strength of coupling between coinciding alterations in blood pressure and heart rate. No significant effect of time (p=0.28) or treatment (p=0.29) was observed on sBR gain (sensitivity) with this method (Figure 9). In both groups, the gain of the sBR was maintained near naïve values at approximately 2-2.5 mmHg-1 throughout the study. Analysis of acute time points in the immediate days post-injury were not included due to high variability associated with the confounding effects of recovery from surgical anesthesia and SCI.

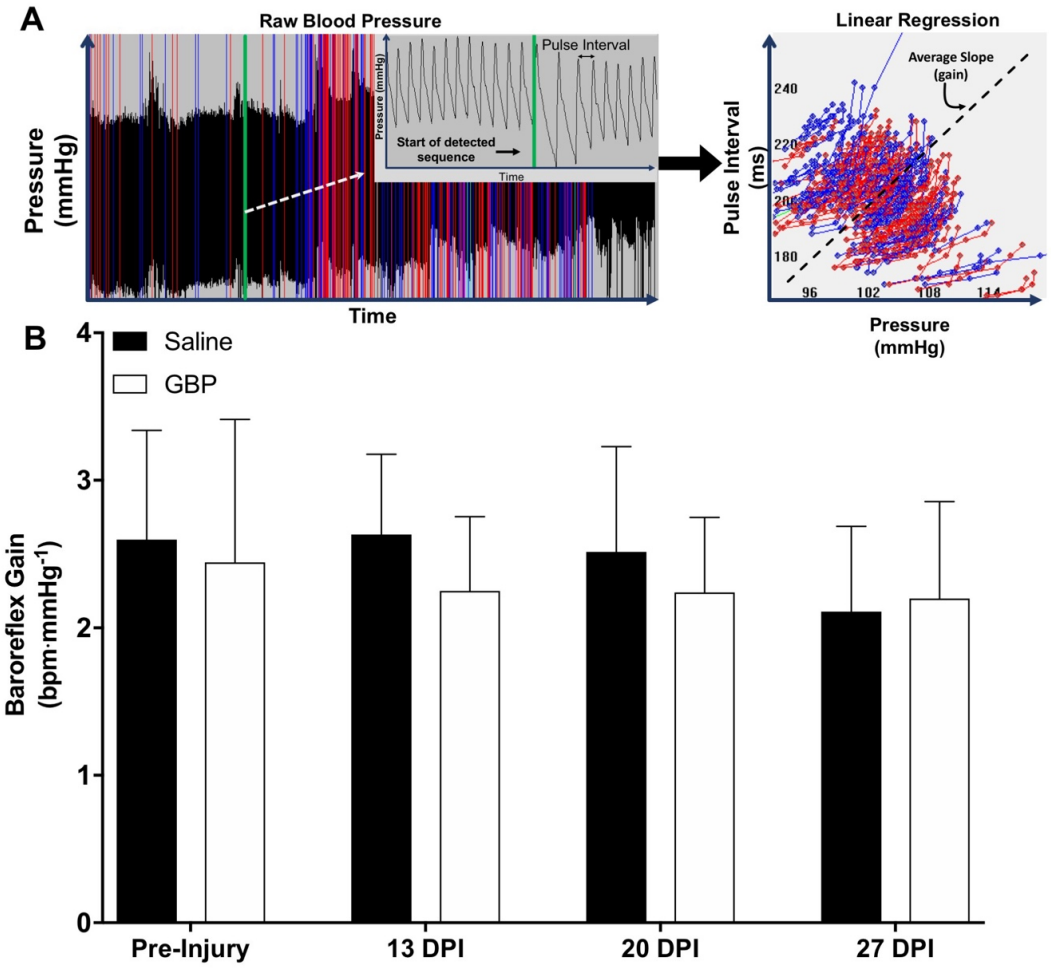

Figure 4.9. Effect of SCI and GBP on the spontaneous baroreflex (sBR). The gain (sensitivity) of the sBR was measured using 2-hour segments of raw blood pressure data collected in a 2-hour window following the 12:00 p.m. injections at corresponding days post-injury (DPI). (**A**) Representative trace depicts typical

sequence detections (**A**; left) and subsequent linear regression (**A**; right) from which the average slope is calculated as a measure of sBR gain. (**B**) No significant effect of injury or GBP treatment was observed at the evaluated time-points. N=11 Saline, N=10 GBP. Bars are mean ± SD.

4.3.8 Effects of SCI and GBP treatment on spleen weight

While there was no significant effect of injury on spleen size ($p>0.99$), GBP treatment significantly increased spleen size after injury (**Figure 4.10**). Compared to naïve and saline treated SCI rats, GBP treated SCI rats had significantly larger spleens ($p<0.05$).

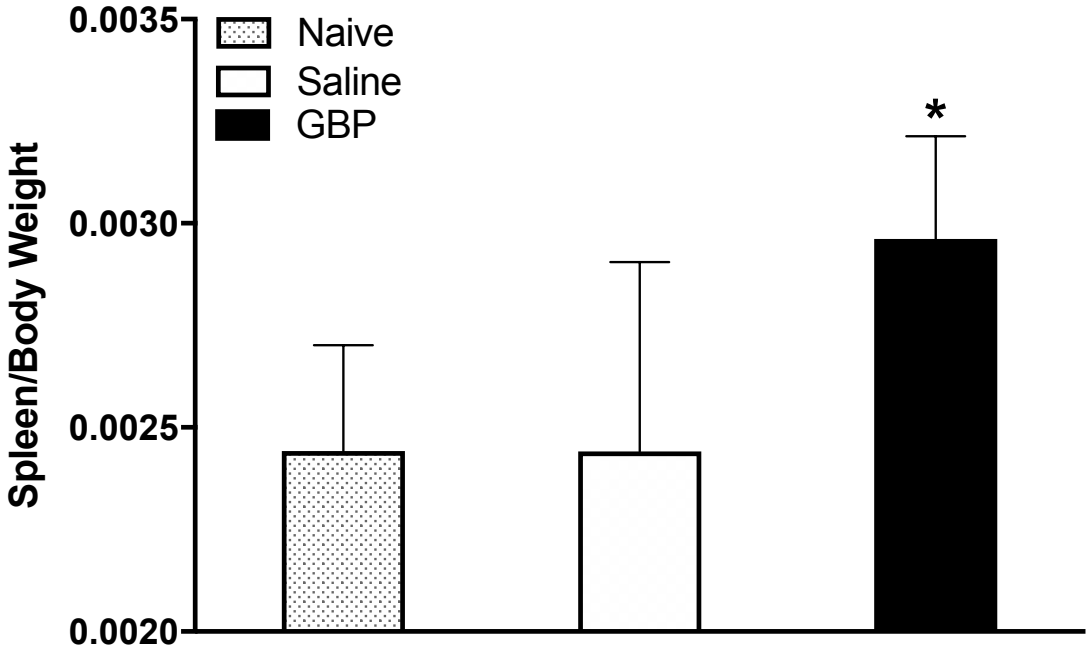

Figure 4.10. Effect of injury and GBP on terminal spleen weights. Spleen wet weights were recorded and normalized to terminal body weights at 4 weeks post-injury. While no effect of injury was observed, spleens from the GBP-treated injured group were significantly heavier in comparison to saline treated, as well as to age and body-weight matched naïve control rats. N=8 Naïve, N=11 Saline,

N=10 GBP. *p<0.05 vs naive control and saline treated SCI rats. Bars are mean ± SD.

4.3.9 Effects of SCI and GBP treatment on pre-synaptic densities

To investigate potential effects of SCI and chronic GBP treatment on synaptic connectivity in the lumbosacral spinal cord, we measured the immunoreactivity of presynaptic synaptophysin$^+$, VGLUT2$^+$ and VGAT$^+$ puncta in the dorsal horn (lamina I-II; R1) and dorsal gray commissure (lamina X; R2) of the L6/S1 spinal cord. These regions of interest contain the central terminals of c-fibers conveying colorectal afferent stimuli into the dorsal horn (R1) and the ascending propriospinal neurons (R2) believed to relay afferent stimuli rostrally towards the SPN. Representative images demonstrate apparent decreases in immunoreactivity for synaptophysin (**Figure 4.11A,B,E,F**), VGLUT2 (**Figure 4.11C,D**) as well as VGAT (**Figure 4.11G,H**) associated with SCI. The normalized percent area covered by synaptophysin in both regions of interest was reduced by SCI (**Figure 4.11I,L**). In the VGAT staining set, synaptophysin coverage was significantly lower ($p<0.001$; **Figure 4.11L**) in the SCI+saline and SCI+GBP treated groups compared to naïve controls, however this reduction was not significant in the VGLUT2 set ($p=0.09$; **Figure 4.11I**), perhaps due to higher staining variability. No effect of GBP treatment on synaptophysin area was observed in either staining set ($p>0.05$; **Figure 4.11I,L**). Similar to synaptophysin, SCI also significantly reduced the area occupied by VGLUT2$^+$ ($p<0.01$; **Figure 4.11J**) and VGAT$^+$ ($p<0.01$; **Figure 4.11M**) immunoreactivity in both regions of interest, with no observed effect of GBP treatment ($p>0.1$).

We also evaluated the percent area occupied by the overlap of synaptophysin/VGLUT2 puncta as well as synaptophysin/VGAT puncta. The area occupied by the union of synaptophysin and VGLUT2 immunoreactivity was significantly reduced in both regions of interest after injury ($p<0.05$; **Figure 4.11K**). Moreover, injury decreased the area occupied by the overlap of synaptophysin and VGAT puncta in R1 and R2 ($p<0.05$; **Figure 4.11N**). No effect of GBP treatment was observed on the overlap of either synaptophysin/VGLUT2

or synaptophysin/VGAT (p>0.5). Therefore, despite decreases in synaptic density in the lumbosacral dorsal horn after SCI, there was no effect of GBP on synaptic re-organization in these regions of interest believed to be involved in the viscero-sympathetic relay pathway.

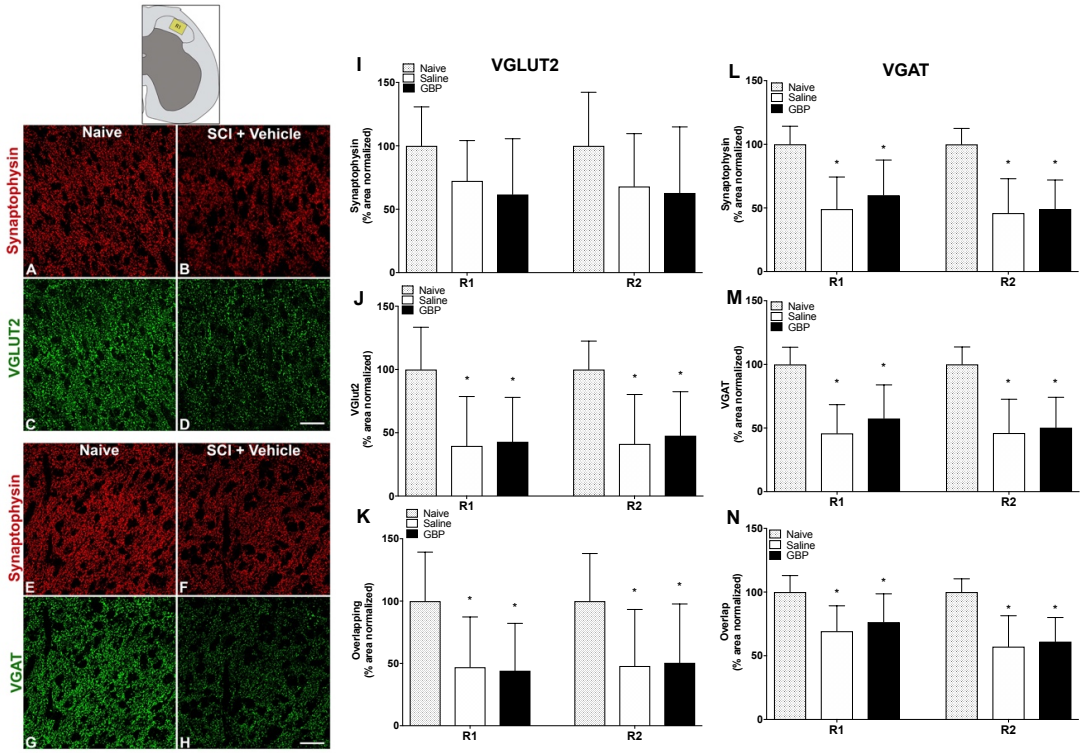

Figure 4.11. Density of synaptic puncta following complete spinal cord injury (SCI). Analyses were performed as described in **Figures 4.1** and **4.2**. Representative images (**A-H**) demonstrate VGLUT2 (**C,D**), VGAT (**G,H**) and synaptophysin (**A,B** and **E,F**) immunoreactivity in the lumbosacral dorsal horn (inset, top left) 4 weeks after injury. Widespread punctate immunoreactivity of all three markers was observed throughout the spinal cord gray matter. SCI decreased the density of VGLUT2 (**J**), VGAT (**M**), synaptophysin (**I,L**) and the overlap of VGLUT/synaptophysin (**K**) and VGAT/ synaptophysin (**N**), suggesting an overall decrease in excitatory and inhibitory synapses. Immunoreactive density was not altered by prolonged gabapentin (GBP) treatment. N=8 naïve,

N=11 Saline, N=10 GBP. *p<0.05 vs naive control. Symbols are mean +/- SD. Scale bar= 10 uM.

4.3.10 Effects of SCI and GBP treatment on pre-synaptic colocalization

The Manders' coefficients, tM1 and tM2, and Manders' overlap coefficient (MOC) were calculated for presynaptic immunoreactivities to corroborate density measures. The fraction of total VGLUT2 signal overlapping with SYN (tM1) was not significantly altered by SCI or treatment in either region of interest (p>0.05), whereas the fraction of total VGAT signal overlapping with SYN was significantly decreased by SCI in the R2 region (p=0.014; **Figure 12A**). No effect of GBP treatment was observed on tM1 in the VGLUT2 or VGAT staining sets (p>0.1). The converse relationship, defined as the fraction of total SYN signal overlapping with VGLUT2 or VGAT (tM2; **Figure 12B**) showed that in both the VGLUT2/SYN and VGAT/SYN staining sets, tM2 was significantly decreased after injury in both regions of interest (p<0.01). Like tM1, no significant effect of GBP treatment was observed on the tM2 overlap coefficient (p>0.05). The MOC for each pair of markers (VGLUT2/SYN and VGAT/SYN) indicated a high degree of signal overlap; >0.9 in R1 and R2 regions of interest (**Figure 4.12C**). Injury significantly increased the MOC of VGLUT2/SYN and VGAT/SYN relative to naïve controls in R1 (p=0.0003; p<0.01). MOC was unaffected by GBP treatment in either staining set (p>0.5).

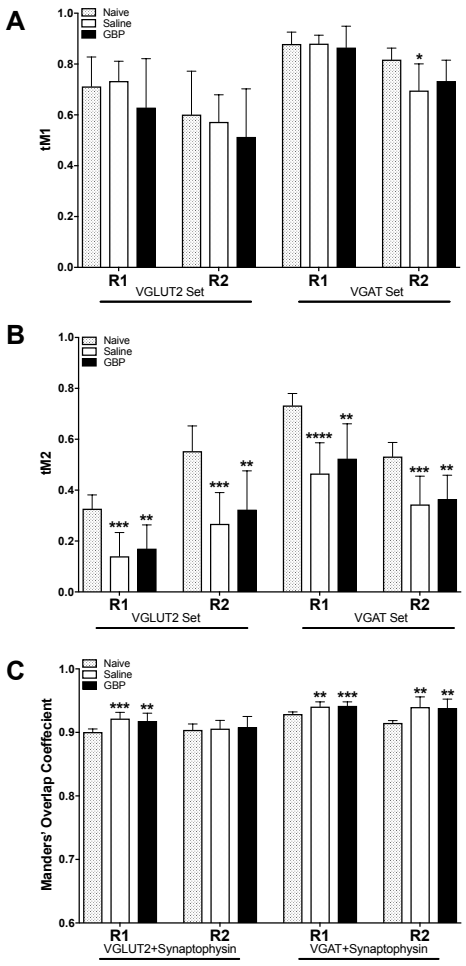

Figure 4.12. Quantitative colocalization analysis of synaptic immunostaining. The Manders' fractional overlap coefficients, tM1 and tM2 (A,B), and Manders' overall overlap coefficient (MOC; C) were calculated to assess the co-localization of VGLUT2/synaptophysin and VGAT/synaptophysin staining in the same regions of interest (R1 and R2) used for density measurements. (**A**) The fraction of total VGLUT2 or VGAT signal overlapping with synaptophysin (tM1) was largely unaffected by injury or GBP treatment. (**B**) Conversely, injury significantly decreased the fraction of synaptophysin signal overlapping with VGLUT2 or VGAT (tM2). (**C**) An MOC greater than 0.9 was observed in all groups. MOC was significantly increased by injury, with no effect of GBP treatment. N=8 naïve, N=11 Saline, N=10 GBP. *$p<0.05$; **$p<0.01$; ***$p<0.001$; ****$p<0.001$ vs naive control. Bars are mean +/- SD.

4.4 Discussion

We found that continuous high dose GBP treatment reduced blood pressure during CRD, and decreased bradycardia typically observed during AD as well as the MAP recovery time after CRD. However, GBP treated rats also had higher sAD frequency and failed to return to pre-injury body weight. Moreover, we observed that SCI reduced the density of putative excitatory ($VGLUT2^+$) and inhibitory ($VGAT^+$) synaptic puncta in the lumbosacral cord, although GBP did not alter these parameters. These results suggest that continuous GBP treatment offers clinical benefit in decreasing the magnitude and duration of CRD-induced AD, but appears to have paradoxical effects on spontaneously occurring AD.

Our finding that continuous GBP treatment significantly lowers the MAP achieved during CRD stimulation after complete SCI is similar to our previous reports (Rabchevsky et al., 2011; Rabchevsky et al., 2012) in which we found that a single acute administration of 50 mg/kg GBP reduces the magnitude of MAP change during CRD over 4-weeks post injury. We expected to see a similar effect on the change in MAP with our present study, since we increased both the treatment frequency and drug dosage (4x daily, 100 mg/kg). This higher dosage was chosen based on reports that 100-400 mg/kg of GBP daily prevents excitatory synaptogenesis in mice (Eroglu et al., 2009; Takahashi et al., 2018). Furthermore, we distributed the daily dosage across 4 injections to maintain relatively stable drug concentrations in spite of the 2-3 hour half-life in rats (Vollmer et al., 1986). However, we did not observe a significant treatment effect on the MAP change relative to baseline. We determined that this was due to a concomitant decrease in the baseline MAP prior to CRD which we attribute to the well-established anxiolytic effects of GBP (Houghton et al., 2017; Markota and Morgan, 2017). This is supported by our finding that relative to saline controls, GBP treated rats had a significantly smaller increase in blood pressure associated with experimental handling and restraint. As these experimental manipulations can present considerable stressors for rodents (Crestani, 2016), it

is likely that pretreatment with GBP attenuated levels of stress or anxiety and subsequent cardiovascular responses.

Body weight analysis of all injured rats revealed an acute gain of body weight in the immediate days post-injury, followed by a significant loss of body weight over the next two weeks. The reduction in body weight observed after SCI is likely attributable to loss of bone and muscle mass below the injury where the musculoskeletal system undergoes atrophic plasticity in response to disuse and unloading (Baldi et al., 1998; Castro et al., 1999; Giangregorio and McCartney, 2006; Gordon and Mao, 1994). Others have similarly reported an initial gain in body weight after traumatic SCI in rats (Krishna et al., 2013), which may be due to a combination of fluid retention and reduced metabolic demand as motor activity is dramatically suppressed during recovery from surgical anesthesia and SCI. Approximately two-weeks after injury, saline control-treated rats started to regain weight, reaching pre-injury body weight levels by three weeks post-injury. In contrast, GBP treated rats did not return to pre-injury body weight before termination 4 weeks post-injury. GBP treated rats did not lose additional body weight compared to saline controls, suggesting that treatment did not promote weight loss after SCI, rather it impeded body weight recovery during the chronic phase of injury.

The gradual return to pre-injury weight beginning approximately 2-weeks after SCI occurs in parallel to the development of muscle spasticity in rats after SCI. For example, Bennett et al. (2004) demonstrated the development of intense and long-lasting spasms of the tail musculature by two-weeks after complete sacral transection SCI. Multiple studies suggest that muscular contractions during spasm after SCI can help maintain or even increase muscle mass (Baldi et al., 1998; Gorgey and Gater, 2012). This indicates that the return to pre-injury body weight in our study could be attributable to muscle hypertrophy resulting from muscle spasticity. We previously demonstrated that GBP is effective for decreasing the intensity of tail spasticity in rats after SCI (Rabchevsky et al., 2011; Rabchevsky et al., 2012). Therefore, given the continuous 4x daily GBP administration in our current study, it is feasible that the

failure of GBP rats to return to pre-injury weight is due to a lack of spasticity-induced muscle hypertrophy. It is clinically important to understand whether a continuous GBP dosage paradigm could abrogate the potentially beneficial effects of muscle spasticity, as a preservation of muscle tone could also be expected to help prevent musculoskeletal issues such as joint contractures (Pingel et al., 2017).

We observed changes in daily MAP and HR after SCI which reflect the changes in cardiovascular control associated with our complete T4-transection model. The marked drop in MAP in the first days after injury likely reflects two phenomena: 1) the recovery from surgical ketamine and xylazine anesthesia, the latter of which has demonstrated cardiac depressant effects in Wistar rats (Albrecht et al., 2014), and 2) the sudden and complete removal of supraspinal drive to SPN. In the absence of supraspinal drive, the tonic activity of SPN is decreased, leading to a reduction of vasomotor tone and peripheral arterial resistance which manifests as reduced MAP (Mathias et al., 1979; Mathias and Frankel, 1988). Daily HR similarly decreased dramatically immediately after SCI, likely due to the potent effects of xylazine on the α_2-adrenergic receptors (Hsu et al., 1985). Xylazine functions both centrally and on peripheral vasculature, causing side effects such as hypertension or hypotension, bradycardia and sedation. Xylazine induced reductions in heart rate are caused by a combination of reflex-bradycardia in response to peripheral vasoconstriction, which increases systemic vascular resistance, and through reduced sympathetic tone as a result of reduced norepinephrine release from sympathetic terminals (Sinclair, 2003). By 2 DPI, daily HR was significantly increased compared to pre-injury and remained elevated for the duration of the study. We observed that GBP treated SCI rats had daily HR 20-30 bpm higher than saline-treated controls. This trend was non-significant ($p=0.06$), perhaps due to inherent variability commonly observed in daily HR measurements. It indicates, however, that this GBP treatment regimen has cardiovascular effects after SCI which have not previously been reported. Notably, the $\alpha_2\delta_1$ subunit which GBP binds to is found ubiquitously in many tissues and is highly abundant in the myocardium, vascular

smooth muscle, skeletal muscle and many brain regions (Fuller-Bicer et al., 2009; Klugbauer et al., 2003; Taylor and Garrido, 2008). Fuller-Bicer et al. (2009) created a mouse knockout model with a targeted disruption of the $\alpha_2\delta_1$ calcium channel subunit and investigated electrophysiological and mechanical properties of the heart in mice lacking this subunit. They reported decreased Ca^{2+} currents in cardiomyocytes and reduced basal contractility and relaxation parameters in ex-vivo heart preparations in knockout mice. These findings suggest important roles of the $\alpha_2\delta_1$ subunit in cardiac function and further suggest possible effects of GBP on daily HR in our model. Based on the work of Fuller-Bicer et al. (2009), it is feasible that SCI rats receiving GBP have reduced cardiac contractility and output. As described in **Chapter 1**, the cardiovascular and autonomic nervous systems function together to maintain an appropriate cardiac output, which is determined by the product of stroke volume and heart rate (CO=SV x HR). Therefore, one could expect to observe a compensatory increase in heart rate mediated by elevated cardiac sympathetic drive in GBP treated rats if this drug decreases myocardial contractility and stroke volume.

We set our sAD algorithm thresholds to detect small events consisting of a MAP increase ≥ 10 with a HR reduction ≥ 10 bpm, as well as larger events with a MAP increase ≥ 20 and HR reduction ≥ 20 bpm. Similar to our previous studies using the smaller threshold of 10mmHg/10 bpm, we observed a negligible number of detections prior to injury (Eldahan et al., 2018; Rabchevsky et al., 2012). This validates that our algorithm detects abnormal physiological phenomena reflecting the loss of regular cardiovascular control and is likely to reflect true AD events. Compared to other sAD algorithms which utilized more stringent threshold of a change >20 mmHg/bpm (Mironets et al., 2018; West et al., 2015), thresholds of 10 mmHg and 10 bpm are relatively lenient. However, the smaller events reflect abnormal physiological patterns which may be important to monitor. Recent reports suggest that the abnormal fluctuations in blood pressure associated with SCI may contribute to cerebrovascular dysfunction (Phillips et al., 2016; Phillips et al., 2018). This indicates that the moderate sAD events that we detected may be clinically relevant outcome

measures. Moreover, there is evidence to suggest that increased blood pressure variability is associated with poor cardiovascular outcomes (Stevens et al., 2016). Therefore, our finding that chronic administration of GBP increases the frequency of relatively small as well as moderate hemodynamic fluctuations after SCI warrants careful consideration of potentially negative effects on cardiovascular outcomes after SCI.

We hypothesized that continuous treatment with GBP would reduce the frequency of spontaneous AD. It is surprising, therefore, that our current treatment paradigm, which delivers eight times the daily amount of GBP, had the effect of increasing sAD frequency. Although the exact mechanisms of sAD generation have not been examined, it is possible that a subset of these events could be due to spontaneous firing of the SPN or pre-sympathetic interneurons. In this case, it would suggest that continuous GBP treatment somehow increases spontaneous sympathetic neural activity. One intriguing possibility is that prolonged attenuation of primary afferent activity by continual GBP delivery deprives sympathetic interneurons of peripheral stimulation. Studies on the effects of long-term application of gabapentinoids on spinal cord slice preparations demonstrate that prolonged exposure to GBP decreases spontaneous excitatory post-synaptic potentials in the substantia gelatinosa (Biggs et al., 2014). This was associated with a significant decrease in Ca^{2+} release sparking, suggesting that GBP reduces overall spinal network excitability. Similarly, Coderre et al. (2005) and Coderre et al. (2007) reported that GBP decreases intraspinal release of glutamate from afferent terminals. These observations present the possibility that prolonged GBP treatment increases spontaneous spinal sympathetic activity through a homeostatic mechanism in which sustained decreases in peripheral stimulation of SPN or sympathetically correlated interneurons promotes increased excitability of SPN, perhaps manifesting as increased sAD events.

Cardiovascular regulation is dynamic multifactorial. Among the many variables involved in cardiovascular regulation, psychological and emotional stressors can introduce acute alterations in blood pressure and heart rate.

Indeed, many animal studies have demonstrated the importance of controlling for potential sources of stress during monitoring of the cardiovascular or autonomic systems (Crestani, 2016). We observed an increase in the resting blood pressure of saline treated rats after experimental manipulations to conduct CRD, whereas GBP treated rats had a significantly reduced pressor response to identical handling. GBP is well known to have anxiolytic effects in humans and rodents (Greenblatt and Greenblatt, 2018; SM et al., 2011), suggesting that the reduced pressor response is likely attributable to a reduction in emotional distress during handling, drug injection, gentle cloth restraint and colorectal catheter placement.

We quantified the density of synaptic puncta in the lumbosacral spinal cord to investigate the effects of complete SCI and GBP treatment on synaptic connectivity in regions receiving primary afferent terminations from the colorectum (Kyloh et al., 2011). In the caudal spinal cord 4 weeks after injury, we observed significantly reduced density of the vesicular neurotransmitter transporters VGLUT2 and VGAT in conjunction with the pre-synaptic marker synaptophysin, suggesting an overall decrease in excitatory and inhibitory synapses, respectively. VGLUT2 and VGAT are widely accepted markers of glutamatergic and GABAergic synapses, and utilizing double-labeling of VGLUT2 or VGAT in conjunction with the specific presynaptic marker synaptophysin (Wiedenmann and Franke, 1985) shows puncta of excitatory or inhibitory synapses, respectively (Herzog et al., 2006; Lee et al., 2017; Li et al., 2003).

The identification of neurochemical markers specific to particular synaptic populations and structural components has been a non-trivial challenge in neuroscience research (Rees et al., 2017). In recent decades, a number of neurochemical markers have been identified and utilized to observe synaptic structures in tissue. Synaptophysin is the most abundant protein in presynaptic vesicles, accounting for approximately 7% of total vesicular membrane proteins (Jahn and Sudhof, 1993). Despite its abundance, knockout mice lacking this protein appear healthy and maintain normal synaptic function (McMahon et al., 1996; Valtorta et al., 2004). While the exact function of synaptophysin remains unknown, this vesicular glycoprotein is widely used as a universal marker of

chemical presynaptic terminals in the brain and spinal cord (Kwon and Chapman, 2011; Vulovic et al., 2018). How specific is synaptophysin to the presynaptic compartment compared to, for example, intra-axonal transport pathways? In their seminal study, Wiedenmann and Franke (1985), who were the first to characterize synaptophysin as a presynaptic identifier, observed immunogold labeled synaptophysin virtually exclusively in synaptic terminals of the brain using electron microscopy. Immunogold labeled puncta were markedly enriched in presynaptic terminals but not observed in the cell bodies or axons. Wiedenmann and Franke (1985) also observed synaptophysin in the adrenal medulla, suggesting possible non-synaptic roles of this protein. However, this study was not sufficient to conclusively determine whether low levels of neuronal synaptophysin may also be found outside of synaptic vesicles. Subsequent studies designed to assess the pre-synaptic specificity of synaptophysin within neurons concluded that it is highly specific to small synaptic vesicles (SSV) (Navone et al., 1986). In contrast to large dense-core vesicles, which are continually transported to the synapse after being reloaded with peptide transmitters in the cell body, SSVs are recycled and re-loaded locally in the synapse and therefore do not undergo continual axonal transport from the soma to terminal (Ceccarelli et al., 1973; Navone et al., 1986; Reichardt and Kelly, 1983). Labeling and trafficking studies have demonstrated that newly synthesized synaptophysin is shuttled to synaptic terminals using fast transport mechanisms (Elluru et al., 1995; Tang et al., 2013), indicating that it only briefly exists outside of the synapse. Systematic analysis of the metabolic turnover of synaptic proteins in primary cortical neuron cultures revealed that synaptophysin has a half-life of approximately 96 hours and suggested that as little as 0.7% of total synaptophysin protein is replaced every hour (Cohen et al., 2013). An earlier study, which used intact brain tissue, estimated a half-life of approximately 500 hours, indicating that synaptophysin may have a substantially slower turnover rate *in-vivo* (Price et al., 2010). The fast-transport and slow turnover of synaptophysin suggests that newly synthesized protein *en route* to synaptic terminals likely accounts for a small proportion of total observable synaptophysin.

Lastly, the immunoreactive staining pattern of synaptophysin is also consistent with other well-characterized and specific presynaptic markers such as synapsin I (De Camilli et al., 1983; Fletcher et al., 1991; Navone et al., 1986). Collectively, these studies indicate that synaptophysin is useful as a high-fidelity marker of presynaptic terminals.

Presently, three isoforms of the VGLUT (VGLUT1-3) have been identified in the central nervous system (Bai et al., 2001; Bellocchio et al., 2000; Gras et al., 2002; Herzog et al., 2001; Liguz-Lecznar and Skangiel-Kramska, 2007; Ni et al., 1994; Schafer et al., 2002; Takamori et al., 2001). Specific VGLUTs are typically found in discrete subsets of neurons, with a mostly complementary and non-overlapping pattern of distribution observed throughout the CNS (Herzog et al., 2001; Kaneko and Fujiyama, 2002). In the spinal cord, VGLUT1 and VGLUT2 are the primary isoforms observed with only low levels of VGLUT3 mRNA and protein being detected (Alvarez et al., 2004; Landry et al., 2004; Li et al., 2003; Oliveira et al., 2003; Todd et al., 2003). We chose to examine VGLUT2^{+} synaptic puncta based on previous studies showing that this is the predominant VGLUT expressed in the upper dorsal horn and lamina X regions of interest in our model (Alvarez et al., 2004; Landry et al., 2004; Llewellyn-Smith et al., 2007; Oliveira et al., 2003; Todd et al., 2003; Varoqui et al., 2002). Spinal VGLUT2 may arise from three sources: 1) incoming primary afferents, 2) descending fibers or 3) local propriospinal neurons. Evidence suggests that most VGLUT2 in the spinal dorsal horn is derived from propriospinal sources. For example, Alvarez et al. (2004) and Oliveira et al. (2003) observed a marked decrease in the density of VGLUT1 varicosities in the upper dorsal horn one week following lumbar dorsal rhizotomy, whereas VGLUT2 density was not significantly altered. Others have identified VGLUT3 expression in dorsal root ganglia along with low-levels of VGLUT3 immunoreactivity in the upper dorsal laminae (Seal et al., 2009). These observations indicate that primary afferent terminals are comprised mostly of VGLUT1 and, perhaps to a lesser extent, VGLUT3. Llewellyn-Smith et al. (2007) reported no change in VGLUT2 density throughout the thoracolumbar lateral horn caudal to complete T4-transection and observed significantly decreased

VGLUT1 labeling, but did not look at lower spinal levels or dorsal horn. This suggests that intraspinal VGLUT2 may be more specific for propriospinal sources, whereas VGLUT1 is more likely associated with supraspinal and primary afferent fibers. Some descending tracts are known to contain VGLUT2. For example, 97% of axons from the descending rubrospinal and vestibulospinal tracts projecting to the spinal cord contain VGLUT2 exclusively (Du Beau et al., 2012). However, because these tracts project to ventral motor regions they cannot account for the reduction in VGLUT2 we have observed in dorsal horn and lamina X regions. Others (Maxwell et al., 2007; Todd et al., 2003) have contended that VGLUT2 in the dorsal cord is likely expressed by excitatory interneurons, which would indicate that the reduced VGLUT2 density that we observed is of a propriospinal origin.

4.4.1 Methodological Considerations

Advancements in confocal microscopy have enabled accurate measurement of sub-cellular structures using immunofluorescent labeling. Improved resolution power of confocal microscopes have permitted the use of this technique to quantify specific synaptic populations (Vulovic et al., 2018). While electron microscopy (EM) remains the gold standard for precise quantification of individual synapses, confocal microscopy has the distinct advantage of allowing comparatively high throughput of large sets of biological replicates and analysis of larger fields of tissue. Moreover, quantified results obtained with confocal imaging of synapses have been corroborated with electrophysiological functional measurements (Nikonenko et al., 2006; Vulovic et al., 2018). As previously discussed (Burette et al., 2015; Rossler et al., 2017), confocal imaging of synapses in intact tissue has important caveats. The resolution of conventional light microscopy compared to the relatively small size of synapses makes it difficult to accurately resolve neighboring synapses, which are typically very dense in tissue. Combined with inherent limitations of tissue immunofluorescence such as uneven antibody penetration, variable tissue fixation and light scattering at deeper optical planes, it becomes very difficult to

obtain accurate synaptic counts from a field of tissue. We therefore chose to quantify the density of our presynaptic markers to circumvent this limitation. Others have used similar area measurements to quantify the density of supra-threshold immunoreactivity of presynaptic markers in the brain and spinal cord (Beauparlant et al., 2013; Carasatorre et al., 2015; Cloutier et al., 2016; McKillop et al., 2016). Threshold based methods have also been employed to measure overlapping synaptic puncta (Alvarez et al., 2004). Such density-based measurements of large regions of interest can provide broad indication of changes synaptic connectivity. Future studies combining the use of retrograde tracers and synaptic labeling may be useful in characterizing synaptic connectivity within discrete neuronal pathways in our model. For example, retrograde labeling of primary c-fiber afferents innervating the distal colon, in conjunction with synaptic labeling after SCI could provide a method of measure the effects of experimental treatments on specific neuronal populations known to be involved in the etiology of AD.

Quantitative colocalization analyses were used to corroborate synaptic density measurements. Such colocalization methods are increasingly used to quantify the overall spatial and stoichiometric relationship between a set of fluorescent probes on a pixel-by-pixel basis (Aaron et al., 2018; Bolte and Cordelieres, 2006; Cordelieres and Bolte, 2014; Dunn et al., 2011). Although some researchers rely on relatively simple visual assessments of signal overlap, this approach is highly prone to user bias and inappropriate in cases where the intensity of one channel overwhelms the signal from the second (Bolte and Cordelieres, 2006; Sheng et al., 2016; Zinchuk and Zinchuk, 2008). Therefore, we chose to implement these more rigorous colocalization techniques. The Manders' overlap coefficient (MOC) is well-suited for quantifying the co-occurrence of two probes. Although the MOC is primarily sensitive to spatial overlap (Dunn et al., 2011), pixel intensity is also factored into its calculation. Hence, in cases where a direct linear relationship exists between the number of target antigen and fluorescence intensity, the MOC represents the colocalization of total labeled antigens to provide a more comprehensive metric. Compared to

the Pearson's correlation coefficient, which is another commonly used colocalization metric, the MOC is arguably more appropriate in cases where the fluorescent probes utilized differ in intensity (Zinchuk and Grossenbacher-Zinchuk, 2009).

We observed a high degree of co-occurrence between synaptophysin/VGLUT2 or synaptophysin/VGAT, with MOC values above 0.9. Considering that a MOC of 1.0 indicates complete signal overlap, our results demonstrate that these pairs of pre-synaptic markers are highly colocalized and further suggests that the majority of staining represents pre-synaptic puncta. While our density measurements revealed a significant decrease in the area covered by overlapping synaptophysin/VGLUT2 and synaptophysin/VGAT puncta after injury, we observed an increase in the MOC after injury. Since MOC factors marker co-occurrence and pixel intensity, this could suggest a differential effect of SCI on the co-occurrence and relative stoichiometry of these markers (i.e. reduced co-occurrence but increased intensity correlation). However, examination of the MOC equation suggests that alterations in pixel intensity would have relatively minor effects on the MOC since this variable is present in both the numerator and denominator. Alternatively, it is possible that SCI decreases the overall area occupied by these markers but that a higher proportion of the remaining synaptophysin, VGLUT2 and VGAT protein is present together in the pre-synaptic compartment. For example, it is conceivable that spinal transection and subsequent degeneration of descending fibers results in a reduction of non-synaptic synaptophysin, VGLUT2 and VGAT protein being transported from the soma to presynaptic terminals. Such a scenario would be expected to result in a lower overall density but higher proportion of co-occurring markers. Lastly, because SCI increased the MOC values from approximately 0.9 to 0.95, this relatively minor increase is consistent with the notion that the vast majority of these markers are normally present in the presynaptic compartment (Vulovic et al., 2018; Wiedenmann and Franke, 1985).

We also evaluated the Manders' fractional overlap coefficients tM1 and tM2, which reflect the proportion of total VGLUT2 or VGAT signal that overlaps

with synaptophysin, and vice versa. Based on the reduced density we observed with all three markers, it may be expected that the relative fraction of overlap would not be altered after SCI. This was true of tM1, which is the proportion of total VGLUT2 or VGAT signal coinciding with synaptophysin. However, we found that SCI significantly decreased the proportion of synaptophysin signal that colocalizes with VGLUT2 or VGAT (tM2). Therefore, SCI decreased the proportion of synaptophysin signal which overlaps with VGLUT2 or VGAT (tM2), while the amount of total VGLUT2 or VGAT signal overlapping with synaptophysin was unaffected. These metrics might represent that the same proportion of VGLUT2/VGAT signal after SCI remains in the pre-synaptic compartment along with synaptophysin, whereas an increased proportion of synaptophysin signal may be associated with other synaptic populations such as those expressing VGLUT1 or glycine transporters GLYT1/2. This would be consistent with studies suggesting that dorsal horn VGLUT1 is primarily derived from incoming primary afferents (Alvarez et al., 2004; Oliveira et al., 2003) which would not be expected to decrease after SCI.

VGAT is a presynaptic protein widely used as marker of presynaptic inhibitory synapses. Although initially used as a GABAergic presynaptic marker, it is now understood to be present in both GABAergic and glycinergic synapses (Chaudhry et al., 1998). Co-release of GABA and glycine from the same synaptic vesicle has also been observed in the brain and spinal cord, suggesting that VGAT may be involved in the transport of both of these inhibitory neurotransmitters (Jonas et al., 1998; Wojcik et al., 2006). It is likely, therefore, that our observed decrease in VGAT immunoreactivity after transection SCI indicates a reduction of both GABAergic and glycinergic synapses in our ROIs. Sources of VGAT within the spinal cord are limited to descending pathways and spinal interneurons, as incoming primary afferents are thought to be exclusively excitatory. In the intact animal, descending GABAergic fibers from the periaqueductal gray (PAG) and rostral ventromedial medulla (RVM) innervate ascending nociceptive neurons in the dorsal horn and are believed to play an important role in the endogenous analgesic system (Basbaum and Fields, 1984;

Lau and Vaughan, 2014; Taylor and Corder, 2014). GABAergic interneurons are present throughout the spinal dorsal horn, with an estimated 25-40% of neurons in the upper dorsal lamina being immunoreactive for GABA (Polgar et al., 2003). Notably, decreases in the number of dorsal inhibitory neurons after SCI has been documented and proposed to contribute to the development of injury-induced neuropathic pain (Meisner et al., 2010). Drew et al. (2004) demonstrated a decreased sensitivity to bicuculline (GABA antagonist) applied locally to dorsal horn neurons, which was proposed to occur in response to decreased GABA release resulting from reduced VGAT expression. Song et al. (2001) used GeneChip analysis to examine shifts in gene transcription in a rat model of acute SCI. Following T9 contusion injury, a segment of cord centered on the epicenter was isolated and processed for RNA isolation. They demonstrated a 3.5-fold decrease in VGAT mRNA expression at 3-hours, and a 10-fold decreased at 24-hours post-injury. This study suggests that SCI may result in decreased VGAT protein production throughout the cord immediately after injury. However, it is unclear whether this downregulation is maintained into the chronic phase of injury. GABAergic interneurons are also located in lamina X (Alvarez et al., 1996; Blok et al., 1998). It is unclear in our study whether the reductions of VGAT density are associated with the loss of descending fibers or alterations within propriospinal circuits. Additional experiments are needed to determine the relative contributions of these two sources. Future studies using a series of spinal lesions may be useful in determine the relative contributions. For example, comparison of VGAT density in rats with a rostral spinal transection to rats receiving a subsequent second lesion in the nearby caudal cord may help determine the relative contribution of descending vs. local inhibitory neurons.

An important limitation of our study is that, because we have not counted the number of synapses, we are unable to determine conclusively whether the observed decrease in immunoreactive density is attributed to a reduction in synapse size, number of presynaptic vesicles per neurotransmitter release site, or a general reduction of presynaptic vesicle protein expression. Evidence indicates that the expression of VGLUT2 and VGAT protein in the neocortex is

positively correlated with synaptic activity (De Gois et al., 2005; Doyle et al., 2010). Therefore the loss of descending supraspinal synaptic drive after cord transection could result in decreased expression of VGLUT2 and VGAT protein and account for the reduced VGLUT2/VGAT density observed in our study, rather than a decrease in the actual number of synapses.

A number of other studies in rodents have similarly observed decreased immunoreactivity of synaptic markers caudal to a spinal lesion. Beauparlant et al. (2013) reported decreased density of VGLUT1 and VGLUT2 in the lumbosacral cord one week after a staggered T7/T10 hemisection before returning to intact control levels by 9 weeks. Their study suggests that following the initial loss of supraspinally derived synapses, the decentralized spinal cord compensates with reactive sprouting and synaptogenesis in an attempt to re-establish a normal level of synaptic connectivity and activity. The authors contend that this compensatory response proceeds in an undirected manner, resulting in the formation of aberrant circuitry contributing to neuronal dysfunction and, perhaps, muscle spasticity, pain and autonomic dysfunction. We terminated our experiment 4 weeks after injury, so it is unclear whether there is a similar restoration in the density of synaptic markers in more chronic phases after complete SCI.

Kapitza et al. (2012) reported a 10-50% decrease in the density of VGLUT1^{+} and VGLUT2^{+} puncta in laminae VII caudal to the lesion at 1 and 12 weeks following S2 transection, however no significant decrease was observed at 4 weeks suggesting a dynamic time-dependent shift in synaptic architecture. These results are in contrast to a study by Kitzman (2006), who observed an increase in the number of VGLUT2^{+} boutons in contact with ventral motoneurons. This discrepancy may be related to methodological differences, or due to laminae specific re-arrangements of glutamatergic terminals after injury. Using a contusion model in mice, McKillop et al. (2016) quantified the immunoreactive area of VGLUT2, synaptophysin and VGAT in the ventral horn at 48-hours and 10-weeks post-injury. Although their study utilized a different species injury model and focused on the ventral rather than the dorsal horn, they reported

injury-related decreases in synaptic markers at both 2 days and 10 weeks after injury, similar to our results in the rat dorsal horn 4 weeks post injury. This study suggests that SCI causes a widespread decrease in synaptic density throughout the dorsal-ventral axis since they observed similar results in the ventral horn as we observed in the dorsal horn and laminae X region.

It is difficult to compare studies directly due to differences in injury model, spinal level, time after injury, method of quantification and laminar distribution examined across various studies. However, with these studies in mind it is apparent that SCI provokes temporally and spatially dynamic changes in synaptic organization that are likely to be involved in sensorimotor and autonomic dysfunction.

4.5 Conclusion

Our findings indicate that continuous high dose GBP treatment may offer clinical benefit in reducing the magnitude and duration of AD induced by noxious stimulation of the pelvic viscera, however potential deleterious effects such as increased spontaneous AD and reduced gain in body weight must also be considered. The absence of treatment effect on the density of synaptic immunoreactivity after SCI suggests that prolonged high-dose GBP does not alter synaptic density in the lumbosacral cord and likely acts through an alternative mechanism to reduce the severity of AD. Moreover, the reduced density of synaptic markers indicates that altered synaptic connectivity in the lumbosacral cord may contribute to the etiology of AD. Future investigations using more detailed approaches to study synaptic connectivity in discrete neuronal pathways may reveal a nuanced and previously unappreciated contribution of lumbosacral synaptic remodeling in the etiology of AD.

Copyright © Khalid C. Eldahan 2019

CHAPTER 5

Discussion, Future Research Directions and Conclusions

5.1 Conclusions

This dissertation has presented the investigation of two FDA-approved drugs, rapamycin (RAP) and gabapentin (GBP), for their potential to suppress maladaptive plasticity associated with the development of AD. Collectively, our results give important new insights into possible cellular signaling mechanisms and synaptic re-organization involved in the development of AD, and inspire a number of novel future research directions to push forward the effort to discover treatments capable of mitigating AD development.

These two drugs were tested for distinct reasons. We chose to test RAP based on an emergence of evidence implicating the mammalian target of rapamycin (mTOR) pathway as a critical signaling hub coordinating the cellular processes required for neurons to sprout and regenerate. RAP is employed both as an experimental tool to investigate the role of mTOR signaling in health and disease, as well as a clinically important immunosuppressant used to reduce the chance of post-organ transplant rejection. Moreover, some researchers have proposed RAP treatment after SCI to promote tissue sparing and functional recovery, yet we are the first to critically assess this drug for potential autonomic or cardiovascular side effects, notably in a population which is already susceptible to cardio-autonomic dysfunction. We found that prolonged treatment with RAP after complete SCI exacerbates cardiovascular dysfunction without modifying markers of intraspinal plasticity associated with AD, as assessed by $CGRP^+$ fiber sprouting and interneuronal c-fos expression. The present results suggest a limited role of this major signaling hub in aberrant sensory fiber sprouting after SCI and further indicate that a number of alternative and targetable pathways may be more critically involved.

We tested GBP based on previous reports from our lab demonstrating that acute administration reduces the severity of experimentally induced AD (Rabchevsky et al., 2011; Rabchevsky et al., 2012), and other research

suggesting that daily treatment with GBP can block the formation of new excitatory synapses in the brain and spinal cord (Eroglu et al., 2009; Lau et al., 2017; Yu et al., 2018). For over a decade, it has been thought that the formation of new synapses between newly sprouted c-fibers and propriospinal neurons is necessary for the development of exaggerated sympathetic reflexes produced during AD (Weaver et al., 2002). Therefore, we sought to determine if continuous delivery of this purported anti-synaptogenic drug could prevent alterations in synaptic density of intraspinal primary afferents or interneurons thought to contribute to AD. We found that continuous delivery of high dose GBP reduced the absolute blood pressure achieved during experimentally induced AD, prevented normally observed bradycardia during CRD and reduced the amount of time for blood pressure to return to baseline after an induced AD event. Our continuous treatment paradigm was also associated with apparent anxiolytic effects not observed in our previous studies using a smaller dosage of GBP. Unexpectedly, GBP also increased the frequency of spontaneously occurring AD through an uncertain mechanism. Consistent with previous reports (Beauparlant et al., 2013; Freria et al., 2017; McKillop et al., 2016), we observed a decrease in the density of excitatory and inhibitory pre-synaptic markers in the dorsal lumbosacral cord from injury alone. However, these reductions in synaptic immunoreactivity were not altered by GBP treatment, suggesting an alternative mechanism of action in reducing the severity of AD.

This chapter discusses the relevance of these findings in the broader context of SCI and AD research. Moreover, future directions are presented with the ultimate goal of better understanding maladaptive changes at the molecular and neuronal level within spinal sympathetic circuits which may aid in the discovery of treatments capable of preventing the development of this condition.

5.2 Discussion

We investigated the possible role of the mammalian target of rapamycin (mTOR), a major intracellular signaling pathway in mammalian cells, in the pathophysiology of AD. mTOR signaling has been the focus of much recent

research for its role in structural and functional plasticity of the central nervous system and as a potential therapeutic target to promote functional recovery after SCI. Approximately a decade ago, Park et al. (2008) demonstrated that disinhibition of the mTOR pathway can markedly enhance axonal regeneration after optic nerve injury. Soon after, others demonstrated that decreased mTOR activity in adult neurons is associated with the loss of regrowth potential, but that experimentally increased mTOR signaling can 're-awaken' neuronal growth and sprouting potential after SCI (Liu et al., 2010). These studies generated considerable interest in the role of mTOR in CNS injury and disease. Numerous subsequent studies demonstrated similar roles of mTOR in neuronal plasticity in a number of models, including epilepsy, autism and neurodegenerative disease (Lipton and Sahin, 2014).

Despite the promising studies proposing mTOR as a critical mediator of CNS plasticity (Hu, 2015), other researchers presented evidence that mTOR may play a more subtle and perhaps replaceable role in post-injury sprouting. For example, Lee et al. (2014b) demonstrated that collateral branching of descending corticospinal axons after pyramidotomy in adult mice proceeds normally during RAP treatment, indicating that mTOR activity is dispensable for reactive sprouting. Furthermore, collateral sprouting in young mice was shown to be substantially impeded by RAP treatment which suggested that mTOR plays a more essential in plasticity early in development. We observed a pattern of enhanced intraspinal mTOR activity weeks after spinal transection, indicating a potential role in mediating maladaptive plasticity. Our hypothesis was that pharmacological inhibition of the mTOR pathway with RAP would impede maladaptive c-fiber sprouting after spinal cord transection and mitigate the development of AD. We did not, however, observe an effect of chronic mTOR inhibition with RAP on the sprouting of primary $CGRP^+$ afferents after SCI, suggesting that mTOR signaling is not involved.

An important caveat with this interpretation arises in the context of studies demonstrating cross-talk and compensatory signaling between mTOR and parallel signaling pathways which can counteract the effects of mTOR

suppression. As discussed in **Chapter 3**, the work of Melemedjian et al. (2013) demonstrated that mTOR inhibition can increase the activity of related signaling pathways in sensory neurons to produce paradoxical effects. This concept is well known in the field of cancer research which often utilizes drugs targeting pro-growth signaling pathways. For example, the development of rapamycin-resistant tumors and failure of otherwise promising tumor suppressing drugs has been attributed to the complex redundancy of important intracellular signaling pathways (Gruppuso et al., 2011; Rozengurt et al., 2014). Notably, mTOR forms two distinct signaling hubs: mammalian target of rapamycin complex 1 and complex 2 (mTORC1 and mTORC2). These protein complexes mediate distinct aspects of cellular activity and metabolism and are classically described as "rapamycin-sensitive" (mTORC1) and "rapamycin-insensitive" (mTORC2) pathways (Laplante and Sabatini, 2009). Acute RAP administration selectively inhibits mTORC1, as this complex contains the specific binding protein targeted by RAP (the FK506 binding protein) which is absent from mTORC2. However, long-term RAP administration is also known to inhibit mTORC2 (Laplante and Sabatini, 2009; Sarbassov et al., 2006). Therefore, it is possible that our prolonged treatment paradigm may have inadvertently suppressed two major signaling hubs, creating even further feedback stimulation of compensatory pathways.

The lessons learned from cancer research elucidate an additional challenge of inhibiting intracellular signaling pathways for therapeutic purposes after SCI; namely that of redundancy within signal transduction networkds. This redundancy is an important feature of intracellular signaling networks that lends an organism resiliency on the sub-cellular level (Logue and Morrison, 2012), however it also presents significant challenges in developing targeted drug therapies. Newer drugs, such as the dual PI3K/mTOR inhibitors, were developed to suppress multiple pathways in hopes of overcoming such drug resistant tumors. Some of these dual inhibitors have been successful in blocking the growth of tumors (Fourneaux et al., 2017; Stankovic et al., 2018). Future studies using dual pathway inhibitors may similarly prove more successful in blocking

maladaptive plasticity by avoiding compensatory signaling through parallel pathways. There are, however, reports suggesting that even dual PI3K/mTOR inhibitors can result in compensatory signaling through MEK/ERK (mitogen-activated protein kinase-kinase/extracellular signal-regulated kinases) signaling (Fourneaux et al., 2017; Soares et al., 2015). Therefore, future experiments utilizing such inhibitors must still assess related pathways and monitor for paradoxical effects.

Similar to previous studies in our lab (Rabchevsky et al., 2011; Rabchevsky et al., 2012), the current GBP study was performed with intraperitoneal drug delivery. An important question regarding the mechanism of GBP in treating AD is whether our observed effects on AD are due to central or peripheral actions of GBP. As the $\alpha_2\delta$–1 and $\alpha_2\delta$–2 subunits targeted by GBP are found throughout various central and peripheral tissues (Taylor and Garrido, 2008), there are numerous locations throughout the body which could feasibly be involved, including the spinal cord, brain, dorsal root ganglia, peripheral sympathetic ganglia and vasculature. Unlike GABA, which has high structural similarity, GBP readily traverses the blood-brain barrier (BBB) and permeates tissue of the central nervous system. In rats, high levels of GBP binding have been documented in membrane extracts from brain, heart and skeletal muscle tissue (Gee et al., 1996). Passage of GBP through the BBB and into neurons is mediated by the L-type amino acid transporter 1 (LAT1) (Uchino et al., 2002). The transport of GBP by LAT1 has been shown to increase in proportion to the plasma concentration of GBP, although this process likely has a saturation limit (Luer et al., 1999). These characteristics indicate that GBP can have multiple sites of action in the central and peripheral nervous systems.

Studies conducted by Taylor and Garrido (2008) characterizing the expression patterns of the $\alpha_2\delta$–1 subunit targeted by GBP found widespread distribution throughout much of the body, including the central nervous system, skeletal muscle, heart, and to a milder extent in the spleen, liver and kidneys. A particularly high staining density is seen in the spinal dorsal and lateral horns, the latter of which is the region containing the majority of SPN. This distribution

pattern suggests that GBP could act on primary afferents, SPNs or some combination thereof. *Ex-vivo* studies using spinal cord slice preparations indicate that GBP reduces excitatory glutamatergic neurotransmission in the dorsal horn through a pre-synaptic mechanism (Patel et al., 2000; Shimoyama et al., 2000). Because the primary subunit targeted by GBP is found at a high density in the lateral horn of the rat thoracic cord where SPN are located (Taylor and Garrido, 2008), future studies using spinal cord slice preparations could be designed to determine whether GBP directly modulates electrophysiological properties of SPN or pre-sympathetic interneurons. Notably, retrograde viral tracing methods could be used to identify SPN in slice preparations from naïve and injured rats to determine possible effects of GBP treatment on the electrophysiological properties of SPN after injury (Derbenev et al., 2010; Ueno et al., 2016; Wilson et al., 2002). Moreover, additional insights could be gained through future studies comparing the effects of systemic (i.p.) versus localized (i.t.) drug delivery on the magnitude of CRD-induced AD. These future directions could be useful for identifying the site of action of GBP and also contribute to our understanding of mechanisms underlying AD.

Another possible site of action is smooth muscle of the vasculature. $\alpha_2\delta$-1 is expressed throughout the smooth muscle of arteries, which indicates a potential role of this subunit in the regulation of peripheral resistance and blood pressure. Pregabalin (PGB), which is a gabapentinoid with similar binding properties to the $\alpha_2\delta$-1 and $\alpha_2\delta$-2, has been shown to induce vasodilation in rat arteries *ex-vivo* (Bannister et al., 2009; Bannister et al., 2012). Isolated and pressurized cerebral arteries had significantly reduced myogenic tone following incubation with PGB, with the arterial tone returning to normal control levels several hours after drug washout. This effect corresponded with an increased ratio of cytosolic:membrane-bound $\alpha_2\delta$-1 subunits suggesting that the vasodilatory effect of PGB results from reduced membrane trafficking of calcium channels and consequent reductions in calcium channel current. Moreover, the 12-hour delay between PGB washout and restoration of myogenic tone is consistent with the time-frame needed for membrane density and trafficking of

calcium channels to return to normal (Bannister et al., 2009). Because these studies were conducted on cerebral arteries, further study is required to determine if gabapentinoid drugs exert similar effects on the systemic vasculature. However, these findings present the possibility that GBP attenuates blood pressure during AD, at least in part, via actions on the peripheral vasculature. It is conceivable that GBP reduces the capacity of vascular smooth muscle to constrict and increase total peripheral resistance. If GBP has vasoactive effects, we would expect a reduction in daily MAP with 4x daily drug administration. Since we did not observe an alteration in the daily MAP in rats receiving GBP, it does not appear that GBP altered vascular tone after SCI. On the other hand, the slight but consistent elevation of daily HR in injured GBP rats relative to saline controls may reflect an increase in cardiac sympathetic drive increasing cardiac output to compensate for possible vasodilatory effects of GBP.

5.3 Alternative Approaches and Future Directions

5.3.1 Determining the mechanism by which GBP suppresses AD

Despite a long history of use in treating epilepsy, neuropathic pain and, more recently, mental illnesses, GBP's primary mechanism of action remains uncertain. A number of mechanisms have been proposed over the past three decades including activation of inhibitory GABA receptors, alteration of intra- and extracellular amino acid concentrations, modification of glutamatergic neurotransmission, prevention of excitatory synaptogenesis, suppression of descending serotonergic facilitation, and inhibition of voltage-gated Na^+, K^+ or Ca^{2+} channels (Chincholkar, 2018; Sills, 2006; Su et al., 2005; Taylor et al., 1998). Following the discovery of Gee et al. (1996) and Wang et al. (1999) that GBP is a ligand for the L-type Ca^{2+} channels (LTCC), many researchers have focused on this interaction to generate a steady accumulation of evidence supporting this as the primary and most clinically relevant target of the gabapentinoid drugs. LTCCs are multimeric complexes with a vast functional diversity (Dolphin, 2016). These channels all contain an obligate α_1 pore-forming subunit through which Ca^{2+} ions flow into the cell upon depolarization, as well as

three auxillary subunits known as the β, γ and $\alpha_2\delta$ subunits (Bourinet et al., 2004). Moreover, these auxillary subunits are each found in multiple isoforms which provide the structural basis for a wide functional diversity of the LTCCs (Dolphin, 2016). The $\alpha_2\delta$ subunit is expressed in four isoforms ($\alpha_2\delta$-1, $\alpha_2\delta$-2, $\alpha_2\delta$-3 and $\alpha_2\delta$-4) of which GBP and pregabalin are known to bind with high affinity to the $\alpha_2\delta$-1 and $\alpha_2\delta$-2 (Gee et al., 1996). Notably, mutation of the $\alpha_2\delta$-1 subunit has been demonstrated to significantly decrease GBP binding and its therapeutic effect in mice (Hendrich et al., 2008; Taylor, 2004), further implicating this subunit as the primary pharmacologically relevant target of GBP. The functional significance of the GBP-$\alpha_2\delta$-1 interaction on LTCCs and neuronal function remains unclear. Work by Annette Dolphin and colleagues suggests that GBP binding to $\alpha_2\delta$-1 disrupts the trafficking of calcium channels to the surface plasma membrane of neurons, resulting in reduced calcium flux and presynaptic neurotransmitter release (Bauer et al., 2010; Dolphin, 2016; Hendrich et al., 2008; Sarantopoulos et al., 2002; Taylor, 2009). Of note, this proposed mechanism is consistent with the delayed-onset effects of GBP in some models (Baba et al., 2016), purportedly due to the time necessary for the cell to traffic new Ca^{2+} channels to the plasma membrane which is likely between 6 and 16 hours *in vitro* (Bauer et al., 2010; Heblich et al., 2008). However, because gabapentin has rapid onset effects with some *in vivo* models this mechanism does not satisfactorily account for its clinical properties (Alles and Smith, 2017; Chincholkar, 2018). In relation to our studies, reduced membrane trafficking of calcium channels also fails to explain the rapid effect of acutely delivered GBP to reduce the magnitude of induced AD (Rabchevsky et al., 2011; Rabchevsky et al., 2012).

Recently, Chen et al. (2018) presented a novel mechanism of action of GBP which involves modulation of N-Methyl-D-aspartic acid receptor (NMDAR) activity. Their study showed that the $\alpha_2\delta$-1subunit coimmunoprecipitates with NMDAR subunits in membrane fractions of rat dorsal spinal cord extract as well as membrane extracts from HEK293 cells *in vitro*, suggesting the formation of a $\alpha_2\delta$-1-NMDAR complex (Chen et al., 2018). Moreover, they demonstrated that exposure to GBP decreases the trafficking of $\alpha_2\delta$-1-NMDAR complexes to

synaptic terminals and reduces NMDA current, suggesting that the $\alpha_2\delta$-1-NMDAR complex potentiates excitatory neurotransmission. This was a remarkable finding, as Chen et al. (2018) challenge the notion that $\alpha_2\delta$-1 functions solely in the context of LTCCs and instead suggest more broad functions independent of LTCCs. Interestingly, this research group has found that the $\alpha_2\delta$-1-NMDAR interaction is involved in spinal cord primary afferents, as well as nuclei within the brain involved in sympathetic nerve activity regulation. These studies suggest that the $\alpha_2\delta$-1-NMDAR is relevant in multiple physiological systems and may account for discrepancies between studies. These novel findings also indicate that GBP may decrease the magnitude of AD by decreasing the density of $\alpha_2\delta$-1-NMDA complexes in primary afferent terminals, leading to a reduction of excitatory neurotransmission through c-fiber afferents during CRD. Notably, $\alpha_2\delta$-1 expression is particularly dense in the spinal cord dorsal horn (Taylor and Garrido, 2008), which supports the hypothesis that GBP suppresses AD by blocking the $\alpha_2\delta$-1-NMDA interaction in the dorsal horn. Future studies may elucidate whether this novel mechanism accounts for the effect of GBP in mitigating experimental AD. Chen et al. (2018) demonstrated that nerve injury increases $\alpha_2\delta$-1-NMDA complexes, implicating this interaction part of the underlying mechanism of GBP. Similar co-immunoprecipitation experiments after T4x SCI would be an important future direction to test the hypothesis that SCI increases $\alpha_2\delta$-1-NMDA complexes in correlation with the development of AD. Moreover, it is feasible to intrathecally or intraperitoneally inject the $\alpha_2\delta$-1 Tat c-terminus peptide as used by Chen et al. (2018) to disrupt the interaction between $\alpha_2\delta$-1 and NMDAR subunits to determine whether blocking this interaction mimics the effects of GBP.

How might this recently proposed mechanism relate to the findings of Eroglu and colleagues (Eroglu et al., 2009; Lau et al., 2017; Yu et al., 2018) indicating that GBP's clinical effects are associated with reduced excitatory synaptogenesis? An intriguing possibility is that a reduction in excitatory neurotransmitter release resulting from GBP's interference with the $\alpha_2\delta$-1-NMDA

complex decreases synapse formation driven by neurotransmitter release (Chen et al., 2018). Viewed in light of other recent findings that suggest thrombospondin-4 (TSP-4) does not interact with $\alpha_2\delta$-1 expressed on the cell surface (Lana et al., 2016), and therefore may not be physiologically relevant, it is possible that much of GBP's purported anti-synaptogenic effects are alternatively due to a reduction of activity-driven synapse formation. The role of neurotransmission in the formation of new synapses has been the subject of investigation for some time. This relationship remains incompletely understood and appears to depend on the specific circuits being investigated and experimental conditions (Andreae and Burrone, 2014). However, a considerable number of studies indicate that synapse formation or maintenance may be driven or enhanced by neurotransmitter release in some systems (Andreae and Burrone, 2014; Brandon et al., 2003; Kozorovitskiy et al., 2015; Reese and Kavalali, 2015).

If GBP prevents the formation of new synapses without altering existing connections (Eroglu et al., 2009), we would expect deleterious effects on memory and learning. Moreover, *in utero* exposure to this commonly prescribed drug might be expected to create developmental defects. However, studies investigating potential effects of *in utero* GBP exposure on the incidence of major birth defects have not reported such a relationship (Fujii et al., 2013; Molgaard-Nielsen and Hviid, 2011; Morrow et al., 2006). This suggests that typical clinical dosages of GBP do not block *de novo* synapse formation *in vivo*. Investigations in rats examining the effect of three weeks of daily GBP treatment (30 mg/kg i.p.) on memory formation also did not find such a relationship, although the closely related drug pregabalin (PGB, 30 mg/kg i.p.) significantly reduced indices of memory consolidation (Salimzade et al., 2017). One important consideration is the relatively short 2-4 hour half-life of GBP in rats, suggesting that plasma concentrations are minimal for the majority of the day when single daily doses are used (Vollmer et al., 1986). In addition, the discrepancy between the effects of GBP and PGB, both of which bind to the $\alpha_2\delta$-1 and $\alpha_2\delta$-2 subunits, may be due to the significantly higher potency of PGB (Shamsi Meymandi and

Keyhanfar, 2013). Several studies examining memory and cognition in humans did not observe an effect of GBP treatment on memory and cognition (Cilio et al., 2001; Leach et al., 1997; Shannon and Love, 2004). However, some conflicting reports exist as well that indicate GBP may actually enhance memory retention and cognitive performance (Acosta et al., 2000; Celikyurt et al., 2011). Recently, Zhou et al. (2018) found that the $\alpha_2\delta$-1-NMDA complex plays an important role in long term potentiation within the corticostriatal pathway and that treatment with either GBP or $\alpha_2\delta$-1 c-terminus peptide interrupts the $\alpha_2\delta$-1-NMDA complex to interfere with memory formation in mice. These discrepant findings likely reflect the inconsistencies in drug dosage, route of delivery, cognitive tests and experimental models utilized.

Could GBP treatment be optimized to more efficiently mitigate AD without numerous possible off-target effects? As described above, the passage of GBP through the BBB and into cells is mediated by LAT1 (Uchino et al., 2002). LAT1 transport of GBP increases in proportion to the plasma concentration of GBP, however this transporter is relatively slow (Palacin et al., 1998) and has a saturation limit beyond which increased plasma GBP does not increase the rate of exposure to central neurons (Luer et al., 1999). Because numerous other tissues throughout the body also bind GBP and can sequester it from the circulation (Gong et al., 2001; Taylor and Garrido, 2008), it is challenging to deliver large doses of GBP to the central nervous system specifically by way of systemic administration. Moreover, LAT1 is found in many cell types and therefore cellular uptake of GBP is non-specific. Intriguing work by Biggs et al. (2015) indicates that the capsaicin-activated TRPV1 (transient receptor/vanilloid receptor 1) cation channel can provide an additional route of entry for GBP into cells that is hundreds of times faster than LAT1 transport (Biggs et al., 2015). Because TRPV1$^+$ sensory neurons play an important role in AD (Ramer et al., 2012), this suggests that combined treatment with GBP and TRPV1 activators could markedly increase the specificity of GBP for TRPV1$^+$ neurons to more potently suppress AD at lower systemic dosages. Additionally, it is currently unclear whether GBP acts at an extracellular or intracellular site to suppress AD.

Therefore, enhancing the cytoplasmic concentration of GBP in TRPV1$^+$ cells could also help elucidate the relevant site of action.

5.3.2 Dissecting the cellular signaling driving maladaptive plasticity

What other signaling pathways might drive maladaptive sprouting associated with the development of AD? One clue in the relevant signaling pathway comes from studies demonstrating the role of nerve growth factor (NGF) in sprouting of c-fibers after SCI (Brown et al., 2004; Cameron et al., 2006; Krenz et al., 1999). As discussed in **Chapter 2**, NGF expression is upregulated throughout the spinal cord in response to traumatic SCI (Bakhit et al., 1991). Sequestration of intraspinal NGF with anti-NGF antibodies decreases c-fiber sprouting in correlation with a reduced magnitude of AD (Krenz et al., 1999), and viral-mediated overexpression of NGF has been shown to increase c-fiber sprouting and AD severity (Cameron et al., 2006). Upon binding to its high-affinity receptor, tropomyosin receptor kinase A (trkA), NGF can stimulate a number of intracellular signaling cascades (Wang et al., 2014). Protein kinase B (a.k.a. Akt) has garnered interest for its role in mediating the protective effects of NGF on neurons (Crowder and Freeman, 1998; Xia et al., 2015). The survival of rat sympathetic neurons maintained *in vitro* is enhanced with NGF treatment, though this effect is blocked with PI3K-Akt inhibitors (Crowder and Freeman, 1998). The mitogen-activated protein kinase (MAPK) pathway is also believed to function downstream of NGF to promote neuronal plasticity (Blum and Konnerth, 2005). Further experimentation in rodent AD models using Akt or MAPK inhibitors (English and Cobb, 2002; Nitulescu et al., 2016), for example, may provide new insight into pathways related to AD development.

An important consideration that must be addressed when attempting to block maladaptive plasticity is that many aspects of post-injury plasticity are desirable for functional recovery (Brown and Weaver, 2012). Therefore, an ideal prophylactic treatment for AD would be capable of blocking pathways involved specifically with maladaptive plasticity without compromising signaling pathways driving adaptive plasticity. Because unmyelinated c-fibers are thought to be the

primary fiber type involved in the pathophysiology of AD (Hou et al., 2009), it may be possible to target signaling pathways specific to these neurons without impeding beneficial plasticity of motoneuron circuits or other myelinated sensory fibers. This would require a detailed comparative understanding of the transcriptional and proteomic profiles of specific neuronal populations after SCI. Modern technologies such as single-cell laser capture microdissection and high-fidelity transcriptome sequencing allow for such characterization of transcriptional programs in specific cell types. For example, these methods have been used recently in the rodent spinal cord to characterize the transcriptomes of spatially distinct neuronal populations isolated with laser microdissection (Bandyopadhyay et al., 2014; Nichterwitz et al., 2016). These studies indicate that this may be a viable approach to drive forward our understanding of cellular mechanisms involved in maladaptive sprouting.

5.3.3 Homeostatic plasticity: does it play a role in the pathogenesis of AD?

Homeostatic control is found in many biological systems and is a powerful mechanism that allows cells and organisms to operate with optimal physiological function despite changing environmental conditions. In the nervous system, homeostatic plasticity (HP) refers to a process whereby neurons behave in a self-regulatory manner to maintain activity within a relatively stable range. These mechanisms may include alterations in the number of synapses, ion channel expression, altered neurotransmitter release quanta, and changes in neurotransmitter receptor expression (Lazarevic et al., 2013; O'Brien et al., 1998; Turrigiano, 2012; Turrigiano, 2008; Wenner, 2014). Schaukowitch et al. (2017) demonstrated *in vitro* that a global decrease in network activity following exposure to the Na^+ channel blocker tetrodotoxin triggers a specific transcriptional program which enhances synaptic strength, indicating that neurons have archetypal transcription programs for mechanisms of HP. Substantial evidence suggests a role of HP in the pathophysiology of SCI and subsequent dysfunctions. For example, previous studies show that the loss of descending inputs onto spinal neurons after SCI results in increased

spontaneous neuronal firing and compensatory sprouting in attempt to maintain an normal level of activity (Beauparlant et al., 2013; Ferguson et al., 2012). Studies on spinal respiratory networks indicate that HP is a feature of respiratory neurons that helps to maintain appropriate blood arterial gas levels (Braegelmann et al., 2017) and also indicates that mechanisms of HP may be seen in other spinal networks including autonomic neurons.

Within the theoretical framework of HP, a potential role in the etiology of AD can be speculated. Presently, it is known that primary afferent c-fibers and ascending propriospinal neurons sprout after SCI (Hou et al., 2008; Hou et al., 2009). This plasticity is believed to be a compensatory response to the denervation and loss of supraspinal inputs. What is not yet clear, however, is whether the sprouting of these two populations are interrelated. One possibility is that the reactive sprouting of primary afferents and subsequent increase in sensory input provides the stimulus for the sprouting and plasticity of propriospinal neurons. Future studies designed to limit the effects of primary afferent sprouting may elucidate a possible relationship. Dorsal rhizotomy, which triggers the degeneration of intraspinal afferents from the associated dermatome(s) (Coimbra et al., 1984; Muneton-Gomez et al., 2004), may be performed after SCI to test the hypothesis that segmental propriospinal sprouting is driven or enhanced by sprouting of primary afferents. Combined with propriospinal labeling methods such as those previously employed in our lab (Hou et al., 2008), deafferentation may yield insights into a possible relationship between the sprouting of these two neuronal populations. Conversely, it is also possible that the sprouting of both populations is driven by a common stimulus such as increased NGF expression (Brown et al., 2004). Although injury-induced upregulation of NGF has been demonstrated to induce c-fiber sprouting after SCI (Cameron et al., 2006; Krenz et al., 1999), the hypothesis that ascending propriospinal neurons similarly sprout in response to elevated NGF remains untested.

Prolonged exposure to GBP has been observed to decrease the overall activity of dorsal horn networks (Biggs et al., 2014). This implies that our 4x daily

treatment paradigm feasibly reduced overall sensory input into the spinal cord after injury. In this case, we can speculate that a long-term reduction in afferent stimulation would also reduce activity of intraspinal networks influenced by sensory inputs, such as the SPN. Large-scale changes in network activity are known to induce HP, whereby a sustained reduction of synaptic inputs or activity results in an increase of spontaneous activity or membrane excitability (Braegelmann et al., 2017). When extended to our current GBP study, this indicates that a prolonged reduction in afferent stimulation of sympathetic or pre-sympathetic interneurons could provide impetus for SPN to increase their intrinsic excitability in effort to maintain their activity around a “set-point”. While this hypothesis must be assessed directly with future experiments, it may explain our finding that continuous high dose GBP treatment paradoxically increases the frequency of spontaneous AD.

5.3.4 Further elucidation of the neuronal circuitry underlying AD

Our current understanding of the interneurons influencing SPN in both the naïve and injured spinal cord remains fragmented, in part because of earlier technical challenges of confidently identifying sympathetic interneurons as described by Schramm (2006) and Deuchars (2007). In the intact animal, spinal interneurons are believed to play a minor role in regulating SPN. Rather, the descending inputs from supraspinal sympathetic nuclei are the major controllers of SPN (Laskey and Polosa, 1988; Schramm, 2006). After SCI, the loss of descending connections leaves the SPN isolated from the brain and completely reliant on spinal interneurons or primary afferents for excitatory or inhibitory modulation. Because spinal interneuron networks undergo extensive reorganization and form new circuits after injury (Bareyre et al., 2004; Cote et al., 2012; Hou et al., 2008; Rabchevsky, 2006; Ueno et al., 2016), it is not presently clear how sympathetic and pre-sympathetic spinal interneurons are organized after SCI.

During CRD, the activation of thoracic SPN by lumbosacral pelvic afferents originating several spinal segments caudal to the IML indicates the

presence of long-distance intersegmental interneurons or a series of shorter segmental interneurons relaying afferent inputs to rostral thoracic SPN. These propriospinal "relay" neurons are known to sprout after transection SCI, suggesting that plasticity of this pathway may contribute to the development of AD (Hou et al., 2008). What is not clear, however, is the relative contribution of long inter-segmental interneurons traversing several segments to form a di-synaptic pathway (pelvic afferent→intersegmental interneuron→SPN), compared to a series of segmental interneurons connected to form a poly-synaptic pathway (primary afferent→segmental interneuron→segmental neuron(n_x)→ SPN; **Figure 5.1**).

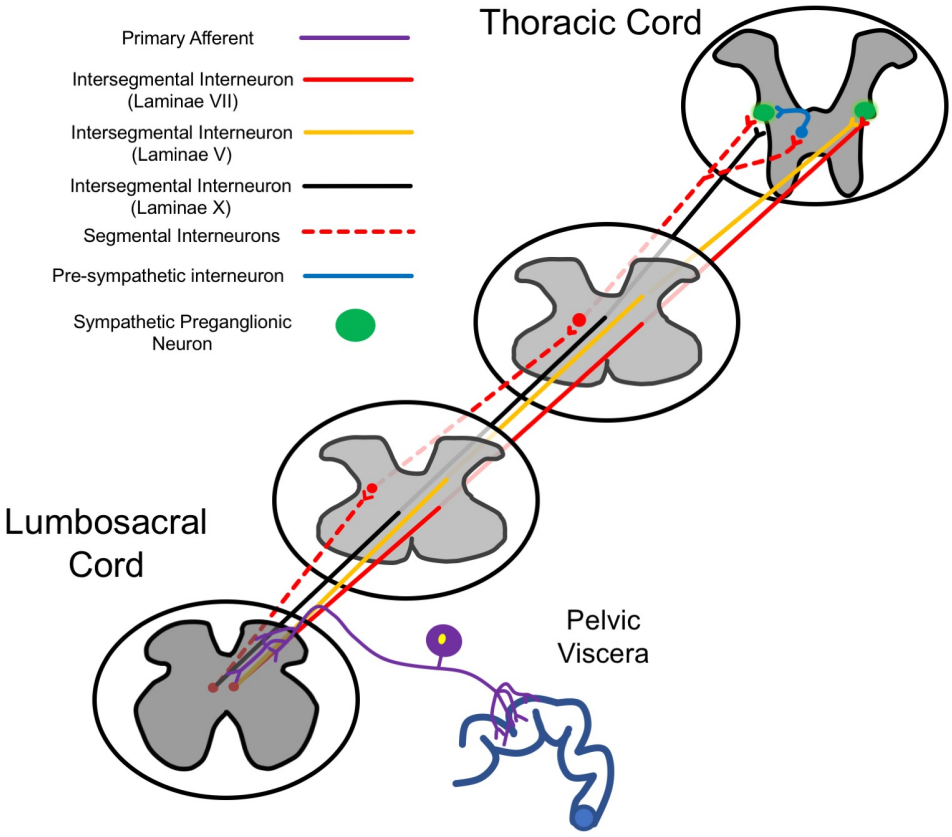

Figure 5.1. Proposed ascending pathways relaying visceral stimulation to sympathetic preganglionic neurons (SPN). Segmental (dotted red lines) and intersegmental (solid red, orange and black lines) interneurons may contribute to AD. These "relay" neurons may be a single long projection spanning several segments or a series of shorter segmental connections. These propriospinal

projection neurons originating in the dorsal gray commissure have been identified in lamina VII (red), V (orange) and X (black). The relative importance of these distinct neural pathways in relaying noxious pelvic stimulation to the SPN is currently unknown, however the future use of chemogenetic or optogenetic silencing methods may enable the dissection of circuitry critical in AD elicited by noxious pelvic stimuli.

Novel tract tracing and silencing techniques may be applied in our AD model to dissect this pathway in more detail. As discussed in Chapter 2, chemogenetic silencing of discrete neuronal pathways has been applied in the CNS to examine the role of specific neuronal tracts (**Figure 2.1**). In addition to the experiments proposed in **Chapter 2**, DREADDs and chemogenetic silencing methods may also be applied to determine the relative contributions of long intersegmental projections compared to series of short segmental projections in relaying lumbosacral visceral afferents to thoracic SPN. The two-vector system described in **Chapter 2** is comprised of a high-efficiency retrograde virus expressing tetanus toxin (HiRET-eTeNT) and a second virus carrying a doxycycline sensitive activation gene (AAV-rtTAV). After doxycycline treatment, HiRET-eTeNT becomes activated to block pre-synaptic neurotransmitter release. Notably, however, only neurons transfected with both vectors are silenced. With this system, it is feasible to inject HiRET-eTeNT into thoracic segments containing vasomotor SPN and AAV-rtTAV into the lumbosacral laminae X to silence long intersegmental projection neurons. Alternatively, HiRET-eTeNT may be injected throughout intervening thoracolumbar segments with AAV-rtTAV similarly injected into the lumbosacral lamina X in order to silence shorter segmental projection neurons. Pairing this silencing paradigm with cardiophysiological monitoring in SCI rats, it may be possible to compare the importance of these two proposed pathways to the magnitude of CRD-induced AD. As described in the review by Roth (2016), similar approaches have been used with vectors expressing the hM4Di DREADD (designer receptor exclusively activated by designer drugs), which activates K+ channels to hyperpolarize neurons when the designer drug clozapine-n-oxide (CNO) is delivered.

While DREADDs and other chemogenetic methods hold the potential for significantly advancing our understanding of the pathophysiology of SCI and AD, caution must be used in interpreting the results of CNO mediated DREADD activation in lieu of recent studies demonstrating that metabolites of CNO create confounding physiological effects (Manvich et al., 2018). Additionally, while double vector systems can target specific neuronal projections, chemogenetic techniques do not provide temporal and spatial precision as the activation drugs require time to become active and may last for several hours before elimination. An alternative technique is that of optogenetic modulation of neural activity. This technology utilizes the light-activated cation or anion-conducting channelrhodopsins to excite or inhibit neural activity, respectively (Iyer et al., 2014). In contrast to chemogenetic methods, optogenetic modulation provides a high degree of temporal and spatial precision due to the ability to expose discrete areas of tissue with a controllable light source. These characteristics make it well suited for identifying the role of specific neurons in network-level activity such as viscerosympathetic circuits important to AD. While a majority of optogenetic studies have been focused on brain pathways, a number of groups have adapted this technique for use in the spinal cord (Christensen et al., 2016; Rahman et al., 2018). Considerable technical challenges exist in the implementation of spinal cord optogenetics (Montgomery et al., 2016), although researchers have recently developed a wireless, battery free and flexible optical device which circumvents several technical hurdles (Samineni et al., 2017).

5.3.5 Interaction between AD and the Immune System

As discussed in detail in **Chapter 2**, we are now beginning to appreciate that the dramatic fluctuations in blood pressure and circulating catecholamines (Leman et al., 2000) during recurrent AD can produce deleterious effects on multiple physiological functions. SCI-induced immune depression syndrome (SCI-IDS), which has been linked with recurrent AD in mice, is one example which has significant clinical relevance (Riegger et al., 2007; Zhang et al., 2013). This relationship is believed to be mediated through abnormal levels of

immunosuppressive catecholamine and glucocorticoids released during AD, although other mechanisms such as atrophy of the hemaepoetic niche in bone marrow have been proposed as well (see **Chapter 2**). Unlike studies in mice (Zhang et al., 2013), we did not observe gross spleen atrophy in our rat AD model despite using a similar injury method and experimental timeline. Taken alone, our data implies that the association between AD and SCI-IDS may be species specific. In contrast, Mironets et al. (2018) recently utilized flow cytometry and reported splenic leucopenia (decreased white blood cells) in wistar rats after T3-transection SCI. They did not, however, report spleen wet weights for comparison to our data. It is possible that leucopenia occurred after injury in our study without being reflected in spleen size or weight. Future AD studies in rats should employ flow-cytometry to quantify markers of white blood cells such as CD45R (B cell), CD4 (T cell), CD8 (T cell), CD11b/c and CD68. Notably, flow cytometry is the preferred method of analysis, as spleen tissue is notoriously difficult to analyze histologically due to high levels of autofluorescence which contribute significant false-positive readings (Franken et al., 2015; Li et al., 2012a).

Paradoxically, we found that continuous GBP treatment after SCI caused splenomegaly (enlarged spleen). Although there are no readily apparent connections between GBP and spleen weight, there are clinical reports of splenomegaly associated with GBP administration. Ragucci and Cohen (2001) described a patient receiving 200 mg/kg GBP once daily who developed GBP hypersensitivity syndrome, which included splenomegaly and elevated hepatic enzymes. The spleen returned to normal size rapidly after discontinuation of GBP. A number of possible causes of GBP-induced splenomegaly can be speculated. The primary calcium channel subunit targeted by GBP is modestly expressed in splenic tissue, indicating a possible direct effect of GBP on spleen. As reviewed by (Petroianu, 2007), a variety of drugs can cause splenomegaly through direct effects on spleen cells or through indirect effects on other organ systems leading to congestion and enlargement of the spleen. The $\alpha_2\delta$–1 subunit is sparsely expressed in the spleen, however liver hepatocytes show moderate

expression (Taylor and Garrido, 2008). As the portal vein carries blood from the spleen to the liver, it is feasible that an effect of GBP on venous resistance in the liver led to splenic congestion. Furthermore, blood vessels express the $\alpha_2\delta$–1 subunit (Bannister et al., 2009) and, therefore, splenic congestion and enlargement may have resulted from effects on the vascular smooth muscle.

5.4 Summary of Thesis

This dissertation has confirmed maladaptive neuroanatomical changes which contribute to autonomic dysfunction and AD after SCI, as well as the investigation of two drugs that were hypothesized to impede maladaptive plasticity and prevent the development of AD. We discovered previously undescribed cardiovascular side effects of RAP after SCI. Our results demonstrate that prolonged RAP treatment exacerbates cardiovascular dysfunction without modifying c-fiber sprouting, and suggest that mTOR signaling plays a minor or dispensable role in maladaptive plasticity. Our findings also highlight the challenges involved in targeting complex signaling pathways for therapeutic outcomes. However other viable research avenues exist such as the dual-kinase inhibitors which may prove more effective in suppressing the cellular processes required for maladaptive sprouting.

Continuous GBP treatment was found to decrease the magnitude of hypertension during AD and to reduce the time required for blood pressure to return to normal after CRD. These represent clinically valuable effects, however the dosage paradigm we used was also associated with more frequent sAD and inhibited weight gain. We found that SCI decreases markers of excitatory and inhibitory synapses in the lumbosacral cord, suggesting that synaptic remodeling in the dorsal horn may contribute to dysfunctional sympathetic activity after SCI. Further and more detailed analyses will be necessary to better understand how synaptic re-arrangements contribute to AD. Although GBP treatment did not alter synaptic measurements as hypothesized, multiple other unexplored mechanisms have been presented that may be the subject of valuable future research. Ultimately, GBP remains a valuable tool in the current arsenal of drugs which can

alleviate AD, however the dosage, frequency and route of delivery must be optimized to reduce potentially deleterious side effects.

Copyright © Khalid C. Eldahan 2019

Appendix 1. Abbreviations

ACh	Acetylcholine
AD	Autonomic dysreflexia
ADP	Adenosine diphosphate
AMPA	α-amino-3-hydroxy-5-methyl-4-isoxazolepropionic acid receptor
APN	Ascending propriospinal neuron
BTX	Botulinum toxin
CGRP	Calcitonin gene related peptide
CNO	Clozapine-n-oxide
CRD	Colorectal distension
CVS	Cardiovascular system
DGC	Dorsal gray commissure
DREADD	Designer receptor exclusively activated by designer drug
GABA	Gamma-aminobutyric acid
GBP	Gabapentin
GC	Glucocorticoid
GIRK	G protein-coupled inwardly rectifying potassium channel
HP	Homeostatic plasticity
HPA	Hypothalamic pituitary axis
IML	Intermediolateral cell column
mTOR	Mammalian target of rapamycin
NDO	Neurogenic detrusor overactivity
NE	Norepinephrine
NGF	Nerve growth factor
NMDA	N-methyl-d-aspartic acid
NMDAR	N-methyl-D-aspartate receptor
PI3K	Phosphoinositide 3-kinase
RAP	Rapamycin
sAD	Spontaneous autonomic dysreflexia
sBR	Spontaneous baroreflex

SCI	Spinal cord injury
SCI-IDS	Spinal cord injury-induced immune depression syndrome
SHR	Spontaneously hypertensive rats
SNS	Sympathetic nervous system
SPN	Sympathetic preganglionic neurons
SYP	Synaptophysin
VGAT	Vesicular gamma-aminobutyric acid transporter
VGLUT	Vesicular glutamate transporter

REFERENCES

Aaron, J.S., Taylor, A.B., Chew, T.L., 2018. Image co-localization - co-occurrence versus correlation. J Cell Sci 131.

Ackerknecht, E.H., 1974. The history of the discovery of the vegatative (autonomic) nervous system. Med Hist 18, 1-8.

Ackery, A.D., Norenberg, M.D., Krassioukov, A., 2007. Calcitonin gene-related peptide immunoreactivity in chronic human spinal cord injury. Spinal Cord 45, 678-686.

Acosta, G.B., Boccia, M.M., Baratti, C.M., 2000. Gabapentin, an antiepileptic drug, improves memory storage in mice. Neurosci Lett 279, 173-176.

Adameova, A., Abdellatif, Y., Dhalla, N.S., 2009. Role of the excessive amounts of circulating catecholamines and glucocorticoids in stress-induced heart disease. Can J Physiol Pharmacol 87, 493-514.

Al Dera, H., Habgood, M.D., Furness, J.B., Brock, J.A., 2012. Prominent contribution of L-type Ca2+ channels to cutaneous neurovascular transmission that is revealed after spinal cord injury augments vasoconstriction. Am J Physiol Heart Circ Physiol 302, H752-762.

Al-Chaer, E.D., Lawand, N.B., Westlund, K.N., Willis, W.D., 1996. Pelvic visceral input into the nucleus gracilis is largely mediated by the postsynaptic dorsal column pathway. J Neurophysiol 76, 2675-2690.

Alan, N., Ramer, L.M., Inskip, J.A., Golbidi, S., Ramer, M.S., Laher, I., Krassioukov, A.V., 2010. Recurrent autonomic dysreflexia exacerbates vascular dysfunction after spinal cord injury. Spine J 10, 1108-1117.

Albrecht, M., Henke, J., Tacke, S., Markert, M., Guth, B., 2014. Effects of isoflurane, ketamine-xylazine and a combination of medetomidine, midazolam and fentanyl on physiological variables continuously measured by telemetry in Wistar rats. BMC Vet Res 10, 198.

Alles, S.R.A., Smith, P.A., 2017. The Anti-Allodynic Gabapentinoids: Myths, Paradoxes, and Acute Effects. Neuroscientist 23, 40-55.

Alvarez, F.J., Taylor-Blake, B., Fyffe, R.E., De Blas, A.L., Light, A.R., 1996. Distribution of immunoreactivity for the beta 2 and beta 3 subunits of the GABAA receptor in the mammalian spinal cord. J Comp Neurol 365, 392-412.

Alvarez, F.J., Villalba, R.M., Zerda, R., Schneider, S.P., 2004. Vesicular glutamate transporters in the spinal cord, with special reference to sensory primary afferent synapses. J Comp Neurol 472, 257-280.

Amiya, E., Watanabe, M., Komuro, I., 2014. The Relationship between Vascular Function and the Autonomic Nervous System. Ann Vasc Dis 7, 109-119.

Anderson, K.D., 2004. Targeting recovery: priorities of the spinal cord-injured population. Journal of neurotrauma 21, 1371-1383.

Andreae, L.C., Burrone, J., 2014. The role of neuronal activity and transmitter release on synapse formation. Curr Opin Neurobiol 27, 47-52.

Apostolidis, A., Popat, R., Yiangou, Y., Cockayne, D., Ford, A.P., Davis, J.B., Dasgupta, P., Fowler, C.J., Anand, P., 2005. Decreased sensory receptors P2X3 and TRPV1 in suburothelial nerve fibers following intradetrusor injections of

botulinum toxin for human detrusor overactivity. J Urol 174, 977-982; discussion 982-973.
Armbruster, B.N., Li, X., Pausch, M.H., Herlitze, S., Roth, B.L., 2007. Evolving the lock to fit the key to create a family of G protein-coupled receptors potently activated by an inert ligand. Proc Natl Acad Sci U S A 104, 5163-5168.
Armour, J.A., Murphy, D.A., Yuan, B.X., Macdonald, S., Hopkins, D.A., 1997. Gross and microscopic anatomy of the human intrinsic cardiac nervous system. Anat Rec 247, 289-298.
Arnold, J.M., Feng, Q.P., Delaney, G.A., Teasell, R.W., 1995. Autonomic dysreflexia in tetraplegic patients: evidence for alpha-adrenoceptor hyper-responsiveness. Clin Auton Res 5, 267-270.
Asante, C.O., Wallace, V.C., Dickenson, A.H., 2009. Formalin-induced behavioural hypersensitivity and neuronal hyperexcitability are mediated by rapid protein synthesis at the spinal level. Mol Pain 5, 27.
Baba, H., Petrenko, A.B., Fujiwara, N., 2016. Clinically relevant concentration of pregabalin has no acute inhibitory effect on excitation of dorsal horn neurons under normal or neuropathic pain conditions: An intracellular calcium-imaging study in spinal cord slices from adult rats. Brain Res 1648, 445-458.
Baeyens, N., Nicoli, S., Coon, B.G., Ross, T.D., Van den Dries, K., Han, J., Lauridsen, H.M., Mejean, C.O., Eichmann, A., Thomas, J.L., Humphrey, J.D., Schwartz, M.A., 2015. Vascular remodeling is governed by a VEGFR3-dependent fluid shear stress set point. Elife 4.
Bai, L., Xu, H., Collins, J.F., Ghishan, F.K., 2001. Molecular and functional analysis of a novel neuronal vesicular glutamate transporter. J Biol Chem 276, 36764-36769.
Bakhit, C., Armanini, M., Wong, W.L., Bennett, G.L., Wrathall, J.R., 1991. Increase in nerve growth factor-like immunoreactivity and decrease in choline acetyltransferase following contusive spinal cord injury. Brain Res 554, 264-271.
Baldi, J.C., Jackson, R.D., Moraille, R., Mysiw, W.J., 1998. Muscle atrophy is prevented in patients with acute spinal cord injury using functional electrical stimulation. Spinal Cord 36, 463-469.
Baldwin, K.T., Eroglu, C., 2017. Molecular mechanisms of astrocyte-induced synaptogenesis. Curr Opin Neurobiol 45, 113-120.
Bandyopadhyay, U., Fenton, W.A., Horwich, A.L., Nagy, M., 2014. Production of RNA for transcriptomic analysis from mouse spinal cord motor neuron cell bodies by laser capture microdissection. J Vis Exp, e51168.
Bannister, J.P., Adebiyi, A., Zhao, G., Narayanan, D., Thomas, C.M., Feng, J.Y., Jaggar, J.H., 2009. Smooth muscle cell alpha2delta-1 subunits are essential for vasoregulation by CaV1.2 channels. Circ Res 105, 948-955.
Bannister, J.P., Bulley, S., Narayanan, D., Thomas-Gatewood, C., Luzny, P., Pachuau, J., Jaggar, J.H., 2012. Transcriptional upregulation of alpha2delta-1 elevates arterial smooth muscle cell voltage-dependent Ca2+ channel surface expression and cerebrovascular constriction in genetic hypertension. Hypertension 60, 1006-1015.

Bareyre, F.M., Kerschensteiner, M., Raineteau, O., Mettenleiter, T.C., Weinmann, O., Schwab, M.E., 2004. The injured spinal cord spontaneously forms a new intraspinal circuit in adult rats. Nat Neurosci 7, 269-277.
Barth, E., Albuszies, G., Baumgart, K., Matejovic, M., Wachter, U., Vogt, J., Radermacher, P., Calzia, E., 2007. Glucose metabolism and catecholamines. Crit Care Med 35, S508-518.
Basbaum, A.I., Fields, H.L., 1984. Endogenous pain control systems: brainstem spinal pathways and endorphin circuitry. Annu Rev Neurosci 7, 309-338.
Bauer, C.S., Rahman, W., Tran-van-Minh, A., Lujan, R., Dickenson, A.H., Dolphin, A.C., 2010. The anti-allodynic alpha(2)delta ligand pregabalin inhibits the trafficking of the calcium channel alpha(2)delta-1 subunit to presynaptic terminals in vivo. Biochem Soc Trans 38, 525-528.
Beauparlant, J., van den Brand, R., Barraud, Q., Friedli, L., Musienko, P., Dietz, V., Courtine, G., 2013. Undirected compensatory plasticity contributes to neuronal dysfunction after severe spinal cord injury. Brain 136, 3347-3361.
Bellocchio, E.E., Reimer, R.J., Fremeau, R.T., Jr., Edwards, R.H., 2000. Uptake of glutamate into synaptic vesicles by an inorganic phosphate transporter. Science 289, 957-960.
Benarroch, E.E., 1993. The central autonomic network: functional organization, dysfunction, and perspective. Mayo Clin Proc 68, 988-1001.
Bennett, D.J., Sanelli, L., Cooke, C.L., Harvey, P.J., Gorassini, M.A., 2004. Spastic long-lasting reflexes in the awake rat after sacral spinal cord injury. J Neurophysiol 91, 2247-2258.
Bertinieri, G., di Rienzo, M., Cavallazzi, A., Ferrari, A.U., Pedotti, A., Mancia, G., 1985. A new approach to analysis of the arterial baroreflex. J Hypertens Suppl 3, S79-81.
Bevan, R.D., Dodge, J., Nichols, P., Penar, P.L., Walters, C.L., Wellman, T., Bevan, J.A., 1998. Weakness of sympathetic neural control of human pial compared with superficial temporal arteries reflects low innervation density and poor sympathetic responsiveness. Stroke 29, 212-221.
Biggs, J.E., Boakye, P.A., Ganesan, N., Stemkowski, P.L., Lantero, A., Ballanyi, K., Smith, P.A., 2014. Analysis of the long-term actions of gabapentin and pregabalin in dorsal root ganglia and substantia gelatinosa. J Neurophysiol 112, 2398-2412.
Biggs, J.E., Stemkowski, P.L., Knaus, E.E., Chowdhury, M.A., Ballanyi, K., Smith, P.A., 2015. Suppression of network activity in dorsal horn by gabapentin permeation of TRPV1 channels: implications for drug access to cytoplasmic targets. Neurosci Lett 584, 397-402.
Birder, L.A., Nakamura, Y., Kiss, S., Nealen, M.L., Barrick, S., Kanai, A.J., Wang, E., Ruiz, G., De Groat, W.C., Apodaca, G., Watkins, S., Caterina, M.J., 2002. Altered urinary bladder function in mice lacking the vanilloid receptor TRPV1. Nat Neurosci 5, 856-860.
Bjelakovic, B., Dimitrijevic, L., Lukic, S., Golubovic, E., 2014. Hypertensive encephalopathy as a late complication of autonomic dysreflexia in a 12-year-old boy with a previous spinal cord injury. Eur J Pediatr 173, 1683-1684.

Blackmer, J., 2003. Rehabilitation medicine: 1. Autonomic dysreflexia. CMAJ 169, 931-935.
Blok, B.F., van Maarseveen, J.T., Holstege, G., 1998. Electrical stimulation of the sacral dorsal gray commissure evokes relaxation of the external urethral sphincter in the cat. Neurosci Lett 249, 68-70.
Blum, R., Konnerth, A., 2005. Neurotrophin-mediated rapid signaling in the central nervous system: mechanisms and functions. Physiology (Bethesda) 20, 70-78.
Bluvshtein, V., Korczyn, A.D., Pinhas, I., Vered, Y., Gelernter, I., Catz, A., 2011. Insulin resistance in tetraplegia but not in mid-thoracic paraplegia: is the mid-thoracic spinal cord involved in glucose regulation? Spinal Cord 49, 648-652.
Bohr, D.F., 1967. Adrenergic receptors in coronary arteries. Ann N Y Acad Sci 139, 799-807.
Bolte, S., Cordelieres, F.P., 2006. A guided tour into subcellular colocalization analysis in light microscopy. J Microsc 224, 213-232.
Bourinet, E., Mangoni, M.E., Nargeot, J., 2004. Dissecting the functional role of different isoforms of the L-type Ca2+ channel. J Clin Invest 113, 1382-1384.
Brack, K.E., 2015. The heart's 'little brain' controlling cardiac function in the rabbit. Exp Physiol 100, 348-353.
Braddom, R.L., Rocco, J.F., 1991. Autonomic dysreflexia. A survey of current treatment. Am J Phys Med Rehabil 70, 234-241.
Braegelmann, K.M., Streeter, K.A., Fields, D.P., Baker, T.L., 2017. Plasticity in respiratory motor neurons in response to reduced synaptic inputs: A form of homeostatic plasticity in respiratory control? Exp Neurol 287, 225-234.
Brandon, E.P., Lin, W., D'Amour, K.A., Pizzo, D.P., Dominguez, B., Sugiura, Y., Thode, S., Ko, C.P., Thal, L.J., Gage, F.H., Lee, K.F., 2003. Aberrant patterning of neuromuscular synapses in choline acetyltransferase-deficient mice. J Neurosci 23, 539-549.
Brock, J.A., Yeoh, M., McLachlan, E.M., 2006. Enhanced neurally evoked responses and inhibition of norepinephrine reuptake in rat mesenteric arteries after spinal transection. Am J Physiol Heart Circ Physiol 290, H398-405.
Brommer, B., Engel, O., Kopp, M.A., Watzlawick, R., Muller, S., Pruss, H., Chen, Y., DeVivo, M.J., Finkenstaedt, F.W., Dirnagl, U., Liebscher, T., Meisel, A., Schwab, J.M., 2016. Spinal cord injury-induced immune deficiency syndrome enhances infection susceptibility dependent on lesion level. Brain 139, 692-707.
Brown, A., Ricci, M.J., Weaver, L.C., 2004. NGF message and protein distribution in the injured rat spinal cord. Exp Neurol 188, 115-127.
Brown, A., Weaver, L.C., 2012. The dark side of neuroplasticity. Exp Neurol 235, 133-141.
Budde, K., Becker, T., Arns, W., Sommerer, C., Reinke, P., Eisenberger, U., Kramer, S., Fischer, W., Gschaidmeier, H., Pietruck, F., Investigators, Z.S., 2011. Everolimus-based, calcineurin-inhibitor-free regimen in recipients of de-novo kidney transplants: an open-label, randomised, controlled trial. Lancet 377, 837-847.
Burette, A., Collman, F., Micheva, K.D., Smith, S.J., Weinberg, R.J., 2015. Knowing a synapse when you see one. Front Neuroanat 9, 100.

Burnstock, G., 1969. Evolution of the autonomic innervation of visceral and cardiovascular systems in vertebrates. Pharmacol Rev 21, 247-324.
Cabot, J.B., Alessi, V., Carroll, J., Ligorio, M., 1994. Spinal cord lamina V and lamina VII interneuronal projections to sympathetic preganglionic neurons. J Comp Neurol 347, 515-530.
Calaresu, F.R., Yardley, C.P., 1988. Medullary basal sympathetic tone. Annu Rev Physiol 50, 511-524.
Cameron, A.A., Smith, G.M., Randall, D.C., Brown, D.R., Rabchevsky, A.G., 2006. Genetic manipulation of intraspinal plasticity after spinal cord injury alters the severity of autonomic dysreflexia. J Neurosci 26, 2923-2932.
Campagnolo, D.I., Bartlett, J.A., Keller, S.E., Sanchez, W., Oza, R., 1997. Impaired phagocytosis of Staphylococcus aureus in complete tetraplegics. Am J Phys Med Rehabil 76, 276-280.
Campagnolo, D.I., Keller, S.E., DeLisa, J.A., Glick, T.J., Sipski, M.L., Schleifer, S.J., 1994. Alteration of immune system function in tetraplegics. A pilot study. Am J Phys Med Rehabil 73, 387-393.
Cano, G., Sved, A.F., Rinaman, L., Rabin, B.S., Card, J.P., 2001. Characterization of the central nervous system innervation of the rat spleen using viral transneuronal tracing. J Comp Neurol 439, 1-18.
Canon, S., Shera, A., Phan, N.M., Lapicz, L., Scheidweiler, T., Batchelor, L., Swearingen, C., 2015. Autonomic dysreflexia during urodynamics in children and adolescents with spinal cord injury or severe neurologic disease. J Pediatr Urol 11, 32 e31-34.
Carasatorre, M., Ochoa-Alvarez, A., Velazquez-Campos, G., Lozano-Flores, C., Ramirez-Amaya, V., Diaz-Cintra, S.Y., 2015. Hippocampal Synaptic Expansion Induced by Spatial Experience in Rats Correlates with Improved Information Processing in the Hippocampus. PLoS One 10, e0132676.
Caruso, D., Gater, D., Harnish, C., 2015. Prevention of recurrent autonomic dysreflexia: a survey of current practice. Clin Auton Res 25, 293-300.
Castro, M.J., Apple, D.F., Jr., Hillegass, E.A., Dudley, G.A., 1999. Influence of complete spinal cord injury on skeletal muscle cross-sectional area within the first 6 months of injury. Eur J Appl Physiol Occup Physiol 80, 373-378.
Cavero, I., Roach, A.G., 1980. The pharmacology of prazosin, a novel antihypertensive agent. Life Sci 27, 1525-1540.
Ceccarelli, B., Hurlbut, W.P., Mauro, A., 1973. Turnover of transmitter and synaptic vesicles at the frog neuromuscular junction. J Cell Biol 57, 499-524.
Celikyurt, I.K., Mutlu, O., Ulak, G., Akar, F.Y., Erden, F., 2011. Gabapentin, A GABA analogue, enhances cognitive performance in mice. Neurosci Lett 492, 124-128.
Cersosimo, M.G., Benarroch, E.E., 2013. Central control of autonomic function and involvement in neurodegenerative disorders. Handb Clin Neurol 117, 45-57.
Chalmers, J., Arnolda, L., Llewellyn-Smith, I., Minson, J., Pilowsky, P., Suzuki, S., 1994. Central neurons and neurotransmitters in the control of blood pressure. Clin Exp Pharmacol Physiol 21, 819-829.
Chaudhry, F.A., Reimer, R.J., Bellocchio, E.E., Danbolt, N.C., Osen, K.K., Edwards, R.H., Storm-Mathisen, J., 1998. The vesicular GABA transporter, VGAT,

localizes to synaptic vesicles in sets of glycinergic as well as GABAergic neurons. J Neurosci 18, 9733-9750.
Chen, J., Li, L., Chen, S.R., Chen, H., Xie, J.D., Sirrieh, R.E., MacLean, D.M., Zhang, Y., Zhou, M.H., Jayaraman, V., Pan, H.L., 2018. The alpha2delta-1-NMDA Receptor Complex Is Critically Involved in Neuropathic Pain Development and Gabapentin Therapeutic Actions. Cell Rep 22, 2307-2321.
Chincholkar, M., 2018. Analgesic mechanisms of gabapentinoids and effects in experimental pain models: a narrative review. Br J Anaesth 120, 1315-1334.
Chirinos, J.A., Rietzschel, E.R., De Buyzere, M.L., De Bacquer, D., Gillebert, T.C., Gupta, A.K., Segers, P., Asklepios, i., 2009. Arterial load and ventricular-arterial coupling: physiologic relations with body size and effect of obesity. Hypertension 54, 558-566.
Chobanian, A.V., Bakris, G.L., Black, H.R., Cushman, W.C., Green, L.A., Izzo, J.L., Jones, D.W., Materson, B.J., Oparil, S., Wright, J.T., Roccella, E.J., 2003. Seventh Report of the Joint National Committee on Prevention, Detection, Evaluation, and Treatment of High Blood Pressure. Hypertension 42, 1206-1252.
Christensen, A.J., Iyer, S.M., Francois, A., Vyas, S., Ramakrishnan, C., Vesuna, S., Deisseroth, K., Scherrer, G., Delp, S.L., 2016. In Vivo Interrogation of Spinal Mechanosensory Circuits. Cell Rep 17, 1699-1710.
Cilio, M.R., Bolanos, A.R., Liu, Z., Schmid, R., Yang, Y., Stafstrom, C.E., Mikati, M.A., Holmes, G.L., 2001. Anticonvulsant action and long-term effects of gabapentin in the immature brain. Neuropharmacology 40, 139-147.
Ciriello, J., Calaresu, F.R., 1982. Medullary origin of vagal preganglionic axons to the heart of the cat. J Auton Nerv Syst 5, 9-22.
Clarke, H.A., Dekaban, G.A., Weaver, L.C., 1998. Identification of lamina V and VII interneurons presynaptic to adrenal sympathetic preganglionic neurons in rats using a recombinant herpes simplex virus type 1. Neuroscience 85, 863-872.
Cloughesy, T.F., Yoshimoto, K., Nghiemphu, P., Brown, K., Dang, J., Zhu, S., Hsueh, T., Chen, Y., Wang, W., Youngkin, D., Liau, L., Martin, N., Becker, D., Bergsneider, M., Lai, A., Green, R., Oglesby, T., Koleto, M., Trent, J., Horvath, S., Mischel, P.S., Mellinghoff, I.K., Sawyers, C.L., 2008. Antitumor activity of rapamycin in a Phase I trial for patients with recurrent PTEN-deficient glioblastoma. PLoS Med 5, e8.
Cloutier, F., Kalincik, T., Lauschke, J., Tuxworth, G., Cavanagh, B., Meedeniya, A., Mackay-Sim, A., Carrive, P., Waite, P., 2016. Olfactory ensheathing cells but not fibroblasts reduce the duration of autonomic dysreflexia in spinal cord injured rats. Auton Neurosci 201, 17-23.
Cockayne, D.A., Hamilton, S.G., Zhu, Q.M., Dunn, P.M., Zhong, Y., Novakovic, S., Malmberg, A.B., Cain, G., Berson, A., Kassotakis, L., Hedley, L., Lachnit, W.G., Burnstock, G., McMahon, S.B., Ford, A.P., 2000. Urinary bladder hyporeflexia and reduced pain-related behaviour in P2X3-deficient mice. Nature 407, 1011-1015.
Coderre, T.J., Kumar, N., Lefebvre, C.D., Yu, J.S., 2005. Evidence that gabapentin reduces neuropathic pain by inhibiting the spinal release of glutamate. J Neurochem 94, 1131-1139.

Coderre, T.J., Kumar, N., Lefebvre, C.D., Yu, J.S., 2007. A comparison of the glutamate release inhibition and anti-allodynic effects of gabapentin, lamotrigine, and riluzole in a model of neuropathic pain. J Neurochem 100, 1289-1299.
Cohen, L.D., Zuchman, R., Sorokina, O., Muller, A., Dieterich, D.C., Armstrong, J.D., Ziv, T., Ziv, N.E., 2013. Metabolic turnover of synaptic proteins: kinetics, interdependencies and implications for synaptic maintenance. PLoS One 8, e63191.
Coimbra, A., Ribeiro-da-Silva, A., Pignatelli, D., 1984. Effects of dorsal rhizotomy on the several types of primary afferent terminals in laminae I-III of the rat spinal cord. An electron microscope study. Anat Embryol (Berl) 170, 279-287.
Colachis, S.C., 3rd, Clinchot, D.M., 1997. Autonomic hyperreflexia associated with recurrent cardiac arrest: case report. Spinal Cord 35, 256-257.
Collins, H.L., Rodenbaugh, D.W., DiCarlo, S.E., 2006. Spinal cord injury alters cardiac electrophysiology and increases the susceptibility to ventricular arrhythmias. Prog Brain Res 152, 275-288.
Comeau, J.W., Costantino, S., Wiseman, P.W., 2006. A guide to accurate fluorescence microscopy colocalization measurements. Biophys J 91, 4611-4622.
Consortium for Spinal Cord, M., 2002. Acute management of autonomic dysreflexia: individuals with spinal cord injury presenting to health-care facilities. J Spinal Cord Med 25 Suppl 1, S67-88.
Coote, J.H., 1988. The organisation of cardiovascular neurons in the spinal cord. Rev Physiol Biochem Pharmacol 110, 147-285.
Coote, J.H., 2013. Myths and realities of the cardiac vagus. J Physiol 591, 4073-4085.
Coote, J.H., Chauhan, R.A., 2016. The sympathetic innervation of the heart: Important new insights. Auton Neurosci 199, 17-23.
Cordelieres, F.P., Bolte, S., 2014. Experimenters' guide to colocalization studies: finding a way through indicators and quantifiers, in practice. Methods Cell Biol 123, 395-408.
Costa, M., Brookes, S.J., Hennig, G.W., 2000. Anatomy and physiology of the enteric nervous system. Gut 47 Suppl 4, iv15-19; discussion iv26.
Cote, M.P., Detloff, M.R., Wade, R.E., Jr., Lemay, M.A., Houle, J.D., 2012. Plasticity in ascending long propriospinal and descending supraspinal pathways in chronic cervical spinal cord injured rats. Front Physiol 3, 330.
Cragg, J.J., Noonan, V.K., Krassioukov, A., Borisoff, J., 2013. Cardiovascular disease and spinal cord injury: results from a national population health survey. Neurology 81, 723-728.
Crawford, P., Ghadiali, E., Lane, R., Blumhardt, L., Chadwick, D., 1987. Gabapentin as an antiepileptic drug in man. J Neurol Neurosurg Psychiatry 50, 682-686.
Crestani, C.C., 2016. Emotional Stress and Cardiovascular Complications in Animal Models: A Review of the Influence of Stress Type. Front Physiol 7, 251.
Crosby, N.D., Zaucke, F., Kras, J.V., Dong, L., Luo, Z.D., Winkelstein, B.A., 2015. Thrombospondin-4 and excitatory synaptogenesis promote spinal sensitization after painful mechanical joint injury. Exp Neurol 264, 111-120.

Crowder, R.J., Freeman, R.S., 1998. Phosphatidylinositol 3-kinase and Akt protein kinase are necessary and sufficient for the survival of nerve growth factor-dependent sympathetic neurons. J Neurosci 18, 2933-2943.
Curt, A., Nitsche, B., Rodic, B., Schurch, B., Dietz, V., 1997. Assessment of autonomic dysreflexia in patients with spinal cord injury. J Neurol Neurosurg Psychiatry 62, 473-477.
Davidoff, G.N., Roth, E.J., Haughton, J.S., Ardner, M.S., 1990. Cognitive dysfunction in spinal cord injury patients: sensitivity of the Functional Independence Measure subscales vs neuropsychologic assessment. Arch Phys Med Rehabil 71, 326-329.
De Camilli, P., Cameron, R., Greengard, P., 1983. Synapsin I (protein I), a nerve terminal-specific phosphoprotein. I. Its general distribution in synapses of the central and peripheral nervous system demonstrated by immunofluorescence in frozen and plastic sections. J Cell Biol 96, 1337-1354.
De Gois, S., Schafer, M.K., Defamie, N., Chen, C., Ricci, A., Weihe, E., Varoqui, H., Erickson, J.D., 2005. Homeostatic scaling of vesicular glutamate and GABA transporter expression in rat neocortical circuits. J Neurosci 25, 7121-7133.
Deblon, N., Bourgoin, L., Veyrat-Durebex, C., Peyrou, M., Vinciguerra, M., Caillon, A., Maeder, C., Fournier, M., Montet, X., Rohner-Jeanrenaud, F., Foti, M., 2012. Chronic mTOR inhibition by rapamycin induces muscle insulin resistance despite weight loss in rats. Br J Pharmacol 165, 2325-2340.
Debru, A., 1997. Galen on pharmacology : philosophy, history, and medicine : proceedings of the Vth International Galen Colloquium, Lille, 16-18 March 1995. Brill, Leiden ; New York.
Derbenev, A.V., Duale, H., Rabchevsky, A.G., Smith, B.N., 2010. Electrophysiological characteristics of identified kidney-related neurons in adult rat spinal cord slices. Neurosci Lett 474, 168-172.
Deuchars, S.A., 2007. Multi-tasking in the spinal cord--do 'sympathetic' interneurones work harder than we give them credit for? J Physiol 580, 723-729.
Deuchars, S.A., Brooke, R.E., Frater, B., Deuchars, J., 2001. Properties of interneurones in the intermediolateral cell column of the rat spinal cord: role of the potassium channel subunit Kv3.1. Neuroscience 106, 433-446.
Deuchars, S.A., Lall, V.K., 2015. Sympathetic preganglionic neurons: properties and inputs. Compr Physiol 5, 829-869.
Devivo, M.J., 2012. Epidemiology of traumatic spinal cord injury: trends and future implications. Spinal Cord 50, 365-372.
Dhein, S., van Koppen, C.J., Brodde, O.E., 2001. Muscarinic receptors in the mammalian heart. Pharmacol Res 44, 161-182.
Dibble, C.C., Manning, B.D., 2013. Signal integration by mTORC1 coordinates nutrient input with biosynthetic output. Nat Cell Biol 15, 555-564.
Ditunno, J.F., Little, J.W., Tessler, A., Burns, A.S., 2004. Spinal shock revisited: a four-phase model. Spinal Cord 42, 383-395.
Dolly, O., 2003. Synaptic transmission: inhibition of neurotransmitter release by botulinum toxins. Headache 43 Suppl 1, S16-24.
Dolphin, A.C., 2016. Voltage-gated calcium channels and their auxiliary subunits: physiology and pathophysiology and pharmacology. J Physiol 594, 5369-5390.

Doyle, S., Pyndiah, S., De Gois, S., Erickson, J.D., 2010. Excitation-transcription coupling via calcium/calmodulin-dependent protein kinase/ERK1/2 signaling mediates the coordinate induction of VGLUT2 and Narp triggered by a prolonged increase in glutamatergic synaptic activity. J Biol Chem 285, 14366-14376.
Dragunow, M., Faull, R., 1989. The use of c-fos as a metabolic marker in neuronal pathway tracing. J Neurosci Methods 29, 261-265.
Drew, G.M., Siddall, P.J., Duggan, A.W., 2004. Mechanical allodynia following contusion injury of the rat spinal cord is associated with loss of GABAergic inhibition in the dorsal horn. Pain 109, 379-388.
Du Beau, A., Shakya Shrestha, S., Bannatyne, B.A., Jalicy, S.M., Linnen, S., Maxwell, D.J., 2012. Neurotransmitter phenotypes of descending systems in the rat lumbar spinal cord. Neuroscience 227, 67-79.
Duckworth, W.C., Solomon, S.S., Jallepalli, P., Heckemeyer, C., Finnern, J., Powers, A., 1980. Glucose intolerance due to insulin resistance in patients with spinal cord injuries. Diabetes 29, 906-910.
Dunn, K.W., Kamocka, M.M., McDonald, J.H., 2011. A practical guide to evaluating colocalization in biological microscopy. Am J Physiol Cell Physiol 300, C723-742.
Dykstra, D.D., 2003. Botulinum toxin in the management of bowel and bladder function in spinal cord injury and other neurologic disorders. Phys Med Rehabil Clin N Am 14, 793-804, vi.
Dykstra, D.D., Sidi, A.A., Anderson, L.C., 1987. The effect of nifedipine on cystoscopy-induced autonomic hyperreflexia in patients with high spinal cord injuries. J Urol 138, 1155-1157.
Dykstra, D.D., Sidi, A.A., Scott, A.B., Pagel, J.M., Goldish, G.D., 1988. Effects of botulinum A toxin on detrusor-sphincter dyssynergia in spinal cord injury patients. J Urol 139, 919-922.
Ehrlich, M.E., Evinger, M., Regunathan, S., Teitelman, G., 1994. Mammalian adrenal chromaffin cells coexpress the epinephrine-synthesizing enzyme and neuronal properties in vivo and in vitro. Dev Biol 163, 480-490.
Eldahan, K.C., Cox, D.H., Gollihue, J.L., Patel, S.P., Rabchevsky, A.G., 2018. Rapamycin Exacerbates Cardiovascular Dysfunction after Complete High-Thoracic Spinal Cord Injury. J Neurotrauma 35, 842-853.
Eldahan, K.C., Rabchevsky, A.G., 2018. Autonomic dysreflexia after spinal cord injury: Systemic pathophysiology and methods of management. Auton Neurosci 209, 59-70.
Elkelini, M.S., Bagli, D.J., Fehlings, M., Hassouna, M., 2012. Effects of intravesical onabotulinumtoxinA on bladder dysfunction and autonomic dysreflexia after spinal cord injury: role of nerve growth factor. BJU Int 109, 402-407.
Elluru, R.G., Bloom, G.S., Brady, S.T., 1995. Fast axonal transport of kinesin in the rat visual system: functionality of kinesin heavy chain isoforms. Mol Biol Cell 6, 21-40.
Eltorai, I., Kim, R., Vulpe, M., Kasravi, H., Ho, W., 1992. Fatal cerebral hemorrhage due to autonomic dysreflexia in a tetraplegic patient: case report and review. Paraplegia 30, 355-360.
Emmelin, N., 1987. Nerve interactions in salivary glands. J Dent Res 66, 509-517.

Engeland, W.C., Arnhold, M.M., 2005. Neural circuitry in the regulation of adrenal corticosterone rhythmicity. Endocrine 28, 325-332.
English, J.M., Cobb, M.H., 2002. Pharmacological inhibitors of MAPK pathways. Trends Pharmacol Sci 23, 40-45.
Erickson, R.P., 1980. Autonomic hyperreflexia: pathophysiology and medical management. Arch Phys Med Rehabil 61, 431-440.
Eroglu, C., Allen, N.J., Susman, M.W., O'Rourke, N.A., Park, C.Y., Ozkan, E., Chakraborty, C., Mulinyawe, S.B., Annis, D.S., Huberman, A.D., Green, E.M., Lawler, J., Dolmetsch, R., Garcia, K.C., Smith, S.J., Luo, Z.D., Rosenthal, A., Mosher, D.F., Barres, B.A., 2009. Gabapentin receptor alpha2delta-1 is a neuronal thrombospondin receptor responsible for excitatory CNS synaptogenesis. Cell 139, 380-392.
Esmail, Z., Shalansky, K.F., Sunderji, R., Anton, H., Chambers, K., Fish, W., 2002. Evaluation of captopril for the management of hypertension in autonomic dysreflexia: a pilot study. Arch Phys Med Rehabil 83, 604-608.
Espinosa-Medina, I., Saha, O., Boismoreau, F., Chettouh, Z., Rossi, F., Richardson, W.D., Brunet, J.F., 2016. The sacral autonomic outflow is sympathetic. Science 354, 893-897.
Fang, Y., Westbrook, R., Hill, C., Boparai, R.K., Arum, O., Spong, A., Wang, F., Javors, M.A., Chen, J., Sun, L.Y., Bartke, A., 2013. Duration of rapamycin treatment has differential effects on metabolism in mice. Cell Metab 17, 456-462.
Fausel, R.A., Paski, S.C., 2014. Autonomic Dysreflexia Resulting in Seizure After Colonoscopy in a Patient With Spinal Cord Injury. ACG Case Rep J 1, 187-188.
Ferguson, A.R., Christensen, R.N., Gensel, J.C., Miller, B.A., Sun, F., Beattie, E.C., Bresnahan, J.C., Beattie, M.S., 2008. Cell death after spinal cord injury is exacerbated by rapid TNF alpha-induced trafficking of GluR2-lacking AMPARs to the plasma membrane. J Neurosci 28, 11391-11400.
Ferguson, A.R., Huie, J.R., Crown, E.D., Baumbauer, K.M., Hook, M.A., Garraway, S.M., Lee, K.H., Hoy, K.C., Grau, J.W., 2012. Maladaptive spinal plasticity opposes spinal learning and recovery in spinal cord injury. Front Physiol 3, 399.
Feustel, D., 1976. Autonomic hyperreflexia. Am J Nurs 76, 228-230.
Fletcher, T.L., Cameron, P., De Camilli, P., Banker, G., 1991. The distribution of synapsin I and synaptophysin in hippocampal neurons developing in culture. J Neurosci 11, 1617-1626.
Fougere, R.J., Currie, K.D., Nigro, M.K., Stothers, L., Rapoport, D., Krassioukov, A.V., 2016a. Reduction in Bladder-Related Autonomic Dysreflexia after OnabotulinumtoxinA Treatment in Spinal Cord Injury. J Neurotrauma.
Fougere, R.J., Currie, K.D., Nigro, M.K., Stothers, L., Rapoport, D., Krassioukov, A.V., 2016b. Reduction in Bladder-Related Autonomic Dysreflexia after OnabotulinumtoxinA Treatment in Spinal Cord Injury. J Neurotrauma 33, 1651-1657.
Fourneaux, B., Chaire, V., Lucchesi, C., Karanian, M., Pineau, R., Laroche-Clary, A., Italiano, A., 2017. Dual inhibition of the PI3K/AKT/mTOR pathway suppresses the growth of leiomyosarcomas but leads to ERK activation through mTORC2: biological and clinical implications. Oncotarget 8, 7878-7890.

Frankel, H.L., Michaelis, L.S., Golding, D.R., Beral, V., 1972. The blood pressure in paraplegia. I. Paraplegia 10, 193-200.
Franken, L., Klein, M., Spasova, M., Elsukova, A., Wiedwald, U., Welz, M., Knolle, P., Farle, M., Limmer, A., Kurts, C., 2015. Splenic red pulp macrophages are intrinsically superparamagnetic and contaminate magnetic cell isolates. Sci Rep 5, 12940.
Freria, C.M., Hall, J.C., Wei, P., Guan, Z., McTigue, D.M., Popovich, P.G., 2017. Deletion of the Fractalkine Receptor, CX3CR1, Improves Endogenous Repair, Axon Sprouting, and Synaptogenesis after Spinal Cord Injury in Mice. J Neurosci 37, 3568-3587.
Fujii, H., Goel, A., Bernard, N., Pistelli, A., Yates, L.M., Stephens, S., Han, J.Y., Matsui, D., Etwell, F., Einarson, T.R., Koren, G., Einarson, A., 2013. Pregnancy outcomes following gabapentin use: results of a prospective comparative cohort study. Neurology 80, 1565-1570.
Fuller-Bicer, G.A., Varadi, G., Koch, S.E., Ishii, M., Bodi, I., Kadeer, N., Muth, J.N., Mikala, G., Petrashevskaya, N.N., Jordan, M.A., Zhang, S.P., Qin, N., Flores, C.M., Isaacsohn, I., Varadi, M., Mori, Y., Jones, W.K., Schwartz, A., 2009. Targeted disruption of the voltage-dependent calcium channel alpha2/delta-1-subunit. Am J Physiol Heart Circ Physiol 297, H117-124.
Furlan, J.C., Fehlings, M.G., 2008. Cardiovascular complications after acute spinal cord injury: pathophysiology, diagnosis, and management. Neurosurg Focus 25, E13.
Furlan, J.C., Fehlings, M.G., Halliday, W., Krassioukov, A.V., 2003. Autonomic dysreflexia associated with intramedullary astrocytoma of the spinal cord. Lancet Oncol 4, 574-575.
Furness, J.B., 2012. The enteric nervous system and neurogastroenterology. Nat Rev Gastroenterol Hepatol 9, 286-294.
Furness, J.B., Callaghan, B.P., Rivera, L.R., Cho, H.J., 2014. The enteric nervous system and gastrointestinal innervation: integrated local and central control. Adv Exp Med Biol 817, 39-71.
Furusawa, K., Tokuhiro, A., Sugiyama, H., Ikeda, A., Tajima, F., Genda, E., Uchida, R., Tominaga, T., Tanaka, H., Magara, A., Sumida, M., 2011. Incidence of symptomatic autonomic dysreflexia varies according to the bowel and bladder management techniques in patients with spinal cord injury. Spinal Cord 49, 49-54.
Gao, S.A., Ambring, A., Lambert, G., Karlsson, A.K., 2002. Autonomic control of the heart and renal vascular bed during autonomic dysreflexia in high spinal cord injury. Clin Auton Res 12, 457-464.
Garshick, E., Kelley, A., Cohen, S.A., Garrison, A., Tun, C.G., Gagnon, D., Brown, R., 2005. A prospective assessment of mortality in chronic spinal cord injury. Spinal Cord 43, 408-416.
Gaskell, W.H., 1886. On the Structure, Distribution and Function of the Nerves which innervate the Visceral and Vascular Systems. J Physiol 7, 1-80 89.
Gassmann, M., Grenacher, B., Rohde, B., Vogel, J., 2009. Quantifying Western blots: pitfalls of densitometry. Electrophoresis 30, 1845-1855.

Gee, N.S., Brown, J.P., Dissanayake, V.U., Offord, J., Thurlow, R., Woodruff, G.N., 1996. The novel anticonvulsant drug, gabapentin (Neurontin), binds to the alpha2delta subunit of a calcium channel. J Biol Chem 271, 5768-5776.
Gensel, J.C., Zhang, B., 2015. Macrophage activation and its role in repair and pathology after spinal cord injury. Brain Res 1619, 1-11.
Giangregorio, L., McCartney, N., 2006. Bone loss and muscle atrophy in spinal cord injury: epidemiology, fracture prediction, and rehabilitation strategies. J Spinal Cord Med 29, 489-500.
Goldstein, D.S., McCarty, R., Polinsky, R.J., Kopin, I.J., 1983. Relationship between plasma norepinephrine and sympathetic neural activity. Hypertension 5, 552-559.
Gong, H.C., Hang, J., Kohler, W., Li, L., Su, T.Z., 2001. Tissue-specific expression and gabapentin-binding properties of calcium channel alpha2delta subunit subtypes. J Membr Biol 184, 35-43.
Gordon, T., Mao, J., 1994. Muscle atrophy and procedures for training after spinal cord injury. Phys Ther 74, 50-60.
Gorgey, A.S., Dolbow, D.R., Dolbow, J.D., Khalil, R.K., Castillo, C., Gater, D.R., 2014. Effects of spinal cord injury on body composition and metabolic profile - part I. J Spinal Cord Med 37, 693-702.
Gorgey, A.S., Gater, D.R., 2012. Insulin growth factors may explain relationship between spasticity and skeletal muscle size in men with spinal cord injury. J Rehabil Res Dev 49, 373-380.
Gras, C., Herzog, E., Bellenchi, G.C., Bernard, V., Ravassard, P., Pohl, M., Gasnier, B., Giros, B., El Mestikawy, S., 2002. A third vesicular glutamate transporter expressed by cholinergic and serotoninergic neurons. J Neurosci 22, 5442-5451.
Greenblatt, H.K., Greenblatt, D.J., 2018. Gabapentin and Pregabalin for the Treatment of Anxiety Disorders. Clin Pharmacol Drug Dev 7, 228-232.
Greenway, C.V., Lister, G.E., 1974. Capacitance effects and blood reservoir function in the splanchnic vascular bed during non-hypotensive haemorrhage and blood volume expansion in anaesthetized cats. J Physiol 237, 279-294.
Grobecker, H., 1990. Pharmacology and clinical pharmacology of organic nitrates. Eur J Clin Pharmacol 38 Suppl 1, S3-7.
Gruppuso, P.A., Boylan, J.M., Sanders, J.A., 2011. The physiology and pathophysiology of rapamycin resistance: implications for cancer. Cell Cycle 10, 1050-1058.
Guimaraes, S., Moura, D., 2001. Vascular adrenoceptors: an update. Pharmacol Rev 53, 319-356.
Guo, D., Zeng, L., Brody, D.L., Wong, M., 2013. Rapamycin attenuates the development of posttraumatic epilepsy in a mouse model of traumatic brain injury. PLoS One 8, e64078.
Guttmann, L., Whitteridge, D., 1947. Effects of bladder distension on autonomic mechanisms after spinal cord injuries. Brain 70, 361-404.
Guyenet, P., Cabot, J., 1981. Inhibition of sympathetic preganglionic neurons by catecholamines and clonidine: mediation by an alpha-adrenergic receptor. The Journal of Neuroscience 1, 908-917.
Guyton, A.C., Hall, J.E., 2006. Textbook of medical physiology, 11th ed. Elsevier Saunders, Philadelphia, Pa.

Hagemann, D., Xiao, R.P., 2002. Dual site phospholamban phosphorylation and its physiological relevance in the heart. Trends Cardiovasc Med 12, 51-56.
Harlan, S.M., Guo, D.F., Morgan, D.A., Fernandes-Santos, C., Rahmouni, K., 2013. Hypothalamic mTORC1 signaling controls sympathetic nerve activity and arterial pressure and mediates leptin effects. Cell Metab 17, 599-606.
Hartzell, H.C., 1988. Regulation of cardiac ion channels by catecholamines, acetylcholine and second messenger systems. Prog Biophys Mol Biol 52, 165-247.
Harvey, R.D., Belevych, A.E., 2003. Muscarinic regulation of cardiac ion channels. Br J Pharmacol 139, 1074-1084.
Harvey, R.D., Hume, J.R., 1989. Autonomic regulation of delayed rectifier K+ current in mammalian heart involves G proteins. Am J Physiol 257, H818-823.
Hebert, M., Licursi, M., Jensen, B., Baker, A., Milway, S., Malsbury, C., Grant, V.L., Adamec, R., Hirasawa, M., Blundell, J., 2014. Single rapamycin administration induces prolonged downward shift in defended body weight in rats. PLoS One 9, e93691.
Heblich, F., Tran Van Minh, A., Hendrich, J., Watschinger, K., Dolphin, A.C., 2008. Time course and specificity of the pharmacological disruption of the trafficking of voltage-gated calcium channels by gabapentin. Channels (Austin) 2, 4-9.
Hendrich, J., Van Minh, A.T., Heblich, F., Nieto-Rostro, M., Watschinger, K., Striessnig, J., Wratten, J., Davies, A., Dolphin, A.C., 2008. Pharmacological disruption of calcium channel trafficking by the alpha2delta ligand gabapentin. Proc Natl Acad Sci U S A 105, 3628-3633.
Herzog, E., Bellenchi, G.C., Gras, C., Bernard, V., Ravassard, P., Bedet, C., Gasnier, B., Giros, B., El Mestikawy, S., 2001. The existence of a second vesicular glutamate transporter specifies subpopulations of glutamatergic neurons. J Neurosci 21, RC181.
Herzog, E., Takamori, S., Jahn, R., Brose, N., Wojcik, S.M., 2006. Synaptic and vesicular co-localization of the glutamate transporters VGLUT1 and VGLUT2 in the mouse hippocampus. J Neurochem 99, 1011-1018.
Hickey, K.J., Vogel, L.C., Willis, K.M., Anderson, C.J., 2004. Prevalence and etiology of autonomic dysreflexia in children with spinal cord injuries. J Spinal Cord Med 27 Suppl 1, S54-60.
Higgins, C.B., Vatner, S.F., Braunwald, E., 1973. Parasympathetic control of the heart. Pharmacol Rev 25, 119-155.
Horn, J.P., 2018. The sacral autonomic outflow is parasympathetic: Langley got it right. Clin Auton Res 28, 181-185.
Hosoya, Y., Nadelhaft, I., Wang, D., Kohno, K., 1994. Thoracolumbar sympathetic preganglionic neurons in the dorsal commissural nucleus of the male rat: an immunohistochemical study using retrograde labeling of cholera toxin subunit B. Exp Brain Res 98, 21-30.
Hosoya, Y., Sugiura, Y., Okado, N., Loewy, A.D., Kohno, K., 1991. Descending input from the hypothalamic paraventricular nucleus to sympathetic preganglionic neurons in the rat. Exp Brain Res 85, 10-20.
Hou, S., Duale, H., Cameron, A.A., Abshire, S.M., Lyttle, T.S., Rabchevsky, A.G., 2008. Plasticity of lumbosacral propriospinal neurons is associated with the

development of autonomic dysreflexia after thoracic spinal cord transection. J Comp Neurol 509, 382-399.
Hou, S., Duale, H., Rabchevsky, A.G., 2009. Intraspinal sprouting of unmyelinated pelvic afferents after complete spinal cord injury is correlated with autonomic dysreflexia induced by visceral pain. Neuroscience 159, 369-379.
Hou, S., Rabchevsky, A.G., 2014. Autonomic consequences of spinal cord injury. Compr Physiol 4, 1419-1453.
Houghton, K.T., Forrest, A., Awad, A., Atkinson, L.Z., Stockton, S., Harrison, P.J., Geddes, J.R., Cipriani, A., 2017. Biological rationale and potential clinical use of gabapentin and pregabalin in bipolar disorder, insomnia and anxiety: protocol for a systematic review and meta-analysis. BMJ Open 7, e013433.
Hsu, W.H., Lu, Z.X., Hembrough, F.B., 1985. Effect of xylazine on heart rate and arterial blood pressure in conscious dogs, as influenced by atropine, 4-aminopyridine, doxapram, and yohimbine. J Am Vet Med Assoc 186, 153-156.
Hu, Y., 2015. The necessary role of mTORC1 in central nervous system axon regeneration. Neural Regen Res 10, 186-188.
Huang, Y.J., Lee, K.H., Murphy, L., Garraway, S.M., Grau, J.W., 2016. Acute spinal cord injury (SCI) transforms how GABA affects nociceptive sensitization. Exp Neurol 285, 82-95.
Hubli, M., Gee, C.M., Krassioukov, A.V., 2015. Refined assessment of blood pressure instability after spinal cord injury. Am J Hypertens 28, 173-181.
Hubli, M., Krassioukov, A.V., 2014. Ambulatory blood pressure monitoring in spinal cord injury: clinical practicability. J Neurotrauma 31, 789-797.
Iencean, S.M., 2003. Classification of spinal injuries based on the essential traumatic spinal mechanisms. Spinal Cord 41, 385-396.
Irwin, M.R., Cole, S.W., 2011. Reciprocal regulation of the neural and innate immune systems. Nat Rev Immunol 11, 625-632.
Iversen, P.O., Hjeltnes, N., Holm, B., Flatebo, T., Strom-Gundersen, I., Ronning, W., Stanghelle, J., Benestad, H.B., 2000. Depressed immunity and impaired proliferation of hematopoietic progenitor cells in patients with complete spinal cord injury. Blood 96, 2081-2083.
Iyer, S.M., Montgomery, K.L., Towne, C., Lee, S.Y., Ramakrishnan, C., Deisseroth, K., Delp, S.L., 2014. Virally mediated optogenetic excitation and inhibition of pain in freely moving nontransgenic mice. Nat Biotechnol 32, 274-278.
Iyer, S.M., Vesuna, S., Ramakrishnan, C., Huynh, K., Young, S., Berndt, A., Lee, S.Y., Gorini, C.J., Deisseroth, K., Delp, S.L., 2016. Optogenetic and chemogenetic strategies for sustained inhibition of pain. Sci Rep 6, 30570.
Jahn, R., Sudhof, T.C., 1993. Synaptic vesicle traffic: rush hour in the nerve terminal. J Neurochem 61, 12-21.
Jaillon, P., 1980. Clinical pharmacokinetics of prazosin. Clin Pharmacokinet 5, 365-376.
Jain, A., Ghai, B., Jain, K., Makkar, J.K., Mangal, K., Sampley, S., 2013. Severe autonomic dysreflexia induced cardiac arrest under isoflurane anesthesia in a patient with lower thoracic spine injury. J Anaesthesiol Clin Pharmacol 29, 241-243.

Jamali, H.K., Waqar, F., Gerson, M.C., 2017. Cardiac autonomic innervation. J Nucl Cardiol 24, 1558-1570.
Janig, W., Neuhuber, W., 2017. Reclassification of the Sacral Autonomic Outflow to Pelvic Organs as the Caudal Outpost of the Sympathetic System Is Misleading. J Am Osteopath Assoc 117, 416-417.
Jansen, A.S., Nguyen, X.V., Karpitskiy, V., Mettenleiter, T.C., Loewy, A.D., 1995. Central command neurons of the sympathetic nervous system: basis of the fight-or-flight response. Science 270, 644-646.
Jin, D., Liu, Y., Sun, F., Wang, X., Liu, X., He, Z., 2015. Restoration of skilled locomotion by sprouting corticospinal axons induced by co-deletion of PTEN and SOCS3. Nat Commun 6, 8074.
Jonas, P., Bischofberger, J., Sandkuhler, J., 1998. Corelease of two fast neurotransmitters at a central synapse. Science 281, 419-424.
Jose, A.D., Collison, D., 1970. The normal range and determinants of the intrinsic heart rate in man. Cardiovasc Res 4, 160-167.
Jose, A.D., Taylor, R.R., 1969. Autonomic blockade by propranolol and atropine to study intrinsic myocardial function in man. J Clin Invest 48, 2019-2031.
Joshi, S., Levatte, M.A., Dekaban, G.A., Weaver, L.C., 1995. Identification of spinal interneurons antecedent to adrenal sympathetic preganglionic neurons using trans-synaptic transport of herpes simplex virus type 1. Neuroscience 65, 893-903.
Kaji, A., Maeda, T., Watanabe, S., 1991. Parasympathetic innervation of cutaneous blood vessels examined by retrograde tracing in the rat lower lip. J Auton Nerv Syst 32, 153-158.
Kaneko, T., Fujiyama, F., 2002. Complementary distribution of vesicular glutamate transporters in the central nervous system. Neurosci Res 42, 243-250.
Kapitza, S., Zorner, B., Weinmann, O., Bolliger, M., Filli, L., Dietz, V., Schwab, M.E., 2012. Tail spasms in rat spinal cord injury: changes in interneuronal connectivity. Exp Neurol 236, 179-189.
Karim, F., Wang, C.C., Gereau, R.W.t., 2001. Metabotropic glutamate receptor subtypes 1 and 5 are activators of extracellular signal-regulated kinase signaling required for inflammatory pain in mice. J Neurosci 21, 3771-3779.
Karlsson, A.K., 1999. Autonomic dysreflexia. Spinal Cord 37, 383.
Karlsson, A.K., Elam, M., Friberg, P., Sullivan, L., Attvall, S., Lonnroth, P., 1997. Peripheral afferent stimulation of decentralized sympathetic neurons activates lipolysis in spinal cord-injured subjects. Metabolism 46, 1465-1469.
Kewalramani, L.S., 1980. Autonomic dysreflexia in traumatic myelopathy. Am J Phys Med 59, 1-21.
Kinoshita, M., Matsui, R., Kato, S., Hasegawa, T., Kasahara, H., Isa, K., Watakabe, A., Yamamori, T., Nishimura, Y., Alstermark, B., Watanabe, D., Kobayashi, K., Isa, T., 2012. Genetic dissection of the circuit for hand dexterity in primates. Nature 487, 235-238.
Kitzman, P., 2006. Changes in vesicular glutamate transporter 2, vesicular GABA transporter and vesicular acetylcholine transporter labeling of sacrocaudal motoneurons in the spastic rat. Exp Neurol 197, 407-419.

Klugbauer, N., Marais, E., Hofmann, F., 2003. Calcium channel alpha2delta subunits: differential expression, function, and drug binding. J Bioenerg Biomembr 35, 639-647.
Kozorovitskiy, Y., Peixoto, R., Wang, W., Saunders, A., Sabatini, B.L., 2015. Neuromodulation of excitatory synaptogenesis in striatal development. Elife 4.
Krassioukov, A., Warburton, D.E., Teasell, R., Eng, J.J., Spinal Cord Injury Rehabilitation Evidence Research, T., 2009. A systematic review of the management of autonomic dysreflexia after spinal cord injury. Arch Phys Med Rehabil 90, 682-695.
Krassioukov, A.V., Bunge, R.P., Pucket, W.R., Bygrave, M.A., 1999. The changes in human spinal sympathetic preganglionic neurons after spinal cord injury. Spinal Cord 37, 6-13.
Krassioukov, A.V., Furlan, J.C., Fehlings, M.G., 2003. Autonomic dysreflexia in acute spinal cord injury: an under-recognized clinical entity. J Neurotrauma 20, 707-716.
Krassioukov, A.V., Harkema, S.J., 2006. Effect of harness application and postural changes on cardiovascular parameters of individuals with spinal cord injury. Spinal Cord 44, 780-786.
Krassioukov, A.V., Johns, D.G., Schramm, L.P., 2002. Sensitivity of sympathetically correlated spinal interneurons, renal sympathetic nerve activity, and arterial pressure to somatic and visceral stimuli after chronic spinal injury. J Neurotrauma 19, 1521-1529.
Krassioukov, A.V., Weaver, L.C., 1995. Episodic hypertension due to autonomic dysreflexia in acute and chronic spinal cord-injured rats. American Journal of Physiology - Heart and Circulatory Physiology 268, H2077-H2083.
Krassioukov, A.V., Weaver, L.C., 1996. Morphological changes in sympathetic preganglionic neurons after spinal cord injury in rats. Neuroscience 70, 211-225.
Krenz, N.R., Meakin, S.O., Krassioukov, A.V., Weaver, L.C., 1999. Neutralizing intraspinal nerve growth factor blocks autonomic dysreflexia caused by spinal cord injury. J Neurosci 19, 7405-7414.
Krenz, N.R., Weaver, L.C., 1998a. Changes in the morphology of sympathetic preganglionic neurons parallel the development of autonomic dysreflexia after spinal cord injury in rats. Neurosci Lett 243, 61-64.
Krenz, N.R., Weaver, L.C., 1998b. Sprouting of primary afferent fibers after spinal cord transection in the rat. Neuroscience 85, 443-458.
Krishna, V., Andrews, H., Jin, X., Yu, J., Varma, A., Wen, X., Kindy, M., 2013. A contusion model of severe spinal cord injury in rats. J Vis Exp.
Krum, H., Louis, W.J., Brown, D.J., Clarke, S.J., Fleming, J.A., Howes, L.G., 1992a. Cardiovascular and vasoactive hormone responses to bladder distension in spinal and normal man. Paraplegia 30, 348-354.
Krum, H., Louis, W.J., Brown, D.J., Howes, L.G., 1992b. Pressor dose responses and baroreflex sensitivity in quadriplegic spinal cord injury patients. J Hypertens 10, 245-250.
Krum, H., Louis, W.J., Brown, D.J., Howes, L.G., 1992c. A study of the alpha-1 adrenoceptor blocker prazosin in the prophylactic management of autonomic dysreflexia in high spinal cord injury patients. Clin Auton Res 2, 83-88.

Kulcu, D.G., Akbas, B., Citci, B., Cihangiroglu, M., 2009. Autonomic dysreflexia in a man with multiple sclerosis. J Spinal Cord Med 32, 198-203.
Kumar, R., Lim, J., Mekary, R.A., Rattani, A., Dewan, M.C., Sharif, S.Y., Osorio-Fonseca, E., Park, K.B., 2018. Traumatic Spinal Injury: Global Epidemiology and Worldwide Volume. World Neurosurg 113, e345-e363.
Kwon, S.E., Chapman, E.R., 2011. Synaptophysin regulates the kinetics of synaptic vesicle endocytosis in central neurons. Neuron 70, 847-854.
Kyloh, M., Nicholas, S., Zagorodnyuk, V.P., Brookes, S.J., Spencer, N.J., 2011. Identification of the visceral pain pathway activated by noxious colorectal distension in mice. Front Neurosci 5, 16.
Laird, A.S., Carrive, P., Waite, P.M., 2006. Cardiovascular and temperature changes in spinal cord injured rats at rest and during autonomic dysreflexia. J Physiol 577, 539-548.
Lana, B., Page, K.M., Kadurin, I., Ho, S., Nieto-Rostro, M., Dolphin, A.C., 2016. Thrombospondin-4 reduces binding affinity of [(3)H]-gabapentin to calcium-channel alpha2delta-1-subunit but does not interact with alpha2delta-1 on the cell-surface when co-expressed. Sci Rep 6, 24531.
Landry, M., Bouali-Benazzouz, R., El Mestikawy, S., Ravassard, P., Nagy, F., 2004. Expression of vesicular glutamate transporters in rat lumbar spinal cord, with a note on dorsal root ganglia. J Comp Neurol 468, 380-394.
Lane, R.D., McRae, K., Reiman, E.M., Chen, K., Ahern, G.L., Thayer, J.F., 2009. Neural correlates of heart rate variability during emotion. Neuroimage 44, 213-222.
Langley, J.N., 1898. On the Union of Cranial Autonomic (Visceral) Fibres with the Nerve Cells of the Superior Cervical Ganglion. J Physiol 23, 240-270.
Lanzafame, A.A., Christopoulos, A., Mitchelson, F., 2003. Cellular signaling mechanisms for muscarinic acetylcholine receptors. Receptors Channels 9, 241-260.
Laplante, M., Sabatini, D.M., 2009. mTOR signaling at a glance. J Cell Sci 122, 3589-3594.
Laplante, M., Sabatini, D.M., 2012. mTOR signaling in growth control and disease. Cell 149, 274-293.
Laskey, W., Polosa, C., 1988. Characteristics of the sympathetic preganglionic neuron and its synaptic input. Prog Neurobiol 31, 47-84.
Lau, B.K., Vaughan, C.W., 2014. Descending modulation of pain: the GABA disinhibition hypothesis of analgesia. Curr Opin Neurobiol 29, 159-164.
Lau, L.A., Noubary, F., Wang, D., Dulla, C.G., 2017. alpha2delta-1 Signaling Drives Cell Death, Synaptogenesis, Circuit Reorganization, and Gabapentin-Mediated Neuroprotection in a Model of Insult-Induced Cortical Malformation. eNeuro 4.
Lazarevic, V., Pothula, S., Andres-Alonso, M., Fejtova, A., 2013. Molecular mechanisms driving homeostatic plasticity of neurotransmitter release. Front Cell Neurosci 7, 244.
Le Douarin, N.M., Smith, J., 1988. Development of the peripheral nervous system from the neural crest. Annu Rev Cell Biol 4, 375-404.

Leach, J.P., Girvan, J., Paul, A., Brodie, M.J., 1997. Gabapentin and cognition: a double blind, dose ranging, placebo controlled study in refractory epilepsy. J Neurol Neurosurg Psychiatry 62, 372-376.
LeDoux, J.E., Iwata, J., Cicchetti, P., Reis, D.J., 1988. Different projections of the central amygdaloid nucleus mediate autonomic and behavioral correlates of conditioned fear. J Neurosci 8, 2517-2529.
Lee, B.B., Cripps, R.A., Fitzharris, M., Wing, P.C., 2014a. The global map for traumatic spinal cord injury epidemiology: update 2011, global incidence rate. Spinal Cord 52, 110-116.
Lee, D.H., Luo, X., Yungher, B.J., Bray, E., Lee, J.K., Park, K.K., 2014b. Mammalian target of rapamycin's distinct roles and effectiveness in promoting compensatory axonal sprouting in the injured CNS. J Neurosci 34, 15347-15355.
Lee, H.J., White, J.M., Chung, J., Tansey, K.E., 2017. Peripheral and central anatomical organization of cutaneous afferent subtypes in a rat nociceptive intersegmental spinal reflex. J Comp Neurol 525, 2216-2234.
Lee, J.S., Fang, S.Y., Roan, J.N., Jou, I.M., Lam, C.F., 2016. Spinal cord injury enhances arterial expression and reactivity of alpha1-adrenergic receptors-mechanistic investigation into autonomic dysreflexia. Spine J 16, 65-71.
Leman, S., Bernet, F., Sequeira, H., 2000. Autonomic dysreflexia increases plasma adrenaline level in the chronic spinal cord-injured rat. Neurosci Lett 286, 159-162.
Li, F., Yang, M., Wang, L., Williamson, I., Tian, F., Qin, M., Shah, P.K., Sharifi, B.G., 2012a. Autofluorescence contributes to false-positive intracellular Foxp3 staining in macrophages: a lesson learned from flow cytometry. J Immunol Methods 386, 101-107.
Li, H., Graber, K.D., Jin, S., McDonald, W., Barres, B.A., Prince, D.A., 2012b. Gabapentin decreases epileptiform discharges in a chronic model of neocortical trauma. Neurobiol Dis 48, 429-438.
Li, J.L., Fujiyama, F., Kaneko, T., Mizuno, N., 2003. Expression of vesicular glutamate transporters, VGluT1 and VGluT2, in axon terminals of nociceptive primary afferent fibers in the superficial layers of the medullary and spinal dorsal horns of the rat. J Comp Neurol 457, 236-249.
Li, K.W., Yu, Y.P., Zhou, C., Kim, D.S., Lin, B., Sharp, K., Steward, O., Luo, Z.D., 2014. Calcium channel alpha2delta1 proteins mediate trigeminal neuropathic pain states associated with aberrant excitatory synaptogenesis. J Biol Chem 289, 7025-7037.
Liang, S., Li, J., Gou, X., Chen, D., 2016. Blocking mammalian target of rapamycin alleviates bladder hyperactivity and pain in rats with cystitis. Mol Pain 12.
Liguz-Lecznar, M., Skangiel-Kramska, J., 2007. Vesicular glutamate transporters (VGLUTs): the three musketeers of glutamatergic system. Acta Neurobiol Exp (Wars) 67, 207-218.
Lindan, R., Joiner, E., Freehafer, A., Hazel, C., 1980. Incidence and clinical features of autonomic dysreflexia in patients with spinal cord injury. Spinal Cord 18, 285-292.
Lipton, J.O., Sahin, M., 2014. The neurology of mTOR. Neuron 84, 275-291.

Liu, G., Detloff, M.R., Miller, K.N., Santi, L., Houle, J.D., 2012. Exercise modulates microRNAs that affect the PTEN/mTOR pathway in rats after spinal cord injury. Exp Neurol 233, 447-456.
Liu, K., Lu, Y., Lee, J.K., Samara, R., Willenberg, R., Sears-Kraxberger, I., Tedeschi, A., Park, K.K., Jin, D., Cai, B., Xu, B., Connolly, L., Steward, O., Zheng, B., He, Z., 2010. PTEN deletion enhances the regenerative ability of adult corticospinal neurons. Nat Neurosci 13, 1075-1081.
Llewellyn-Smith, I.J., 2009. Anatomy of synaptic circuits controlling the activity of sympathetic preganglionic neurons. J Chem Neuroanat 38, 231-239.
Llewellyn-Smith, I.J., Martin, C.L., Fenwick, N.M., Dicarlo, S.E., Lujan, H.L., Schreihofer, A.M., 2007. VGLUT1 and VGLUT2 innervation in autonomic regions of intact and transected rat spinal cord. J Comp Neurol 503, 741-767.
Llewellyn-Smith, I.J., Weaver, L.C., 2001. Changes in synaptic inputs to sympathetic preganglionic neurons after spinal cord injury. J Comp Neurol 435, 226-240.
Lockwood, G., Durkee, C., Groth, T., 2016. Intravesical Botulinum Toxin for Persistent Autonomic Dysreflexia in a Pediatric Patient. Case Rep Urol 2016, 4569684.
Loffelholz, K., Pappano, A.J., 1985. The parasympathetic neuroeffector junction of the heart. Pharmacol Rev 37, 1-24.
Logue, J.S., Morrison, D.K., 2012. Complexity in the signaling network: insights from the use of targeted inhibitors in cancer therapy. Genes Dev 26, 641-650.
Lorton, D., Bellinger, D.L., 2015. Molecular mechanisms underlying beta-adrenergic receptor-mediated cross-talk between sympathetic neurons and immune cells. Int J Mol Sci 16, 5635-5665.
Loukas, M., Klaassen, Z., Merbs, W., Tubbs, R.S., Gielecki, J., Zurada, A., 2010. A review of the thoracic splanchnic nerves and celiac ganglia. Clin Anat 23, 512-522.
Lu, Y., Inokuchi, H., McLachlan, E.M., Li, J.S., Higashi, H., 2001. Correlation between electrophysiology and morphology of three groups of neuron in the dorsal commissural nucleus of lumbosacral spinal cord of mature rats studied in vitro. J Comp Neurol 437, 156-169.
Lucin, K.M., Sanders, V.M., Jones, T.B., Malarkey, W.B., Popovich, P.G., 2007. Impaired antibody synthesis after spinal cord injury is level dependent and is due to sympathetic nervous system dysregulation. Exp Neurol 207, 75-84.
Luer, M.S., Hamani, C., Dujovny, M., Gidal, B., Cwik, M., Deyo, K., Fischer, J.H., 1999. Saturable transport of gabapentin at the blood-brain barrier. Neurol Res 21, 559-562.
Machhada, A., Marina, N., Korsak, A., Stuckey, D.J., Lythgoe, M.F., Gourine, A.V., 2016. Origins of the vagal drive controlling left ventricular contractility. J Physiol 594, 4017-4030.
Maiorov, D.N., Krenz, N.R., Krassioukov, A.V., Weaver, L.C., 1997. Role of spinal NMDA and AMPA receptors in episodic hypertension in conscious spinal rats. Am J Physiol 273, H1266-1274.
Manvich, D.F., Webster, K.A., Foster, S.L., Farrell, M.S., Ritchie, J.C., Porter, J.H., Weinshenker, D., 2018. The DREADD agonist clozapine N-oxide (CNO) is

reverse-metabolized to clozapine and produces clozapine-like interoceptive stimulus effects in rats and mice. Sci Rep 8, 3840.
Marcus, B., Gillette, P.C., Garson, A., Jr., 1990. Intrinsic heart rate in children and young adults: an index of sinus node function isolated from autonomic control. Am Heart J 119, 911-916.
Markham, J.A., Vaughn, J.E., 1990. Ultrastructural analysis of choline acetyltransferase-immunoreactive sympathetic preganglionic neurons and their dendritic bundles in rat thoracic spinal cord. Synapse 5, 299-312.
Markota, M., Morgan, R.J., 2017. Treatment of Generalized Anxiety Disorder with Gabapentin. Case Rep Psychiatry 2017, 6045017.
Marsh, D.R., Weaver, L.C., 2004. Autonomic dysreflexia, induced by noxious or innocuous stimulation, does not depend on changes in dorsal horn substance p. J Neurotrauma 21, 817-828.
Martins, L., Fernandez-Mallo, D., Novelle, M.G., Vazquez, M.J., Tena-Sempere, M., Nogueiras, R., Lopez, M., Dieguez, C., 2012. Hypothalamic mTOR signaling mediates the orexigenic action of ghrelin. PLoS One 7, e46923.
Maruyama, Y., Mizuguchi, M., Yaginuma, T., Kusaka, M., Yoshida, H., Yokoyama, K., Kasahara, Y., Hosoya, T., 2008. Serum leptin, abdominal obesity and the metabolic syndrome in individuals with chronic spinal cord injury. Spinal Cord 46, 494-499.
Massard, C., Fizazi, K., Gross-Goupil, M., Escudier, B., 2010. Reflex sympathetic dystrophy in patients with metastatic renal cell carcinoma treated with everolimus. Invest New Drugs 28, 879-881.
Mathias, C.J., Christensen, N.J., Corbett, J.L., Frankel, H.L., Spalding, J.M., 1976. Plasma catecholamines during paroxysmal neurogenic hypertension in quadriplegic man. Circ Res 39, 204-208.
Mathias, C.J., Christensen, N.J., Frankel, H.L., Spalding, J.M., 1979. Cardiovascular control in recently injured tetraplegics in spinal shock. Q J Med 48, 273-287.
Mathias, C.J., Frankel, H.L., 1988. Cardiovascular control in spinal man. Annu Rev Physiol 50, 577-592.
Matsushita, M., 1998. Ascending propriospinal afferents to area X (substantia grisea centralis) of the spinal cord in the rat. Exp Brain Res 119, 356-366.
Maxwell, D.J., Belle, M.D., Cheunsuang, O., Stewart, A., Morris, R., 2007. Morphology of inhibitory and excitatory interneurons in superficial laminae of the rat dorsal horn. J Physiol 584, 521-533.
Mayet, J., Hughes, A., 2003. Cardiac and vascular pathophysiology in hypertension. Heart 89, 1104-1109.
Mayorov, D.N., Adams, M.A., Krassioukov, A.V., 2001. Telemetric blood pressure monitoring in conscious rats before and after compression injury of spinal cord. J Neurotrauma 18, 727-736.
McBride, F., Quah, S.P., Scott, M.E., Dinsmore, W.W., 2003. Tripling of blood pressure by sexual stimulation in a man with spinal cord injury. J R Soc Med 96, 349-350.
McCaughey, E.J., Purcell, M., McLean, A.N., Fraser, M.H., Bewick, A., Borotkanics, R.J., Allan, D.B., 2016. Changing demographics of spinal cord injury over a 20-

year period: a longitudinal population-based study in Scotland. Spinal Cord 54, 270-276.
McCormack, F.X., Inoue, Y., Moss, J., Singer, L.G., Strange, C., Nakata, K., Barker, A.F., Chapman, J.T., Brantly, M.L., Stocks, J.M., Brown, K.K., Lynch, J.P., 3rd, Goldberg, H.J., Young, L.R., Kinder, B.W., Downey, G.P., Sullivan, E.J., Colby, T.V., McKay, R.T., Cohen, M.M., Korbee, L., Taveira-DaSilva, A.M., Lee, H.S., Krischer, J.P., Trapnell, B.C., National Institutes of Health Rare Lung Diseases, C., Group, M.T., 2011. Efficacy and safety of sirolimus in lymphangioleiomyomatosis. N Engl J Med 364, 1595-1606.
McKillop, W.M., York, E.M., Rubinger, L., Liu, T., Ossowski, N.M., Xu, K., Hryciw, T., Brown, A., 2016. Conditional Sox9 ablation improves locomotor recovery after spinal cord injury by increasing reactive sprouting. Exp Neurol 283, 1-15.
McMahon, H.T., Bolshakov, V.Y., Janz, R., Hammer, R.E., Siegelbaum, S.A., Sudhof, T.C., 1996. Synaptophysin, a major synaptic vesicle protein, is not essential for neurotransmitter release. Proc Natl Acad Sci U S A 93, 4760-4764.
Meisner, J.G., Marsh, A.D., Marsh, D.R., 2010. Loss of GABAergic interneurons in laminae I-III of the spinal cord dorsal horn contributes to reduced GABAergic tone and neuropathic pain after spinal cord injury. J Neurotrauma 27, 729-737.
Melemedjian, O.K., Asiedu, M.N., Tillu, D.V., Peebles, K.A., Yan, J., Ertz, N., Dussor, G.O., Price, T.J., 2010. IL-6- and NGF-induced rapid control of protein synthesis and nociceptive plasticity via convergent signaling to the eIF4F complex. J Neurosci 30, 15113-15123.
Melemedjian, O.K., Khoutorsky, A., Sorge, R.E., Yan, J., Asiedu, M.N., Valdez, A., Ghosh, S., Dussor, G., Mogil, J.S., Sonenberg, N., Price, T.J., 2013. mTORC1 inhibition induces pain via IRS-1-dependent feedback activation of ERK. Pain 154, 1080-1091.
Mironets, E., Osei-Owusu, P., Bracchi-Ricard, V., Fischer, R., Owens, E.A., Ricard, J., Wu, D., Saltos, T., Collyer, E., Hou, S., Bethea, J.R., Tom, V.J., 2018. Soluble TNFalpha Signaling within the Spinal Cord Contributes to the Development of Autonomic Dysreflexia and Ensuing Vascular and Immune Dysfunction after Spinal Cord Injury. J Neurosci 38, 4146-4162.
Moeller, B.A., Jr., Scheinberg, D., 1973. Autonomic dysreflexia in injuries below the sixth thoracic segment. JAMA 224, 1295.
Molgaard-Nielsen, D., Hviid, A., 2011. Newer-generation antiepileptic drugs and the risk of major birth defects. JAMA 305, 1996-2002.
Molina, M.G., Diekmann, F., Burgos, D., Cabello, M., Lopez, V., Oppenheimer, F., Navarro, A., Campistol, J., 2008. Sympathetic dystrophy associated with sirolimus therapy. Transplantation 85, 290-292.
Moncada, S., Higgs, A., 1993. The L-arginine-nitric oxide pathway. N Engl J Med 329, 2002-2012.
Montgomery, K.L., Iyer, S.M., Christensen, A.J., Deisseroth, K., Delp, S.L., 2016. Beyond the brain: Optogenetic control in the spinal cord and peripheral nervous system. Sci Transl Med 8, 337rv335.
Morrow, J., Russell, A., Guthrie, E., Parsons, L., Robertson, I., Waddell, R., Irwin, B., McGivern, R.C., Morrison, P.J., Craig, J., 2006. Malformation risks of antiepileptic

drugs in pregnancy: a prospective study from the UK Epilepsy and Pregnancy Register. J Neurol Neurosurg Psychiatry 77, 193-198.
Muneton-Gomez, V., Taylor, J.S., Averill, S., Priestley, J.V., Nieto-Sampedro, M., 2004. Degeneration of primary afferent terminals following brachial plexus extensive avulsion injury in rats. Biomedica 24, 183-193.
Muzumdar, A.S., 1982. The mass reflex: an emergency in a quadriplegic patients. Can Med Assoc J 126, 369-370, 376.
Myers, J., Lee, M., Kiratli, J., 2007. Cardiovascular disease in spinal cord injury: an overview of prevalence, risk, evaluation, and management. Am J Phys Med Rehabil 86, 142-152.
Navone, F., Jahn, R., Di Gioia, G., Stukenbrok, H., Greengard, P., De Camilli, P., 1986. Protein p38: an integral membrane protein specific for small vesicles of neurons and neuroendocrine cells. J Cell Biol 103, 2511-2527.
Neuhuber, W., McLachlan, E., Janig, W., 2017. The Sacral Autonomic Outflow Is Spinal, but Not "Sympathetic". Anat Rec (Hoboken) 300, 1369-1370.
Ni, B., Rosteck, P.R., Jr., Nadi, N.S., Paul, S.M., 1994. Cloning and expression of a cDNA encoding a brain-specific Na(+)-dependent inorganic phosphate cotransporter. Proc Natl Acad Sci U S A 91, 5607-5611.
Nichterwitz, S., Chen, G., Aguila Benitez, J., Yilmaz, M., Storvall, H., Cao, M., Sandberg, R., Deng, Q., Hedlund, E., 2016. Laser capture microscopy coupled with Smart-seq2 for precise spatial transcriptomic profiling. Nat Commun 7, 12139.
Nikonenko, A.G., Sun, M., Lepsveridze, E., Apostolova, I., Petrova, I., Irintchev, A., Dityatev, A., Schachner, M., 2006. Enhanced perisomatic inhibition and impaired long-term potentiation in the CA1 region of juvenile CHL1-deficient mice. Eur J Neurosci 23, 1839-1852.
Nilsson, S., 1983. Autonomic nerve function in the vertebrates. Springer-Verlag, Berlin ; New York.
Nilsson, S., 2011. Comparative anatomy of the autonomic nervous system. Auton Neurosci 165, 3-9.
Nishimaru, K., Tanaka, Y., Tanaka, H., Shigenobu, K., 2000. Positive and negative inotropic effects of muscarinic receptor stimulation in mouse left atria. Life Sci 66, 607-615.
Nitulescu, G.M., Margina, D., Juzenas, P., Peng, Q., Olaru, O.T., Saloustros, E., Fenga, C., Spandidos, D., Libra, M., Tsatsakis, A.M., 2016. Akt inhibitors in cancer treatment: The long journey from drug discovery to clinical use (Review). Int J Oncol 48, 869-885.
O'Brien, R.J., Kamboj, S., Ehlers, M.D., Rosen, K.R., Fischbach, G.D., Huganir, R.L., 1998. Activity-dependent modulation of synaptic AMPA receptor accumulation. Neuron 21, 1067-1078.
O'Connell, T.D., Jensen, B.C., Baker, A.J., Simpson, P.C., 2014. Cardiac alpha1-adrenergic receptors: novel aspects of expression, signaling mechanisms, physiologic function, and clinical importance. Pharmacol Rev 66, 308-333.
Obara, I., Tochiki, K.K., Geranton, S.M., Carr, F.B., Lumb, B.M., Liu, Q., Hunt, S.P., 2011. Systemic inhibition of the mammalian target of rapamycin (mTOR) pathway reduces neuropathic pain in mice. Pain 152, 2582-2595.

Olive, J.L., Dudley, G.A., McCully, K.K., 2003. Vascular remodeling after spinal cord injury. Med Sci Sports Exerc 35, 901-907.
Oliveira, A.L., Hydling, F., Olsson, E., Shi, T., Edwards, R.H., Fujiyama, F., Kaneko, T., Hokfelt, T., Cullheim, S., Meister, B., 2003. Cellular localization of three vesicular glutamate transporter mRNAs and proteins in rat spinal cord and dorsal root ganglia. Synapse 50, 117-129.
Orasanu, B., Mahajan, S.T., 2013. The use of botulinum toxin for the treatment of overactive bladder syndrome. Indian J Urol 29, 2-11.
Orr, M.B., Gensel, J.C., 2017. Interactions of primary insult biomechanics and secondary cascades in spinal cord injury: implications for therapy. Neural Regen Res 12, 1618-1619.
Palacin, M., Estevez, R., Bertran, J., Zorzano, A., 1998. Molecular biology of mammalian plasma membrane amino acid transporters. Physiol Rev 78, 969-1054.
Pardini, B.J., Lund, D.D., Schmid, P.G., 1989. Organization of the sympathetic postganglionic innervation of the rat heart. J Auton Nerv Syst 28, 193-201.
Pardini, B.J., Lund, D.D., Schmid, P.G., 1990. Innervation patterns of the middle cervical--stellate ganglion complex in the rat. Neurosci Lett 117, 300-306.
Park, K.K., Liu, K., Hu, Y., Smith, P.D., Wang, C., Cai, B., Xu, B., Connolly, L., Kramvis, I., Sahin, M., He, Z., 2008. Promoting axon regeneration in the adult CNS by modulation of the PTEN/mTOR pathway. Science 322, 963-966.
Pascual, J.I., Insausti, R., Gonzalo, L.M., 1993. Urinary bladder innervation in male rat: termination of primary afferents in the spinal cord as determined by transganglionic transport of WGA-HRP. J Urol 150, 500-504.
Patel, M.K., Gonzalez, M.I., Bramwell, S., Pinnock, R.D., Lee, K., 2000. Gabapentin inhibits excitatory synaptic transmission in the hyperalgesic spinal cord. Br J Pharmacol 130, 1731-1734.
Petroianu, A., 2007. Drug-induced splenic enlargement. Expert Opin Drug Saf 6, 199-206.
Phillips, A.A., Elliott, S.L., Zheng, M.M., Krassioukov, A.V., 2015. Selective alpha adrenergic antagonist reduces severity of transient hypertension during sexual stimulation after spinal cord injury. J Neurotrauma 32, 392-396.
Phillips, A.A., Matin, N., Frias, B., Zheng, M.M., Jia, M., West, C., Dorrance, A.M., Laher, I., Krassioukov, A.V., 2016. Rigid and remodelled: cerebrovascular structure and function after experimental high-thoracic spinal cord transection. J Physiol 594, 1677-1688.
Phillips, A.A., Matin, N., Jia, M., Squair, J.W., Monga, A., Zheng, M.M.Z., Sachdeva, R., Yung, A., Hocaloski, S., Elliott, S., Kozlowski, P., Dorrance, A.M., Laher, I., Ainslie, P.N., Krassioukov, A.V., 2018. Transient Hypertension after Spinal Cord Injury Leads to Cerebrovascular Endothelial Dysfunction and Fibrosis. J Neurotrauma 35, 573-581.
Phillips, A.A., Warburton, D.E., Ainslie, P.N., Krassioukov, A.V., 2014. Regional neurovascular coupling and cognitive performance in those with low blood pressure secondary to high-level spinal cord injury: improved by alpha-1 agonist midodrine hydrochloride. J Cereb Blood Flow Metab 34, 794-801.

Pingel, J., Bartels, E.M., Nielsen, J.B., 2017. New perspectives on the development of muscle contractures following central motor lesions. J Physiol 595, 1027-1038.
Ploumis, A., Yadlapalli, N., Fehlings, M.G., Kwon, B.K., Vaccaro, A.R., 2010. A systematic review of the evidence supporting a role for vasopressor support in acute SCI. Spinal Cord 48, 356-362.
Polgar, E., Hughes, D.I., Riddell, J.S., Maxwell, D.J., Puskar, Z., Todd, A.J., 2003. Selective loss of spinal GABAergic or glycinergic neurons is not necessary for development of thermal hyperalgesia in the chronic constriction injury model of neuropathic pain. Pain 104, 229-239.
Popok, D., West, C.R., Hubli, M., Currie, K.D., Krassioukov, A.V., 2016. Characterising the severity of autonomic cardiovascular dysfunction after spinal cord injury using a novel 24 hour ambulatory blood pressure analysis software. J Neurotrauma.
Post, S.R., Hammond, H.K., Insel, P.A., 1999. Beta-adrenergic receptors and receptor signaling in heart failure. Annu Rev Pharmacol Toxicol 39, 343-360.
Price, J.C., Guan, S., Burlingame, A., Prusiner, S.B., Ghaemmaghami, S., 2010. Analysis of proteome dynamics in the mouse brain. Proc Natl Acad Sci U S A 107, 14508-14513.
Pyner, S., Coote, J.H., 1994. Evidence that sympathetic preganglionic neurones are arranged in target-specific columns in the thoracic spinal cord of the rat. J Comp Neurol 342, 15-22.
Rabchevsky, A.G., 2006. Segmental organization of spinal reflexes mediating autonomic dysreflexia after spinal cord injury. 152, 265-274.
Rabchevsky, A.G., Patel, S.P., Duale, H., Lyttle, T.S., O'Dell, C.R., Kitzman, P.H., 2011. Gabapentin for spasticity and autonomic dysreflexia after severe spinal cord injury. Spinal Cord 49, 99-105.
Rabchevsky, A.G., Patel, S.P., Lyttle, T.S., Eldahan, K.C., O'Dell, C.R., Zhang, Y., Popovich, P.G., Kitzman, P.H., Donohue, K.D., 2012. Effects of gabapentin on muscle spasticity and both induced as well as spontaneous autonomic dysreflexia after complete spinal cord injury. Front Physiol 3, 329.
Radulovic, L.L., Turck, D., von Hodenberg, A., Vollmer, K.O., McNally, W.P., DeHart, P.D., Hanson, B.J., Bockbrader, H.N., Chang, T., 1995. Disposition of gabapentin (neurontin) in mice, rats, dogs, and monkeys. Drug Metab Dispos 23, 441-448.
Ragucci, M.V., Cohen, J.M., 2001. Gabapentin-induced hypersensitivity syndrome. Clin Neuropharmacol 24, 103-105.
Rahman, M.H., Nam, Y., Kim, J.H., Lee, W.H., Suk, K., 2018. Optogenetics of the Spinal Cord: Use of Channelrhodopsin Proteins for Interrogation of Spinal Cord Circuits. Curr Protein Pept Sci 19, 714-724.
Ramer, L.M., van Stolk, A.P., Inskip, J.A., Ramer, M.S., Krassioukov, A.V., 2012. Plasticity of TRPV1-Expressing Sensory Neurons Mediating Autonomic Dysreflexia Following Spinal Cord Injury. Front Physiol 3, 257.
Rando, T.A., Bowers, C.W., Zigmond, R.E., 1981. Localization of neurons in the rat spinal cord which project to the superior cervical ganglion. J Comp Neurol 196, 73-83.
Rao, M., Gershon, M.D., 2016. The bowel and beyond: the enteric nervous system in neurological disorders. Nat Rev Gastroenterol Hepatol 13, 517-528.

Rees, C.L., White, C.M., Ascoli, G.A., 2017. Neurochemical Markers in the Mammalian Brain: Structure, Roles in Synaptic Communication, and Pharmacological Relevance. Curr Med Chem 24, 3077-3103.
Reese, A.L., Kavalali, E.T., 2015. Spontaneous neurotransmission signals through store-driven Ca(2+) transients to maintain synaptic homeostasis. Elife 4.
Reichardt, L.F., Kelly, R.B., 1983. A molecular description of nerve terminal function. Annu Rev Biochem 52, 871-926.
Reis, F., Parada, B., Teixeira de Lemos, E., Garrido, P., Dias, A., Piloto, N., Baptista, S., Sereno, J., Eufrasio, P., Costa, E., Rocha-Pereira, P., Santos-Silva, A., Figueiredo, A., Mota, A., Teixeira, F., 2009. Hypertension induced by immunosuppressive drugs: a comparative analysis between sirolimus and cyclosporine. Transplant Proc 41, 868-873.
Rhen, T., Cidlowski, J.A., 2005. Antiinflammatory action of glucocorticoids--new mechanisms for old drugs. N Engl J Med 353, 1711-1723.
Riegger, T., Conrad, S., Liu, K., Schluesener, H.J., Adibzahdeh, M., Schwab, J.M., 2007. Spinal cord injury-induced immune depression syndrome (SCI-IDS). Eur J Neurosci 25, 1743-1747.
Rizzoni, D., Porteri, E., Boari, G.E., De Ciuceis, C., Sleiman, I., Muiesan, M.L., Castellano, M., Miclini, M., Agabiti-Rosei, E., 2003. Prognostic significance of small-artery structure in hypertension. Circulation 108, 2230-2235.
Rossler, W., Spaethe, J., Groh, C., 2017. Pitfalls of using confocal-microscopy based automated quantification of synaptic complexes in honeybee mushroom bodies (response to Peng and Yang 2016). Sci Rep 7, 9786.
Roth, B.L., 2016. DREADDs for Neuroscientists. Neuron 89, 683-694.
Rowell, L.B., 1990. Importance of scintigraphic measurements of human splanchnic blood volume. J Nucl Med 31, 160-162.
Rozengurt, E., Soares, H.P., Sinnet-Smith, J., 2014. Suppression of feedback loops mediated by PI3K/mTOR induces multiple overactivation of compensatory pathways: an unintended consequence leading to drug resistance. Mol Cancer Ther 13, 2477-2488.
Ruffolo, R.R., Jr., Nichols, A.J., Stadel, J.M., Hieble, J.P., 1991. Structure and function of alpha-adrenoceptors. Pharmacol Rev 43, 475-505.
Rummery, N.M., Tripovic, D., McLachlan, E.M., Brock, J.A., 2010. Sympathetic vasoconstriction is potentiated in arteries caudal but not rostral to a spinal cord transection in rats. J Neurotrauma 27, 2077-2089.
Ruocco, I., Cuello, A.C., Parent, A., Ribeiro-da-Silva, A., 2002. Skin blood vessels are simultaneously innervated by sensory, sympathetic, and parasympathetic fibers. J Comp Neurol 448, 323-336.
Sabre, L., Rekand, T., Asser, T., Korv, J., 2013. Mortality and causes of death after traumatic spinal cord injury in Estonia. J Spinal Cord Med 36, 687-694.
Salimzade, A., Hosseini-Sharifabad, A., Rabbani, M., 2017. Comparative effects of chronic administrations of gabapentin, pregabalin and baclofen on rat memory using object recognition test. Res Pharm Sci 12, 204-210.
Samineni, V.K., Yoon, J., Crawford, K.E., Jeong, Y.R., McKenzie, K.C., Shin, G., Xie, Z., Sundaram, S.S., Li, Y., Yang, M.Y., Kim, J., Wu, D., Xue, Y., Feng, X., Huang, Y., Mickle, A.D., Banks, A., Ha, J.S., Golden, J.P., Rogers, J.A., Gereau,

R.W.t., 2017. Fully implantable, battery-free wireless optoelectronic devices for spinal optogenetics. Pain 158, 2108-2116.
Sandsmark, D.K., Pelletier, C., Weber, J.D., Gutmann, D.H., 2007. Mammalian target of rapamycin: master regulator of cell growth in the nervous system. Histol Histopathol 22, 895-903.
Santos, E.A., Filho, W.J., Possatti, L.L., Bittencourt, L.R., Fontoura, E.A., Botelho, R.V., 2009. Epidemiology of severe cervical spinal trauma in the north area of Sao Paulo City: a 10-year prospective study. Clinical article. J Neurosurg Spine 11, 34-41.
Sarantopoulos, C., McCallum, B., Kwok, W.M., Hogan, Q., 2002. Gabapentin decreases membrane calcium currents in injured as well as in control mammalian primary afferent neurons. Reg Anesth Pain Med 27, 47-57.
Sarbassov, D.D., Ali, S.M., Sengupta, S., Sheen, J.H., Hsu, P.P., Bagley, A.F., Markhard, A.L., Sabatini, D.M., 2006. Prolonged rapamycin treatment inhibits mTORC2 assembly and Akt/PKB. Mol Cell 22, 159-168.
Schafer, M.K., Varoqui, H., Defamie, N., Weihe, E., Erickson, J.D., 2002. Molecular cloning and functional identification of mouse vesicular glutamate transporter 3 and its expression in subsets of novel excitatory neurons. J Biol Chem 277, 50734-50748.
Schaukowitch, K., Reese, A.L., Kim, S.K., Kilaru, G., Joo, J.Y., Kavalali, E.T., Kim, T.K., 2017. An Intrinsic Transcriptional Program Underlying Synaptic Scaling during Activity Suppression. Cell Rep 18, 1512-1526.
Schiffrin, E.L., 2004. Remodeling of resistance arteries in essential hypertension and effects of antihypertensive treatment. Am J Hypertens 17, 1192-1200.
Schmelzle, T., Hall, M.N., 2000. TOR, a central controller of cell growth. Cell 103, 253-262.
Schnegelsberg, B., Sun, T.T., Cain, G., Bhattacharya, A., Nunn, P.A., Ford, A.P., Vizzard, M.A., Cockayne, D.A., 2010. Overexpression of NGF in mouse urothelium leads to neuronal hyperinnervation, pelvic sensitivity, and changes in urinary bladder function. Am J Physiol Regul Integr Comp Physiol 298, R534-547.
Schramm, L.P., 2006. Spinal sympathetic interneurons: their identification and roles after spinal cord injury. Prog Brain Res 152, 27-37.
Schurch, B., de Seze, M., Denys, P., Chartier-Kastler, E., Haab, F., Everaert, K., Plante, P., Perrouin-Verbe, B., Kumar, C., Fraczek, S., Brin, M.F., Botox Detrusor Hyperreflexia Study, T., 2005. Botulinum toxin type a is a safe and effective treatment for neurogenic urinary incontinence: results of a single treatment, randomized, placebo controlled 6-month study. J Urol 174, 196-200.
Schurch, B., Hauri, D., Rodic, B., Curt, A., Meyer, M., Rossier, A.B., 1996. Botulinum-A toxin as a treatment of detrusor-sphincter dyssynergia: a prospective study in 24 spinal cord injury patients. J Urol 155, 1023-1029.
Schurch, B., Stohrer, M., Kramer, G., Schmid, D.M., Gaul, G., Hauri, D., 2000. Botulinum-A toxin for treating detrusor hyperreflexia in spinal cord injured patients: a new alternative to anticholinergic drugs? Preliminary results. J Urol 164, 692-697.

Scott, M.B., Morrow, J.W., 1978. Phenoxybenzamine in neurogenic bladder dysfunction after spinal cord injury. II. Autonomic dysreflexia. J Urol 119, 483-484.
Seal, R.P., Wang, X., Guan, Y., Raja, S.N., Woodbury, C.J., Basbaum, A.I., Edwards, R.H., 2009. Injury-induced mechanical hypersensitivity requires C-low threshold mechanoreceptors. Nature 462, 651-655.
Sebastian, S., Ang, R., Abramowitz, J., Weinstein, L.S., Chen, M., Ludwig, A., Birnbaumer, L., Tinker, A., 2013. The in vivo regulation of heart rate in the murine sinoatrial node by stimulatory and inhibitory heterotrimeric G proteins. Am J Physiol Regul Integr Comp Physiol 305, R435-442.
Secomb, T.W., 2016. Hemodynamics. Compr Physiol 6, 975-1003.
Sekiguchi, A., Kanno, H., Ozawa, H., Yamaya, S., Itoi, E., 2012. Rapamycin promotes autophagy and reduces neural tissue damage and locomotor impairment after spinal cord injury in mice. J Neurotrauma 29, 946-956.
Shamsi Meymandi, M., Keyhanfar, F., 2013. Relative potency of pregabalin, gabapentin, and morphine in a mouse model of visceral pain. Can J Anaesth 60, 44-49.
Shannon, H.E., Love, P.L., 2004. Effects of antiepileptic drugs on working memory as assessed by spatial alternation performance in rats. Epilepsy Behav 5, 857-865.
Sheng, H., Stauffer, W., Lim, H.N., 2016. Systematic and general method for quantifying localization in microscopy images. Biol Open 5, 1882-1893.
Sheng, Y., Zhu, L., 2018. The crosstalk between autonomic nervous system and blood vessels. Int J Physiol Pathophysiol Pharmacol 10, 17-28.
Shimoyama, M., Shimoyama, N., Hori, Y., 2000. Gabapentin affects glutamatergic excitatory neurotransmission in the rat dorsal horn. Pain 85, 405-414.
Showkathali, R., Antionios, T.F., 2007. Autonomic dysreflexia; a medical emergency. J R Soc Med 100, 382-383.
Sieber-Blum, M., 2000. Factors controlling lineage specification in the neural crest. Int Rev Cytol 197, 1-33.
Sills, G.J., 2006. The mechanisms of action of gabapentin and pregabalin. Curr Opin Pharmacol 6, 108-113.
Silver, A.E., Vita, J.A., 2006. Shear-stress-mediated arterial remodeling in atherosclerosis: too much of a good thing? Circulation 113, 2787-2789.
Silver, J.R., 2000. Early autonomic dysreflexia. Spinal Cord 38, 229-233.
Sinclair, M.D., 2003. A review of the physiological effects of alpha2-agonists related to the clinical use of medetomidine in small animal practice. Can Vet J 44, 885-897.
Sirven, J.I., 2010. New uses for older drugs: the tales of aspirin, thalidomide, and gabapentin. Mayo Clin Proc 85, 508-511.
SM, O.M., Coelho, A.M., Fitzgerald, P., Lee, K., Winchester, W., Dinan, T.G., Cryan, J.F., 2011. The effects of gabapentin in two animal models of co-morbid anxiety and visceral hypersensitivity. Eur J Pharmacol 667, 169-174.
Snow, J.C., Sideropoulos, H.P., Kripke, B.J., Freed, M.M., Shah, N.K., Schlesinger, R.M., 1978. Autonomic hyperreflexia during cystoscopy in patients with high spinal cord injuries. Paraplegia 15, 327-332.

Soares, H.P., Ming, M., Mellon, M., Young, S.H., Han, L., Sinnet-Smith, J., Rozengurt, E., 2015. Dual PI3K/mTOR Inhibitors Induce Rapid Overactivation of the MEK/ERK Pathway in Human Pancreatic Cancer Cells through Suppression of mTORC2. Mol Cancer Ther 14, 1014-1023.
Song, G., Cechvala, C., Resnick, D.K., Dempsey, R.J., Rao, V.L., 2001. GeneChip analysis after acute spinal cord injury in rat. J Neurochem 79, 804-815.
Song, Y., Xue, H., Liu, T.T., Liu, J.M., Chen, D., 2015. Rapamycin plays a neuroprotective effect after spinal cord injury via anti-inflammatory effects. J Biochem Mol Toxicol 29, 29-34.
Squair, J.W., West, C.R., Popok, D., Assinck, P., Liu, J., Tetzlaff, W., Krassioukov, A.V., 2017. High Thoracic Contusion Model for the Investigation of Cardiovascular Function after Spinal Cord Injury. J Neurotrauma 34, 671-684.
Stachniak, T.J., Ghosh, A., Sternson, S.M., 2014. Chemogenetic synaptic silencing of neural circuits localizes a hypothalamus-->midbrain pathway for feeding behavior. Neuron 82, 797-808.
Stankovic, T., Dinic, J., Podolski-Renic, A., Musso, L., Buric, S.S., Dallavalle, S., Pesic, M., 2018. Dual Inhibitors as a New Challenge for Cancer Multidrug Resistance Treatment. Curr Med Chem.
Stevens, S.L., Wood, S., Koshiaris, C., Law, K., Glasziou, P., Stevens, R.J., McManus, R.J., 2016. Blood pressure variability and cardiovascular disease: systematic review and meta-analysis. BMJ 354, i4098.
Stjernberg, L., Blumberg, H., Wallin, B.G., 1986. Sympathetic activity in man after spinal cord injury. Outflow to muscle below the lesion. Brain 109 (Pt 4), 695-715.
Strack, A.M., Sawyer, W.B., Hughes, J.H., Platt, K.B., Loewy, A.D., 1989. A general pattern of CNS innervation of the sympathetic outflow demonstrated by transneuronal pseudorabies viral infections. Brain Res 491, 156-162.
Su, T.Z., Feng, M.R., Weber, M.L., 2005. Mediation of highly concentrative uptake of pregabalin by L-type amino acid transport in Chinese hamster ovary and Caco-2 cells. J Pharmacol Exp Ther 313, 1406-1415.
Sullivan, P.G., Krishnamurthy, S., Patel, S.P., Pandya, J.D., Rabchevsky, A.G., 2007. Temporal characterization of mitochondrial bioenergetics after spinal cord injury. J Neurotrauma 24, 991-999.
Sun, F., Park, K.K., Belin, S., Wang, D., Lu, T., Chen, G., Zhang, K., Yeung, C., Feng, G., Yankner, B.A., He, Z., 2011. Sustained axon regeneration induced by co-deletion of PTEN and SOCS3. Nature 480, 372-375.
Sun, Z., Hu, L., Wen, Y., Chen, K., Sun, Z., Yue, H., Zhang, C., 2013. Adenosine triphosphate promotes locomotor recovery after spinal cord injury by activating mammalian target of rapamycin pathway in rats. Neural Regen Res 8, 101-110.
Sundaram, K., Murugaian, J., Sapru, H., 1989. Cardiac responses to the microinjections of excitatory amino acids into the intermediolateral cell column of the rat spinal cord. Brain Res 482, 12-22.
Sved, A.F., Cano, G., Card, J.P., 2001. Neuroanatomical specificity of the circuits controlling sympathetic outflow to different targets. Clin Exp Pharmacol Physiol 28, 115-119.

Takahashi, D.K., Jin, S., Prince, D.A., 2018. Gabapentin Prevents Progressive Increases in Excitatory Connectivity and Epileptogenesis Following Neocortical Trauma. Cereb Cortex 28, 2725-2740.
Takamori, S., Rhee, J.S., Rosenmund, C., Jahn, R., 2001. Identification of differentiation-associated brain-specific phosphate transporter as a second vesicular glutamate transporter (VGLUT2). J Neurosci 21, RC182.
Tang, F.R., Tan, C.K., Ling, E.A., 1995. A light-microscopic study of the intermediolateral nucleus following injection of CB-HRP and fluorogold into the superior cervical ganglion of the rat. J Auton Nerv Syst 50, 333-338.
Tang, X., Neckel, N.D., Schramm, L.P., 2004a. Spinal interneurons infected by renal injection of pseudorabies virus in the rat. Brain Res 1004, 1-7.
Tang, X.Q., Tanelian, D.L., Smith, G.M., 2004b. Semaphorin3A inhibits nerve growth factor-induced sprouting of nociceptive afferents in adult rat spinal cord. J Neurosci 24, 819-827.
Tang, Y., Scott, D., Das, U., Gitler, D., Ganguly, A., Roy, S., 2013. Fast vesicle transport is required for the slow axonal transport of synapsin. J Neurosci 33, 15362-15375.
Tateda, S., Kanno, H., Ozawa, H., Sekiguchi, A., Yahata, K., Yamaya, S., Itoi, E., 2017. Rapamycin suppresses microglial activation and reduces the development of neuropathic pain after spinal cord injury. J Orthop Res 35, 93-103.
Taylor, B.K., Corder, G., 2014. Endogenous analgesia, dependence, and latent pain sensitization. Curr Top Behav Neurosci 20, 283-325.
Taylor, C.P., 2004. The biology and pharmacology of calcium channel alpha2-delta proteins Pfizer Satellite Symposium to the 2003 Society for Neuroscience Meeting. Sheraton New Orleans Hotel, New Orleans, LA November 10, 2003. CNS Drug Rev 10, 183-188.
Taylor, C.P., 2009. Mechanisms of analgesia by gabapentin and pregabalin--calcium channel alpha2-delta [Cavalpha2-delta] ligands. Pain 142, 13-16.
Taylor, C.P., Garrido, R., 2008. Immunostaining of rat brain, spinal cord, sensory neurons and skeletal muscle for calcium channel alpha2-delta (alpha2-delta) type 1 protein. Neuroscience 155, 510-521.
Taylor, C.P., Gee, N.S., Su, T.Z., Kocsis, J.D., Welty, D.F., Brown, J.P., Dooley, D.J., Boden, P., Singh, L., 1998. A summary of mechanistic hypotheses of gabapentin pharmacology. Epilepsy Res 29, 233-249.
Teasell, R.W., Arnold, J.M., Krassioukov, A., Delaney, G.A., 2000. Cardiovascular consequences of loss of supraspinal control of the sympathetic nervous system after spinal cord injury. Arch Phys Med Rehabil 81, 506-516.
Thomas, G.D., 2011. Neural control of the circulation. Adv Physiol Educ 35, 28-32.
Thyberg, M., Ertzgaard, P., Gylling, M., Granerus, G., 1994. Effect of nifedipine on cystometry-induced elevation of blood pressure in patients with a reflex urinary bladder after a high level spinal cord injury. Paraplegia 32, 308-313.
Todd, A.J., Hughes, D.I., Polgar, E., Nagy, G.G., Mackie, M., Ottersen, O.P., Maxwell, D.J., 2003. The expression of vesicular glutamate transporters VGLUT1 and VGLUT2 in neurochemically defined axonal populations in the rat spinal cord with emphasis on the dorsal horn. Eur J Neurosci 17, 13-27.

Trop, C.S., Bennett, C.J., 1991. Autonomic dysreflexia and its urological implications: a review. J Urol 146, 1461-1469.
Turrigiano, G., 2012. Homeostatic synaptic plasticity: local and global mechanisms for stabilizing neuronal function. Cold Spring Harb Perspect Biol 4, a005736.
Turrigiano, G.G., 2008. The self-tuning neuron: synaptic scaling of excitatory synapses. Cell 135, 422-435.
Uchino, H., Kanai, Y., Kim, D.K., Wempe, M.F., Chairoungdua, A., Morimoto, E., Anders, M.W., Endou, H., 2002. Transport of amino acid-related compounds mediated by L-type amino acid transporter 1 (LAT1): insights into the mechanisms of substrate recognition. Mol Pharmacol 61, 729-737.
Ueno, M., Ueno-Nakamura, Y., Niehaus, J., Popovich, P.G., Yoshida, Y., 2016. Silencing spinal interneurons inhibits immune suppressive autonomic reflexes caused by spinal cord injury. Nat Neurosci 19, 784-787.
Valles, M., Benito, J., Portell, E., Vidal, J., 2005. Cerebral hemorrhage due to autonomic dysreflexia in a spinal cord injury patient. Spinal Cord 43, 738-740.
Valtorta, F., Pennuto, M., Bonanomi, D., Benfenati, F., 2004. Synaptophysin: leading actor or walk-on role in synaptic vesicle exocytosis? Bioessays 26, 445-453.
Varoqui, H., Schafer, M.K., Zhu, H., Weihe, E., Erickson, J.D., 2002. Identification of the differentiation-associated Na+/PI transporter as a novel vesicular glutamate transporter expressed in a distinct set of glutamatergic synapses. J Neurosci 22, 142-155.
Vegiopoulos, A., Herzig, S., 2007. Glucocorticoids, metabolism and metabolic diseases. Mol Cell Endocrinol 275, 43-61.
Verghese, M., 1989. Autonomic dysreflexia: a life threatening emergency. Nurs J India 80, 134-135.
Verstraelen, P., Van Dyck, M., Verschuuren, M., Kashikar, N.D., Nuydens, R., Timmermans, J.P., De Vos, W.H., 2018. Image-Based Profiling of Synaptic Connectivity in Primary Neuronal Cell Culture. Front Neurosci 12, 389.
Vizzard, M.A., 2000. Increased expression of spinal cord Fos protein induced by bladder stimulation after spinal cord injury. Am J Physiol Regul Integr Comp Physiol 279, R295-305.
Vollmer, K.O., von Hodenberg, A., Kolle, E.U., 1986. Pharmacokinetics and metabolism of gabapentin in rat, dog and man. Arzneimittelforschung 36, 830-839.
Vulovic, M., Divac, N., Jakovcevski, I., 2018. Confocal Synaptology: Synaptic Rearrangements in Neurodegenerative Disorders and upon Nervous System Injury. Front Neuroanat 12, 11.
Wake, E., Brack, K., 2016. Characterization of the intrinsic cardiac nervous system. Auton Neurosci 199, 3-16.
Wallin, B.G., Stjernberg, L., 1984. Sympathetic activity in man after spinal cord injury. Outflow to skin below the lesion. Brain 107 (Pt 1), 183-198.
Wang, H., Wang, R., Thrimawithana, T., Little, P.J., Xu, J., Feng, Z.P., Zheng, W., 2014. The nerve growth factor signaling and its potential as therapeutic target for glaucoma. Biomed Res Int 2014, 759473.

Wang, M., Offord, J., Oxender, D.L., Su, T.Z., 1999. Structural requirement of the calcium-channel subunit alpha2delta for gabapentin binding. Biochem J 342 (Pt 2), 313-320.
Wang, X., Li, X., Huang, B., Ma, S., 2016. Blocking mammalian target of rapamycin (mTOR) improves neuropathic pain evoked by spinal cord injury. Transl Neurosci 7, 50-55.
Watts, S.W., Morrison, S.F., Davis, R.P., Barman, S.M., 2012. Serotonin and blood pressure regulation. Pharmacol Rev 64, 359-388.
Weaver, L.C., Cassam, A.K., Krassioukov, A.V., Llewellyn-Smith, I.J., 1997. Changes in immunoreactivity for growth associated protein-43 suggest reorganization of synapses on spinal sympathetic neurons after cord transection. Neuroscience 81, 535-551.
Weaver, L.C., Fleming, J.C., Mathias, C.J., Krassioukov, A.V., 2012. Disordered cardiovascular control after spinal cord injury. Handb Clin Neurol 109, 213-233.
Weaver, L.C., Marsh, D.R., Gris, D., Meakin, S.O., Dekaban, G.A., 2002. Central mechanisms for autonomic dysreflexia after spinal cord injury. Prog Brain Res 137, 83-95.
Wecht, J.M., Bauman, W.A., 2013. Decentralized cardiovascular autonomic control and cognitive deficits in persons with spinal cord injury. J Spinal Cord Med 36, 74-81.
Wenner, P., 2014. Homeostatic synaptic plasticity in developing spinal networks driven by excitatory GABAergic currents. Neuropharmacology 78, 55-62.
West, C.R., Alyahya, A., Laher, I., Krassioukov, A., 2013. Peripheral vascular function in spinal cord injury: a systematic review. Spinal Cord 51, 10-19.
West, C.R., Popok, D., Crawford, M.A., Krassioukov, A.V., 2015. Characterizing the temporal development of cardiovascular dysfunction in response to spinal cord injury. J Neurotrauma 32, 922-930.
West, C.R., Squair, J.W., McCracken, L., Currie, K.D., Somvanshi, R., Yuen, V., Phillips, A.A., Kumar, U., McNeill, J.H., Krassioukov, A.V., 2016. Cardiac Consequences of Autonomic Dysreflexia in Spinal Cord Injury. Hypertension.
Wiedenmann, B., Franke, W.W., 1985. Identification and localization of synaptophysin, an integral membrane glycoprotein of Mr 38,000 characteristic of presynaptic vesicles. Cell 41, 1017-1028.
Wilson, J.M., Coderre, E., Renaud, L.P., Spanswick, D., 2002. Active and passive membrane properties of rat sympathetic preganglionic neurones innervating the adrenal medulla. J Physiol 545, 945-960.
Wojcik, S.M., Katsurabayashi, S., Guillemin, I., Friauf, E., Rosenmund, C., Brose, N., Rhee, J.S., 2006. A shared vesicular carrier allows synaptic corelease of GABA and glycine. Neuron 50, 575-587.
Xia, B., Liu, H., Xie, J., Wu, R., Li, Y., 2015. Akt enhances nerve growth factor-induced axon growth via activating the Nrf2/ARE pathway. Int J Mol Med 36, 1426-1432.
Yekutiel, M., Brooks, M.E., Ohry, A., Yarom, J., Carel, R., 1989. The prevalence of hypertension, ischaemic heart disease and diabetes in traumatic spinal cord injured patients and amputees. Paraplegia 27, 58-62.

Yu, Y.P., Gong, N., Kweon, T.D., Vo, B., Luo, Z.D., 2018. Gabapentin prevents synaptogenesis between sensory and spinal cord neurons induced by thrombospondin-4 acting on pre-synaptic Cav alpha2 delta1 subunits and involving T-type Ca(2+) channels. Br J Pharmacol 175, 2348-2361.

Zagon, A., Smith, A.D., 1993. Monosynaptic projections from the rostral ventrolateral medulla oblongata to identified sympathetic preganglionic neurons. Neuroscience 54, 729-743.

Zeng, L.H., Xu, L., Gutmann, D.H., Wong, M., 2008. Rapamycin prevents epilepsy in a mouse model of tuberous sclerosis complex. Ann Neurol 63, 444-453.

Zhang, Y., Guan, Z., Reader, B., Shawler, T., Mandrekar-Colucci, S., Huang, K., Weil, Z., Bratasz, A., Wells, J., Powell, N.D., Sheridan, J.F., Whitacre, C.C., Rabchevsky, A.G., Nash, M.S., Popovich, P.G., 2013. Autonomic dysreflexia causes chronic immune suppression after spinal cord injury. J Neurosci 33, 12970-12981.

Zhou, J.J., Li, D.P., Chen, S.R., Luo, Y., Pan, H.L., 2018. The alpha2delta-1-NMDA receptor coupling is essential for corticostriatal long-term potentiation and is involved in learning and memory. J Biol Chem.

Zhu, H., Roth, B.L., 2014. Silencing synapses with DREADDs. Neuron 82, 723-725.

Zinchuk, V., Grossenbacher-Zinchuk, O., 2009. Recent advances in quantitative colocalization analysis: focus on neuroscience. Prog Histochem Cytochem 44, 125-172.

Zinchuk, V., Zinchuk, O., 2008. Quantitative colocalization analysis of confocal fluorescence microscopy images. Curr Protoc Cell Biol Chapter 4, Unit 4 19.

VITA

Khalid C. Eldahan
Birthplace: Middlesboro, KY, USA

Education:

2013- present	PhD Candidate	Department of Physiology University of Kentucky, Lexington, KY
2010	Bachelor of Arts	Department of Biology Kenyon College, Gambier, OH

AWARDS AND HONORS:

- NIH T32 Predoctoral Fellowship, University of Kentucky, 2016- 2018
- KSCHIRT Predoctoral Fellowship, University of Kentucky, 2014-2016
- Graduate Student Representative, Department of Physiology, University of Kentucky, 2017-2018
- 1st place, "The Art of Science" competition, Biomedical Graduate Student Association, University of Kentucky, 2018
- Graduate Student Representative, Bluegrass Society for Neuroscience, University of Kentucky, 2017-2018
- Integrated Biomedical Sciences Scholarship, University of Kentucky, 2013
- Elected to Dean's Advisory Committee, Kenyon College, 2009
- Community Advisor student leadership award, Kenyon College 2009
- Undergraduate Research Fellowship, Kenyon College, 2009
- Deans Honor Roll, Kenyon College, 2007

Publications:

Eldahan K.C. and Rabchevsky A.G. (2018) Autonomic dysreflexia after spinal cord injury: Systemic pathophysiology and methods of management. Special Issue "Spinal cord injury (SCI) and the autonomic nervous system," Autonomic Neuroscience: Basic and Clinical, 209: 59-70. Epub 2017 May 8 **PMID: 28506502**, **PMCID: PMC5677594**

Gollihue J.L., Patel S.P., Mashburn C., **Eldahan K.C.**, Cox D.H., Donahue R.R., Taylor B.K., Sullivan P.G. and Rabchevsky A.G. (2018) Effects of mitochondrial transplantation on bioenergetics, cellular incorporation and functional recovery after spinal cord injury. Journal of Neurotrauma 35:842–853. Epub 2017 Dec 15 **PMID:29648982**, **PMCID: PMC6053898**

Eldahan K.C., Cox DH, Gollihue, J.L., Patel S.P. and Rabchevsky A.G. (2017) Rapamycin exacerbates cardiovascular dysfunction after complete high-thoracic spinal cord injury. Journal of Neurotrauma 35:842–853. Epub 2017 Dec 15 **PMID: 29205090**, **PMCID: PMC5863090**

Gollihue J.L., Patel S.P., Mashburn C., **Eldahan K.C.**, Sullivan P.G. and Rabchevsky A.G. (2017) Optimization of mitochondrial isolation techniques for intraspinal transplantation procedures. Journal of Neuroscience Methods 287: 1–12. Epub 2017 May 26 **PMID: 28554833**, **PMCID: PMC5533517**

Patel S.P., Sullivan P.G., Pandy J.D., Goldstein G.A., VanRooyen J.L., Yonutas H.M., **Eldahan K.C.**, Morehouse J., Magnuson D.S.K. and Rabchevsky A.G. (2014) N-acetylcysteine amide preserves mitochondrial bioenergetics and improves functional recovery following spinal trauma. Experimental Neurology 257: 95-105. Epub 2014 May 5 **PMID: 24805071**, **PMCID: PMC4114148**

Rabchevsky A.G., Patel S.P., Lyttle T.S., **Eldahan K.C.**, O'Dell C.R., Zhang Y., Popovich P.G., Kitzman P.H., and Donohue, K.D. (2012) Effects of gabapentin on muscle spasticity and both induced as well as spontaneous autonomic dysreflexia after complete spinal cord injury. Frontiers in Physiology 3: 329-350. Epub 2012 Aug 31 **PMID: 22934077**, **PMCID**: **PMC3429097**

Noguchi K., Riggins D.P., **Eldahan K.C.**, Kitko R.D., Slonczewski J.L. (2010) Hydrogenase-3 Contributes to Anaerobic Acid Resistance of Escherichia coli. PLoS ONE 5(4): e10132.
PMID: 20405029, **PMCID: PMC2853565**

<u>Oral Presentations:</u>

T*argeting Maladaptive Plasticity to Improve Cardiovascular Function After Spinal Cord Injury*. Departmental Research Retreat, Department of Physiology, Lexington, KY (May 2018).

Presentations (Posters/Abstracts):

Patel S.P., Gollihue J.L., **Eldahan K.C.**, Cox D.H., Sullivan P.G. and Rabchevsky A.G. (2017) Mitochondrial transplantation following contusion spinal cord injury. *The 19th International Spinal Research Trust Network Meeting*, London, UK.

Patel S.P., Gollihue J.L., **Eldahan K.C.**, Cox D.H., Sullivan P.G. and Rabchevsky A.G. (2017) Transplantation of mitochondria following spinal trauma. *Society for Neuroscience Annual Meeting*, Washington, D.C.

Patel S.P., Gollihue J.L., **Eldahan K.C.**, Cox D., Sullivan P.G. and Rabchevsky A.G. (2017) Mitochondrial transplantation following contusion spinal cord injury. *The 2nd Annual Clinical-Translational Research Symposium*, Kentucky Neuroscience Institute, UK Albert B. Chandler Hospital, Lexington, KY

Eldahan K.C., Cox D., Gollihue J., Patel S. and Rabchevsky A. (2017) Effects of continuous gabapentin administration on the incidence and severity of autonomic dysreflexia. *The 35th Annual National Neurotrauma Society Symposium*, Snowbird, UT J. Neurotrauma 34 (A-142), p. B26-01.

Patel S.P., Gollihue J.L., **Eldahan K.C.**, Cox D.H., Sullivan P.G. and Rabchevsky A.G. (2017) Mitochondrial transplantation following contusion spinal cord injury. *The 35th Annual National Neurotrauma Society Symposium*, Snowbird, UT J. Neurotrauma 34 (A-66), p. A18-11.

Gollihue J., Patel S., **Eldahan K.C.**, Cox D. and Rabchevsky A. (2017) Mitochondrial transplantation restores bioenergetics after spinal cord injury. *Experimental Biology Annual Meeting*, Chicago, IL

Hou S., Saltos T., Connors T., **Eldahan K.C.**, Rabchevsky A.G., Lu P., Tom V.J. (2016) Grafting embryonic raphe nuclei cells into a complete spinal cord injury site reestablishes serotonergic modulation of sympathetic activity and improves cardiovascular regulation. *Society for Neuroscience Annual Meeting*, San Diego, CA

Eldahan K.C., Cox D.H., Gollihue J.L., Patel S.P. and Rabchevsky A. (2016) Chronic rapamycin administration after high-thoracic spinal cord injury exacerbates cardiovascular dysfunction. *The 1st Annual Clinical-Translational Research Symposium*, Kentucky Neuroscience Institute, UK Albert B. Chandler Hospital, Lexington, KY

Gollihue J.L., Patel S.P., Mashburn C., **Eldahan K.C.**, Cox D., Sullivan P.G. and Rabchevsky A.G. (2016) Mitochondrial transplantation into the injured spinal cord improves cellular respiration. *1st Annual Clinical-Translational Research Symposium*, Kentucky Neuroscience Institute, UK Albert B. Chandler Hospital, Lexington, KY

Eldahan K.C., VanRooyen J., Patel S.P. and Rabchevsky A.G. (2016) Modulation of the mammalian target of rapamycin to alter maladaptive plasticity associated with autonomic dysreflexia. *The 34th Annual National Neurotrauma Society Symposium*, Lexington, KY J. Neurotrauma 33(13): A-67, PSA-154.

VanRooyen J.V., Patel S., Mashburn C., **Eldahan K.C.**, Cox D., Sullivan P. and Rabchevsky A. (2016) Transplanted mitochondria significantly maintain cellular respiration after acute contusion spinal cord injury. *The 34th Annual National Neurotrauma Society Symposium*, Lexington, KY J. Neurotrauma 33(13): A-8, T01-10.

Eldahan K.C., VanRooyen J.L., Patel S.P. and Rabchevsky A.G. (2015) Pharmacological manipulation of maladaptive plasticity to prevent autonomic dysreflexia. *The 16th International Symposium on Neural Regeneration*, Asilomar Conference, Pacific Grove, CA

Eldahan K.C., VanRooyen J.L., Patel S.P. and Rabchevsky A.G. (2015) Pharmacological manipulation of mTOR activity to modulate maladaptive intraspinal plasticity and autonomic dysreflexia. *The 33rd Annual National Neurotrauma Society Symposium*, Santa Fe, NM J. Neurotrauma 32, p. A-38.

VanRooyen J.L., Patel S.P., **Eldahan K.C.**, Smith T.L., Cox D.H. and Rabchevsky A.G. (2015) Mitochondrial transplantation to restore cellular bioenergetics after spinal cord injury. *The 22nd Annual American Society for Neural Therapy and Repair Conference*, Clearwater, FL

VanRooyen J.L., Patel S.P., **Eldahan K.C.**, Smith T.L., Cox D.H. and Rabchevsky A.G. (2016) Mitochondrial transplantation into the injured spinal cord improves bioenergetic integrity. *Keystone Symposium on Mitochondrial Dynamics*, Steamboat Springs, CO

VanRooyen J.L., Patel S.P., **Eldahan K.C.**, Smith T.L., Cox D.H. and Rabchevsky A.G. (2015) Mitochondrial supplementation after spinal cord injury maintains cellular bioenergetics, *Bluegrass Society for Neuroscience Day*, Lexington Convention Center, Lexington, KY

Rabchevsky A.G., **Eldahan K.C.**, VanRooyen J.L., Wang C.Y., Smith T.L., Cox D.H. and Patel S.P. (2014) Gabapentin management of autonomic dysreflexia:

Effects on systemic inflammation. *Society for Neuroscience Annual Meeting*, Washington, D.C.

Rabchevsky A.G., **Eldahan K.C.**, Nall D.A., VanRooyen J.L., Wang C.Y., Patel S.P. (2013) Influences of systemic inflammation and gabapentin on the severity of autonomic dysreflexia in relation to the expression of inflammatory cytokines in both visceral and neural tissues. *Society for Neuroscience Annual Meeting*, San Diego, CA

Patel S.P, Sullivan P.G., Yonutas H. M., VanRooyen J.L., **Eldahan K.C.** and Rabchevsky A.G. (2013) Effects of continuous N-acetylcysteine amide (NACA treatment on acute and chronic pathophysiology after contusion spinal cord injury. *Society for Neuroscience Annual Meeting*, San Diego, CA

Patel S.P., Sullivan P.G., Yonutas H.M., VanRooyen J.L, Pandya J.D., **Eldahan K.C.**, and Rabchevsky A.G. (2013) Effects of continuous subcutaneous delivery of N-acetylcysteine amide (NACA) on acute and chronic pathophysiology after spinal cord injury". Selected for oral presentation, *The 31th Annual National Neurotrauma Society Symposium*, Nashville, TN J. Neurotrauma 30, p. A-18.

Rabchevsky A.G., **Eldahan K.C.**, Kline R.H. and Patel S.P. (2012) Mitigation of autonomic dysreflexia by gabapentin treatment after complete spinal cord injury: Effects on pERK expression in spinal cord neurons and neuroglial cells. *Society for Neuroscience Annual Meeting*, New Orleans, LA

Patel S.P., Sullivan P.G., Pandya J.D., Visavadiya N.P., **Eldahan K.C.**, Kline, R.H. and Rabchevsky A.G. (2012) Neuroprotective effects of N-acetylcysteine amide (NACA) following contusion spinal cord injury in rats. *Society for Neuroscience Annual Meeting*, 252.19/M18, New Orleans, LA

Patel S.P., Pandya J.D., **Eldahan K.C.**, Sullivan P.G. and Rabchevsky A.G. (2012) N-acetylcysteine amide (NACA) treatment improved mitochondrial bioenergetics and hindlimb functional recovery following contusion spinal cord injury. Selected for oral presentation, *The 30th Annual National Neurotrauma Society Symposium*, Phoenix, AZ

Rabchevsky A.G., Patel S.P., Lyttle T.S., O'Dell C.R., **Eldahan K.C.**, Donohue, K.D. and Kitzman P.H. (2011) Gabapentin mitigates both induced and spontaneous autonomic dysreflexia, as well as reflexive spasticity after severe spinal cord injury. *Society for Neuroscience Annual Meeting*, Washington, D.C.

Rabchevsky A.G., Patel S.P., Lyttle T.S., O'Dell C.R., **Eldahan K.C.**, Donohue, K.D. and Kitzman P.H. (2011) Gabapentin alleviates spasticity and both induced and spontaneous autonomic dysreflexia after severe spinal cord injury. *The 29th Annual National Neurotrauma Symposium*, Ft. Lauderdale, FL